National Library of Canada
Acquisitions and Bibliographic Services Branch
395 Wellington Street
Ottawa, Ontario
K1A 0N4

Bibliothèque nationale du Canada
Direction des acquisitions et des services bibliographiques
395, rue Wellington
Ottawa (Ontario)
K1A 0N4

Your file Votre référence

Our file Notre référence

NOTICE

The quality of this microform is heavily dependent upon the quality of the original thesis submitted for microfilming. Every effort has been made to ensure the highest quality of reproduction possible.

If pages are missing, contact the university which granted the degree.

Some pages may have indistinct print especially if the original pages were typed with a poor typewriter ribbon or if the university sent us an inferior photocopy.

Reproduction in full or in part of this microform is governed by the Canadian Copyright Act, R.S.C. 1970, c. C-30, and subsequent amendments.

AVIS

La qualité de cette microforme dépend grandement de la qualité de la thèse soumise au microfilmage. Nous avons tout fait pour assurer une qualité supérieure de reproduction.

S'il manque des pages, veuillez communiquer avec l'université qui a conféré le grade.

La qualité d'impression de certaines pages peut laisser à désirer, surtout si les pages originales ont été dactylographiées à l'aide d'un ruban usé ou si l'université nous a fait parvenir une photocopie de qualité inférieure.

La reproduction, même partielle, de cette microforme est soumise à la Loi canadienne sur le droit d'auteur, SRC 1970, c. C-30, et ses amendements subséquents.

Canada

University of Alberta

Development of a Serotonergic Neuron in Embryos of *Helisoma trivolvis*: Developmental and Behavioral Consequences of Serotonin Expression

by

Thomas John Diefenbach

A thesis submitted to the Faculty of Graduate Studies and Research in partial fulfillment of the requirements for the degree of Doctor of Philosophy

Department of Biological Sciences

Edmonton, Alberta
Fall 1995.

National Library
of Canada

Acquisitions and
Bibliographic Services Branch

395 Wellington Street
Ottawa, Ontario
K1A 0N4

Bibliothèque nationale
du Canada

Direction des acquisitions et
des services bibliographiques

395, rue Wellington
Ottawa (Ontario)
K1A 0N4

Your file Votre référence

Our file Notre référence

THE AUTHOR HAS GRANTED AN IRREVOCABLE NON-EXCLUSIVE LICENCE ALLOWING THE NATIONAL LIBRARY OF CANADA TO REPRODUCE, LOAN, DISTRIBUTE OR SELL COPIES OF HIS/HER THESIS BY ANY MEANS AND IN ANY FORM OR FORMAT, MAKING THIS THESIS AVAILABLE TO INTERESTED PERSONS.

L'AUTEUR A ACCORDE UNE LICENCE IRREVOCABLE ET NON EXCLUSIVE PERMETTANT A LA BIBLIOTHEQUE NATIONALE DU CANADA DE REPRODUIRE, PRETER, DISTRIBUER OU VENDRE DES COPIES DE SA THESE DE QUELQUE MANIERE ET SOUS QUELQUE FORME QUE CE SOIT POUR METTRE DES EXEMPLAIRES DE CETTE THESE A LA DISPOSITION DES PERSONNE INTERESSEES.

THE AUTHOR RETAINS OWNERSHIP OF THE COPYRIGHT IN HIS/HER THESIS. NEITHER THE THESIS NOR SUBSTANTIAL EXTRACTS FROM IT MAY BE PRINTED OR OTHERWISE REPRODUCED WITHOUT HIS/HER PERMISSION.

L'AUTEUR CONSERVE LA PROPRIETE DU DROIT D'AUTEUR QUI PROTEGE SA THESE. NI LA THESE NI DES EXTRAITS SUBSTANTIELS DE CELLE-CI NE DOIVENT ETRE IMPRIMES OU AUTREMENT REPRODUITS SANS SON AUTORISATION.

ISBN 0-612-06201-5

Canada

University of Alberta

Library Release Form

Name of Author: Thomas John Diefenbach

Title of Thesis: Development of a Serotonergic Neuron in Embryos of *Helisoma trivolvis*: Developmental and Behavioral Consequences of Serotonin Expression.

Degree: Doctor of Philosophy

Year this Degree Granted: 1995.

Permission is hereby granted to the University of Alberta Library to reproduce single copies of this thesis and to lend or sell such copies for private, scholarly, or scientific research purposes only.

The author reserves all other publication and other rights in association with the copyright in the thesis, and except as herein before provided, neither the thesis nor any substantial portion thereof may be printed or otherwise reproduced in any material form whatever without the author's prior written permission.

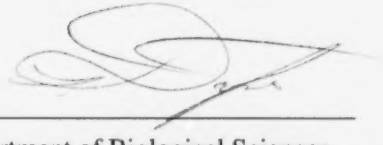

Department of Biological Sciences,
CW303 Biological Sciences Centre,
University of Alberta,
Edmonton, Alberta,
Canada T6G 2E9

September 15, 1995.

University of Alberta

Faculty of Graduate Studies and Research

The undersigned certify that they have read, and recommend to the Faculty of Graduate Studies and Research for acceptance, a thesis entitled **Development of a Serotonergic Neuron in Embryos of *Helisoma trivolvis*: Developmental and Behavioral Consequences of Serotonin Expression** submitted by **Thomas John Diefenbach** in partial fulfillment of the requirements for the degree of **Doctor of Philosophy**.

Dr. J. I. Goldberg (Supervisor)

Dr. T. Gordon (Committee Member)

Dr. A. N. Spencer (Committee Member)

Dr. S. Zalik (Committee Member)

Dr. J. P. Chang (Department appointee)

Dr. J. Lauder (External Examiner)

Dr. M. Belosevic (Examination Chairman)

Sep. 15, 1995

Dedicational

I dedicate this thesis to my loving wife, Angela.

Abstract

Neurotransmitters affect cellular development in addition to serving as chemical messengers. In embryos of the snail *Helisoma trivolvis*, serotonin is first expressed in a pair of neurons, embryonic neurons C1 (ENC1). The early differentiation of ENC1 prompted the hypothesis that serotonin functions as both a neurotransmitter and developmental regulator in *Helisoma* embryos.

In a study of the development of ENC1, its neurites were found to project ventrally toward the pedal ciliary band, where they branched extensively. ENC1 also extended an apical dendrite to the embryonic surface, which was tipped with a chemoreceptor-like structure. ENC1 thus displayed morphological characteristics of both a motor and sensory neuron.

To test the hypothesis that serotonin regulates the outgrowth of ENC1 neurites, p-chlorophenylalanine (pCPA) and 5-hydroxytryptophan (5-HTP) were used to lower and raise embryonic serotonin content, respectively. ENC1 neurite branching was increased after pCPA treament, whereas it was decreased after 5-HTP treatment. Therefore, serotonin released from ENC1 during development may limit neurite branching through an autoregulatory mechanism.

Given that ENC1 neurites innervate the pedal ciliary band, serotonin released from ENC1 may regulate cilia-driven rotational behavior of the embryo. The pedal ciliary band was found to generate rotational surges responsible for a developmental increase in rotation rate. Applied serotonin produced dose-dependent increases in rotation rate that were blocked by the serotonin receptor antagonist, mianserin. Mianserin applied alone reduced basal rotation by preventing the expression of surges. These results suggest that rotational surges are generated by the episodic release of serotonin from ENC1 onto pedal ciliated cells.

Lymnaea stagnalis was also examined to determine if an ENC1-like neuron is present in a related species. $ENC1_{Lym}$ was identified based on its cellular morphology and

uptake of 5,7-dihydroxytryptamine. However, $ENC1_{Lym}$ expressed tyrosine hydroxylase immunoreactivity rather than serotonin immunoreactivity. Furthermore, results from a pharmacological study suggested that $ENC1_{Lym}$ may utilize dopamine rather than serotonin as its cilioexcitatory neurotransmitter.

These results support a dual role for serotonin as both neurotransmitter and developmental regulator during development. Furthermore, homologous neurons from different species may express different neurotransmitters.

Acknowledgments

I wish to acknowledge the patient and excellent supervision of Dr. Jeffrey I. Goldberg, my supervisor, friend, and future good colleague. I will always admire his straightforward, uncluttered approach to science and his exemplary ability to communicate scientific principles. Thank-you, Jeff, for showing confidence in me that I could succeed in graduate studies. I am also indebted to Dr. John P. Chang, who served as interim supervisor during Dr. Goldberg's sabbatical, as well as "supervisor at large" for the rest of my program. John has a great sense of humour intermingled with a deep understanding of almost everything. His example of generosity, dedication and critical thinking will leave a lasting impression for me. I wish to acknowledge Dr. Sudarshan K. Malhotra for his wise counsel and for the opportunity to work on vertebrate tissue in his lab. I wish to acknowledge past and present committee members and externals including Dr. Andrew N. Spencer (who gave me an opportunity to work with jellyfish neurons), Dr. Warren Gallin (whose helpfully critical tutorials in the core course helped me to reassess my perspective of science), Dr. Sarah Zalik, Dr. Mike Belosevic (for never being boring), Dr. Tessa Gordon, Dr. Ruben R. Kaufman (who helped me to appreciate ticks), and Dr. Robert Berdan (who appreciated the visual poetry of neuronal form). I would especially like to thank Dr. Jean M. Lauder for venturing to the Great White North to serve as the external for the defense.

Thanks go to Dr. Rakesh Bhatnager and Ron Koss for interesting discussions and technical assistance with the confocal microscope, as well as Bruce Wakeford for lively discussions about goldfish and snails. I wish to acknowledge the technical assistance of Kimberly McKenney, who did a scanning electron microscopic study of *Helisoma* embryos, Dr. B. Duff Sloley for teaching me HPLC and providing some biogenic amines, Niels Koehncke, who performed some of the initial mianserin and specificity tests in the

pharmacological study, and Ken Cavers for for his help with the blind analysis of neurite branching.

During my program I have had the pleasure to be aquainted with many graduate and undergraduate students, all of whom have enriched my experience in this department. These include Dr. Ken Cavers, Dr. Niels Koehncke, Dr. André Martel, Dr. Jun-Mo Chung, James Lin, Dr. Chun Peng, Dr. Nikita Grigoryev, Dr. Jan Przysiezniak, Dr. B. Duff Sloley, Dr. Karl Schwalme, Dr. Christopher Price, Kimberly Christopher, Robert Zalitak, Rafe Garofalo, Susan Kirkpatrick, Fred Van Goor, Paul Klatt, Katherine Neumann, Norm Neumann, Randy Marsh, David Spafford, Geoff Zbitnew, Kevin Young, and Dennis Djogovic.

I am also grateful to the Alberta Heritage Foundation for Medical Research for providing me with Studentship support, in addition to the previous Department of Zoology for two years of Graduate Teaching Assistantship support.

I would especially like to acknowledge my wife, Angela, to whom this thesis is dedicated, for her love, patience and support, as well as my parents, Hedy and Bernie Diefenbach, and my sister Christine, for their love, support and good advice over the years. I am also indebted to God, the Father, and his son, the Lord Jesus Christ, for much spiritual guidance over the years.

Table of Contents

Introduction..... 1

I) Neurotransmitters as regulators of development..... 2

i) Early evidence implicating serotonin as a regulator of development during embryogenesis..... 2

ii) Serotonin as morphogen and mitogen..... 5

iii) Serotonin as a regulator of neuronal development in vertebrates..... 6

iv) Serotonin as a regulator of neuronal development in molluscs..... 8

v) Role of other neurotransmitters in neuronal development..... 10

II) Nervous system organization and development in gastropod molluscs..... 11

i) Organization and structure of the central ganglia..... 11

ii) Gangliogenesis..... 13

iii) Benefits of the gastropod nervous system in neurobiology..... 14

III) Regulation of neurite outgrowth by neurotransmitters..... 15

i) The growth cone is the motile structure of growing neurites..... 16

ii) Neurotransmitter effects on neurite outgrowth in *Helisoma*..... 19

iii) Neurotransmitter effects on neurite outgrowth in vertebrate neurons..... 20

iv) Mechanisms of neurotransmitter-induced changes in neurite outgrowth..... 21

IV) Serotonin expression and function in gastropods..... 26

i) Prevalence of serotonin expression..... 26

ii) Serotonin expression in the giant cerebral neurons of gastropods..... 27

iii) Serotonin as a possible neurohormone in gastropods..... 28

iv) Serotonin turnover in gastropods: uptake and inactivation..... 28

v) Role of serotonin in molluscan behavior..... 29

V) Objectives..... 32

i) Development of ENC1..... 32

ii) Serotonin regulation of ENC1 development..... 33
iii) Serotonin regulation of an embryonic behavior..... 33
iv) Identification of an ENC1-like cell in *Lymnaea stagnalis*..... 34
Materials and Methods..... 35
i) Animals..... 35
ii) Staging of Embryos..... 35
iii) Serotonin and tyrosine hydroxylase immunohistochemistry..... 38
iv) ENC1 identification *in vivo*..... 40
v) High performance liquid chromatography and ganglia dissection..... 41
vi) Quantification of neurite branching..... 43
vii) Drug treatment for neurite branching assays..... 44
viii) Analysis of rotational behavior..... 45
ix) Drug treatment for behavioral experiments: *Helisoma*..... 46
x) Drug treatment for behavioral experiments: *Lymnaea*..... 47
xi) Figures..... 49
Results..... 51
I) Development of ENC1 *in vivo*..... 51
i) Initial expression of serotonin..... 51
ii) Neurite outgrowth initiation, pathway formation and target selection..... 52
iii) Migration of ENC1..... 54
iv) Identification of putative guidance cells: interactions with ENC1 primary neurites..... 54
v) Identification of ENC1 *in vivo*..... 56
vi) Morphology of ENC1 soma and apical dendrite..... 57
vii) Identification and development of pedal ciliated target cells..... 59
viii) Developmental branching of primary ENC1 neurites: role of target cell differentiation..... 61

a) Unbranched EPN outgrowth..... 62
b) Back-branching of EPNs..... 62
c) Fasciculation of EPNs..... 64
ix) Later development of ENC1..... 65
a) ENC1 is present throughout embryogenesis..... 65
b) ENC1 as potential pioneer neuron..... 66
c) ENC1 expresses serotonin transiently..... 66
x) Figures..... 68
II) Role of serotonin in the development of ENC1..... 103
i) Effect of pCPA on whole embryo serotonin content..... 103
ii) Effect of pCPA on serotonin content of mature CNS of *Helisoma*..... 104
iii) Effect of pCPA on serotonin immunoreactivity..... 105
iv) Effect of pCPA on ENC1 neurites..... 106
v) Effects of 5-HTP..... 107
vi) Effects of dopamine on ENC1 neurites..... 108
vii) Figures..... 109
III) Role of serotonin in the development of rotational behavior in *Helisoma* embryos. 121
i) Rotational behavior: characteristics of rotation..... 121
ii) Developmental changes in rotation..... 122
iii) Effects of serotonin on rotation..... 123
iv) Effects of a serotonin antagonist on rotation..... 124
v) Figures..... 126
IV) Identification of ENC1 homologues in embryos of *Lymnaea stagnalis*..... 143
i) Serotonin immunostaining..... 144
ii) Tyrosine hydroxylase immunostaining..... 145
iii) Identification of an ENC1-like cell *in vivo*..... 146
iv) Dynamics of rotational behavior of *Lymnaea* embryos..... 148

v) Effects of serotonin and dopamine on rotation..... 149
vi) Effects of dopamine receptor antagonists on rotation..... 150
vii) Figures..... 152
Discussion..... 176
I) Development of ENC1 in *Helisoma*..... 176
i) Identity of ENC1 as possible sensorimotor neuron..... 177
ii) ENC1 as potential pioneer neuron..... 180
II) Chronology of differentiation events..... 181
i) Expression of serotonin immunoreactivity..... 181
ii) Serotonin immunoreactivity in the EPN growth cone..... 183
iii) Uptake of serotonin by ENC1..... 184
iv) Initial neurite outgrowth and contact with putative guidance cells..... 185
v) Target-localized branching outgrowth..... 187
vi) Fasciculation of EPNs on medial ciliated cells 189
vii) Possible factors influencing EPN outgrowth..... 189
viii) Asymmetries in the development of ENC1 homologues..... 190
ix) Transient expression of serotonin in ENC1..... 191
III) Role of serotonin in the development of ENC1 neurites..... 193
i) pCPA and ENC1 serotonin content..... 194
ii) 5-HTP and neurite branching..... 196
iii) Serotonin regulation of neurite branching..... 197
iv) Possible role of the target in neurite branch development..... 200
v) Significance of serotonin immunoreactivity in the growth cones of ENC1..... 203
IV) Role of serotonin in the development of rotational behavior of *Helisoma* embryos..... 204

i) Development of embryonic rotational behavior..... 205

ii) Significance of rotation and surges for *Helisoma* embryogenesis..... 208

iii) Serotonin and embryonic rotational behavior..... 209

iv) Serotonin and rotational surges..... 212

V) Potential homologue of ENC1 in *Lymnaea* and other molluscs..... 214

i) Morphological and neurotransmitter phenotype of $ENC1_{Lym}$..... 215

ii) Characteristics of rotational behavior in *Lymnaea*..... 220

iii) Dopamine, serotonin and embryonic rotational behavior..... 221

VI) Figures..... 225

Footnotes..... 230

Literature cited..... 231

List of Tables

Table 1: Summary of qualitative developmental changes in rotational behavior and ciliogenesis of *Helisoma* embryos.....126

List of Figures

Figure 1: SEM images of early embryonic stages of *Helisoma* 50

Figure 2: Initial expression of serotonin 69

Figure 3: EPN contact of G1 cells 71

Figure 4: G-cells in pedal region 73

Figure 5: EPN growth cone contact of G3 cells 75

Figure 6: Progression of EPN outgrowth over the pedal region 77

Figure 7: Identification of ENC1 *in vivo* 79

Figure 8: Prevalence of serotonin immunoreactivity and serotonin-like uptake expression as a function of developmental stage 80

Figure 9: Morphology of ENC1 soma *in vivo* 82

Figure 10: Identification of pedal ciliated epithelial cells *in vivo* 84

Figure 11: Schematic illustrating the initial development of the pedal ciliary band from stage E15 to E35 86

Figure 12: EPNs associate with pedal ciliated cells *in vivo* 88

Figure 13: Development of EPN outgrowth pathway 90

Figure 14: Quantification of primary and total branch point number of EPNs between stages E15 and E30 92

Figure 15: EPN fasciculation is confined to the medial ciliated epithelial cells 94

Figure 16: Fasciculation of EPNs posteriorly along the foot primordium 96

Figure 17: ENC1 is present in later staged embryos 98

Figure 18: Evidence for pioneering of outgrowth pathways by EPNs 100

Figure 19: Transient expression of serotonin in ENC1 102

Figure 20: Effect of pCPA treatment on embryonic serotonin and dopamine content 110

Figure 21: pCPA specifically reduced serotonin content of isolated ganglia

from adult *Helisoma*.....111

Figure 22: Reduction of serotonin immunoreactivity in ENC1 after pCPA treatment.....113

Figure 23: Recovery of serotonin immunostaining after pCPA treatment.....114

Figure 24: Effect of pCPA and 5-HTP on ENC1 morphology.....116

Figure 25: Effect of pCPA treatment on number of ENC1 branch points.....117

Figure 26: Effect of 5-HTP treatment on serotonin content of *Helisoma* embryos.....118

Figure 27: Effect of 5-HTP treatment on ENC1 morphology.....119

Figure 28: Dopamine treatment did not alter ENC1 morphology.....120

Figure 29: Scanning electron micrographs of stage E25 embryos.....128

Figure 30: Surge and non-surge components of rotation.....130

Figure 31: Surges are quantifiable changes in rotation rate.....132

Figure 32: Developmental changes in rotation rate.....133

Figure 33: Developmental changes in rotational surge frequency.....134

Figure 34: Effect of serotonin on rotation rate in stage E25 embryos.....136

Figure 35: Test for the specificity of the behavioral response of stage E25 embryos to serotonin.....137

Figure 36: Effect of serotonin on frequency of rotational surges in stage E25 embryos.....139

Figure 37: Dose-dependency of serotonin effects on rotation rate at different embryonic stages.....140

Figure 38: Effects of mianserin on rotation rate and surge frequency.....142

Figure 39: ENC1 in *Helisoma* is serotonin immunoreactive.....153

Figure 40: *Lymnaea* embryos lack a serotonin-immunoreactive ENC1.....155

Figure 41: An ENC1-like cell in *Lymnaea* embryos shows TH immunoreactivity.....157

Figure 42: Identification of ENC1 in *Helisoma in vivo* using 5,7-DHT..... 159
Figure 43: Morphology of $ENC1_{Lym}$ under DIC optics..... 161
Figure 44: $ENC1_{Lym}$s unique morphology permitted consistent identification *in vivo*..... 163
Figure 45: $ENC1_{Lym}$ resembled ENC1 *in vivo*..... 165
Figure 46: Putative neurites were observed associated with the pedal ciliary band of *Lymnaea*..... 167
Figure 47: Effects of serotonin, dopamine and octopamine on rotation rate and surge frequency of *Lymnaea* embryos..... 169
Figure 48: Dose-dependent effects of dopamine on rotation rate in *Lymnaea* embryos..... 171
Figure 49: Dose-dependent effects of serotonin on rotation rate in *Lymnaea* embryos..... 173
Figure 50: Effects of dopamine receptor antagonists on rotation rate of *Lymnaea* embryos..... 175
Figure 51: Tentative chronology of events associated with the differentiation and early development of ENC1..... 225
Figure 52: Schematic illustrating the developmental progression of neurite outgrowth of the EPNs over the pedal ciliary band..... 226
Figure 53: Model of possible mechanism whereby serotonin autoreceptors regulate neurite outgrowth in the target cell region..... 228
Figure 54: Modeled patterns of neurite branching in the target region..... 229

Introduction

Neuronal development is a process in which a neuronal precursor cell acquires the morphological, biochemical, and electrophysiological features which characterize a neuronal phenotype. Neuronal regeneration is similar to neuronal development in that many features which are functionally relevant to the neuron must be expressed for its reintegration into a neuronal network. An important goal in neurobiology is to understand the mechanisms whereby these two processes can be regulated. In searching for these mechanisms, neurons in a regenerating state have more commonly been the focus of study. Since the developmental state of a neuron can determine the extent to which it responds to factors which regulate regeneration, the success of regeneration will depend on an environment which approximates that experienced during development. It is therefore a goal of neurobiologists to recreate the milieu of development to promote the regeneration of mature neurons. Knowledge of how a neuron develops may also permit treatment of neurological disorders with a developmental basis for their etiology.

Molluscan nervous systems provide excellent experimental systems to address questions relevant to neuronal regeneration and development. Much of the recent molluscan neurobiological literature has concentrated on factors which regulate neurite outgrowth, synaptogenesis, and plasticity underlying behavior in the context of the mature animal. The major advantage of molluscs is that they possess large neurons which are consistently identifiable among conspecifics and between phylogenetically related species. Neurons which have a defined phenotype and are inclusive to a particular neuronal population may be considered identifiable, but molluscs possess neurons which are identifiable even on an individual basis. Other invertebrates with determinate development also possess individually identifiable neurons, yet what distinguishes molluscan neurons is the large size, accessibility and electrical excitability of their cell bodies. A large neuron is readily

amenable to electrophysiological study, provides more cellular material for biochemical assays, and provides a larger subject for microscopic observation both *in vitro* and *in situ*.

This thesis deals with an identified neuron of the freshwater snail, *Helisoma trivolvis*, which was found by Goldberg and Kater (1989) to be the first neuron to express serotonin during embryogenesis. This neuron, which is called embryonic neuron C1 (ENC1; the C indicating that the neuron is associated with the cerebral ganglia; Goldberg and Diefenbach, 1992), differentiates shortly after gastrulation in the embryo. Given the early expression of serotonin in *Helisoma* embryos, this thesis will address, from a developmental, behavioral and comparative standpoint, the functional significance of this early neurotransmitter expression for ENC1, and for the embryo.

I) Neurotransmitters as regulators of development.

i) Early evidence implicating serotonin as a regulator of development during embryogenesis.

Neurotransmitters have been found to exert physiological effects on developing cells. Since ENC1 expresses serotonin, studies which have demonstrated effects of serotonin on development will be highlighted, with minor reference to other neurotransmitters. The conceptual impetus for these studies originated from work by Buznikov *et al.* (1964), who found that sea urchin embryos showed changes in the concentrations of serotonin, epinephrine, norepinephrine, dopamine and acetylcholine during the blastula and gastrula stages, and implicated these changes with a role for these neurotransmitters in development. Monoamines such as serotonin were also found to fluctuate during cell division of the protozoan *Tetrahymena pyriformis* (Sullivan and Sullivan, 1964). Both *Tetrahymena* (Rodriguez and Renaud, 1980) and blastomeres of sea urchin embryos (Buznikov, 1984) release serotonin at particular stages of development. Together, these results suggest that neurotransmitters may act as a diffusible signal to

coordinate non-neuronal cell activity during development. Prior to the appearance of neurons with synapses, serotonin's original role in evolution may thus have been to act as a diffusible intercellular signal to coordinate mitotic activity of cell populations (McMahon, 1974).

Buznikov *et al.* (1970) was the first to experimentally perturb embryogenesis using antagonists of monoamine and catecholamine receptors. By exposing sea urchin embryos to many different indolealkylamine derivatives like 5-methyltryptamine, blastomeric cleavage was inhibited. The inhibitory effects of these agents could be blocked by coincubation with serotonin, norepinephrine or epinephrine, of which serotonin had the greatest blocking effect. Serotonin was similarly effective in a nudibranch mollusc, *Ancula cristata*, but not in three other nudibranch species. Buznikov referred to serotonin as an "endogenous neurohumour", or later a "prenervous neurotransmitter" (Buznikov and Shmukler, 1981) and was first to implicate that serotonin may play a developmental role in embryogenesis (Buznikov and Shmukler, 1981).

The ability of serotonin to block the action of indolealkylamines' effect on cleavage may be a pharmacological rather than a physiological effect. That is, Buznikov tested the blocking effect of serotonin on compounds which were not necessarily endogenous to the sea urchin. Gustafson and Toneby (1970) tested whether serotonin endogenous to the sea urchin is important in gastrulation by reducing serotonin levels in sea urchin embryos with p-chlorophenylalanine (pCPA). pCPA inhibits a synthetic enzyme of serotonin, tryptophan hydroxylase. Serotonin is produced from the amino acid precursor tryptophan, which is converted to 5-hydroxytryptophan by tryptophan hydroxylase. 5-hydroxytryptophan is in turn converted by aeromatic amino acid decarboxylase to 5-hydroxytryptamine, which is serotonin. pCPA treatment impaired gastrulation by impeding the migration of primary mesenchyme. Embryos could be rescued by addition of 5-hydroxytryptophan (5-HTP). Deeb (1972) found that relatively low concentrations of serotonin (52 to 129 μM) inhibited hatching of sea urchin embryos, whereas higher concentrations blocked cleavage. Its effect

on hatching was to prevent digestion of the fertilization membrane and was stage-specific; only when treatment with serotonin occurred between 30 minutes after fertilization to before the 8-cell stage was hatching inhibited. Renaud *et al.* (1983) more recently found that serotonin and serotonin receptor agonists delayed cleavage in sea urchin embryos, an effect that can be modulated by the calcium ionophore A23187 (Buznikov *et al.*, 1984), cyclic nucleotides (Shmukler *et al.*, 1984), and the lipophilicity of the indolealkylamines (Landau *et al.*, 1981).

A more recent example of serotonin having a developmental effect in molluscs includes the *in vitro* stimulation of oocyte maturation of the surf clam, *Spisula solidissima* (Hirai *et al.*, 1988). Serotonin also induced spawning when injected into the gonads of the mature surf clam. The effect of serotonin on oocyte maturation was antagonized most effectively by mianserin and very slightly by ketanserin and metergoline. R+-2-dipropylamino-8-hydroxy-1,2,3,4-tetrahydronaphthalene (8-OH-DPAT) was the most effective agonist tested. With these pharmacological results, Kadam and Koide (1989) suggested that serotonin may act on a 5-HT_{1A} receptor subtype. Although 8-OH-DPAT is a potent agonist for the 5-HT_{1A} receptor, the antagonist results suggest a 5-HT_2 receptor type (Zifa and Fillion, 1992). Associated with its effect on oocyte maturation was an increase in intracellular calcium concentration, as measured using the fluorescent calcium indicator dye, Fura-2 (Juneja *et al.*, 1994). The calcium increase was dependent on extracellular calcium and therefore required calcium influx, although a contribution from intracellular calcium stores was not examined. *Spisula* oocytes which have been arrested in prophase can be induced to reinitate meiosis with serotonin (Hirai *et al.*, 1988). Serotonin binding sites were found on the vitelline envelope and plasma membrane, the latter location sharing the pharmacological profile for meiosis reinitiation suggestive of a novel 5-HT_5 receptor type (Krantic *et al.*, 1993a, 1993b).

ii) Serotonin as morphogen and mitogen.

There is now an extensive literature on the morphogenetic and mitogenic effects of neurotransmitters, including serotonin, on nonneuronal cells (for reviews see Emerit, 1992; Lauder *et al.*, 1982; Lauder, 1988; Lauder, 1993). In addition to inhibiting blastomere cleavage in sea urchin (Deeb, 1972), serotonin acts as a morphogen to inhibit cleavage of chick blastulae (Emanuelsson *et al.*, 1988). Serotonin binds to actin and tubulin in chick neuroepithelium (Emanuelsson *et al.*, 1988), and has been reported to be associated with microfilaments in the cleavage furrow of dividing blastomeres of the polychaete, *Ophryotrocha labronica* (Emanuelsson, 1974). A serotonin antagonist was found to retard cytokinesis in these polychaete embryos (Emanuelsson, 1992). Serotonin can promote the regeneration of cilia in deciliated *Tetrahymena*, a process which is dependent on cyclic adenosine monophosphate (cAMP) and Ca^{2+} and inhibited by pretreatment with pCPA (Rodríguez and Renaud, 1980). Serotonin regulates regeneration of flatworms (Lenicque and Feral, 1976) by promoting DNA (Martelly *et al.*, 1981) and RNA (Franquinet and Martelly, 1981) synthesis. Serotonergic neurons are found near the ventral cilia in the flatworm, *Dugesia dorotocephal* (Welsh and Williams, 1970) and may serve as a source of endogenous serotonin to regulate regeneration.

Serotonin is present in yolk cells and may serve as a source of serotonin during development. Emanuelsson (1974) found that serotonin was synthesized in yolk cells of polychaete embryos. Palén *et al.* (1979) implicated experimentally-induced reduction of serotonin synthesis in the yolk granules of chick blastoderms with morphogenetic aberrations. Serotonin, serotonin receptor antagonists, a serotonin synthesis inhibitor, and a monoamine oxidase (MAO) inhibitor, were applied to chick embryos in the first 48 hr of embryogenesis. These different treatments caused specific defects, including deformations in the primative streak, prevention of blastoderm expansion, neural tube closure and heart formation, and impaired somite formation. Since yolk cells did not degranulate in some of the affected regions, it was thought that exogenous serotonin prevented the breakdown of

yolk. Emanuelsson (1992) found ^{3}H-mesulergine (5-HT_{1c} and 5-HT_2 receptor antagonist) binding associated with decomposing yolk granules in 1 to 4 cell stage polychaete embryos. Thus, serotonin may affect development by regulating the availability of yolk reserves to the embryo.

Some of the morphogenetic effects of serotonin may also result from alterations in cell motility. Craniofacial (Shuey *et al.*, 1993) and cardiac (Yavarone *et al.*, 1994) mesenchyme, in addition to neural crest cells (Lauder, 1993) show reduced migration upon treatment with serotonin uptake inhibitors such as fluoxetine. Motility may be affected through serotonin-induced changes in cytoskeletal organization. Serotonin was found to reduce the level of glial fibrillary acidic protein (GFAP) and GFAP mRNA expression in primary cultures of astroglia from rat brainstem (Prince *et al.*, 1990).

Serotonin can also act as a mitogen. Serotonin stimulates the mitosis of smooth muscle cells (Nemecek *et al.*, 1986) and fibroblasts (Seuwen *et al.*, 1990), but inhibits proliferation of astrocytes by promoting their maturation (Whitaker-Azmitia *et al.*, 1990). The mitogenic effect of serotonin may arise from an ability to promote the transition of a cell from the G_1 phase to the S phase of the cell cycle, as serotonin was found to stimulate DNA synthesis in Chinese hamster lung fibroblasts (Seuwen *et al.*, 1988) and bovine smooth muscle cells (Lee *et al.*, 1991).

iii) Serotonin as a regulator of neuronal development in vertebrates

With the extensive evidence for serotonin acting to regulate development of nonneuronal cells, coupled with its role as a neurotransmitter, it follows that serotonin and neurotransmitters in general may regulate the development of the nervous system. Indeed, serotonin is expressed early in nervous system development of the rat (Lauder and Bloom, 1974; Wallace and Lauder, 1983), three-spined stickleback (Ekstroem *et al.*, 1985), chick (Wallace, 1985). Lauder and colleagues were first to examine the effects of perturbing serotonin synthesis on neuronal development in vertebrate embryos . They treated pregnant

rats with pCPA and monitored the incorporation of ^{3}H-thymidine into neurons to determine the time of differentiation of specific neuronal populations (Lauder and Krebs, 1976; 1978). Results from this study were correlated with the development of serotonergic projections (Lauder *et al.*, 1982). From these two studies, Lauder and colleagues found that pCPA treatment, in reducing serotonin content of the axonal projections, delayed the onset of ^{3}H-thymidine incorporation and therefore of differentiation of neurons receiving serotonergic innervation. In short, axons of future presynaptic neurons may stimulate the differentiation of their undifferentiated postsynaptic target cells.

The results of Lauder and colleagues are significant when considering pathological conditions of *Homo sapiens* such as phenylketonuria. Phenylketonuria is caused by an autosomal recessive gene that codes for a type of phenylalanine hydroxylase with very low enzyme activity, resulting in elevated phenylpyruvate levels in the brain (Nichol *et al.*, 1985). Phenylpyruvate can inhibit the formation of 5,6,7,8-tetrahydrobiopterin, a cofactor of aromatic amino acid decarboxylase (alternatively referred to as dopa decarboxylase), resulting in reduced serotonin and dopamine synthesis during development and mental retardation.

The progression of neuronal development whereby serotoninergic inputs arrive to a target prior to the differentiation of its constituent neurons has also been implicated in the three-spined stickleback (Ekstroem *et al.*, 1985). In the rat, serotonergic projections enter primary sensory cortex during early postnatal development and their number diminishes by adulthood, suggesting that their transient invasion of a brain region may signal neuronal development in that region (D'Amato *et al.*, 1987). A transient serotonergic projection also extends to the developing cerebellum and may affect the stratification of the cerebellum in addition to postnatal migration of granular cells (Bishop *et al.*, 1985). Serotonin may also play a role in the ontogeny of spinal autonomic nuclei in that innervation by serotonergic projections in these nuclei occurs over a prolonged period corresponding to the developmental time frame of the nuclei (Newton *et al.*, 1989).

Further to these effects of serotonin on the development of neurons, many studies have shown more directly that serotonin may initiate neuronal differentiation. Serotonin stimulates the differentiation of hippocampal neurons (Gromova *et al.*, 1983) and cerebral cortical neurons (Chubakov *et al.*, 1986). When dorsal root ganglion (DRG) neurons were co-cultured with dissociated brainstem from rat, the ganglion cells were invaded by serotonergic neurites (Forda and Kelly, 1985). The presence of the serotonergic input promoted the expression of spontaneous electrical activity and sensitivity to serotonin in the DRG neurons. These actions of serotonin may be mediated through glia. Whitaker-Azmitia and Azmitia (1989) found that uptake of serotonin by raphe neurons of rat was promoted by astrocytes which had been pretreated with serotonin. In this study, the uptake of serotonin was considered to be an indicator of serotonergic neuronal differentiation. It was later found that serotonin acts through 5-HT_{1A} receptors on astroglia to stimulate release of a protein called S-100 (Azmitia *et al.*, 1990; Whitaker-Azmitia *et al.*, 1990), which has been found to stimulate the uptake of serotonin in serotonergic neurons from mesencephalic raphe (Azmitia *et al.*, 1990). A number of studies have found that serotonergic neurons project to developing brain regions prior to the differentiation of the target neurons. From these studies it has been hypothesized that serotonergic fibres provide a specific cue for target development. In a study of mesencephalic raphe cells from fetal rats (Azmitia and Whitaker-Azmitia, 1987), serotonergic neurons themselves appeared to be stimulated to mature in the presence of a variety of normal and abnormal targets, as measured by increased uptake of ^{3}H-5-HT.

iv) Serotonin as a regulator of neuronal development in molluscs

Prior to any study of the role of neurotransmitters in the development of molluscan nervous systems, it had been well established that serotonin and other neurotransmitters could reversibly inhibit neurite outgrowth of identified buccal ganglion neurons from adult *Helisoma* (Haydon *et al.*, 1984; Haydon *et al.*, 1987; McCobb and Kater, 1988; McCobb

et al., 1988a; McCobb *et al.*, 1988b), including buccal ganglion neuron B19. It had been known that, in mature snails, the giant serotonergic neuron of the cerebral ganglia, neuron C1 (Granzow and Kater, 1977) innervates neuron B19. It was also known from work on rat that serotonergic neurons may affect the subsequent development of their postsynaptic partners (Lauder and Krebs, 1976; Lauder and Krebs, 1978). Thus, Goldberg and Kater (1989) sought to determine whether the expression of serotonin during embryogenesis of *Helisoma trivolvis* could affect the development of neuron B19. They found that serotonin was first expressed early in *Helisoma* embryogenesis, prior to the development of the buccal ganglia, in a pair of neurons they thought were the embryonic equivalent of neuron C1. By treating embryos with the neurotoxic serotonin analogue, 5,7-dihydroxytryptamine (5,7-DHT), embryonic serotonin content was transiently reduced by close to 50%. As a result of the transient reduction in serotonin content, neurons B19 were found in adult *Helisoma* to have developed an aberrant profile of electrical synaptic transmission, characterized by increased dye coupling with surrounding cells, and increased electrotonic coupling between neuron B19 pairs. This study provided the first evidence that serotonin is expressed early in *Helisoma* embryogenesis and that it may play a role in regulating synaptogenesis. In a later study, serotonin was found to reduce gap junctional conductance in two giant peptidergic neurons of a related gastropod, *Lymnaea stagnalis* (Wildering and Janse, 1992), providing further evidence of serotonin's ability to regulate electrical synapses or their formation. Serotonin is also expressed early in the embryogenesis of *Lymnaea stagnalis* (Marois and Croll, 1992). This thesis builds upon the findings of Goldberg and Kater (1989) by addressing whether serotonin can also regulate the development of the first serotonergic neuron of *Helisoma* embryos described by Goldberg and Kater (1989) and now recognized as embryonic neuron C1.

The finding of Goldberg and Kater (1989) that serotonergic input to a target region can affect the subsequent development of target neurons provided experimental evidence in support of the untested hypothesis of Schacher *et al.*(1979a). They found that neurons in

the abdominal ganglia of planktonic larvae of the marine nudibranch mollusc *Aplysia californica* extended transient axosomatic contacts to undifferentiated cells which later extended axons from the point of contact. Schacher speculated that neurotransmitter release from axosomatic contacts may provide a cue to intiate axonogenesis. The neurotransmitter phenotype of these axons and the ability of these axons to release neurotransmitter has yet to be determined.

v) Role of other neurotransmitters in neuronal development.

Neurotransmitters other than serotonin also affect the development of specific brain regions. A shift in the ocular dominance of neurons in the striate cortex of kittens occurs with closure of one eye during the critical period of postnatal development. The shift in ocular dominance to the open eye can be prevented by combined addition of 6-hydroxydopamine (6-OHDA) and N-methyl-DL-aspartate (NMA) (Bear and Singer, 1986). 6-OHDA produces lesions of noradrenergic terminals and NMA lesions cholinergic terminals. By reducing the noradrenergic and cholinergic innervation of the striate cortex during the critical period, the shift in ocular dominance was prevented. Norepinephrine and acetylcholine may therefore regulate the plasticity of the visual cortex. Norepinephrine promoted increased sensitivity of rat hippocampal neurons to norepinephrine *in vitro* in addition to reducing the number of spontaneously active neurons (Chubakov *et al.*, 1984).

Kalb (1994) found that spinal motor neurons of prenatal rat showed reduced cell body growth and branching of dendrites with N-methyl-D-aspartate (NMDA) treatment. NMDA is an agonist which selectively activates a subtype of a glutamate receptor. Interestingly, motor neurons from postnatal rat were refractory to the morphological effects of NMDA, implicating that glutamate from other neurons may regulate dendrite branching during a critical period of motor neuron development. Indeed, glutamate was found to cause a reduction in the length of dendrites of hippocampal pyramidal neurons in culture (Mattson *et al.*, 1988). Plasticity of ocular dominance columns in cat visual cortex has also

been shown to be regulated in part by NMDA receptors (Kasamatsu, 1991). Further evidence of a role for glutamate in regulating neuronal development comes from work which showed transient expression of an NMDA receptor in the ventral horn of developing rat spinal cord (Kalb *et al.*, 1992). This receptor was distinguished by its higher affinity for L-^{3}H-glutamate than the receptor of the adult. Unlike in the adult, NMDA-type glutamate receptors early in development are insensitive to Mg^{2+} blockade (Ben-Ari *et al.*, 1988; Peterson *et al.*, 1989), which means that glutamate-sensitive neurons would not need to be depolarized for glutamate to gate the channel.

A dopamine D_1 receptor is expressed transiently in chick retina prior to synapse formation (De Mello, 1978), the activation of which was found to inhibit neurite outgrowth of E8C3 retinal neurons (Lankford *et al.*, 1987).

These studies and others underscore the potential for neurotransmitters to regulate the development of the nervous system. The transient expression of specific receptors and alteration of their properties, such as ligand binding affinity and voltage sensitivity, appears to be a trend among vertebrate neurons during development. Whether this strategy is employed in invertebrates awaits further study.

II) Nervous system organization and development in gastropod molluscs

i) Organization and structure of the central ganglia.

The central ganglia of gastropods are enveloped in a bi-layered connective tissue sheath consisting of muscle cells, fibroblasts, and globular cells containing glycogen. Capillaries from arterial branches of the anterior aorta penetrate the sheath. Earlier studies suggested that blood was emptied into a sub-sheath space (Pentreath and Cottrell, 1970), which was later shown to be a fixation artifact (Berdan *et al.*, 1987). However, there are spaces between glia which are thought to channel nutrients and ions (Pentreath *et al.*, 1985). Each ganglion consists of a cortex of neuronal somata called the rind from which

axons project into the centre to form the neuropile (Bulloch and Horridge, 1965). Typically the neurons of gastropods are either unipolar, with one axon emanating from the soma, or pseudo-unipolar, with one axon that bifurcates to relay signals between cells (Kandel, 1991). Dendrite-like processes extend from the axons near the soma rather than directly from the soma as in the case of vertebrate neurons. Peripheral sensory neurons provide an exception in that dendrites arising from the soma are common (Bubel, 1983). In addition to neurons, two types of glial cell have been characterized morphologically (Berdan *et al.*, 1987). The most abundant are type I glia, which separate neuronal somata in the cortical rind and axons in the neuropile. Type II glia are motile phagocytic cells which accumulate at sites of nerve crush and may be similar to microglia of the vertebrate brain. Schacher *et al.* (1979a) reported that the synaptic arrangement is predominantly axo-axonal, with axo-somatic synapses appearing transiently during embryogenesis. In contrast, axo-somatic synapses have since been reported in mature ganglia of *Aplysia* (Shkolnik and Schwartz, 1980), and the land snail, *Helix pomatia* (Zs-Nagy and Sakharov, 1969; Elekes, 1991). Synapses in molluscs often do not possess obvious morphological specializations typical of vertebrate synapses, such as active zones and postsynaptic densities (Pentreath *et al.*, 1973; Elekes, 1991), although active zones have been studied in relation to activity-dependent synaptic plasticity in *Aplysia* (Bailey and Chen, 1988; 1989). The ganglia enlarge as a result of increases in cell size (Kriegstein, 1977; Schacher *et al.*, 1979a) and number (Jacob, 1984; McAllister *et al.*, 1983), with large neurons tending to form first (Kandel *et al.*, 1980). Further enlargement of the ganglia later in development was thought to be a result primarily of increases in neuron size (Jacob, 1984). However, Goldberg and Cavers (1993) employed bromodeoxyuridine labelling of dividing neuronal precursors in juvenile and adult *Helisoma* CNS to reveal that mitosis occurred within ganglia postembryonically. In addition, neuronal counts were made of entire ganglia and revealed increases in neuronal number during postembryonic development. The continued proliferation of CNS neurons in the adult may account for the postembryonic increase in

the number of serotonin-immunoreactive neurons in the pulmonate gastropods *Helisoma trivolvis* (Goldberg and Kater, 1989; Diefenbach and Goldberg, 1990) and *Lymnaea stagnalis* (Croll and Chiasson, 1989).

ii) Gangliogenesis

Gastropod central nervous systems are comprised of ganglia arranged through connectives in a ring around the oesophagus, collectively referred to as the circumoesophageal ganglionic ring. Evolutionarily more advanced gastropods possess ganglia with a greater amount of fusion (Hubendick, 1972). *Lymnaea* and *Helisoma* have ganglia which display relatively little fusion in comparison to species such as the land snail *Helix pomatia* (Raven, 1975). In *Helisoma* , the circumoesophageal ring is comprised of four sets of paired ganglia: the cerebral, pedal, pleural and parietal ganglia, in addition to one unpaired visceral ganglion, alternatively referred to as the abdominal ganglion. Two other ganglionic pairs connected to the circumoesophageal ganglia are the buccal ganglia, which rest on the dorsal surface of the buccal mass, and the tentacular ganglia found at the base of the tentacles. Most of the ganglia form independently, although the pleural ganglia each form as a lateral extension of a cerebral ganglion (Kriegstein, 1977). In *Helisoma*, different ganglia appear at specific times during development, with the cerebral ganglia developing first, followed by the pedal ganglia, then the buccal, pleural, parietal and visceral ganglia appear later in an undetermined sequence (Goldberg and Kater, 1989; Goldberg, 1995). In *Aplysia californica*, and probably most gastropods including *Helisoma*, ganglia form in a rostral-caudal sequence as a result of proliferation of individual cells from ectodermal placodes followed by ingression and condensation (Jacob, 1984). This process of gangliogenesis was deduced by following the inward migration of ^{3}H-thymidine-labeled postmitotic cells from slightly invaginated ectoderm in embryonic *Aplysia californica* (Jacob, 1984). In an autoradiographic analysis of the abdominal ganglion of juvenile *Aplysia*, Hickmott and Carew (1991) found that dividing neurons

were more numerous in the body wall regions adjacent to, as opposed to flanking, the ganglia. There may thus be an inductive influence of the ganglia operating over a distance to stimulate proliferation of neurons from the body wall. The development of ganglia in molluscs is similar to that of vertebrate peripheral nervous system (PNS); ganglionic neurons originate from the neural crest and migrate to the peripheral ganglia (LeDouarin, 1980).

iii) Benefits of the gastropod nervous system in neurobiology.

The molluscan nervous system is well suited to experimentation for some interesting reasons. Since the development of molluscs is potentially determinant, neurons are identifiable on an individual basis by virtue of their neurotransmitter phenotype, morphology, electrophysiological activity and connectivity. In addition, neurons of molluscs are well known for their regenerative capacity, both *in vivo* and *in vitro*. Entire ganglia of the circumoesophageal ganglionic ring have been excised and regenerated over a period of one year (Moffett and Ridgway, 1988). More importantly, the regenerative capacity of identified molluscan neurons has resulted in some of the most useful model systems for investigating neurite outgrowth and synapse formation (see below). The specificity of synapse formation during regeneration *in vivo* and *in vitro* has been the subject of extensive investigation (for review see Bulloch, 1985). Neurons are accessible *in vivo* to electrophysiological analysis on account of their large size (up to 1000 μm in *Aplysia*; Gillette, 1991) and peripheral arrangement within ganglia. Furthermore, cell culture systems for molluscan neurons have been developed as a valuable complement to the analysis of identical neurons *in vivo* (Goldberg *et al.*, 1988; Schacher and Proshansky, 1983; Syed *et al.*, 1990; Wong *et al.*, 1981). Molluscs are also interesting in that they do not appear to undergo neuronal cell death during development (Marois and Carew, 1990), providing for reliable identification of the neurons for most of ontogeny. Cell death is a major event in the development of vertebrate (Clarke, 1985) and some invertebrate (Horvitz

et al., 1982; Shankland, 1984) nervous systems. Marois and Carew (1990) reported the disappearance of an unpaired serotonergic neuron of the cerebral ganglia of *Aplysia* and concluded that it had undergone cell death. However, it is not known whether the neuron continues to function after the serotonin immunoreactivity disappears. Thus, molluscan neurons are advantageous for addressing a variety of basic neurobiological questions.

III) Regulation of neurite outgrowth by neurotransmitters.

During nervous system development, neurons make specific contacts with one another to form functionally relevant neural circuits. The outgrowth of neurites from neuronal somata and their subsequent interconnection with other neurons or with effector cells are fundamental processes in the formation of these circuits. It was originally thought that, once formed, neural circuits were "hard wired"; their configurations were fixed. This concept had to be reconciled with the fact that animals can learn, which implies that neurons may undergo morphological or biochemical changes in the learning process. There is now sufficient evidence to support the idea that neurons continue to remodel their connections as a result of aging (Purves and Hadley, 1985; Purves *et al.*, 1987) and learning (Bailey and Chen, 1983) and that these modifications reflect changes in the biochemistry, morphology and electrophysiology of the neurons.

Neuronal injury is another factor that promotes neuronal remodeling. Normally, an assault such as axotomy triggers a complex regenerative response involving the sprouting of new neurites from the proximal axon tip or cell body of the injured cell. Neurobiologists have long taken advantage of this response to gain access to actively elongating neurites. In *Helisoma*, for example, the identifiability of neurons has permitted extensive examination of factors which affect axotomy-induced sprouting (Berdan and Easaw, 1992; for review see Bulloch, 1985). A major goal of neurobiologists is to understand whether the processes associated with development and regeneration in neurons are regulated by similar

mechanisms. One approach is to examine regeneration and relate the findings back to development. Conversely, study of neuronal development can yield insight into factors which promote neurite outgrowth. In this section of the introduction, the regulation of neurite outgrowth by neurotransmitters will be discussed in detail, with examples from both *in vitro* and *in vivo* studies. Where possible, studies related to factors affecting the outgrowth of molluscan neurons will be emphasized.

i) The growth cone is the motile structure of growing neurites.

The motile sensory terminus of extending neurites is called the growth cone. Although S. Ramón y Cajal (1890) was first to view growth cones *in situ* , it was not until the invention of tissue culture by Ross G. Harrison in 1907 that growth cones were directly observed to extend from neurons of embryonic frog neural tube (Harrison, 1907, 1910). Since the growth cone determines the direction of outgrowth, target cell selection, and in some cases transforms into functional synapses, many of the regulatory factors to be mentioned exert their effects on this structure.

The growth cone consists of two morphologically distinct domains, a central or C domain and a peripheral or P domain (Bridgman, 1992). The two domains differ in their allotment of cytoskeletal proteins, with tubulin, which forms microtubules, being confined to the C domain, and actin being present in both domains but forming an elaborate network of filaments in the P domain. The P domain consists of motile, finger-like projections called filopodia, between which are flattened regions of membrane, much like the webbing between a duck's digits, called lamellipodia.

There is a significant body of evidence supporting a sensory role for growth cone filopodia. A definitive study by Davenport *et al.*(1993) showed that when isolated from the growth cone, filopodia can respond to cues such as extracellular electric fields and neurotransmitters through shortening and an increase in intracellular calcium. Chien *et al.* (1993) found that *Xenopus* retinal growth cones failed to navigate to the tectum when

treated with cytochalasin B, which results in an absence of filopodia. Filopodia of grasshopper Ti1 neurons displayed accumulation of actin proximal to the C-domain when encountering a favourable substrate (O'Connor and Bentley, 1993). Time-lapse video microscopy of rhodamine-phalloidin or rhodamine-actin-injected neurons revealed retrograde transport of filamentous or F-actin down the filopodium. It was thought that the accumulation of actin in the base of the filopodium caused expansion and permitted entry of microtubules, which normally are absent from filopodia. As microtubules enter expanding filopodia, the rest of the growth cone follows, leading to a change in the direction of outgrowth. Asymmetric expansion of the growth cone, termed "micropruning" by Burmeister and Goldberg (1988), is thought to be a mechanism leading to abrupt turns in outgrowth.

In addition to a sensory role, filopodia may also be important for growth cone advance. Lamoureux *et al.* (1989) found that growth cones generated tension in conjunction with their advance, reaffirming the view that the growth cone is responsible for axonal extension rather than extrusion of cytoplasm, as in pseudopodia. The filopodia are implicated in generating part of the force required for growth cone advance. Heidemann *et al.* (1990) found that a single filopodium can exert 50-90 μdyn of force. Bray and Chapman (1985) found that filopodia move laterally towards the base of the growth cone, in a way that they may "row" or "tow" the growth cone body forward. In spite of the force exerted by filopodia, depolymerization of actin in growth cones using cytochalasin B did not prevent growth cone advance, but did prevent growth cone motility (Marsh and Letourneau, 1984). Thus, the contribution filopodia make to growth cone advance remains equivocal.

Axonal extension depends on the polymerization of microtubules. Tubulin is transported anterogradely down an extending axon in polymer phases (Reinsch *et al.*, 1991) to be added to the growth cone (Bamburg *et al.*, 1986). There is evidence that the actin needs to be depolymerized when tubulin is polymerizing for axonal extension to

occur. Neurites of chick dorsal root ganglion neurons could still extend in culture after treatment with cytochalasin B, which depolymerizes actin (Marsh and Letourneau, 1984). This treatment results in a loss of filopodia and lamellipodia. Edson *et al.* (1993) transfected a microtubule-associated protein into a non-neuronal cell line (human hepatoma PLC) and found that, upon treatment with the actin depolymerizing drug cytochalasin B, axon-like processes extended from the cells. When a neurite branch forms from a neurite shaft, microtubules fragment in the shaft and the fragments are transported into the nascent branch to reorganize into the nascent neurite branch (Yu *et al.*, 1994). Taxol, which stabilizes microtubules, prevented branching of cultured neurons from dorsal root ganglia and sympathetic ganglia of chick embryos (Letourneau *et al.*, 1986).

Lein and Higgins (1991) found that protein synthesis was required for initiation, but not the continuation of axonal outgrowth of embryonic rat sympathetic neurons. In contrast to axons, dendrites required protein synthesis throughout the period of extension. Isolated growth cones can sustain protein synthesis, implicating that they can integrate pathfinding cues during outgrowth independent of the neuronal cell body (Davis *et al.*, 1992).

A traditional view of membrane addition during neurite outgrowth holds that membrane is transported down the neurite shaft and incorporated into the growth cone in the form of plasmalemmal precursor vesicles (Pfenninger and Friedman, 1993). However, Popov *et al.* (1993) found that membrane flow was correlated with neurite advance rate and increased with distance from the soma. This result suggested that membrane is added to the soma and neurite shaft continuously during neurite outgrowth rather than to the growth cone.

From these and many other studies of growth cone morphology and motility, one can appreciate that growth cones are complex structures. As will be outlined further, the regulation of their motility by neurotransmitters and other extrinsic factors is equally complex.

ii) Neurotransmitter effects on neurite outgrowth in *Helisoma*.

As previously outlined, neurotransmitters are well known for their ability to regulate cell development. Neurotransmitters can also enhance or inhibit neurite outgrowth. In *Helisoma*, serotonin (Haydon *et al.*, 1984) and dopamine (Haydon *et al.*, 1984; McCobb *et al.*, 1988b) inhibit neurite outgrowth, whereas somatostatin (Bulloch, 1987) promotes sprouting of neurites. Glutamate can also promote sprouting by enhancing the outgrowth-promoting action of *Helisoma* brain-conditioned medium (Bulloch, 1989). Acetylcholine has an interesting effect in that it can block the inhibitory effect of serotonin on neurite outgrowth (McCobb *et al.*, 1988a). Neuropeptides are also candidate regulators of neurite outgrowth. In *Lymnaea*, molluscan insulin-related neuropeptide increased the proportion of cultured neurons which initiate neurite outgrowth (Kits *et al.*, 1990). The effect of serotonin on the growth cone is local. Focal application of serotonin to a single growth cone of a neuron did not affect the motility nor the number of filopodia of other growth cones on the same neuron (Haydon *et al.*, 1985). The outgrowth-inhibitory action of serotonin was also shown *in situ* as it reduced axotomy-induced sprouting of neurons B19 and C1 in *Helisoma*, the latter neuron being of particular interest because it is serotonergic (Murrain *et al.*, 1990). Neuron C1, and a serotonergic pedal ganglion neuron P5, shown inhibition of neurite outgrowth in response to serotonin in culture as well (Haydon *et al.*, 1987). Neuron C1 does not, however, show any gross morphological changes resulting from serotonin depletion *in vivo*. Gadotti *et al.* (1986) injected the serotonin-depleting agent 5,7-dihydroxytryptamine into adult *Helisoma* and found that, although the EPSP induced in neuron B19 by stimulation of neuron C1 was reduced, the axons of neuron C1 appeared normal. Thus, adult *Helisoma* neurons in a stable outgrowth state may be refractory to serotonin. However, embryonic *Helisoma* neurons have been shown to display greater response plasticity to serotonin than adult neurons. Serotonin inhibited outgrowth in close to 50% of an embryonic *Helisoma* neuron population in

culture (Goldberg *et al.*, 1991). Interestingly, close to 50% of embryonic neurons with stable neurites displayed reinitiation of outgrowth. It would be interesting to examine whether the effect of serotonin is dependent upon the time spent in culture after plating for a single identified neuron, since a single neuron may display different responses depending upon its developmental stage.

iii) Neurotransmitter effects on neurite outgrowth in vertebrate neurons.

The effects of neurotransmitters on neurite outgrowth are not limited to *Helisoma* neurons. GABA can block the regressive effect of glutamate on dendrites of hippocampal pyramidal neurons (Mattson and Kater, 1989). Glutamate halts dendritic growth cones whereas axonal growth cones are unaffected (Mattson *et al.*, 1988a). Glutamate can, however, promote neurite sprouting through its action on NMDA receptors (Pearce *et al.*, 1987). Dopamine inhibits neurite outgrowth of chick retinal neurons *in vitro* (Lankford *et al.*, 1988). Furthermore, in retinal neurons cultured from chick embryo, dopamine reduced nonprimary neurite branching (Lankford *et al.*, 1987) during a period of development when a D_1 dopamine receptor subtype is known to be transiently expressed (Ventura *et al.*, 1984). Conversely, stimulation of dopamine D_2 receptors substantially increased neurite branching and neurite length of rat cortical neurons *in vitro* (Todd, 1992).

In rat retinal ganglion cells (Lipton *et al.*, 1988), chick retinal neurons (Lankford *et al.*, 1988) and hippocampal pyramidal neurons (Mattson, 1988), neurite outgrowth is inhibited by acetylcholine. An interesting study by Lipton and colleagues (1988) found that blockade of nicotinic acetylcholine receptors on rat retinal ganglion neurons with antagonists such as d-tubocurarine promoted neurite outgrowth. It was hypothesized that tonic acetylcholine receptor activation in the retina inhibits neurite outgrowth and that the antagonist provided a release from this inhibition. This study is significant in that it suggests that the absence of a neurotransmitter can have outgrowth regulatory effects.

iv) Mechanisms of neurotransmitter-induced changes in neurite outgrowth

Neurotransmitters can exert their effects on neurite outgrowth by altering the electrical properties of neurons. Where possible, neuron B19 of the buccal ganglia of *Helisoma* will be emphasized in this section as it provides a well-characterized example of how serotonin can act to alter the neurite outgrowth of an identified molluscan neuron. Serotonin causes depolarization of the *Helisoma* buccal ganglion neuron B19 (Cohan and Kater, 1986). Experimentally-induced hyperpolarization negates the outgrowth-inhibitory effect of serotonin by preventing depolarization (McCobb and Kater, 1988). Furthermore, after stimulating neurons B19 and B4, outgrowth rates increased during poststimulation recovery (Cohan, 1990), showing that the pattern of electrical activity can determine whether neurite outgrowth is enhanced or inhibited.

In *Helisoma* neurons such as neuron B19, serotonin-induced depolarization is accompanied by an increase in intracellular calcium (Mattson and Kater, 1987; Cohan *et al.*, 1987). The outgrowth-inhibitory effect of serotonin on *Helisoma* neurons can thus be mimicked by agents which increase levels of intracellular calcium, such as the calcium ionophore A23187 (Mattson and Kater, 1987). *Lymnaea* neurons loaded with calcium *in vitro* fail to regenerate neurites (Kostenko *et al.*, 1983). Relevant to the subject of this thesis, cultured neurons from *Helisoma* embryos also respond to serotonin-induced depolarization with an increase in intracellular calcium concentration (Goldberg *et al.*, 1992). It has also been shown that calcium influx through voltage-gated calcium channels is necessary for the inhibition of neurite outgrowth in neuron B19 (Cohan *et al.*, 1987; Mattson and Kater, 1987). The role of calcium in neurotransmitter-induced changes in neurite outgrowth are not limited to molluscan neurons, for similar results have been reported for hippocampal pyramidal neurons in response to glutamate (Mattson and Kater, 1988; Mattson *et al.*, 1988a). From these findings, Kater hypothesized that there is a

"window" of intracellular calcium concentration which is permissive for particular growth cone behaviors (Kater *et al.*, 1988; Kater and Mills, 1991). Specifically, there may exist a narrow range of calcium concentrations which is optimal for neurite outgrowth. Either increasing intracellular calcium concentration above or reducing calcium concentration below a specific range could lead to inhibition of neurite outgrowth. Evidence supporting this "calcium window hypothesis" includes the finding that growth cones of *Helisoma* neurons possess higher levels of intracellular calcium in an actively growing state than when stable (Cohan *et al.*, 1987). In addition, either high intracellular calcium resulting from depolarization or application of A23187 or low extracellular calcium retarded axotomy-induced regeneration of neurites of *Helisoma* neurons *in vitro* (Rehder *et al.*, 1992). Neurite outgrowth of neuroblastoma cells (Silver *et al.*, 1989), chick dorsal root ganglion neurons (Lankford and Letourneau, 1991) and rat sensory neurons (Al-Mohanna *et al.*, 1992) also appears to be regulated within a relatively narrow range of intracellular calcium concentrations. Polak *et al.* (1991) found that a calmodulin antagonist, CGS 9343B, prevented serotonin-induced inhibition of neurite outgrowth of *Helisoma* neurons, whereas by itself had no effect on neurite outgrowth apart from a marginal decrease in outgrowth rate. Therefore, the transduction pathway that leads to altered neurite outgrowth may involve calcium acting through a calmodulin-sensitive kinase to phosphorylate relevant substrates (Hanson and Schulman, 1992), such as components of the cytoskeleton.

Exceptions to this "calcium window hypothesis" have been found. Chick dorsal root ganglion cells show no alterations in intracellular calcium as a result of growth cone contact with retinal ganglion cell neurites, which normally cause growth cone collapse (Ivins *et al.*, 1991). Even in the face of a two to three-fold increase in intracellular calcium resulting from either the calcium ionophore ionomycin or 15 mM KCl, growth cone motility and neurite advance were unaltered in these cells. Similarly, rat superior cervical ganglion neurons showed no changes in neurite outgrowth when stimulated at 10 Hz with extracellular patch electrodes in spite of appreciable increases in intracellular calcium

(Garyantes and Regeher, 1992). These results show that the effect of calcium on neurite outgrowth is cell-specific and, as a corollary, neurons likely employ other second messengers to regulate neurite outgrowth.

In *Helisoma*, specific buccal ganglion neurons such as neuron B19 show outgrowth inhibitory responses to dibutyruyl cAMP and forskolin similar to those observed with serotonin (Mattson *et al.*, 1988b). Serotonin may therefore be acting through a cAMP-dependent pathway. It has recently been found that serotonin acts through cAMP to gate a sodium channel in neuron B19 (Price and Goldberg, 1993a). Interestingly, protein kinase inhibitors had no effect on the action of serotonin, suggesting that cAMP may act directly to gate the sodium channel. This was confirmed in single channel experiments which showed direct gating (Price and Goldberg, 1993b). Activation of the sodium current could therefore cause the depolarization in neuron B19 necessary to gate voltage-sensitive calcium channels (Cohan *et al.*, 1987; Mattson and Kater, 1987), leading to calcium influx. Both N-type and L-type calcium channels have been found in growth cone synaptosomal preparations from rat brain (Vigers and Pfenninger, 1991), and only high voltage-activated currents (combination of N- and L-type calcium currents) were found in the growth cones of a buccal ganglion neuron from *Helisoma* (Haydon and Man-Son-Hing, 1988).

In addition to calcium, other possible second messengers involved in regulating neurite outgrowth include metabolites of arachidonic acid, produced by hydrolysis of phosphatidylinositol by phospholipase. These metabolites show high turnover rates in growth cone particles from fetal rat brain (Negre-Aminou and Pfenninger, 1993). In addition, nucleotides such as ATP, cAMP and cGMP, and products of phospholipase C activity, including inositol trisphosphate and diacylglycerol, may also play active roles. These second messengers are all subject to regulation through G-protein-coupled receptors (Igarashi *et al.*, 1993), making the number of possible regulatory pathways to consider formidable. An intrinsic factor which deserves mention in this regard is GAP-43, a growth-associated protein which is expressed in growth cone membranes during neurite outgrowth

and regeneration (Strittmatter *et al.*, 1992). Like serotonin (Emanuelsson *et al.*, 1988), it binds to actin; unlike serotonin, it also binds to calmodulin and G_o and G_i GTP-binding proteins. Strittmatter *et al* (1994) transfected cDNA coding for the amino terminus of GAP-43 into an epithelial cell line, resulting in filopodial extension. Furthermore, transfection with GAP-43 reduced forskolin-induced increases in cAMP, suggesting that the cAMP second messenger system is involved in the filopodial stimulation by GAP-43.

Effects of neurotransmitters on calcium can impinge upon the cytoskeleton, the stability of which is greatly affected by intracellular calcium. Actin is a cytoskeletal component of the growth cone and its polymerization affects growth cone motility, especially in relation to the filopodia, which contain exclusively actin (Forscher and Smith, 1988; Smith, 1988). There are calcium-sensitive and insensitive forms of α-actinin sublocalized to specific regions of the growth cone (Sobue and Kanda, 1989). Lankford and Letourneau (1989) found that A23187 reduced the polymerization of actin filaments of cultured chick dorsal root ganglion neurons in the lamellipodia, but not in filopodia. However, filopodia isolated from neurons B19 shortened in response to serotonin application, which also increased intracellular calcium levels in filopodia (Davenport *et al.*, 1993). This shortening response is likely a result of depolymerization of actin. Calcium is known to promote the depolymerization of actin through its effect on gelsolin (Forscher, 1989; Cooper, 1991). The depolymerization of actin is known to cause growth cone collapse (Lankford and Letourneau, 1989), and growth cone collapse usually accompanies neurite outgrowth inhibition (Walter *et al.*, 1990).

Microtubules are the major structural component of neuritic shafts and the polymerization of their tubulin subunits is required for axonal extension (Bamburg *et al.*, 1986) and branching (Letourneau *et al.*, 1986; Yu *et al.*, 1994). Calcium is known to affect the action of microtubule associated proteins which regulate the stability and promote polymerization of microtubules (Gordon-Weeks, 1991).

Cell adhesion molecules may also play a role in mediating the effects of neurotransmitters on neurite outgrowth. In presynaptic sensory neurons of *Aplysia*, a cell adhesion molecule (apCAM) was found to be endocytosed via a cAMP-dependent mechanism (Hu *et al.*, 1993) in response to applied serotonin (Bailey *et al.*, 1992; Mayford *et al.*, 1992). With a reduction in apCAM at the plasma membrane surface, the sensory neurites defasciculate and, as a result, are able to extend new branches and varicosities along the axons of the postsynaptic motor neuron L7 (Zhu *et al.*, 1994). FMRFamide had a similar effect, but only on the L7 motor neurons and not the sensory neurons (Peter *et al.*, 1994). The effect of serotonin in *Aplysia* serves to regulate synaptic plasticity underlying long-term facilitation, a possible electrophysiological correlate of long term memory (Glanzman *et al.*, 1990).

Finally, extracellular matrix (ECM) molecules have been shown to be essential factors affecting neurite outgrowth in that they provide suitable or nonpermissive substrates on which neurites can grow. Adhesion to ECM is mediated by a class of receptors called integrins whose expression is governed by two large α and β gene families (Hynes, 1992). A laminin-like molecule was found to be part of brain-conditioned medium from *Helisoma* (Miller and Hadley, 1991). This medium promotes neurite outgrowth (Wong *et al.*, 1981; Wong *et al.*, 1984) of *Helisoma* neurons *in vitro*. Furthermore, a laminin antibody revealed staining in the sheath and basal laminae of *Helisoma* ganglia. Staining was absent from both the rind and the neuropile, but was localized to matrix surrounding nerves and between axonal bundles. Fibronectin was examined as another potential component of brain-conditioned medium (Mattson and Kater, 1988). Fibronectin antibody revealed staining in the ganglionic sheath, in parallel arrays along nerves, and, unlike laminin, was also found within ganglia in the extracellular spaces surrounding neurons in patchy and fibrous arrays. Cultured neurons appeared to retain fibronectin on their surfaces for less than 24 h. Medium conditioned by *Helisoma* ganglia was also immunopositive. Fibronectin was found to reduce neuronal sprouting, neurite branching, and total neurite length, but

promoted neurite extension at low concentration and inhibited neurite extension at high concentration (Mattson and Kater, 1988). Integrins were recently reported to be localized in "small point contacts" at the tips of filopodia and at the periphery of somata of pheochromocytoma (PC12) cells, in addition to "focal contacts" (focal assemblies of cytoskeleton at the termini of stress fibers) uniformly distributed over the whole cell (Arregui *et al.*, 1994).

Other substrate-associated molecules which can influence neurite outgrowth include the plant lectins concanavalin A and wheat germ agglutinin, which bind to cell surface glycoproteins and are believed to substitute for as yet unknown endogenous ligands (Lin and Levitan, 1991).

IV) Serotonin expression and function in gastropods.

i) Prevalence of serotonin expression

In *Helisoma* (Goldberg and Kater, 1989) and *Lymnaea* (Croll and Chiasson, 1989), serotonergic neurons increase in number postembryonically, with different ganglia showing increases at different developmental times. In a study comparing the expression of serotonin in laboratory-reared and wild-type *Helisoma* (Diefenbach and Goldberg, 1990), the two strains displayed nearly identical patterns of serotonin-immunoreactive neurons. However, the laboratory-reared strain was precocial in the appearance of these neurons in comparison to the wild-type, taking half the time to attain the full complement of serotonergic neurons. This study underscores the potential for rearing conditions to alter the developmental time course of gastropod nervous systems.

Serotonin immunoreactive neurons have also been found in the prosobranch gastropod, *Littorina littorea* (Croll and Lo, 1986), which possessed many more smaller serotonin-immunoreactive neurons than the more evolutionarily advanced pulmonates

(*Helisoma* and *Lymnaea*) and opisthobranchs (*Aplysia* and *Pleurobranchia*; Bullock and Horridge, 1965).

Kruglyanskaya and Sakharov (1975) demonstrated that biogenic amines are present in the embryos of *Lymnaea stagnalis* using a modified Falck-Hillarp staining technique. Goldberg and Kater (1989) utilized a serotonin antiserum to detect the initial expression of serotonin in *Helisoma* embryos. This study showed that serotonin first appeared shortly after gastrulation in a pair of neurons which they identified as the embryonic equivalent of the giant cerebral neurons (GCNs) in *Helisoma* called neurons C1 (Granzow and Kater, 1977). These neurons, later identified as embryonic neurons C1 (ENC1; Goldberg and Diefenbach, 1992), are the subject of this thesis and turned out not to be homologous with neurons C1 of adult *Helisoma*. Voronezhskaya and Elekes (1993) conducted an immunohistochemical study of serotonin expression in embryos of lymnaid and planorbid snails. They reported the presence of a serotonin-immunoreactive neuron which they called TS1 (transient serotoninergic 1) which was present in *Helisoma* but absent from *Lymnaea*. TS1 appears morphologically similar to ENC1 of *Helisoma* (Goldberg and Kater, 1989; Goldberg and Diefenbach, 1992), which was already known not to be present in *Lymnaea* (Marois and Croll, 1990). TS1 was so named for its transient expression of serotonin. As will be reported in this thesis, ENC1 also showed transient serotonin expression, and so may be homologous with TS1. Serotonin expression was also examined in developing embryos of the abalone, *Haliotis rufescens* (Barlow and Truman, 1992) . It was found that a pair of neurons, the "V-cells", which innervate the ciliated velum, were lost at metamorphosis when the velum was shed. As will be discussed later, it is possible that the V-cell is also homologous to ENC1 of *Helisoma*.

ii) Serotonin expression in the giant cerebral neurons of gastropods

Giant cerebral neurons (GCNs) are found in the cerebral ganglia of a number of gastropod species (Weiss and Kupfermann, 1976) and are presumed to be homologous

based on their morphology, electrophysiological characteristics, targets, and common expression of serotonin (Granzow and Rowell, 1981; Senseman and Gelperin, 1973). In many of these species, these neurons are useful for investigating the physiological actions of serotonin. Serotonin was first detected in GCNs of the land snail *Helix* (Kerkut and Cottrell, 1963), the slug *Limax maximus* (Cottrell and Osborne, 1970) and the pond snail *Helisoma trivolvis* (Granzow and Kater, 1977) using the Falck-Hillarp or glyoxylic acid fluorescence staining techniques for biogenic amines. Evidence that the GCNs actually contain serotonin was obtained from microchromatography of isolated neurons (Osborne and Cottrell, 1971), and conversion of ^{3}H-5-hydroxytryptophan to serotonin *in vitro* (Cottrell and Powell, 1971) and *in vivo* (Osborne, 1972). Ono and McCaman (1984) were first to employ an antibody raised against a conjugate of serotonin with bovine serum albumin to demonstrate serotonin-immunoreactivity in the GCNs of *Aplysia*. By isolating stained neurons, they were able to employ a radioenzymatic assay to measure the serotonin content within the neurons. Ultrastructural evidence that GCNs may sequester serotonin includes the finding of 100 nm dense-core vesicles in the GCNs of *Aplysia* (Weinreich *et al*., 1973; Shkolnik and Schwartz, 1980) and *Tritonia diomedia* (Weinreich *et al*, 1973).

iii) Serotonin as a possible neurohormone in gastropods.

Elekes (1991) found that serotonergic fibers were distributed throughout *Aplysia* ganglia and penetrated the ganglionic sheath. Similar results were reported for serotonin-immunostained juvenile *Aplysia* (Goldstein, *et al*., 1984). If serotonin is released into the blood cavity or haemolymph of gastropods, it could circulate to tissues directly and exert its effects as a neurohormone. Serotonin has been implicated as a neurohormone in gastropods which regulates heart beating (for review see Skelton *et al*., 1992), neuronal development (Goldberg and Kater, 1989), and neuronal proliferation (Hickmott and Carew, 1991). Serotonin also has wide ranging effects in vertebrate CNS given the relatively broad innervation patterns of serotonergic projections (Hoekfelt *et al*., 1984).

iv) Serotonin turnover in gastropods: uptake and inactivation.

As detected through autoradiograpahy, serotonin uptake systems were found to be present in ganglia of *Aplysia* (Gerschenfeld *et al.*, 1978), *Mytilus* (Burrell and Stefano, 1981) and the land snail *Helix pomatia* (Osborne *et al.*, 1975) in addition to GCNs of *Helix* (Pentreath and Cottrell, 1973). McCaman *et al.* (1984) used a radioenzymatic assay to measure serotonin amounts in ganglia and isolated serotonergic neurons of various gastropod species, including *Helisoma*. By incubating isolated serotonergic neurons C1 (the GCN of *Helisoma*) and P5 in the serotonin precursor 5-hydroxytryptophan (5-HTP), serotonin content was increased. Incubation in serotonin had no effect on isolated neurons, but serotonin, along with 5-HTP, increased serotonin production in isolated ganglia. Thus, gastropod neurons display uptake of both serotonin and its precursor, 5-HTP.

In *Helisoma* (Sloley and Goldberg, 1991), *Aplysia* (McCaman *et al.*, 1985), and the land snail *Helix aspersa* (Sloley and Juorio, 1990), serotonin is converted to γ-glutamyl serotonin through the activity of γ-glutamylamine synthetase (Battelle *et al.*, 1988). This reaction also occurs in invertebrates such as the cockroach (Sloley and Downer, 1990) and earthworm (Sloley, 1994). This is in contrast to the primary vertebrate scheme of enzymatic inactivation of serotonin in which monoamine oxidase converts serotonin to 5-hydroxyindolacetic acid (5-HIAA). Although low levels of monoamine oxidase activity was reported in *Lymnaea stagnalis* (Hiripi, 1970) and *Anodonta cygnea* (Hiripi and Slanki, 1971), a more recent study found no 5-HIAA produced by ganglia of *Helisoma trivolvis* (Sloley and Goldberg, 1991). Furthermore, uptake of serotonin is believed to be the main mechanism of its inactivation at synapses (Gerschenfeld *et al.*, 1978).

v) Role of serotonin in molluscan behavior

Serotonin has been found to function in modifying behaviors associated with learning, feeding, and cilia-driven locomotion in molluscs. *Aplysia* displays a gill withdrawal reflex when its siphon is touched, a form of associative learning. A noxious

stimulus to the tail results in sensitized, more vigorous withdrawal reflexes in response to subsequent touches regardless of their intensity. Serotonin released by interneurons facilitates the release of acetylcholine from the siphon sensory neurons, which results in enhancement of subsequent responses (Castellucci and Kandel, 1976). The mechanism of serotonin's effect has been largely determined. Serotonin receptor binding acts through a GTP-binding protein to activate adenylate cyclase which generates cAMP (Siegelbaum *et al.*, 1982; Pollock *et al.*, 1985). cAMP in turn activates protein kinase A, the catalytic subunit of which phosphorylates the S-channel, a serotonin-sensitive potassium channel, which subsequently closes (Shuster *et al.*, 1985). S-channel closure causes depolarization, which in turn activates two types of voltage-sensitive calcium channels: N-type and L-type calcium channels, which enhance neurotransmitter release, and mobilization of additional vesicles to the release site, respectively (Edmonds *et al.*, 1990). PKC activation via a calcium-dependent mechanism also plays a role in sensitization (Conn *et al.*, 1989; Sossin and Schwartz, 1992).

Feeding behavior in gastropods consists of two behavioral phases: food-induced arousal and satiation. Increased arousal is accompanied by increased heart rate and increased frequency and magnitude of biting (Rosen *et al.*, 1989). Serotonin is known to stimulate the heart of *Aplysia* via a cAMP-dependent second messenger pathway (Mandelbaum *et al.*, 1979; Wolleman and S.-Rózsa, 1975). Thus, serotonergic neurons such as the GCNs may mediate changes in arousal associated with feeding. Serotonin may also affect the kinetics of feeding. Lesioning the GCNs of *Aplysia* prolonged radular protraction, thus reducing the interbite interval (Rosen *et al*, 1983; Rosen *et al.*, 1989). The GCNs have been shown to modulate feeding behavior in many molluscs including *Helisoma* (Granzow and Kater, 1977), *Lymnaea* (McCrohan and Benjamin, 1980) *Pleurobranchia* (Gillette and Davis, 1977), *Planorbis* (Berry and Pentreath, 1976) and *Aplysia* (Weiss *et al.*, 1975). In *Aplysia*, serotonin stimulates a muscle involved in retraction of the radula at the end of a bite, called the accessory radula closer muscle.

Serotonin-induced contraction of the muscle was associated with an increase in cAMP as determined through autoradiographic detection of [α^{32}P]-cAMP produced from [α^{32}P]-ATP (Weiss *et al.*, 1979). These results were later verified using a radioimmunoassay for cAMP (Lloyd *et al.*, 1984). In *Helisoma*, the giant serotonergic neuron C1 of the cerebral ganglia projects to the buccal ganglia to innervate select neurons including neurons B19 (Granzow and Kater, 1977). Serotonin excites neuron B19 in *Helisoma* in a way similar to small cardioactive peptide B (SCP_B) (Zoran *et al.*, 1989). Interestingly, serotonin and SCP_B also directly stimulate contraction of the buccal muscle fibers which neuron B19 innervates, providing an example of a possible neurohumoral effect of serotonin on feeding.

One of the objectives of this thesis is to address the possibility that serotonin may regulate a behavior of *Helisoma* embryos consisting of cilia-driven rotational swimming. In a variety of molluscan species, serotonin has been established as an important regulator of ciliary activity. For example, serotonin stimulates the lateral gill cilia of adult bivalves such as the mussels *Mytilus edulis* and *Modiolus demissus* (Aiello, 1962; Catapane, 1983), the pedal cilia of the nudibranch *Tritonia diomedia* (Audesirk *et al.*, 1979) and the pulmonate *Lymnaea stagnalis* (Syed and Winlow, 1989), and the prototrochal cilia of prosobranch and nudibranch embryos and veligers (Koshtoyants *et al.*, 1961). In *Mytilus*, the gill is ciliated on the abfrontal, lateral, frontal and laterofrontal surfaces. The lateral cilia increase their beat frequency upon addition of serotonin in the absence of external calcium (Murakami, 1983; 1987), whereas dopamine causes ciliary arrest which is dependent on calcium (Paparo and Murphy, 1975). The abfrontal cilia respond only to mechanical stimulation in a calcium-dependent manner (Stommel, 1984). The role of cAMP in activating the lateral cilia of *Mytilus* was demonstrated in experiments using the phosphodiesterase inhibitors theophylline and isobutylmethylxantine (IBMX) (Murakami, 1983; Sanderson *et al.*, 1985), which mimicked or enhanced the effect of serotonin. Dynein is an ATPase which promotes sliding of adjacent microtubules in the ciliary axoneme, thus causing bending of a

cilium (Walczak and Nelson, 1994). cAMP has recently been found in lateral cilia of *Mytilus* and the clam *Spisula solidissima* and to act through a cAMP-dependent protein kinase to phosphorylate dynein light chains via a calcium-independent mechanism (Stephens and Prior, 1990; Stephens and Prior, 1992). However, the effect of this phosphorylation on microtubule gliding has yet to be examined.

A component of cilia-driven swimming behavior in gastropod veligers involves velum-wide, simultaneous arrest of the cilia, which induces settlement of the veliger prior to its metamorphosis into a larva (Chia *et al.*, 1984). Ciliary arrests have been examined in veligers of the gastropods *Mangelia nebula* (Mackie *et al.*, 1976) and *Calliostoma ligatum* (Arkett *et al.*, 1987) and in adult bivalves such as *Mytilus edulis* (Murakami and Takahashi, 1975). These studies have indicated that ciliary arrests result from depolarization of ciliated cells. As will be discussed in this thesis, embryos of *Helisoma* do not experience ciliary arrests during early development.

V) Objectives

Given the early appearance of serotonin in *Helisoma* embryos, the question arises whether serotonin is acting as a neurotransmitter, a developmental regulator, or both. There is sufficient evidence to support the role of serotonin as a developmental regulator in a variety of systems. In addition, serotonin is expressed in gastropod molluscs and subserves a variety of functions as a neurotransmitter. Since ENC1 is the first serotonergic neuron in *Helisoma* embryos and, for a period of development, the only serotonergic neuron present in the embryo, the possibility that serotonin can function as both a neurotransmitter and developmental regulator for a single identified neuron was examined.

i) Development of ENC1

In order to understand the developmental context in which experimental manipulations on ENC1 were performed, the initial development of ENC1 was

characterized. Features such as the expression of serotonin, serotonin-like uptake, initiation of neurite outgrowth, pathfinding of the growth cone to the target region, outgrowth of the ENC1 neurite over the target region, and termination of outgrowth were described. In most experiments, serotonin immunohistofluorescence technique was used in conjunction with laser scanning confocal microscopy and Nomarski differential interference contrast microscopy to follow the development of ENC1 *in situ* and *in vivo*, respectively.

ii) Serotonin regulation of ENC1 development

Serotonin inhibits the neurite outgrowth of serotonergic and non-serotonergic neurons from adult *Helisoma*. The adult serotonergic neurons may therefore have autoreceptors for serotonin. ENC1 may also possess serotonin autoreceptors, which may be linked to the regulation of neurite outgrowth during the development of ENC1. To test whether the availability of serotonin in the embryo can influence neurite outgrowth of ENC1 during embryogenesis, whole embryo serotonin content was either lowered or augmented with agents that affect serotonin metabolism. Serotonin immunohistochemistry was employed to resolve changes in the neurite outgrowth of ENC1 resulting from serotonin perturbation experiments. High performance liquid chromatography was used to verify the effectiveness and specificity of the serotonin-perturbing drugs on the embryonic level of serotonin. Upon reaching the target region, ENC1 neurites extend neurite branches which were quantified and used as a readily measurable parameter of the extent of neurite outgrowth. The effect of perturbations in serotonin content on the branching outgrowth of ENC1 neurites was therefore tested.

iii) Serotonin regulation of an embryonic behavior

Serotonin has stimulatory effects on molluscan cilia. Given that *Helisoma* embryos display cilia-driven rotation within their egg capsules, the role of serotonin in regulating rotational behavior of *Helisoma* was examined during the developmental period in which

ENC1 was the only serotonergic neuron present. Time lapse video microscopy was used to dissect the components of rotational behavior to better characterize the effects of serotonin and other drugs on rotational dynamics. In addition, serotonin receptor antagonists were used to test for the specificity of the serotonin response and to determine whether endogenous serotonin, presumably from ENC1, is an active regulator of cilia-driven rotation.

iv) Identification of an ENC1-like cell in *Lymnaea stagnalis*

To better define the identity of ENC1 in *Helisoma*, it is important to assess whether a related gastropod species such as *Lymnaea stagnalis*, also possesses an ENC1-like cell which shares features which distinguish the ENC1 phenotype. Since homologous neurons of similar neurotransmitter phenotype should be present in related gastropod species, an immunohistochemical analysis of *Lymnaea* embryos was conducted using antibodies against serotonin and tyrosine hydroxylase, one of the enzymes involved in dopamine synthesis. An attempt was also made to identify an ENC1-like cell in *Lymnaea* embryos using a fluorescent serotonin analogue, 5,7-dihydroxytryptamine which labels serotonergic neurons. The effects of serotonin, dopamine, and other pharmacological agents on rotational behavior were then examined to correlate the possible expression of either of these neurotransmitters in an ENC1-like cell with a regulatory role similar to that proposed for ENC1 of *Helisoma*.

Together, these studies will help resolve whether a single identified neuron can utilize its neurotransmitter to simultaneously regulate its own development and the expression of an embryonic behavior.

Materials and Methods

i) Animals

Specimens of the ramshorn snail, *Helisoma trivolvis* (Say, 1816) were obtained from a colony at the University of Alberta. The colony was founded from an Oregon Red albino strain obtained from successive inbreeding (Kater, 1974). The classification of *Helisoma* is: phylum Mollusca, class Gastropoda, subclass Pulmonata, superorder Basommatophora, order Limnophila, superfamily Ancyloidea, family Planorbidae, and subfamily Planorbinae. The genus name has alternatively appeared as *Planorbella* (Haldeman 1842), with a subgenus name of *Pierosoma* (Dall 1905). *Lymnaea stagnalis* (Lamarck) is also in the order Limnophila. *Lymnaea* were kindly supplied by Dr. A. G. M. Bulloch of the University of Calgary. *Helisoma* were raised in filtered, flow-through glass aquaria (45 liter) with oyster shell substrata. The snails were maintained at 25°C on a light:dark cycle of 12:12 h. They were fed a combination of lettuce and Trout Chow (Vextra) or Trout Grower Ration (Rangen Feeds). Since egg masses are preferentially deposited onto flat surfaces, 150 mm plastic petri plates (Falcon) were added to the aquaria to facilitate the collection of embryos (Goldberg *et al.*, 1988). Intact egg masses were detached from the petri plate with a razor blade, transferred to 35 mm plastic petri dishes (Falcon 1008) containing filtered artificial pond water (APW; 0.025% Instant Ocean; Aquarium Systems), and acclimatized in APW at 22°C for at least 24 hr. Embryos were examined under a stereomicroscope (model SR; Carl Zeiss) to determine their stage of embryonic development according to the system of McKenney and Goldberg (1989).

ii) Staging of embryos

Embryos of *Helisoma trivolvis* undergo continuous development within an egg capsule, with many egg capsules arranged collectively within an egg mass. With continuous development, there are no maintained larval stages such as those occurring in

the development of marine gastropods (Kriegstein *et al.*, 1974). The time course of morphological change during embryogenesis is relatively consistent among sibling embryos within a single egg mass. Stages of embryogenesis can therefore be identified based on distinctive morphological characteristics which appear at consistent times during embryogenesis at a given temperature. The embryonic stages of *Helisoma* are assigned percentage values with E0 (0% of embryogenesis) being the zygote and E100 (100% of embryogenesis) the hatchling snail (Goldberg *et al.*, 1988; McKenney and Goldberg, 1989). From observation of egg masses in petri dishes, embryogenesis takes 9 days at 26.5°C (Goldberg *et al.*, 1988), and 11 days at 22.5°C. It should be noted that in comparing the time course of development at these two temperatures, I found that at 22.5°C it takes 5 days to reach 30% of embryogenesis, whereas at 26.5°C it takes only 3 days (McKenney and Goldberg, 1989). However, from stage E30 onward it takes 6 days at both temperatures to reach stage E100. Thus, the early stages of development (E0 to E30) take longer at 22.5°C than at 26.5°C, whereas the later stages appear to follow similar time courses at the two temperatures. The higher temperature may accelerate cell division so that the earlier stages, which have fewer cell divisions, would be attained more quickely. This temperature-dependent difference in development time necessitates the use of the percentage staging system, as used for grasshopper embryos (Bentley *et al.*, 1979). Although embryonic stages beyond stage E30 are reliably staged to an accuracy of 5%, stages E0 to E30 have been characterized to an accuracy of 2%. That is to say that an embryo can be identified with all certainty as a stage E25 embryo, whereas an embryo between stage E20 and E25 can be assigned an approximate stage based on whether it is closer to stage E20 or E25. Although embryos have been staged previously (McKenney and Goldberg, 1989), following is a brief description of developmental events which characterize stages E0 to E30, the stages pertinent to the initial development of ENC1. The description of stages beyond E10 is based on previous descriptive accounts of embryogenesis of species related to *Helisoma* (Raven 1966, 1975; Morrill, 1982) and supported by observations made using

Nomarski differential interference contrast microscopy. For the introduction to staging of *Helisoma* embryos, scanning electron micrographs were kindly provided by my supervisor from a collection of images obtained by Kimberly McKenney (McKenney and Goldberg, 1989).

The staging of *Lymnaea* was originally assigned alphanumerical designations based on the number of days of development (from E1 at 1.5 days old to E11 at 9.0 days old; Cumin, 1972). This system was later replaced by a percentage staging system (Marois, 1989) similar to the one devised by Goldberg and Kater (1989). Since the morphological criteria for assigning percent stages to *Helisoma* and *Lymnaea* are similar, and since the focus of this thesis is on *Helisoma*, description of embryonic stages will be limited to *Helisoma*.

Embryogenesis begins at stage E0 with the zygote. Between stages E1 to E10, the zygote undergoes numerous radially symmetrical cleavages to form the blastula. Gastrulation occurs between stage E10 and E15 as the archenteron invaginates at the vegetal pole, a process characteristic of protostomic development. By stage E15, the stomodaeum or primordial oral region forms, two bilateral sheets of small ectodermal cells called cephalic plates form lateral to the stomodaeum, and a medial apical plate consisting of large-celled ectoderm forms dorsal to the stomodaeum (Figure 1A). Also at stage E15, two bilateral bands of ciliated epithelial cells appear adjacent to the dorsolateral margins of the stomodaeum. These bands, each of which consist of one ciliated epithelial cell at stage E15, constitute the prototroch. For marine gastropods, the embryos hatch after the prototroch develops into a more elaborate structure referred to as the velum. These free-swimming embryos are called veligers (Fretter, 1967). The velum propels the veliger during swimming by the action of numerous cilia. Since freshwater gastropods are thought to have evolved from a marine ancestor (Fretter, 1975), the prototroch of *Helisoma* is considered a reduced velum (Raven, 1966). The yolk cells enlarge by stage E15 and become partitioned to the vegetal pole. Between approximately stage E15 and E20, a second band of cilia, the

pedal ciliary band, develops on the medioventral surface of the foot primordium (Figure 1A). The development of this band is described in detail in the Results (section I-vii). At stage E20, the lateral halves of the prototrochal band each enlarge by the addition of one cell, and the embryo begins to elongate along the saggital plane (Figure 1B). The larval kidney or protonephridium also appears at this stage. Stage E25 is distinguished by the partitioning of the foot primordium from the posterior half of the embryo (Figure 1C). This division is marked by the posterior pedal furrow. The foot develops as an ectodermal thickening ventral to the stomodaeum. At stage E30 (Figure 1D), the shell gland cells begin secreting the larval shell; the foot primordium continues to elongate anteriorly, tentacle buds appear and subepidermal musculature in the dorsal aspect of the head region initiate spontaneous contractions. Also at stage E30, the pedal ciliary band enlarges further along the saggital plane. By stage E35, the foot primordium of the embryo is large enough with enough pedal cilia that the embryo begins to crawl along the interior of the egg capsule.

iii) Serotonin and tyrosine hydroxylase immunohistochemistry

The protocol for indirect immunostaining of stage E15 to E70 embryos was adapted from a wholemount protocol of Goldberg and Kater (1989). Embryos were isolated from their egg capsules using fine forceps and a glass Pasteur pipette and placed in petri dishes (Falcon 1008) containing *Helisoma* saline (NaCl: 51.3 mM; KCl: 1.7 mM; $CaCl_2$: 4.1 mM; $MgCl_2$: 1.5 mM; HEPES: 5.0 mM; pH = 7.3) for 5 to 30 min prior to fixation. Embryos were then transferred to cold (4°C) fixative (Zamboni's 2X: 4% paraformaldehyde, 7.5% saturated picric acid in 0.01 M phosphate buffered saline; pH = 7.5). Embryos were fixed for 3 to 18 h at 4°C in 3 ml plastic microwells lined with silicone rubber (General Electric). Following fixation was a series of four 20 min washes in 0.01 M phosphate-buffered saline (PBS; $NaH_2PO_4 \cdot H_2O$: 1.5 mM; $Na_2HPO_4 \cdot 7H_2O$: 9.7 mM; NaCl: 150.6 mM in double-distilled, de-ionized water; pH 7.5). This and subsequent steps were carried out at room temperature with agitation at 80 rpm (American Rotator V) unless

otherwise stated. Embryos were then washed in a PBS solution containing 10% goat serum (Sigma) and 0.4% Triton X-100 for 1 h. This was followed by incubation in primary serotonin antiserum diluted 1 : 125 in a solution of 1% goat serum and 3.3 mg/ml bovine serum albumin (BSA; Sigma) in PBS + 0.4% Triton X-100 from 12 to 24 h at 4°C, followed by a 6 x 20 min wash in PBS + 0.4% Triton X-100. The secondary antibody was diluted 1 : 50 in a solution of 3.3 mg/ml BSA and 0.4% Triton X-100. Following this was a 5 x 15 min wash in PBS + 0.4% Triton X-100, and then a 6 x 15 min wash in PBS. The embryos were then dehydrated in an ascending ethanol series (70%, 85%, 95%: 1 x 10 min; 100%: 2 x 10 min) and mounted in methyl salicylate (Sigma) on glass slides for microscopy. For the serotonin immunostaining protocol, the primary antibody was a rabbit anti-serotonin antiserum (Incstar) and the secondary antibody was a goat anti-rabbit IgG conjugated to tetramethyl rhodamine isothiocyanate (TRITC; Sigma). For tyrosine hydroxylase immunostaining, the primary antibody was a mouse anti-tyrosine hydroxylase monoclonal antibody (Incstar) and the secondary antibody was a goat, anti-mouse IgG antibody conjugated to fluorescein isothiocyanate (FITC; Sigma). Working dilutions were the same for the serotonin and tyrosine hydroxylase immunostaining protocols (see above). Each immunostaining experiment consisted of embryos which received primary and secondary antibody treatments, and negative controls which received only secondary antibody to determine the contribution of the secondary antibody to background immunostaining. Positive controls for the serotonin antibody consisted of immunostaining ganglia from adult *Helisoma* in wholemount (Diefenbach and Goldberg, 1990). In addition, it was found that incubation in primary serotonin antibody with excess serotonin abolished immunoreactivity (J. I. Goldberg, unpublished observations).

Embryos were examined using fluorescence optics (20X, 40X) on a Nikon Diaphot-TMD inverted microscope. For TRITC, I used a Nikon filter block with 510 to 560 nm excitation, 580 nm emission filters and a dichroic mirror with 580 nm cutoff wavelength. For FITC, I used a Nikon filter block with 450 to 490 nm excitation, 520 nm

emission filters and a dichroic mirror with 580 nm cutoff wavelength. A laser scanning confocal microscope (model Multiprobe 2001; Molecular Dynamics) interfaced with a computer workstation (model *Indigo* ; Silicon Graphics Inc.) was used to generate reconstructions of immunostained embryos. Fluorescence micrographs are reconstructions of a series of confocal images unless otherwise stated.

iii) ENC1 identification *in vivo*

Previous studies of vertebrate retinal neurons (Vaney, 1986), adult (Lent, 1984; Lent and Dickinson, 1984) and embryonic leech neurons (Glover and Kramer, 1982), and adult *Aplysia* neurons (Jahan-Parwar, 1987) demonstrated that serotonergic neurons can selectively accumulate the fluorescent serotonin analogue, 5,7-dihydroxytryptamine (5,7-DHT). It was of interest to determine whether ENC1 could be identified *in vivo* by virtue of its ability to take up 5,7-DHT. In addition, by switching from fluorescence to Nomarski DIC optics, an attempt was made to identify ENC1 *in vivo* based on its location and distinguishing morphological characteristics. The outer egg mass membrane (*tunica capsulis*; Plesch *et al.*, 1971) on the underside of each egg mass was surgically removed using stainless steel forceps to ensure that 5,7-DHT could diffuse into the egg capsules (Beadle, 1969; Goldberg and Kater, 1989). This left the *tunica interna* (intercapsulary fluid), internal and external capsular membranes and perivitelline fluid as the only potential diffusion barriers for 5,7-DHT (Plesch *et al.*, 1971). 5,7-DHT was made up as a 1.0 mM solution in 0.01% ascorbate in artificial pond water (APW; 0.025% Instant Ocean) with a final pH of 6.80 to 6.90. Ascorbic acid effectively reduces the extent of spontaneous autooxidation of 5,7-DHT (Klemm *et al.*, 1980). Embryos were incubated in 1.0 mM 5,7-DHT for 12 to 19 hours at room temperature, isolated from their egg capsules and transferred to either APW or a 1:1 mixture of APW and *Helisoma* saline. Control embryos were immersed in APW with 0.01% ascorbate. Isolated embryos where placed on a glass

slide with an overlying coverslip whose corners were tiered with dental wax to partially compress the embryos.

In experiments comparing the developmental timecourse of the expression of serotonin-like immunoreactivity with serotonin uptake capacity of ENC1, 5,7-DHT fluorescence was used as an indicator of serotonin-like uptake. For this set of experiments, egg masses were cut in half so that sibling embryos could be treated separately. Half egg masses were then immersed in either solution of 1.0 mM 5,7-DHT (0.01% ascorbic acid in APW), or in a 0.01% ascorbic acid control solution. To coordinate embryonic staging, embryos receiving 5,7-DHT treatment were immersed in 5,7-DHT at the same time that the complimentary group sibling embryos was fixed for serotonin-like immunoreactivity.

Embryos were examined using sequential fluorescence and differential interference contrast (DIC; Nomarski) optics (20X, 40X) on an inverted microscope (model Diaphot-TMD; Nikon) and an upright microscope (model Microphot-FXA; Nikon) for observation using 100X oil immersion DIC. 5,7-DHT fluorescence was resolved with a 365 nm excitation and 400 nm emission filter block (Nikon).

All photographs were obtained using a 35 mm single lens reflex camera (model N2000; Nikon) mounted directly to an inverted microscope (model Diaphot-TMD; Nikon). Kodak Technical Pan 2415 black and white reversal film was used.

v) High performance liquid chromatography and ganglia dissection

In the experiments involving reduction of embryonic serotonin content, p-chlorophenylalanine (pCPA) was used to inhibit tryptophan hydroxylase, the enzyme which 5-hydroxylates the amino acid tryptophan to 5-hydroxytryptophan, the immediate precursor of 5-hydroxytryptamine or serotonin (Gál and Whitacre, 1982; Jéquier *et al.*, 1967). Conversely, 5-hydroxytryptophan (5-HTP) is reported to increase serotonin production by acting as a substrate for aromatic amino acid decarboxylase (McCaman *et al.*, 1984). To measure changes in whole embryo serotonin content resulting from pCPA and

5-HTP treatment, high-performance liquid chromatography with electrochemical detection (HPLC-ED) was employed. The apparatus and reagents used were as previously described by Sloley and Goldberg (1991). Embryos were counted and isolated from their egg capsules at the end of the drug treatment period and placed in *Helisoma* saline. The average number of embryos in an egg mass was 23.0 ± 1.2 (range 6 to 50; n = 50). For each sample, 200 to 600 embryos were collected in 20 µl of saline and transferred to 1.5 ml polypropylene centrifuge tubes and frozen on dry ice. Samples were either prepared immediately for HPLC or kept on dry ice overnight for preparation the next day. For preparation, the samples were warmed to room temperature, and 60 µl of 0.2 N perchloric acid containing about 950 nM isoproterenol was added to each tube. Embryos were then dissociated using an ultrasonic cell disrupter (Kontes). The tubes were centrifuged at 1600 g for 5 min in a micro-centrifuge (model 235a; Fisher). A 50 µl aliquot of supernatant from the tube was injected into the HPLC column using an automated injection system (model 231; Gilson). For each run of samples, a standard solution containing 258 nM serotonin and 527 nM dopamine (each 5 µg/50 ml; Sigma) was also run to calculate amine concentrations. Peaks of serotonin (5-HT), 5-hydroxytryptophan (5-HTP), dopamine (DA) and the isoproterenol (ISP) internal standard were integrated by maximum height using an integrator (model HP 3394A; Hewlett-Packard). Calculations yielded ng of amine per sample. Since the exact number of embryos in each sample was known, amine content was presented as ng/embryo. Given that ENC1s are the only serotonin-immunoreactive neurons at stage E15 to E35 (Goldberg and Kater, 1989; Goldberg and Diefenbach, 1992), the serotonin content of an embryo likely approximates the serotonin content of both ENC1s in addition to extracellular serotonin.

For experiments in which adult *Helisoma* ganglia were isolated and treated *in vitro* with pCPA, the sample preparation, solutions and apparatus were identical to those of the embryonic serotonin determinations. Forty-eight Ganglia were isolated from snails with 18 mm vertical shell diameter and placed in either *Helisoma* saline, or in *Helisoma* saline with

0.02 % pCPA. Six to 10 ganglia were then removed after 1, 18, 24, 48 or 72 hr in control or pCPA solutions and prepared for HPLC determination of serotonin and dopamine content. Monoamine content was expressed as µg serotonin or dopamine per g of brain protein. For the spectrophotometric assay of protein content, the method of Bradford (1976) was employed. Protein was extracted from the pellet obtained from the final centrifugation of the ganglia. For the extraction procedure, residual perchloric acid was removed from the 1.5 ml polystyrene sample tubes without disturbing the pellet. Then, 1 ml of 0.1M PBS (pH = 8) was added to the tube, which was subsequently centrifuged at 1000 rpm for 2 to 3 min. The pellet was then dissolved using an ultrasonic cell disrupter. Aliquots of the samples were then combined with a protein standard, and protein content was determined using an automated Biotek ultraviolet spectrophotometer set at 595 nm and interfaced with a computer (Apple MacIntosh with a Biotek program).

vi) Quantification of neurite branching

Serotonin-immunostaining of ENC1s in control and experimental embryos permitted resolution of neurites throughout the full extent of the outgrowth pathway. To quantify the effects of pCPA, 5-HTP and DA treatment on neurite outgrowth, neurite branching was chosen as a growth parameter for two reasons: first, in no instance did treated ENC1s display complete interruptions of primary neurite outgrowth along the outgrowth pathway; nor were neurites observed to deviate from the normal pathway along aberrant routes to novel targets. Second, neurites continue to be remodeled even after the target tissue has been innervated (Bear and Singer, 1986; O'Rourke and Fraser, 1990; Purves *et al.*, 1987). In the present study, ENC1s were observed using fluorescence microscopy and neurite branches were quantified by counting the number of branch points (Sanes and Chokshi, 1992). In cases where neurites completely intersected one another or formed a three-pronged branch, two branch points were scored. ENC1 primary neurites grow towards each other until they meet at the anteroventral midline of the embryo. After

the primary neurites have extended over their target, the pedal band of ciliated epithelial cells, extensive neurite branching occurs between the primary neurites exclusively in the target cell region. Since the arbors of the ENC1 homologues overlap, it was necessary to pool branch point counts for both ENC1s, with the underlying assumption that the homologues are equally responsive to experimental perturbation. Branch point counts were validated by an untrained observer using a single blind procedure. In addition, examination of neurite arbors of serotonin-immunostained ENC1s using laser scanning confocal microscopy supported the assertion that even fine terminal neurite branches were resolved in this study. Thus, it is not likely that the number of neurite branches was underestimated as a result of faintly or differentially-immunostained terminal neurites. Significant differences in branch point numbers were determined using Student's t-test with a 95% confidence level (asterisks in graphs).

vii) Drug treatment for neurite branching assays

For the pCPA treatments, egg masses containing stage E15 (late gastrula) embryos were immersed for 1 hr in either APW or APW containing 0.02% (w/v) DL - p - chlorophenylalanine (Calbiochem). The pH of APW is normally between 6.2 and 6.8. The pH of both the control APW and pCPA solution was brought to between 6.80 and 6.90 with 1 M NaOH. Prior to immersion of egg masses, the outer egg mass membrane of the egg mass base was removed with forceps to facilitate the passage of pCPA through the egg capsule membranes. After treatment, test solutions were replaced with APW. The egg masses were then washed with APW every 12 to 14 hr for 48 hr for recovery of serotonin synthesis sufficient to permit visualization of ENC1 neurites using immunofluorescence (see Results section II-iii). With pCPA treatments of longer durations, serotonin immunoreactivity did not recover sufficiently for quantification of neurite branching. In addition, a 48 hr recovery time permitted development of the embryos to stage E25, by which time the initial pattern of neurite branching was established.

Embryos treated with 5-HTP were prepared as described for the pCPA experiments. Half egg masses were immersed for 48 hr in either pH-adjusted APW containing 1 mM 5-HTP (DL isomers; Sigma) or APW alone. The 5-HTP solution was exchanged once at 24 hr with fresh 5-HTP solution to ensure continued production of serotonin by the embryos. The control solution was also exchanged with fresh APW. After the 5-HTP treatment, embryos were isolated and placed into *Helisoma* saline for between 10 and 30 minutes to wash out excess 5-HTP. Embryos were then fixed and processed for serotonin immunofluorescence.

Dopamine is present in many molluscan species (Boer *et al*, 1984; Trimble *et al.*, 1984) and has significant effects on neurite outgrowth of cultured neurons from adult *Helisoma* (McCobb *et al.*, 1988b). The potential for dopamine to alter neurite branching of ENC1 was therefore tested. Egg masses were prepared as described previously and immersed for 48 hr in a 1.0 mM dopamine (Sigma) with 0.04% (w/v) ascorbic acid. Solutions were exchanged at 24 hr. Control egg masses were immersed in either control APW solution or APW solution with 0.04% ascorbic acid.

viii) Analysis of rotational behavior

Embryos were viewed through a CCD video camera (model TK-860U; JVC) mounted to either a stereomicroscope (model SR; Zeiss) for quantification of rotational behaviors, or an inverted microscope (model Diaphot-TMD; Nikon) for still video image capture and observations of ciliary activity. The output of the camera was either routed directly to a television monitor for live on-line analysis or to a time-lapse video cassette recorder (model AG-6720; Panasonic). The time-lapse recorder facilitated the analyses as it allowed the relatively slow rotational behavior to be examined at 6 times the normal video rate of 30 fps. To quantify the overall rate of rotation, the total number of 360° rotations counted over a ten minute interval was recorded. Rotations could be counted to an accuracy of one-half rotation and the data were averaged over the 10 minute recording period and expressed as

rotations per minute. Transient periods of markedly accelerated rotation, referred to as rotational surges, were quantified as the number of surges in a 10 minute interval and were expressed as surges per minute. Surges were counted by viewing recorded images of embryos at six times normal speed. Since there was a greater than two-fold increase in embryonic rotation rate during surge rotation as compared to non-surge rotation, surges were easily resolved (see Results section III-i). Furthermore, measurement of surge frequency performed in a double-blind format by two investigators revealed identical counts. Thus, surges are discrete, transient events which can be reliably quantified using time-lapse video microscopy. To quantify the dynamics of rotation rate, angular changes in the position of the embryo were measured from a video screen which had a superimposed grid. All of these measurements were made from embryos seen in lateral profile. The angular shift of a line tangential to the ventral-most point of the foot primordium and the ventral-most point of the abdomen was measured over sequential five second time periods. The direction of rotation produced by each band of ciliated cells was determined by viewing the local flow of suspended particles adjacent to the cilia. The direction opposite to which particles were projected was taken as the direction of movement initiated by the band. Student's t-test and ANOVA were both used to determine statistical significance, however, significance levels referred to in the text represent t-test results. ANOVA produced the same levels of statistical significance. Asterisks on graphs denote statistically significant differences from control at the 95% confidence level using Student's t-test.

ix) Drug treatments for rotational behavior experiments: *Helisoma*

In all experiments, egg masses were transferred to fresh APW for 10 minutes prior to incubation in drug-containing medium. Egg masses were then transferred to petri dishes containing 2.5 ml of either serotonin in APW (creatinine sulfate complex; Sigma), mianserin (Research Biochem Inc.), octopamine hydrochloride (Sigma), dopamine (Sigma) or γ-glutamyl serotonin (generous gift from Dr. B. D. Sloley, University of Alberta). All

chemicals were made fresh daily and kept under refrigeration prior to data collection. In control experiments, egg masses were transferred into fresh APW. In all experiments, apart from those which addressed the timecourse of effects, embryos were incubated for 10 min. prior to commencing data acquisition to control for variability in the diffusion time through egg mass compartments. This protocol was adopted as there was no short-term desensitization in the response to serotonin (see Results section III-iii). Control experiments were carried out to ensure that the effects of compounds on rotation were not the result of indirect pH or transfer effects. Egg mass transfer between control dishes containing APW did not result in a significant change in rotation rate of stage E25 embryos ($n = 10$ embryos; Student's t-test). Immersion of stage E25 embryos in APW solution at pH 6.5 did not significantly alter rotation rate ($n = 11$ embryos; Student's t-test). Immersion for 10 min in APW at pH 4.8 did result in a significant reduction in rotation rate from 1.54 ± 0.12 rpm (APW control at pH 6.8) to 1.12 ± 0.08 rpm (pH 4.8; $n = 10$; $p < 0.050$; Student's t-test). However, in the second 10 min interval, rotation rate recovered to a level similar to the control. Thus, embryos accommodate to even large shifts in pH after 10 min in solution. Since data collection occurred in the second 10 min interval after a 10 min acclimation period, pH changes should not affect the response of embryos to drugs.

x) Drug treatments for rotational behavior experiments: *Lymnaea*

The protocol for treating *Lymnaea* embryos with drugs was identical to that for *Helisoma*. Like *Helisoma*, *Lymnaea* were exposed to serotonin, dopamine, octopamine, and mianserin. In addition, *Lymnaea* embryos were exposed to dopamine receptor antagonists: haloperidol, domperidone (both kind gifts of Dr. J. P. Chang, the University of Alberta), and SKF83566 (Research Biochemicals International). Every egg mass treated was monitored 10 minutes prior to drug treatment so that every treatment had its own matched control. For data presentation, the matched control data for each treatment was pooled to give the APW Control. Owing to low availability of *Lymnaea* embryos,

treatments could not always be carried out on the same day so that statistical comparisons were made only between any given treatment and its matched control. For the dose-response curves, the data was also collected within two days. However, the low amount of variability in rotation rate (see standard error bars) among embryos from different experiment days permitted a rough comparison between treatments. For these reasons, asterisks indicating statistically significant differences of treatments in the graphs were omitted.

Figure 1: SEM images of early embryonic stages of *Helisoma*. **A.** Anterior profile of a stage E15 embryo with bilateral halves of the prototrochal ciliary band (p) flanking the invaginating stomodaeum (s). Note the presence of a single pedal ciliated epithelial cell marking the start of pedal band development (small arrow). In the animal pole, the bilateral cephalic plates (c) are located lateral to the medial apical plate (a). **B.** Stage E20 embryo in right lateral profile showing enlargement of the prototrochal (p) and pedal (two small arrows) ciliary band, the latter of which develops at the midline of the foot primordium. **C.** Stage E25 embryo in right anterolateral profile with enlarged foot primordium anterior to the posterior pedal furrow (f) with a well-developed pedal ciliary band (two small arrows). **D**. Stage E30 embryo in right lateral profile showing further development of the foot primordium and first appearance of tentacle buds (t), shell (s), and a single ciliated cell (left small arrow) positioned lateral to the elongating pedal ciliary band (two small arrows). Arrowheads in panels B, C and D indicate ciliated tip of apical dendrite of ENC1. Scale bar in each panel = 50 μm.

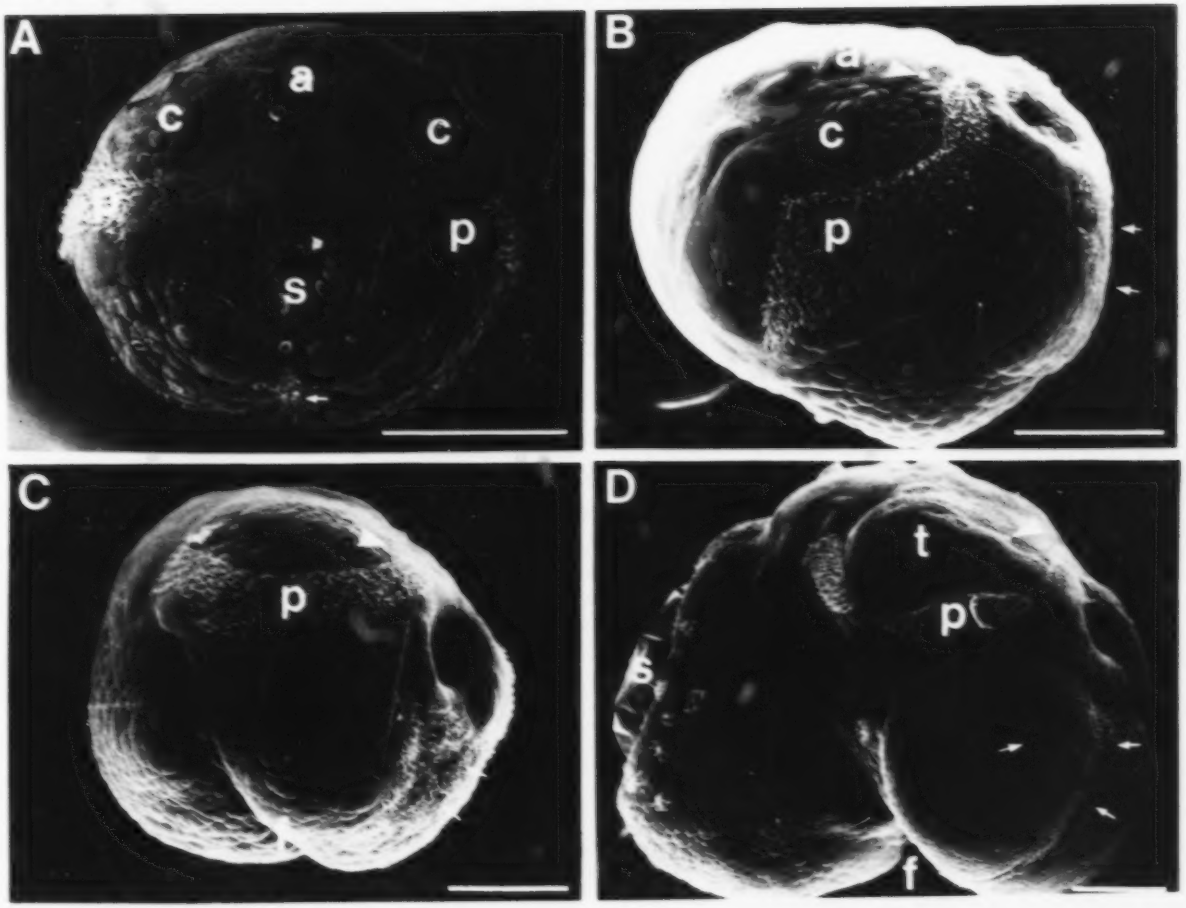
A
a
c
c
p
s
B
a
c
p
C
p
D
t
p
s
f

Results

I) Development of ENC1 *in vivo*

In this section a description will be provided of events associated with the initial development of ENC1, including serotonin expression, serotonin-like uptake, initial neurite outgrowth, target cell contact, and target-localized neurite outgrowth. Using confocal laser scanning microscopy (CLSM) of serotonin-immunostained embryos and Nomarski differential interference contrast (DIC) microscopy of living embryos, these events were examined and arranged in a tentative chronological order. In addition, the neurite outgrowth pathway was characterized in terms of the phases of outgrowth displayed by ENC1 neurites as they approach and arborize over the target.[1,2]

i) Initial expression of serotonin

Embryonic neurons C1 (ENC1s) first appeared at stage E13 as a bilateral pair of serotonin-immunoreactive cells. They were positioned among large ectodermal cells at the lateral margins the apical ectodermal plate, apposing the bilateral cephalic plates (Figure 1A). At this early stage of ENC1 development, serotonin-immunoreactivity was primarily confined to the perikaryon in large immunofluorescent granules (Figure 2A). The distribution of serotonin-immunoreactive granules was polarized in that the granules were concentrated in the apical pole of the cell, which was tapered into a blunt process which will be referred to as the apical dendrite (Figure 2B). This process projected to the ectodermal surface, and was thus in direct contact with the perivitelline fluid of the egg capsule. The immunostaining intensity of the right ENC1 appeared consistently more intense than that of the left homologue ($n > 50$ embryos; Figure 2B). This asymmetry in the apparent amount of serotonin expression persisted up to stage E15, after which an obvious difference between homologues was not consistently evident.

ENC1s at stage E14 onward possessed diffuse serotonin immunostaining throughout the soma in addition to the aforementioned granulated form of immunostaining (Figure 2B). ENC1s with neurites in various stages of outgrowth always possessed serotonin immunostaining. As will be discussed later, these observations suggest that serotonin expression in ENC1 may precede neurite outgrowth. During stages E12 to E15, the only other specific serotonin immunostaining in the embryo was inconsistently observed in select ciliated cells of the prototrochal band, which first appeared at stage E10 and can be seen in Figure 2B.

ii) Neurite outgrowth initiation, pathway formation, and target selection

Although neurite outgrowth of ENC1s at stage E13 to E15 has not been visualized *in vivo*, a sequence of events associated with the outgrowth of ENC1's primary neurite (EPN) will be detailed based on observations of fixed, serotonin-immunostained ENC1 neurites *in situ*. At stage E13 to E14, each ENC1 elaborated a single, ventrally-directed neurite, the outgrowth of which roughly demarcated the lateral boundaries of the stomodaeum when viewed from an anterior profile (Figure 2B). In observing CLSM 3-dimensional reconstructions of ENC1 morphology (n = 9 reconstructions), the EPNs appeared flattened along the basal membrane of ectodermal cells lateral to the margin of the stomodaeum. This observation suggests that these ectodermal cells may provide a suitable substrate for neurite outgrowth. As each EPN extended ventrally about midway past the stomodaeum, it executed an anteromedial turn toward the ventral margin of the buccal mass primordium. At this point in the outgrowth pathway, the EPN growth cones converged over the pedal ciliary band. In every instance that growth cones were observed approaching the pedal band or proceeding over it, the growth cone of the right EPN was in a more advanced position in the outgrowth pathway than the left EPN growth cone (n = 26 embryos; Figure 2B). At stage 15, EPNs were devoid of neuritic branches; no branches

were observed at either the pedal or prototrochal ciliary bands. Thus, the pedal ciliary band is the primary target of EPNs.

Occasionally at stage E15, a medial neurite appeared to extend from each ENC1 soma over the dorsal margin of the stomodaeum toward the contralateral ENC1 (Figure 2B; $n > 20$). In no instance did the medial neurites contact their contralateral homologue and, by stages E16 to E17, the medial neurites were usually absent and assumed to have been retracted. However, a medial neurite was observed on occasion to be retained in later staged embryos.

EPNs whose growth cones were just arriving at the pedal ciliary band displayed a discontinuous distribution of serotonin immunostaining along the length of the neurite. Consistently higher intensities of serotonin immunostaining were observed in the EPN growth cone as compared to the parent neurite ($n = 8$ neurites). Such intensity differences can be seen in Figure 2B, where both the right and left EPN, in addition to the medial neurite of the right ENC1, show greater apparent intensities of serotonin immunostaining in the growth cones and neurite shafts proximal to the growth cones. Sparsely distributed, small, serotonin-immunoreactive granules could be distinguished along the full length of the EPNs (Figure not shown).

Another characteristic of EPN was that the growth cone morphology differed before and after target cell contact (Figure 2B). The left EPN growth cone approaching the pedal ciliary band in Figure 2B appeared to be thin and tapered. In contrast, the right EPN growth cone was proceeding over the ciliary band and had a club-shaped morphology with broadened lamellipodia. Although growth cone morphology was not systematically examined, the distinction between tapered growth cones approaching the target ($n = 6$ neurites) and club-shaped growth cones growing over the target region ($n = 7$ neurites) was a consistent finding.

iii) Migration of ENC1

Another feature of ENC1 development was its migration one cell layer beneath the ectoderm and concomitant lengthening of the apical dendrite beginning after stage E15. This migration is evident by comparing the profile of ENC1 in Figure 2B with ENC1s of stage E25 and E30 embryos in Figure 13. The apical dendrite of ENC1 appears longer and more distinct from the ENC1 soma at stage E25 (Figure 13C) and at stage E30 (Figure 13D) (asterisks) in comparison to ENC1 at stage E15, for which the apical dendrite appears as only a tapered apical pole of the soma (Figure 2B). As the head region enlarged, ENC1 migrated progressively deeper into the embryo up to stage E100, with the apical dendrite maintaining contact with the epithelial surface (Figure not shown).

iv) Identification of putative guidance cells: interactions with ENC1 primary neurites

Putative guidance cells were first observed fortuitously in the course of a study in which *Helisoma* embryos were treated with the inhibitor of serotonin synthesis, pCPA (Results section II). Examination of stage E14 to E15 embryos pretreated with pCPA and immunostained with an anti-serotonin antibody revealed a group of faint, serotonin-immunoreactive cells consistently positioned at intervals along the EPN outgrowth pathway. These cells were spherical and 2 to 3 μm in diameter. The group of cells consisted of three bilateral cell pairs and one unpaired, median cell.

The bilateral pair of cells most proximal to the ENC1 somata were located at the first anteromedial turn in the EPN outgrowth pathway, lateral to the stomodaeum (Figure 3). They were discernible using confocal microscopy in untreated, serotonin-immunostained embyros by virtue of low level granulated fluorescence which approximated background levels (Figure 3A; n = 4). These cells will be referred to as GR1 and GL1, with G specifying a putative guidance function, and R and L specifying the right and left homologues, respectively. Figure 3B shows in left lateral profile a serotonin

immunostained ENC1 in a stage E30 embryo superimposed on a DIC image of the same embryo with identical orientation and magnification. Such an image was achieved by aligning and superimposing the complementary immunofluorescence and DIC negatives (n = 4 superimpositions). In Figure 3B, the anteromedial turn in the EPN outgrowth pathway formed a 90° angle, with the GL1 cell located at the vertex of the angle. In some instances, the EPNs were contorted into an omega-shaped profile at the turn (see also Figure 13C), suggesting that G1 cells may mediate contact-dependent deflection of EPNs toward the pedal ciliary band. Using DIC optics, the G1 cells were consistently identifiable even in living embryos (n > 17 embryos). At high magnification, lamellipodia-like extensions of the G1 cells were observed making direct contact with EPNs (Figure 3C and 3D).

The remaining "G-cells" were located just beneath the basal surface of the pedal ciliary band. Cells of the second bilateral pair (GR2 and GL2) were located just beyond the ventral margin of the stomodaeum (Figure 4) and were spaced between 5 and 10 μm apart at the upper corners of the band. The third cell pair, GR3 and GL3, were located about 5 μm ventral to GR2 and GL2 and were closer to the midline with a separation of about 2 to 5 μm. They were also located within the lateral margins of the band. Near the termination of the EPN outgrowth pathway, a single median cell called Gm was observed. Together, the bilateral G2 and G3 cells and unpaired Gm cell were consistently arranged in a Y-shaped pattern that delineated the EPN outgrowth pathway over the pedal ciliated target cells (n = 19 embryos; Figure 4B, C, and D).

That the "G-cells" may serve as interception points along the outgrowth pathway is illustrated in Figure 4A and schematically in Figure 4B, in which the right EPN growth cone had extended past GR2 and GR3 and appears to be directed towards Gm. The left EPN growth cone intercepted GL2, executed a 60° ventromedial turn and started to approach GL3. In Figure 5B and 5C, the right EPN growth cone can be seen in transit directly between the GR3 and GL3 cells, the GL3 cell being partially outlined by filopodial

extensions that wrap around the GL3 soma. Note in addition that in Figures 4 and 5 the right EPN growth cone had advanced further along its pathway than the left.

The end result of sequential G-cell contacts is convergence of the outgrowth pathways of the left and right EPNs. This convergence is shown by comparing confocal reconstructions of different embryos which show a relative progression of growth cone advancement over the pedal ciliary band to form the basic Y-shaped outgrowth pathway (Figure 6). As the two EPN growth cones reach the pedal ciliary band at stage E14, they first intercept the G2 cells (Figure 6A), then turn ventrally and proceed toward the G3 cells (Figure 6B). The right growth cone leads whereas the trailing left growth cone contacts the neurite shaft of the right EPN at the midline at the level of the G3 cells (Figure 6C). At stage E15, after meeting at the midline, the EPNs appear to undergo fasciculation and proceed in a posteroventral direction along the midline of the future foot primordium until they reach the Gm cell, where outgrowth terminates (Figure 6D).

v) Identification of ENC1 in vivo

Although serotonin immunofluorescence revealed the general location and gross morphology of ENC1 somata, identification of ENC1 in live embryos is necessary for *in vivo* analysis of ENC1 development and physiology. The compound, 5,7-DHT, is a proven fluorescent marker of serotonergic neurons (Glover, 1982; Lent and Dickinson, 1984), and gains access to serotonergic neurons through low and high affinity serotonin uptake systems (Osborne *et al.*, 1975). Embryos treated with 5,7-DHT possessed a single pair of 5,7-DHT stained cells with a morphology and location indistinguishable from serotonin-immunostained ENC1s *in situ* (Figure 7A). Specific fluorescence resulting from 5,7-DHT uptake was confined to ENC1s in addition to a subpopulation of yolk cells. The remainder of the yolk cells which did not display 5,7-DHT fluorescence possesed a white autofluorescence seen in control embryos which did not receive 5,7-DHT treatment. In ENC1, 5,7-DHT fluorescence was prominent in the soma, proximal primary neurite and

apical dendrite, whereas neuritic segments in the ciliated target cell region were always devoid of 5,7-DHT fluorescence. Given the low excitation/emission wavelengths of 5,7-DHT (365/400 nm, respectively), its rapid bleaching and relatively low fluorescent intensity, ENC1s were usually weakly, yet unequivocally stained.

ENC1s initially identified by their 5,7-DHT fluorescence were subsequently examined using DIC optics. DIC observation confirmed that ENC1s were positioned dorsolateral to the stomodaeum at the basal surface of the apical ectodermal plate (Figure 7B). Their characteristic morphology and position permitted consistent identification *in vivo* without a need for prior 5,7-DHT treatment (Figure 7C). 5,7-DHT-stained ENC1s were observed throughout embryogenesis (see Figure 9) and in hatchling embryos (stage P1; figure not shown). Their identity was consistently confirmed by DIC examination of soma morphology.

A notable feature of 5,7-DHT uptake in ENC1 was that it was stage-dependent. 5,7-DHT uptake was observed in ENC1s as early as stage E18. ENC1s of stage E15 embryos did not appear to fluoresce after 5,7-DHT treatment, regardless of treatment duration. Thus, the expression of a 5,7-DHT, and presumably also a 5-HT-uptake system at stage E18 occurred later in the development of ENC1 than the appearance of serotonin-immunoreactivity. To directly compare the developmental schedule of 5,7-DHT uptake and serotonin expression, egg masses containing stage E10 to E30 embryos were bisected; half egg masses were treated with 5,7-DHT and, upon completion of 5,7-DHT treatment, sibling embryos from the other half egg masses were isolated, fixed and processed for serotonin immunohistochemistry. Whereas 80-100% of sibling embryos at stages E15 to E30 possessed ENC1s with serotonin-immunoreactivity, none of the sibling stage E15 embryos displayed 5,7-DHT fluorescence (Figure 8; n = 18 stage E15 embryos). Only about 5% of the sibling stage E20 embryos treated with 5,7-DHT had fluorescently labeled ENC1s (n = 20 embryos), whereas 81% of stage E25 embryos possessed 5,7-DHT fluorescence. Thus, the consistency with which 5,7-DHT staining could be observed was

greater in later staged embryos. The differences in proportions of ENC1s with serotonin-immunostaining versus 5,7-DHT staining were statistically significant ($p=0.0001$, Chi-Square test).

vi) Morphology of ENC1 soma and apical dendrite

The characteristic morphology of ENC1 was evident even in embryos viewed under 20X DIC optics. To best illustrate the finer details of ENC1 morphology, 100X DIC optics were used. ENC1 was typically 13.2 ± 0.6 µm ($n = 10$) along the axis of the EPN at stage E13 to E15 and 15.0 ± 0.6 µm ($n = 5$) at stage E25 to E30. Thus, there was no significant change in the size of ENC1 somata during initial development (Student's t-test; $p > 0.05$). The primary distinguishing feature of ENC1 was a large, spherical nucleus that occupied a significant proportion of the soma. The nucleus was distinct in that it invariably contained a prominent, centrally-situated nucleolus (Figure 9A). Also characteristic were numerous large granules located in the apical cytoplasm. Given that these granules share a similar intracellular distribution as the serotonin-immunoreactive profiles observed in ENC1 somata in immunostained embryos (see Figure 2A), these granules may contain serotonin. The proximal EPN segment extending from the basal pole of the ENC1 soma was thickened relative to the EPN segment distal to the first anteromedial turn (see Figure 3A). Microtubules with attached, motile granules of various sizes were also visible in the proximal EPN segment (Figure 9A).

Consistent with the immunohistochemical observations, ENC1 possessed an apical dendrite. High magnification DIC examination revealed that this process terminated with an unique structure protruding above the ectodermal surface (Figure 9A and B). This surface structure was composed of projections resembling immotile cilia. The cilia were arrayed on a hemispherical base that was slightly less than 5 µm in diameter. Both ENC1 homologues developed this surface structure between stages E14 to E15, and retained it as late as stage

E100 (hatching). 5,7-DHT staining of stage P1 juvenile snails (P refers to a postembryonic juvenile snail; the number refers to the vertical shell diameter in mm; Goldberg and Kater, 1989) also revealed ENC1s with the apical dendrite and surface structure. In keeping with the asymmetrical developmental profile of the two homologous ENC1s, the right ENC1 developed the structure prior to its left homologue. At the SEM level, the structure's dense array of radially projecting cilia-like extensions was more apparent (Figure 9C). Furthermore, there appeared to be two different size classes of projections, one slightly greater than 1 μm and the other about 3 μm. In later embryonic stages, the apical dendrite lengthened to accommodate the inward migration of ENC1 that occurred during enlargement of the head region (Figure not shown). The morphology of the surface structure and its position on the anterodorsal aspect of the snail's head suggests that it may serve a sensory function during embryonic or post-embryonic development, a hypothesis that will be elaborated upon in the discussion.

vii) Identification and development of pedal ciliated target cells

The development of EPNs around the pedal ciliary band involved a stereotyped pattern of primary neurite extension and elaboration of neuritic branches. Initial observations of EPN branch patterns in the target cell region suggested that there may be a relationship between target cell development and the extension of EPN backbranches. Thus, an outline of the initial development of the pedal ciliary band will be presented in regard to the identification of individual ciliated target cells.

Ciliated target cells of ENC1 were identified *in vivo* in stage E15 to E30 embryos by virtue of their surface location and possession of motile cilia (Figure 10). Although the ciliary band is continuous in appearance, individual ciliated cells were distinguished by their large, clear nuclei and motile cilia on the apical membrane when viewed through 100X DIC optics. Pedal ciliated cells were designated using an alphanumerical naming scheme. For a ciliated cell called PeA1, for example, "Pe" specifies the location of the ciliated cell

(pedal band); "A" specifies the cell most dorsal in the band ("B" would be the cell ventral to cell "A", and so forth); the number "1" designates the cell as being the presumed right homologue of a bilateral ciliated cell pair ("2" would refer to the left homologue). Unpaired ciliated cells occupying a medial position in the embryo have no numerical designation (ie: PeA). Figure 10B and C illustrate the distribution of cells at stage E25. At this stage, there is one medially-situated ciliated epithelial cell ventral to the stomodaeum that was identified as cell PeA. Ventral to cell PeA was a bilateral pair of oblong cells identified as cell PeB1 and PeB2. A second bilateral pair of cells were observed directly ventral to and in contact with the PeB1/PeB2 cell pair. This second pair of ciliated cells was identified as PeC1 and PeC2. Also visible was a single medial ciliated cell directly ventral to and in contact with the PeC1/PeC2 cell pair. This posterior medial cell will be identified as cell PeD (Figure 10C).

The developmental pattern of the identified pedal ciliary cells is schematically illustrated in Figure 11 and appears to follow an anterodorsal to posteroventral sequence of differentiation. At stage E15, the core group of six cells PeA, PeB1, PeB2, PeC1, PeC2 and PeD were visible (n = 27 embryos) under both Nomarski optics and CLSM, with cell PeA being the largest and only cell with cilia. The other cells could be identified based on their locations with respect to cell PeA, and their prominent nuclei and nucleoli. The PeB and PeC cell pairs, and the medial PeD cell then increased in size relative to cell PeA and elaborated cilia by stage E20. At stage E15, these cell pairs may be undifferentiated stem cells which, by stage E20, differentiate to complete the core group of six ciliated epithelial cells by stage E25. By stage E30, additional ciliated cells were recruited into the pedal ciliary band. Single medial ciliated cells differentiated in an anterior to posterior sequence, beginning with cell PeE at stage E30 (n = 16 embryos), followed by cell PeF at stage E35 (n = 8 embryos). Between stages E25 and E30, the primordial foot extended along the anterior-posterior axis. During this time, the PeA cell more than doubled in size and the PeB cells shifted to a position more ventrolateral to cell PeA. Also at stage E30, a bilateral

pair of cells appeared at the level of the boundary between the PeB and PeC cell pairs (see Figure 1D). These are the first cells in an anterior to posterior series which eventually covers the remainder of the foot with cilia. These cells were identified as PeLA1 and PeLA2, the first cells of the lateral component of the pedal ciliary band, hence the "L" designation.

By identifying ciliated target cells of ENC1 and characterizing their developmental pattern, we could next examine the development of EPNs in association with these target cells.

viii) Developmental branching of EPNs: role of target cell differentiation

EPNs displayed a stereotyped pattern of neuritic branching over the pedal ciliated target cells. From stage E15 to E30, neurite branches were consistently absent along the length of the EPNs up until the margin of the pedal ciliary band. The restriction of branching outgrowth to the vicinity of pedal ciliated cells prompted an examination of the development of the EPN outgrowth pattern in relation to the developmental pattern of ciliated target cell differentiation, described in the previous section. The EPN outgrowth pattern consisted of four distinct features: 1. The unbranched outgrowth of EPNs along the lateral margins of the pedal ciliated cells, 2. Primary back-branching between the EPN homologues, 3. The elaboration of secondary neuritic branches from EPN back-branches, and 4. Fasciculation of EPNs in the distal outgrowth pathway. We sought to determine if these events may be associated with developmental changes in the pedal ciliary band.

The intimate association between EPNs and pedal ciliated cells was resolved *in vivo* using 100X DIC microscopy. ENC1s were identified and the course of their EPNs followed uninterrupted to the pedal ciliary band. Figure 12A illustrates the EPN of the right ENC1 in lateral profile at the level of the PeC1 cell. Back-branches extending from the EPN toward the ciliated cell are apparent. When the ciliary band was viewed from an

anterior perspective, EPNs and their neurite branches were clearly visible when the focal plane was adjusted to the basal membrane of pedal ciliated cells (Figure 12B). The resemblance of the outgrowth pattern of these processes with that of immunostained EPNs *in situ* (refer to Figure 13 following) and the continuity of these processes with ENC1 somata confirmed their identity as EPNs.

a) Unbranched EPN outgrowth

As outlined in the section on EPN interaction with putative guidance cells, the left and right EPN growth cones initially made contact at stage E15 at the level of the first ciliated epithelial cell identified as cell PeA. The contact of EPNs produced a Y-shaped outgrowth pattern when viewed in anterior profile. Figure 13 shows the development of the neurite outgrowth pattern from stage E15 to stage E30. During this time, the EPNs appear to be displaced laterally from the midline. With the greater separation between EPNs, back-branching could occur between them. Given that the number of ciliated epithelial cells did not change from stage E15 to E25, the increased size of the ciliated cells may account for the separation of EPNs. The EPNs were consistently confined to the lateral margins of the pedal ciliary band and, in cross section under CLSM, EPNs appeared adjoined to the boundary between the very thin pedal ciliated cells and the relatively thick ectodermal cells of the foot primordium (Figure 16B). This association of EPN neurites with the pedal ciliated cells and the foot ectodermal cells could be followed along their length as one progressed through a confocal section series.

b) Back-branching of EPNs

Given that neurite branches are clearly resolved under both conventional epifluorescence and CLSM (Diefenbach *et al.*, 1995), the developmental increase in both back-branching (referred to as primary branch point number) and total neurite branching (total branch point number) were quantified under conventional epifluorescence. This

comparison was made to determine if the extension of neurite branches can be correlated with changes associated with the development of the pedal ciliated cells. To quantify neurite branching, branch points were counted as the number of bifurcations along the full extent of both EPNs from the basal membrane of the ENC1 somata to the terminal growth cones. Since the immunostaining intensity of the EPN homologues was similar during this period of development, we could not reliably determine from which EPN a given neurite originated, necessitating that branch point counts from the left and right EPNs be summed. At stage E15, there were usually zero and occasionally two back-branches extending between EPNs (0.4 ± 0.2 primary branch points; n = 46 embryos; Figure 13A). However, no secondary branching was observed. Thus, at stage E15, the number of primary branch points equaled the total number of branch points (Figure 14A and B). Given that the first identified ciliated epithelial cell, cell PeA, was differentiated at stage E15 (Figure 1A), the initiation of back-branching may depend on the presence of cell PeA.

By stage E20, primary branch point number increased to 3.4 ± 0.5 (n = 48 embryos; Figure 14B). This increase was accompanied by significant secondary, tertiary, etc., branching (Figure 13), resulting in a dramatic increase in the total number of EPN branch points from 0.4 ± 0.2 at stage E15 to 12.4 ± 1.3 at stage E20 (n = 31 embryos; $p<0.0001$; Figure 14A). Thus, between stage E15 and E20, non-primary branching began. This initial elaboration of neuritic branches coincided with the differentiation of the PeB and PeC cell pairs, in addition to the first posteromedial pedal cell, cell PeD.

By stage E25 (Figure 13C), primary branch point number increased to 11.9 ± 0.9 (n = 50 embryos) and total branch point number to 22.2 ± 1.1 (n = 54 embryos; Figure 14A). However, as described previously, there was no change in the number of pedal ciliated cells from stage E20 to E25. Thus, the greatest increase in primary branching occurred between stage E20 and E25, during which there was no change in ciliated cell number and no obvious changes in ciliated cell morphology. By stage E30, primary branch point number increased to 18.7 ± 1.2 (n = 40 embryos) and total branch point number

increased to 38.2 ± 2.0 (n = 50 embryos). The neurite branch pattern underwent some anteroposterior extension by stage E30, which paralleled the enlargement of cell PeA and posterior displacement of the PeB and PeC cell pairs (see Figure 11).

In contrast to the medially-directed branches, a single branch with a small club shaped growth cone extended laterally from each EPN at the level of cell PeA between stages E25 and E30. These lateral branches displayed secondary branching in a circular arrangement between stage E30 (Figure 13D) and E35. These identified branches each extended to one of a bilateral pair of ciliated epithelial cells, which differentiated lateral to the pedal ciliary band by stage E35, long after the branches had entered their vicinity. These lateral branches will be referred to as LBR (lateral branch of the right EPN) and LBL, and extend to the identified lateral ciliated cells PeLA1 and PeLA2, respectively.

c) Fasciculation of EPNs

After EPNs contacted each other at the midline of the pedal ciliary band at stage E15, the EPNs appeared to fasciculate. This fasciculation occurred at the level of the second medial pedal cell, cell PeD. By focusing (or scanning, in the case of CLSM) beneath the apical membrane of ciliated cells, club-shaped growth cones were observed along the margin of cell PeD at stage E20 and appeared to extend posteriorly, using cell PeD as a substrate (Figure 15). The EPN growth cones did not extend beyond the large ectodermal cells of the posterior pedal furrow and appeared to terminate outgrowth in contact with these pedal ectodermal cells, which displayed serotonin immunostaining from stage E25 onward (Figure 16A). Fasciculated EPNs were distinguishable by their growth cones, which remained separated at the terminal extent of the outgrowth pathway. Separations in the contacts of the EPN neurites behind the growth cone pair were observed on occasion, and preclude the interpretation that the two growth cones originated from the bifurcation or splitting of a single neurite.

Collectively, these results suggest that the exclusive localization of EPNs and EPN branches to the developing pedal region results from direct interaction of EPN neurites with differentiating pedal ciliated target cells. Furthermore, the spatially coincident arrangement of pedal target cells and fasciculating EPNs suggests that fasciculation of EPNs is promoted by a subpopulation of pedal ciliated cells that differentiate as medial unpaired cells.

ix) Later development of ENC1

a) ENC1 is present throughout embryogenesis

ENC1 was originally observed by Goldberg and Kater (1989) on the basis of its serotonin immunoreactivity and proximity to the developing cerebral ganglia. It was proposed to be the embryonic homologue of the adult neuron C1, a known regulator of adult feeding behavior (Kater, 1974). However, analysis of later development of ENC1 in this study strongly suggests that ENC1 is distinct from the adult C1 neuron. ENC1s of stage E35 to E100 embryos were identified via 5,7-DHT staining. ENC1's position in the embryo relative to other tissues was then determined using DIC optics. DIC observation revealed that, by stage E100, ENC1s were situated immediately anterodorsal and in contact with the cerebral ganglia, and occupied a deeper position beneath the epidermis. In spite of the insinking of ENC1 beneath the epidermis, the apical dendrite with surface structure was retained up to stage E100. The EPN pathway could be followed posteroventrally into the cerebral ganglion and medially toward the cerebral commissure. Figure 17 shows ENC1 in a stage E80 embryo with its EPN visible. Noteworthy are large granules similar to the serotonin-immunostained granules observed in earlier staged embryos. The gross morphology of the ENC1 soma was also reminiscent of ENC1s in earlier staged embryos with a large spherical nucleus with central nucleolus and numerous cytoplasmic granules concentrated at the apical pole of the cell soma.

b) ENC1 as potential pioneer neuron

In the course of following the development of ENC1 at later stages, it became apparent that other neurons which expressed serotonin subsequent to ENC1 appeared to be directed toward and shared the outgrowth pathway of ENC1. Figure 18A shows a confocal reconstruction of a stage E40 embryo with serotonin-immunostained ENC1 in left lateral profile. At this stage, two neurons in the pedal ganglia expressed serotonin and appeared to extend neurites ventrally toward EPNs in the base of the foot primordium. These two neurons will be referred to as ENP1 (embryonic neuron 1 of the pedal ganglia) and ENP2. Serotonergic neurons in the pedal ganglia also extended neurites up to the proximal segment of the EPN at the base of ENC1 along a pathway which becomes part of the cerebropedal commissure. This pathway is illustrated in Figure 18B in a stage E60 embryo. Also visible at this stage is the first cerebral ganglion neuron to express serotonin which will be referred to as ENC2. By stage E65 (Figure 18C) the left ENC1 had lost most of its serotonin immunostaining, whereas serotonin-immunostained neurites from the pedal ganglion neurons were retained (see also section ix-c following). Thus, neurite outgrowth pathways first established by ENC1 may subsequently be shared with neurites of other serotonergic neurons which differentiate subsequent to ENC1. ENC1 may thus serve to pioneer these routes for neurites which extend later in development.

c) ENC1 expresses serotonin transiently

Surprisingly, examination of serotonin-immunostained embryos revealed that ENC1s lose their serotonin-immunoreactivity between stages E60 and E70. Figure 19 shows confocal reconstructions of stage E60, E65 and E70 embyros. At stage E60 (Figure 19A), ENC1s can be seen anterior to a prominent pair of serotonin-immunostained neurons in the cerebral ganglia. Note that the immunostaining intensity of ENC1s approximates that of the cerebral ganglion neurons. By stage E65 (Figure 19B), the right ENC1 appears

unchanged, whereas the left ENC1 has lost virtually all of its serotonin immunoreactivity. Thus, asymmetry between development of the ENC1 homologues was evident even in regard to the loss of serotonin-immunoreactivity; the right ENC1 homologue retained immunostaining longer than the left homologue. By stage E70 (Figure 19C), both ENC1s have an intensity of immunostaining which is indistinguishable from background. This apparent loss of serotonin expression was not a result of cell death, since 5,7-DHT-stained ENC1s were resolved throughout embryogenesis. These results show that, although ENC1 is present throughout embryogenesis and retains a 5,7-DHT uptake capacity and normal morphology, the expression of serotonin in ENC1 appears to be a transient developmental event.

Figure 2: Initial expression of serotonin. **A**. Epifluorescence micrograph of a left anterolateral profile of a stage E13 embryo with serotonin immunofluorescent granules and no apparent serotonin immunostaining in the EPN. (s): stomodaeum; arrowhead: apical pole of ENC1. The fluorescence in the bottom right quarter of the embryo is a more intense region of nonspecific background fluorescence enhanced in the photographic process. **B.** Anterior profile of stage E14 embryo with the right EPN growth cone proceeding over the pedal ciliary band (faintly immunofluorescent Y-shaped profile; asterisk) ahead of the left EPN growth cone, which has just contacted the left margin of the band. Note the slightly greater intensity of serotonin immunostaining in the right ENC1 compared to the left. In addition, growth cones show stronger staining than the neurites. A transient dorsomedial neurite with a club-shaped growth cone can be seen extending from the right ENC1 (arrowhead). A prototrochal ciliated cell with punctate serotonin-immunostaining can be seen lateral to the left ENC1. s: stomodaeum; arrow: apical dendrite. Scale bar = 10 μm.

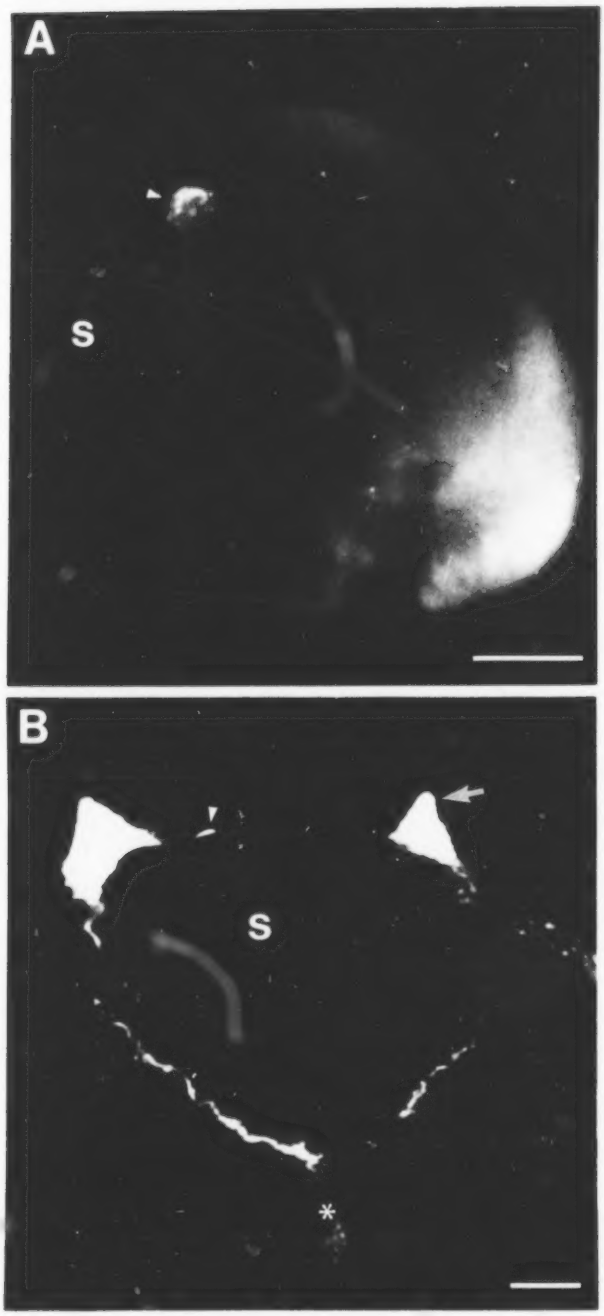
A
S
B
S
*

Figure 3: EPN contact of G1 cells. **A.** Confocal reconstruction of ENC1 in right lateral profile showing the anteromedial turn of the EPN toward the pedal region (stage E30). A faintly immunofluorescent GR1 cell can be seen at the outside angle of the turn (boundaries of cell indicated by arrowheads). **B.** Composite image of conventional epifluorescence micrograph of serotonin-immunostained left ENC1 (stage E30) with corresponding DIC micrograph. The anteromedial deviation of the serotonin-immunoreactive EPN proceeds in a circular arc, subtending an angle of approximately 90^{o} around the DIC profile of the GR1 cell (boundaries indicated with arrowheads). **C.** High magnification DIC micrograph of GR1 cell contacting EPN (arrowheads) with lamellipodia-like extensions. **D.** Complimentary schematic outline of the GR1 cell of panel C. At stage E30 to E35, this cell undergoes cell division. The irregular profile in each dividing half appears to be the segregating chromatids. The fate of these cells has not been followed beyond stage E35. Scale bar = 10 μm (A and B) and 5 μm (C and D).

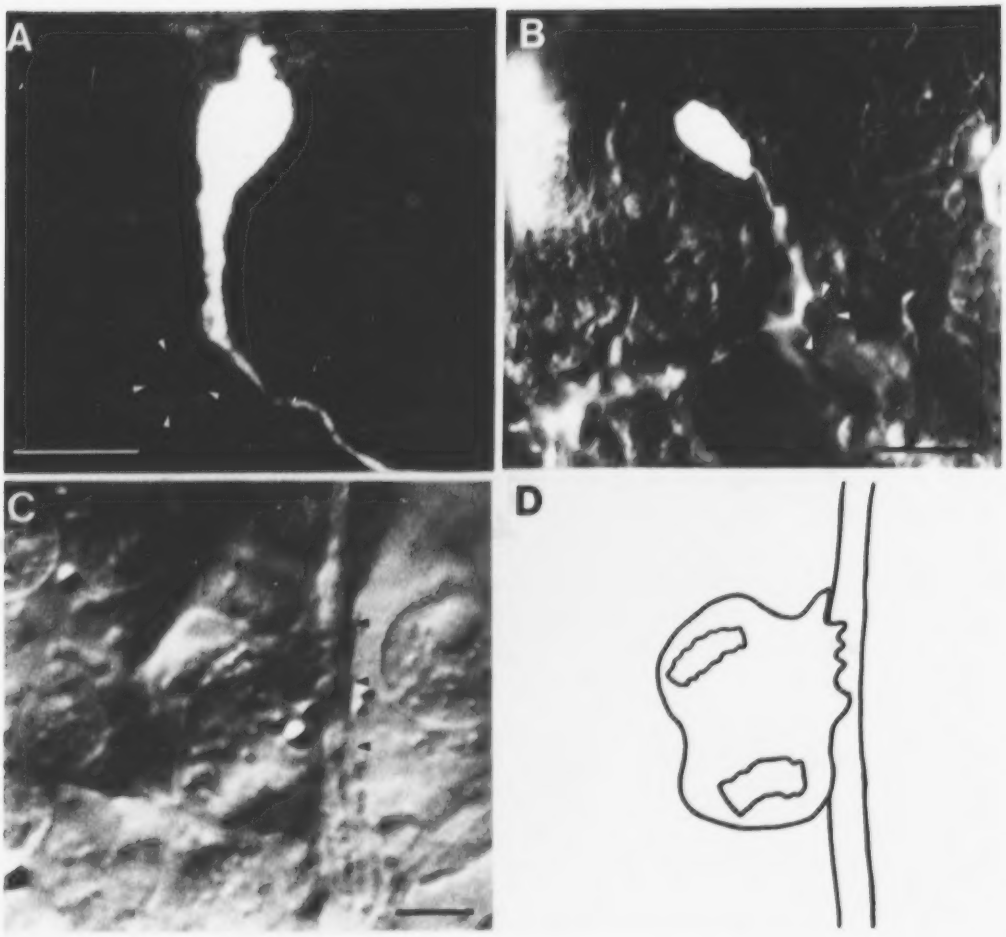
A
B
C
D

Figure 4: G-cells in pedal region. Conventional epifluorescence micrographs (A and C). **A.** Stage E14 to E15 embryo showing EPNs interacting with a collection of five G-cells in a Y-shaped pattern. Bright diffuse staining dorsolateral to the stomodaeum is the serotonin-immunostained ENC1s. **B.** Complimentary schematic of panel A showing the quintet of G-cells: the GR2 and GL2 pair, GR3 and GL3 pair, and the medial unpaired Gm cell. EPN growth cones intersect G-cells on approach to the midline, where the homologous EPNs conjoin and fasciculate. The right EPN has passed GR2 and GR3 and is proceeding to the medial Gm cell. The left EPN has passed the GL2 cell and executed a 60 degree ventromedial turn toward the GL3 cell. The right EPN preceded the left EPN in all embryos examined. (e): left serotonin-immunostained ENC1 out of the focal plane. **C.** pCPA-treated stage E15 embryo with the EPNs having completed their passage to the end of the outgrowth pathway. pCPA treatment permitted resolution of G-cells in the pedal region by virtue of their serotonin immunostaining. A tissue fracture occurred in the ventral region during the immunostaining protocol. **D.** Schematic tracing of panel C showing the identified putative guidance cells. (e): left serotonin-immunostained ENC1 out of the focal plane. Scale bar = 10 μm (A and C).

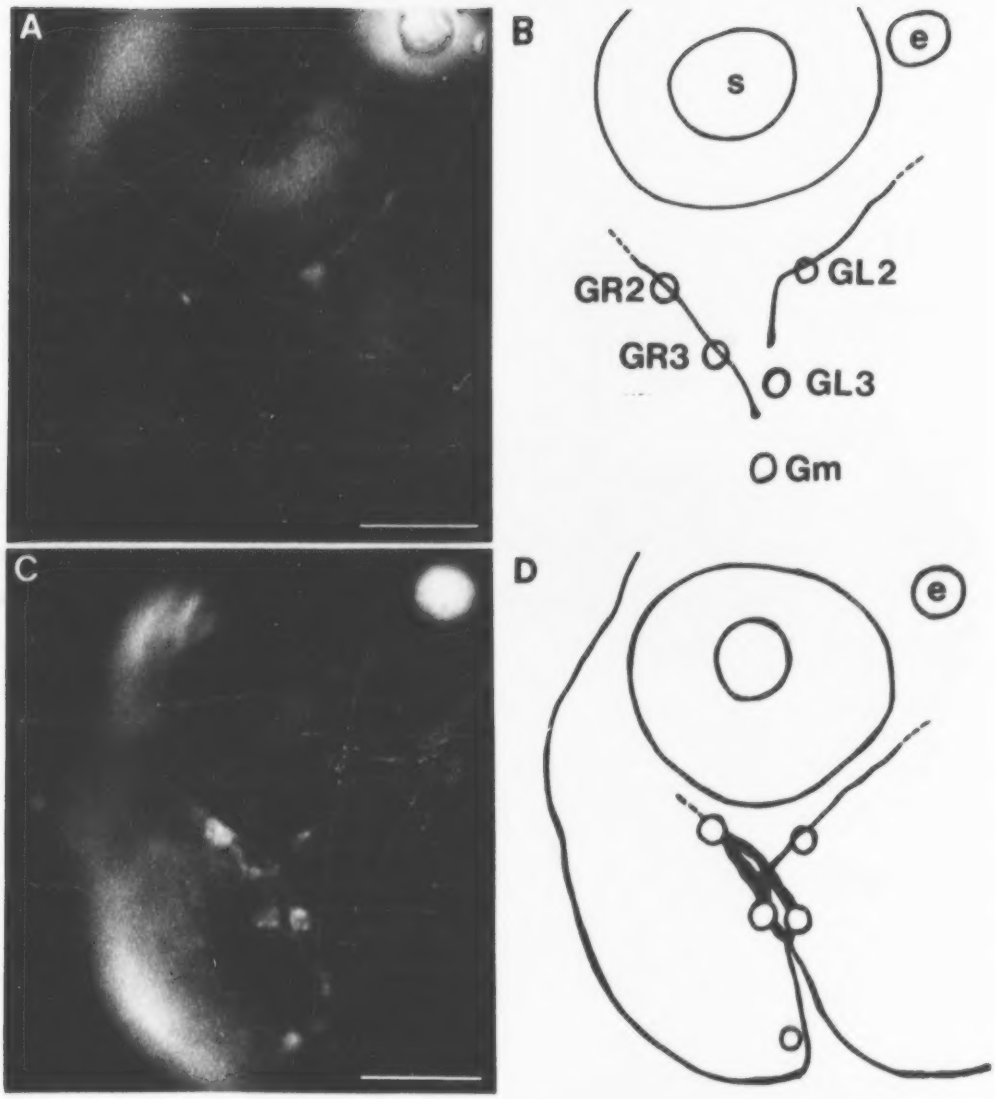
A
B
s
e
GR2
GL2
GR3
GL3
Gm
C
D
e

Figure 5: EPN growth cone contact of G3 cells. **A.** Stage E14 embryo with right EPN growth cone transiting between the GR3 and GL3 cells. The left EPN growth cone is just contacting the pedal band margin. Note the higher intensity of serotonin immunostaining in the right EPN with respect to the left, and the high level of immunostaining in the right EPN growth cone. This confocal reconstruction was not rotated to preserve resolution of the growth cone. **B.** EPN growth cone with two filopodia extending around the GL3 cell. **C.** Schematic of panel B showing the EPN growth cone passing between both G3 cells at the midline. Dotted outline shows the extent of the pedal ciliary band, which can be distinguished by its slightly higher level of background fluorescence. Scale bar = 20 μm (A); 10 μm (B and C).

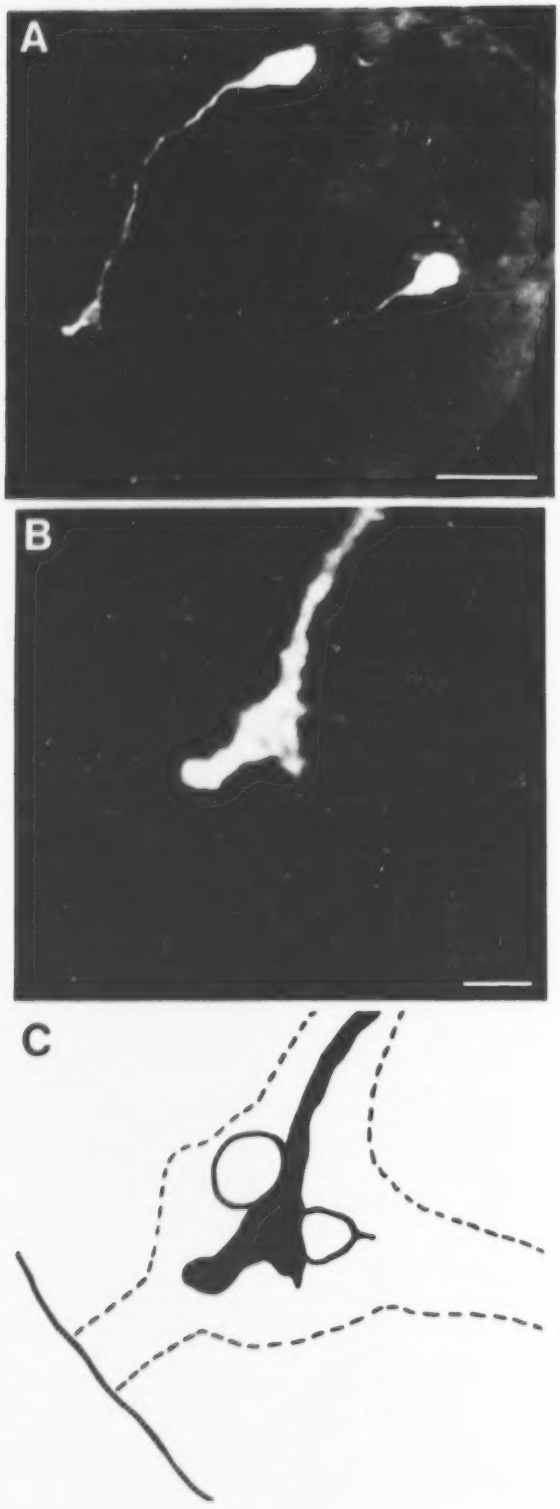
A
B
C

Figure 6: Progression of EPN outgrowth over the pedal region from stages E13 to E15. Confocal reconstruction micrographs. **A.** EPN growth cones reached the pedal region and intercepted the G2 cells at stage E13 (reconstruction from Fig. 2B). **B.** EPN growth cones execute an anteromedial turn toward the G3 cells (reconstruction from Fig. 5A). **C.** Left EPN makes contact with right EPN at the midline at the level of the paired G3 cells at stage E14. Note the higher intensity of serotonin immunostaining in the left EPN growth cone in comparison to panel B. **D.** Around stage E15, left and right EPNs conjoin and fasciculate as they proceed posteroventrally toward the posterior pedal furrow. Scale bar = 10 μm (A, B, C, and D).

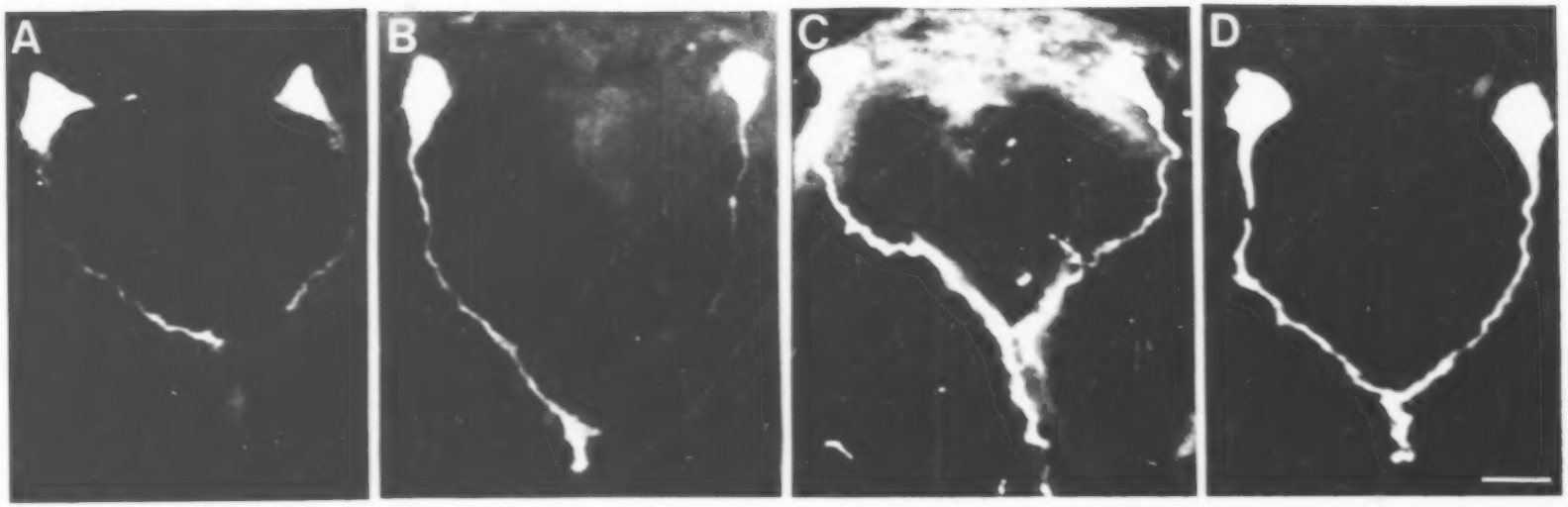
A
B
C
D

Figure 7: Identification of ENC1 *in vivo*. **A.** Conventional epifluorescence micrograph of stage E25 embryo in right lateral profile after treatment with 5,7-DHT. 5,7-DHT fluorescence was observed in ENC1 (arrowhead) in addition to a subset of the yolk cells (asterisk indicates one yolk cell); the remaining yolk cells were dimly autofluorescent. The bright spot to the right of ENC1 is a particle of fluorescent debris. **B.** Matching DIC micrograph of stage E25 embryo from panel A. ENC1 (arrowhead) was located dorsolateral to the stomodaeum (s). **C.** Same embryo as A and B. The distinct morphology of ENC1 (arrowhead) permitted consistent identification using DIC optics, without a need for 5,7-DHT staining. Scale bar = 50 μm (A and B); 10 μm (C).

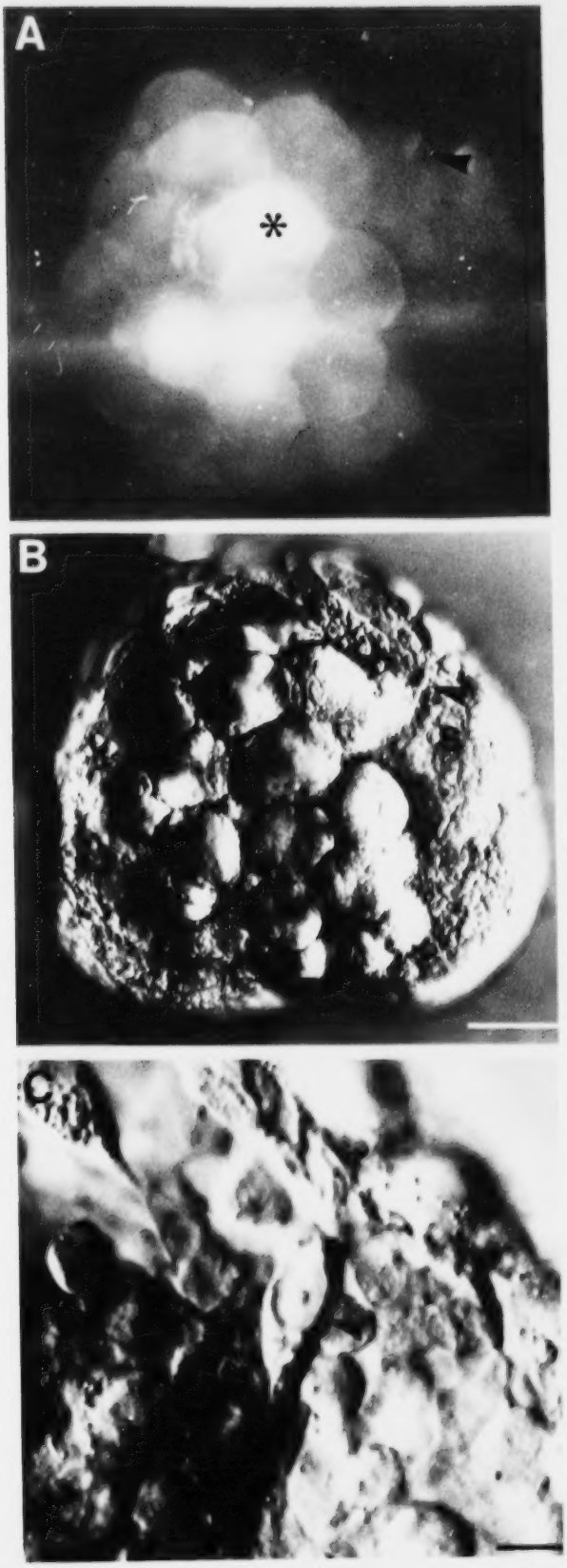
A
*
B
C

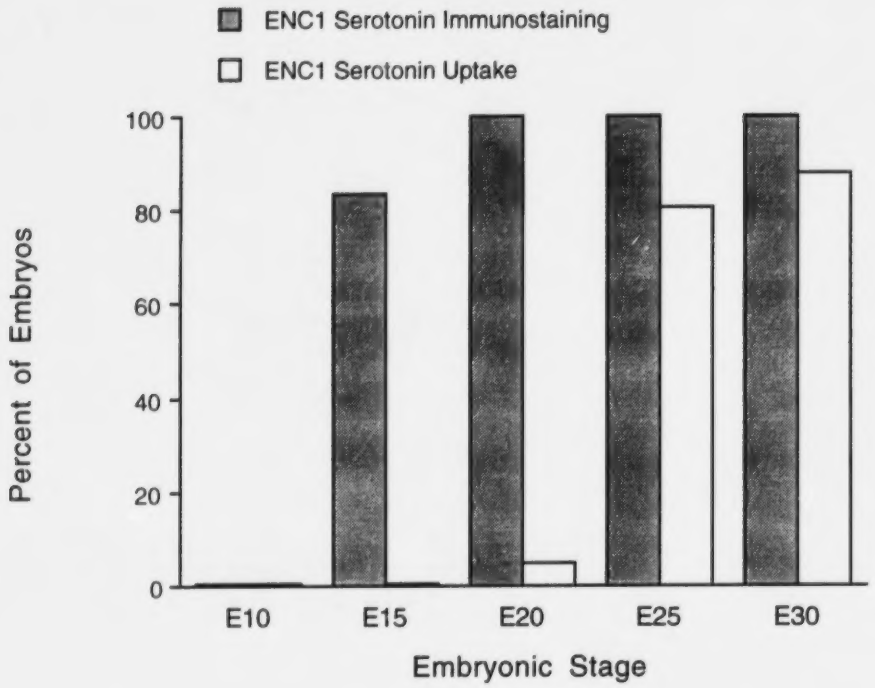

Figure 8: Prevalence of serotonin immunoreactivity and serotonin-like uptake expression as a function of developmental stage. ENC1s expressed serotonin between stages E10 and E15, whereas serotonin-like uptake capacity, as evidenced through 5,7-DHT uptake-induced fluorescence, was initially evident at around stage E20. Number of embryos are shown as follows: stage: serotonin column/5,7-DHT column. E10: 46/197; E15: 12/18 ; E20: 11/20 ; E25: 21/31 ; E30: 55/67 .

Figure 9: Morphology of ENC1 soma *in vivo*. **A.** ENC1 as seen in left lateral profile under high magnification DIC optics in a stage E25 embryo. ENC1 could be readily identified *in vivo* on account of distinguishing morphological features, including a large nucleus with central, prominent nucleolus, numerous granules concentrated in the apical cytoplasm (asterisk), a thickened proximal neurite (arrowhead) and apical dendrite (out of the plane of focus) with surface structure (arrow). **B.** High power DIC micrograph of the ectodermal surface showing the surface structure of ENC1 with its hemispherical base studded with an array of immotile cilia-like projections (arrow). **C.** Scanning electron micrograph of the surface structure with at least two size classes of cilia-like projections (about 1 and 3 μm). The large object to the right of the cilia is a particle of debris. Scale bar = 8 μm (A), 5 μm (B) and 2 μm (C).

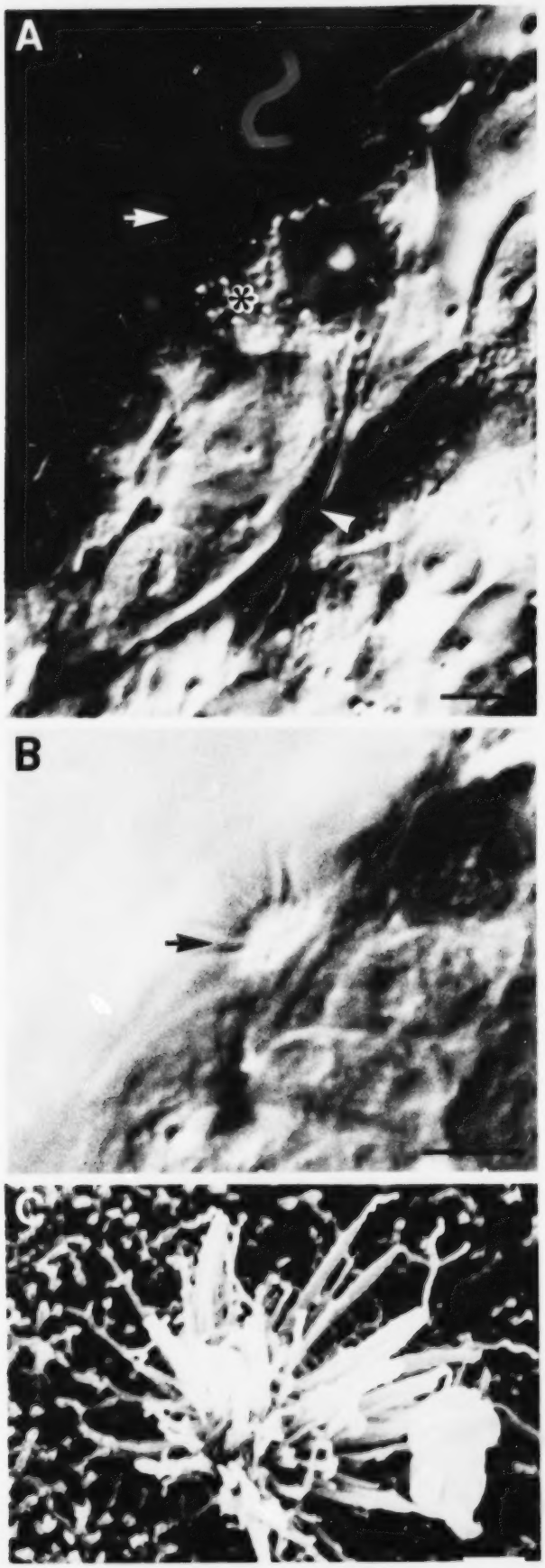
A
B

Figure 10: Identification of pedal ciliated epithelial cells *in vivo*. **A.** DIC micrograph of the pedal ciliary band of a stage E25 embryo in ventral profile with the focal plane at the level of the cilia. Arrows indicate locations of slightly out of focus nucleoli of the individual pedal ciliated cells **B.** Complimentary DIC image of the same pedal ciliary band as in panel A with the focal plane passing through the nuclei and nucleoli (arrows) of the individual ciliated cells. This image was obtained by excessive compression of the embryo so that cells from interior tissues are also visible. Scale bar = 10 μm (A and B). **C.** Schematic of panel B showing the nuclei and nucleoli of cells PeA, PeB1 and PeB2, PeC1 and PeC2. Although the medial cell PeD is not visible in the focal plane of panel B, its nucleus is represented as if one would focus posteriorly through the ciliary band. Although the outlines of the ciliated cell somata were frequently distinguishable, the outlines of the ciliated cell membranes were not completely visible and are partially inferred from observations of other pedal ciliary bands (dashed lines).

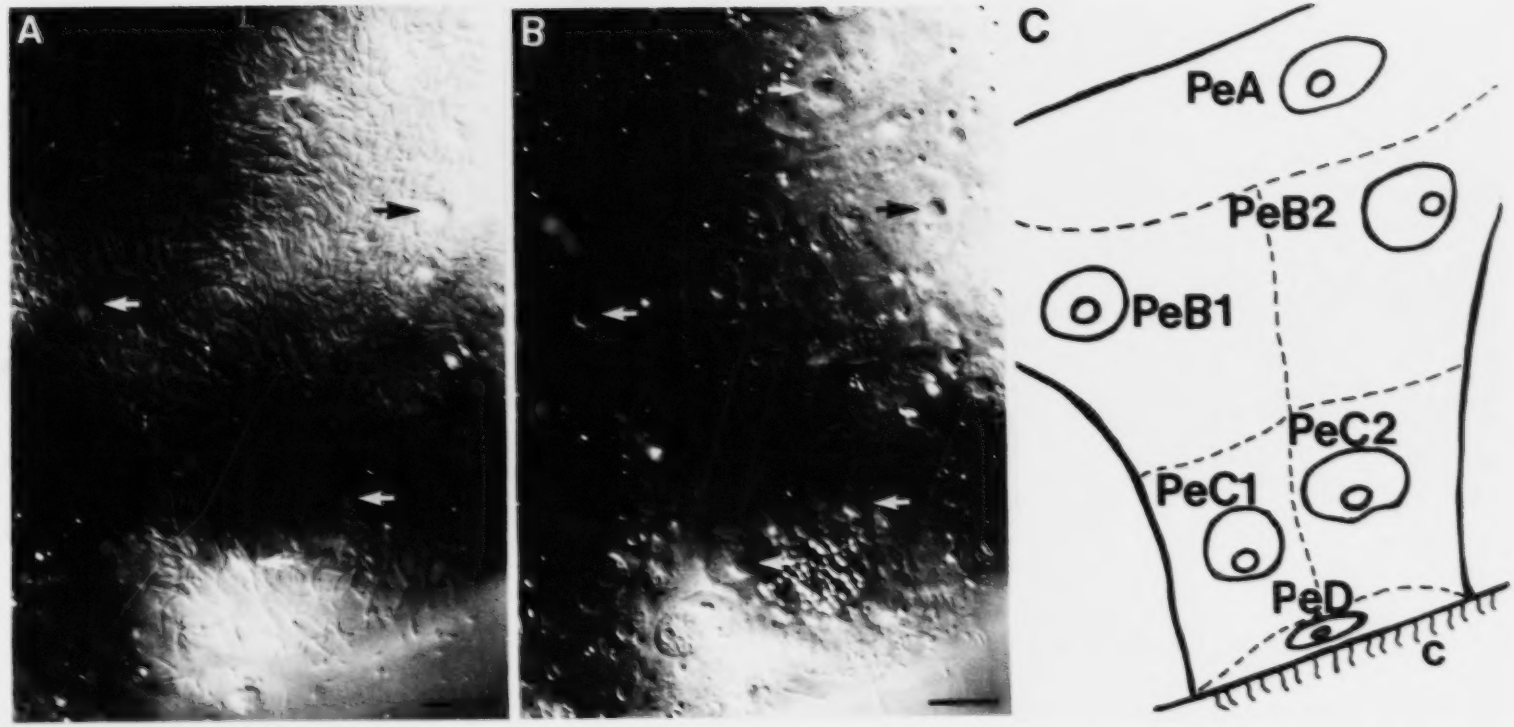
A
B
C
PeA
PeB2
PeB1
PeC2
PeC1
PeD
C

Figure 11. Schematic illustrating the initial development of the pedal ciliary band from stage E15 to E35. At stage E15, only cell PeA is ciliated. The other cells are visible at this stage using Nomarski and confocal microscopy, but have not elaborated cilia (shaded in grey). By stage E20, all the cells in the band are ciliated. Stage E30 marks the addition of a second medial cell, cell PeE, in addition to a pair of cells lateral to the pedal band, PeLA1 and PeLA2, which form the pedal ciliary band of the adult. Note also that, by stage E30, cell PeA increases in size, with the PeB and PeC cell pairs being displaced more ventral to cell PeA.

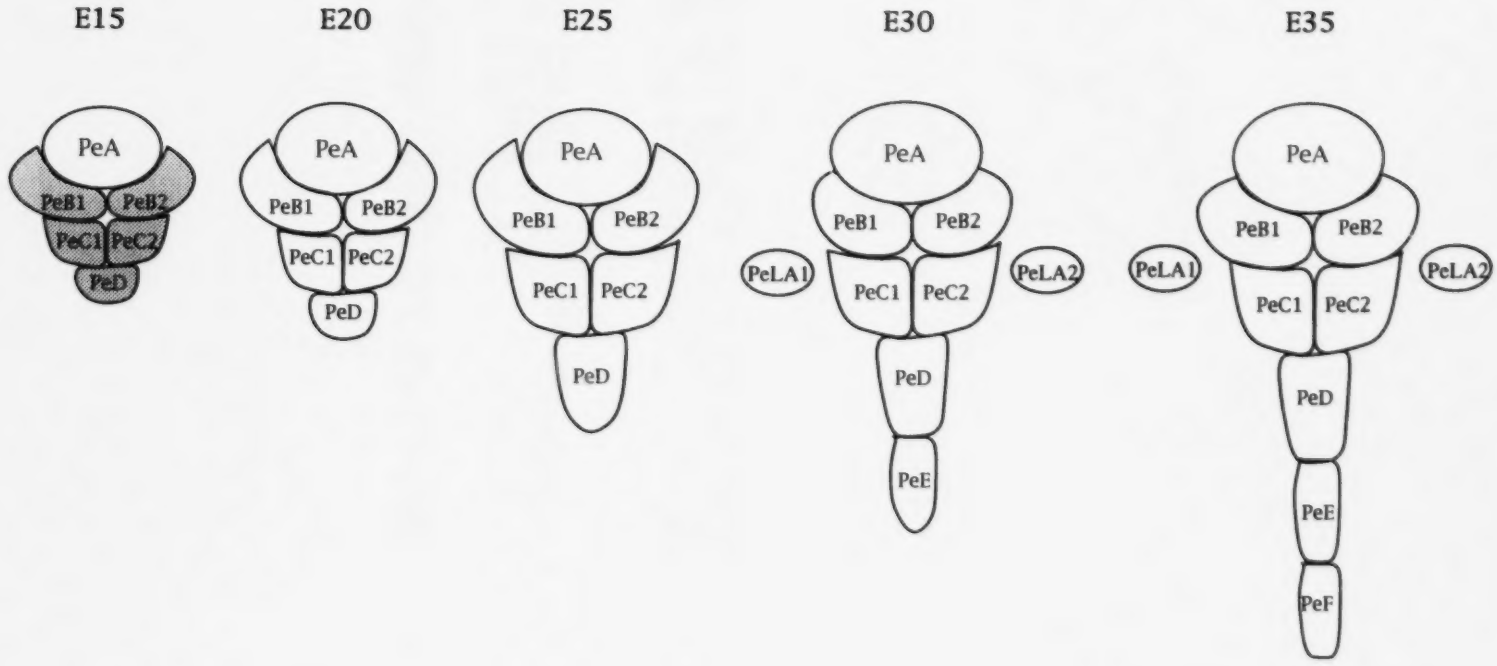
E15
E20
E25
E30
E35
PeA
PeB1
PeB2
PeC1
PeC2
PeD
PeLA1
PeLA2
PeE
PeF

Figure 12: EPNs associate with pedal ciliated cells *in vivo*. **A.** DIC micrograph of living stage E25 embryo in left lateral profile at the level of cell PeC2, identifiable by its large nucleus (n) and numerous cilia (c). The large arrowhead points to the nucleolus of cell PeC2. The EPN is located on the lateral margin of cell PeC2 (p) and extends branches over the basal membrane of the ciliated cell (small arrowheads). **B.** DIC micrograph of living stage E25 embryo in anteroventral profile at the same level as panel A. Visible are the nucleoli (arrowheads) of cell PeC1 (1) and PeC2 (2), which are out of the focal plane, in addition to the nucleolus of the medial cell PeD (D), which is in focus. Neurite branches (small arrowheads) extending from the EPNs (p) are visible at the focal plane of the basal membrane of the pedal ciliated cells. Thus, EPNs are identifiable along the entire length of the outgrowth pathway *in vivo*. Scale bar = 5 μm (A and B).

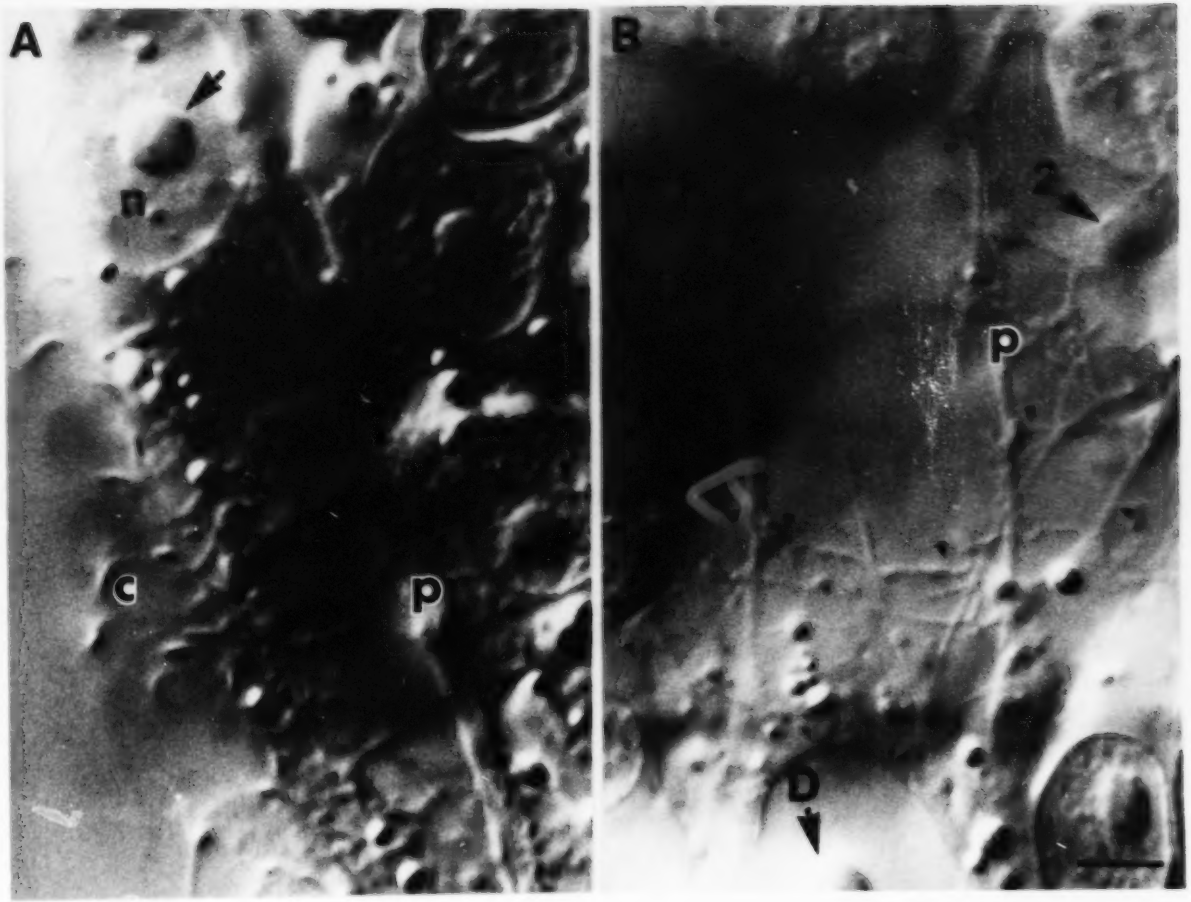
A
n
C
P
B
P
D

Figure 13: Development of EPN outgrowth pathway. Confocal reconstructions of serotonin-immunostained embryos at stage E15 (A), E20 (B), E25 (C), and E30 (D). **A.** The Y-shaped outgrowth pattern is established by stage E15. The break in the right EPN resulted from fracture of the embryo during processing. **B.** Neurite back-branching is initiated between stage E15 and E20. **C.** In this stage E25 embryo, one can see further extension of neurite branches towards a faintly-immunostained ciliated cell PeA (a). Specific transitions in outgrowth are also apparent: unbranched outgrowth toward the pedal band (note the omega-shaped deviation in the pathway of the left EPN at the location of a presumed cell GL1 at the arrowhead), target-localized branching outgrowth, and fasciculation along the medial ciliated cells (arrow). Note the prominent apical dendrite with surface structure (asterisk), and an identified lateral branch, LBL (b), has extended from the left EPN toward the location of the future ciliated pedal cell, PeLA2. **D.** At stage E30, the EPN branching pattern elongates in conjunction with the elongation of the pedal ciliary band. Note again the prominent apical dendrite of the right ENC1 (asterisk). The identified right lateral branch, LBR, has extended secondary branches around the borders of the PeLA1 cell (a); the left branch (b) has not extended around a cell at this time. The EPNs proceed posteroventrally and fasciculate at the level of the arrowhead (a tissue break separates the fasciculating neurites in this embryo at the arrowhead). Scale bar = 10 μm (A, B, C, and D).

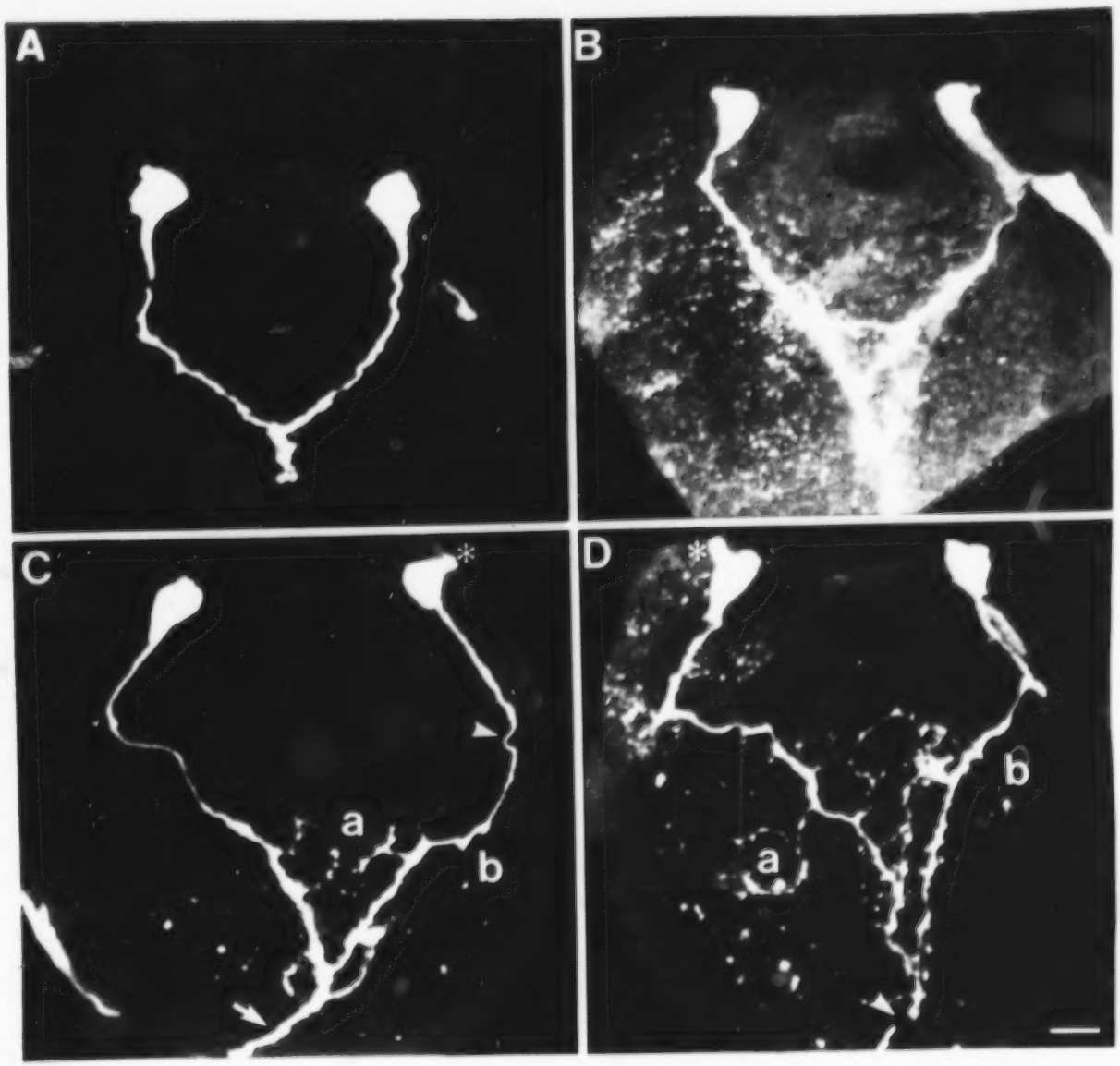
A
B
C
D
a
b
a
b

Figure 14: Quantification of primary and total branch point number of EPNs between stages E15 and E30. **A.** Total branch point number underwent an approximate geometrical increase during development. Number of embryos: E15 (46); E20 (31); E25 (54); E30 (21). **B.** The largest increase in primary branching occurred between stages E20 and E25, when no obvious morphological changes in the pedal ciliary band were observed. Number of embryos: E15 (46); E20 (48); E25 (50); E30 (21).

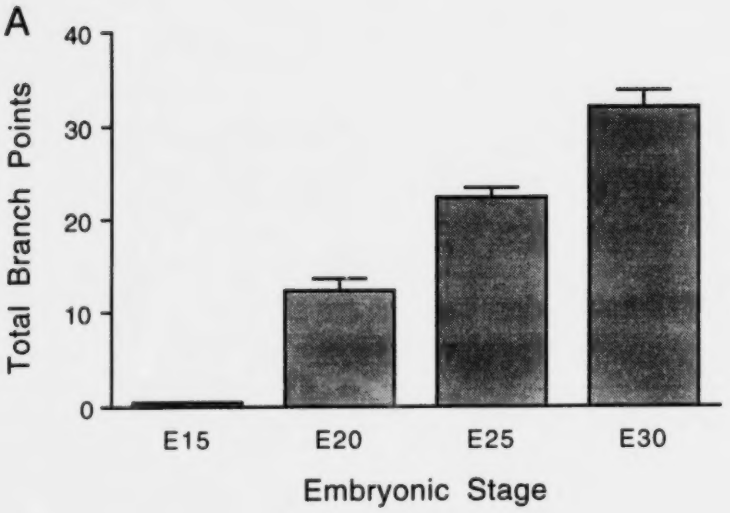
A
Total Branch Points
40
30
20
10
0
E15
E20
E25
E30
Embryonic Stage

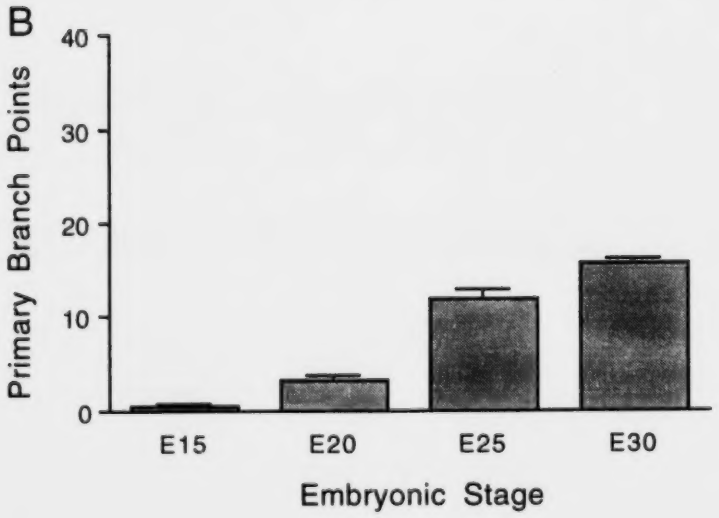
B
Primary Branch Points
40
30
20
10
0
E15
E20
E25
E30
Embryonic Stage

Figure 15. EPN fasciculation is confined to the medial ciliated epithelial cells. **A**. Conventional epifluorescence micrograph of the two EPNs fasciculating along cell PeD at stage E30. In ventral profile (anterior to the top), one can see that the two EPN growth cones (arrowheads) extended posteriorly along the PeD cell while maintaining contact along their neurite shafts along the rest of the length of the PeD cell. Cell PeD was serotonin-immunoreactive in this particular embryo, which permitted resolution of the contact point of the EPNs to be at the anterior boundary of the PeD cell. **B**. Complimentary schematic of panel A, showing the full outline of cell PeD, the anterior margin of which is point of contact and fasciculation of the EPNs. Scale bar = 20 μm.

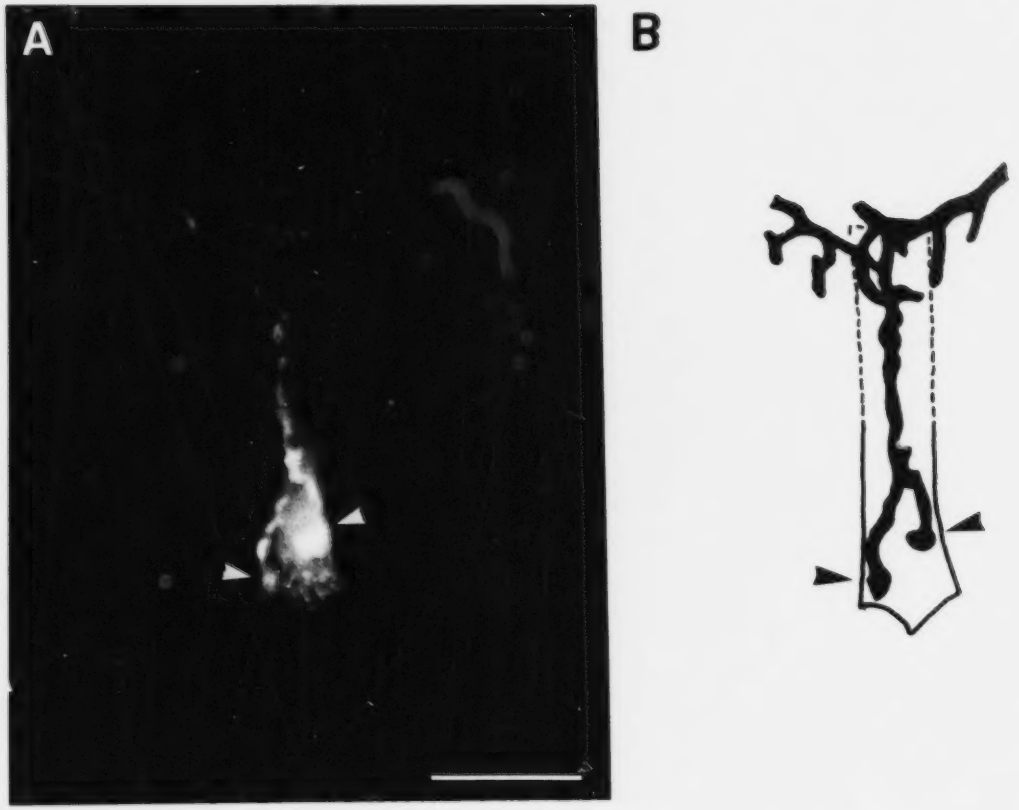
A
B

Figure 16: Fasciculation of EPNs posteriorly along the foot primordium. **A.** Stage E30 embryo in ventral profile showing the sharp transition from branching outgrowth to fasciculated outgrowth along the medial part of the pedal ciliary band (at this stage, along medial cells PeD and PeE). The two EPN growth cones can be seen at the end of the outgrowth pathway, represented by serotonin-immunopositive ectodermal cells of the posterior pedal furrow (p). **B.** Single confocal section through level of reconstruction in panel (A) indicated by the arrow. Apparent are the EPN neurites in frontal section at the transition between lateral margin of the ciliated epithelial cells and the columnar ectodermal cells of the foot primordium. Note that the right EPN (the left immunostained profile) appears to be extending serotonin immunoreactive processes to a small round cell similar to the G-cells. Scale bar = 10 μm (A) and 5 μm (B).

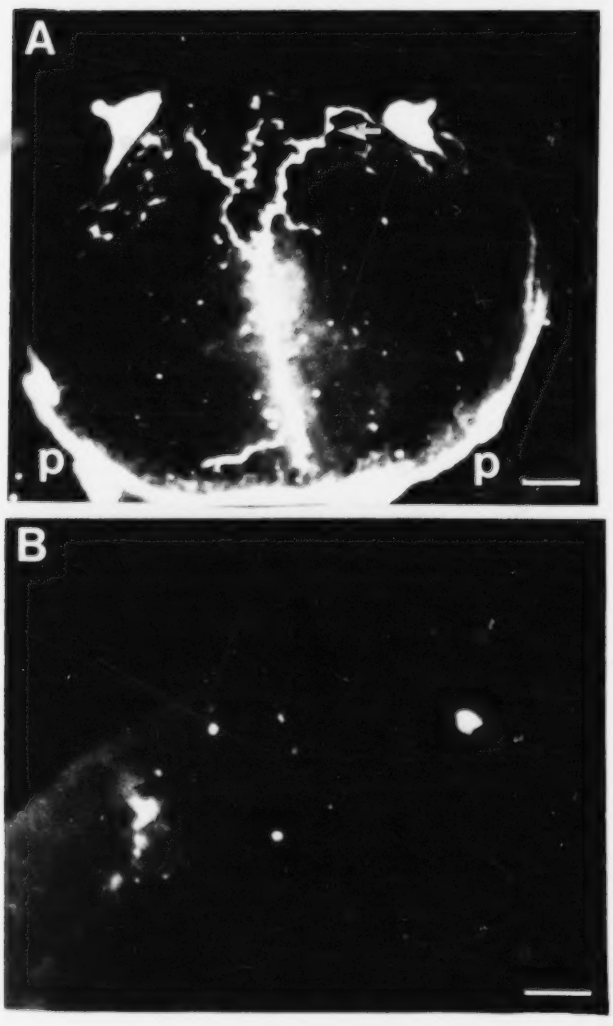
A
p
p
B

Figure 17: ENC1 is present in later staged embryos. DIC micrograph (A) and schematic tracing (B) of a stage E80 embryo in dorsal profile showing a left ENC1 (arrowhead) located anterior to the left cerebral ganglion (c). The EPN of ENC1 can be seen coursing through the ganglion and into the cerebral commissure (hatched lines). Axonal tracts of the neuropile are visible (lines in centre of the ganglion). The base of the left tentacle can be seen on the far left of the panel, in addition to the statocyst (s) with statolyth (a). The large nucleus, granulated cytoplasm, and apical dendrite of ENC1 permitted its identification even up to stage P5 *in vivo*. (b): buccal mass. Scale bar = 50 µm.

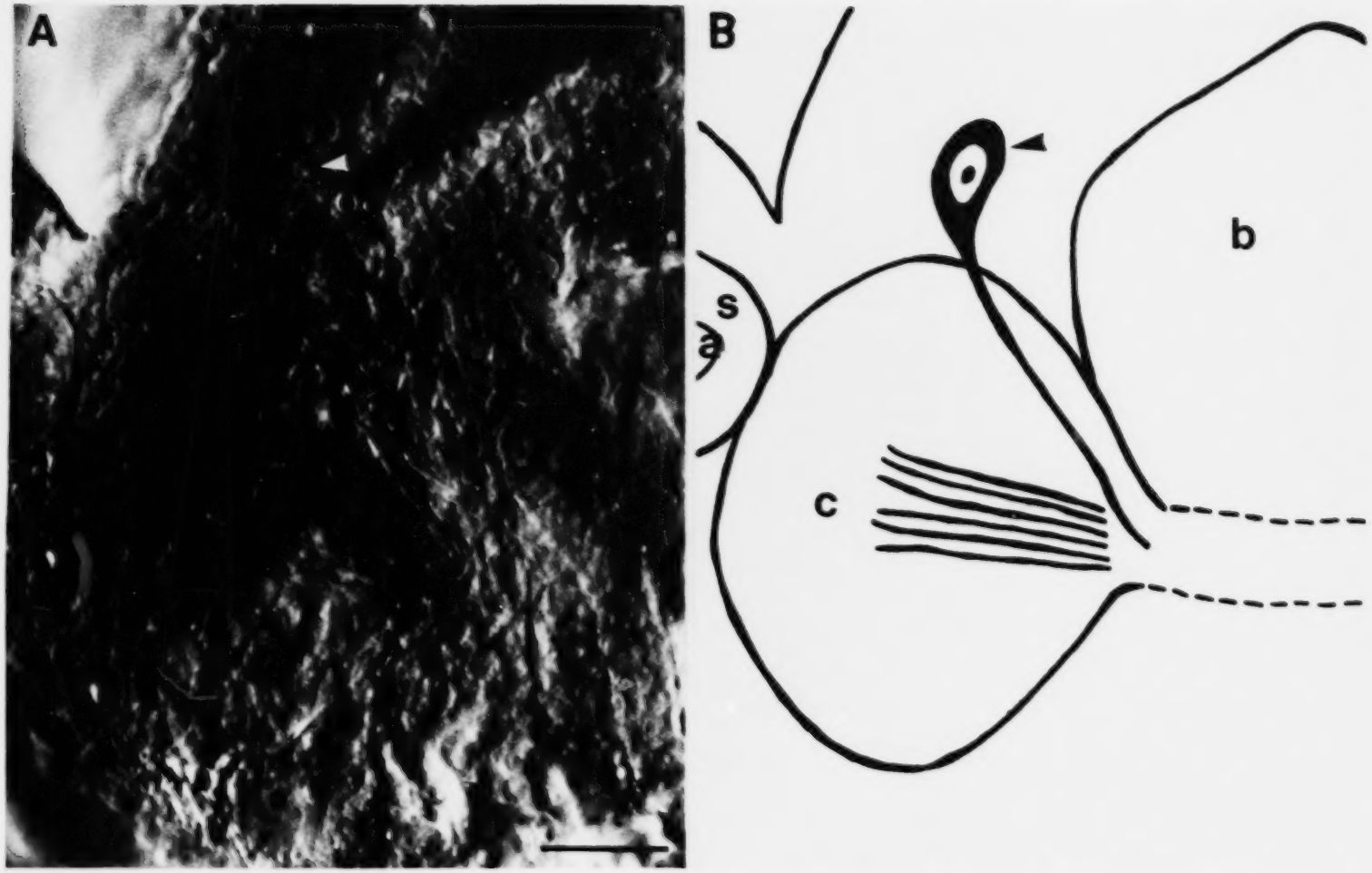
A
B
b
s
a
c

Figure 18: Evidence for pioneering of outgrowth pathways by EPNs. **A.** Stage E40 embryo in left lateral profile showing ENC1 (small arrow) and the full extent of the EPN outgrowth pathway as it extends around the anterior and ventral foot margin. At this stage, two neurons, ENP1 (arrowhead) and ENP2 can be seen in the right pedal ganglion. In this confocal reconstruction, the pedal neurons appear to extend at least one neurite (arrow) ventrally toward the EPNs at the base of the foot (f). Later in development, the pedal neurons also extend neurites dorsally toward the EPN proximal to the ENC1 soma. **B.** At stage E60, the consequence of this outgrowth of pedal serotonergic neurons is the establishment of a pathway between the pedal and cerebral ganglia which is shared by the EPN. In addition, numerous branching neurites extend from the pedal ganglia and grow along the pathway occupied by EPNs in the foot. ENC1 (small arrow) at this stage is still intensely immunofluorescent. ENC2 is also visible at this stage (arrow). **C.** By stage E65, the left ENC1 (small arrow) has lost most of its serotonin immunoreactivity and its outgrowth pathway is no longer visible. Neurites of serotonergic pedal ganglion neurons, however, remain to occupy the ventral foot region (they appear fainter in this confocal series on account of the section thickness chosen, but are as numerous as in panel B). Scale bar = 20 μm (A, B, and C).

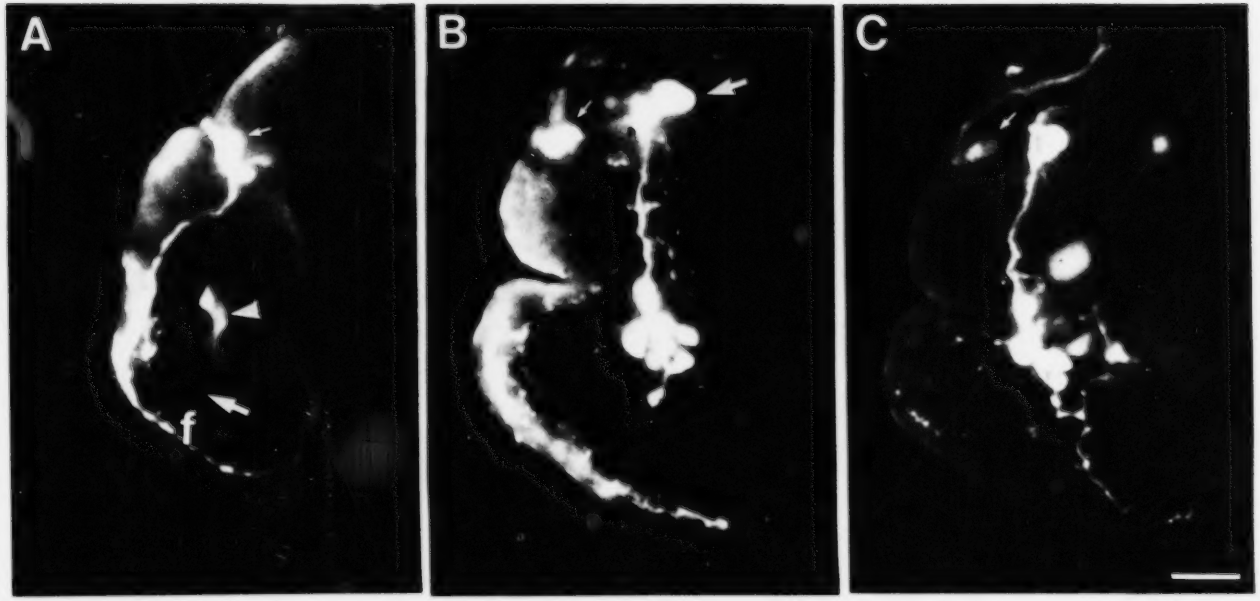
A
B
C
f

Figure 19: Transient expression of serotonin in ENC1. **A.** Dorsal profile of a stage E60 embryo (anterior is toward the bottom of the panel) showing the paired ENC1s (arrows) and the first pair of neurons situated within the cerebral ganglia, the ENC2 (arrowheads). Serotonergic neurites can be seen traversing the cerebral commissure. Note that the EPNs of the ENC1s extend posteriorly to meet with processes of the ENC2 at the level of the cerebral commissure. **B.** Stage E65 embryo showing the right ENC1 with a level of serotonin immunostaining comparable to that of the ipsilateral ENC2. The left ENC1 (arrow), however, has almost completely lost its serotonin immunostaining. **C.** By stage E70, both ENC1s have lost their serotonin immunoreactivity. Arrowheads indicate locations of presence of newly differentiating serotonergic neurons in the cerebral ganglia. Arrows indicate locations of nonimmunoreactive ENC1s. (s): autofluorescent statolyth at the base of the tentacle buds. Scale bar = 20 μm (A, B and C).

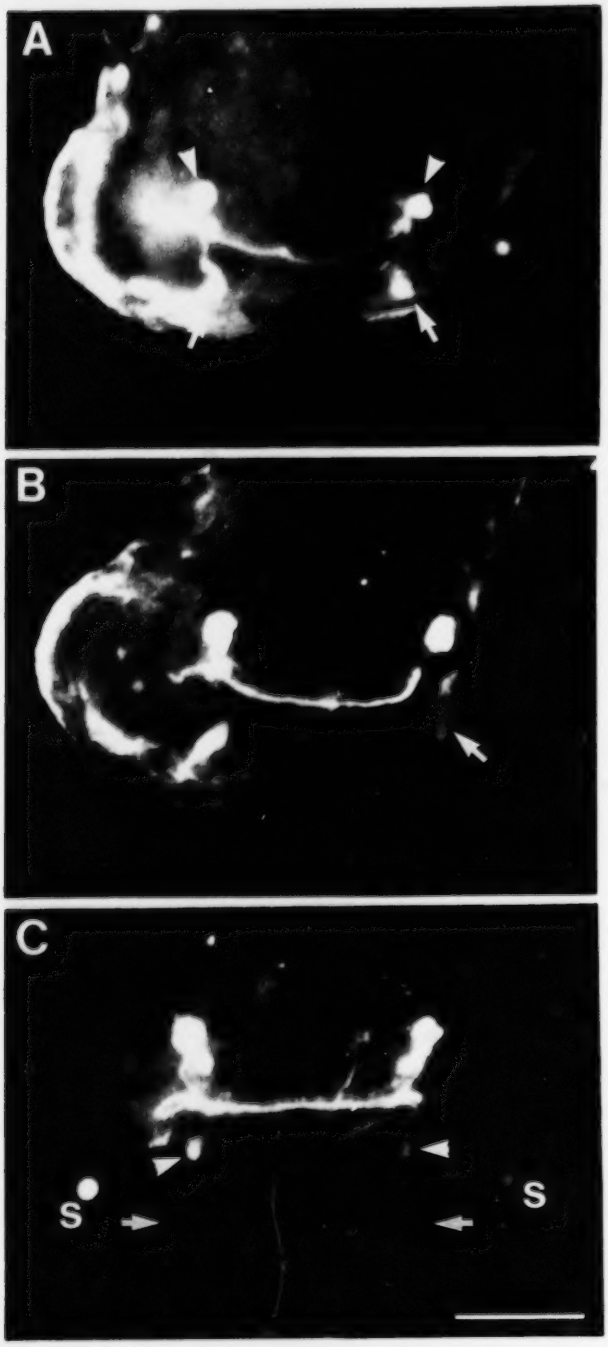
A
B
C
S
S

II) Role of serotonin in the development of ENC1

In this study, I tested the hypothesis that there are serotonin autoreceptors on ENC1 neurites which, when activated, serve to regulate neurite outgrowth. With pCPA treatment, serotonin content in ENC1 should be reduced, thereby reducing the pool of releasable serotonin and therefore the amount of serotonin available to activate serotonin autoreceptors. The effects of pCPA were examined in three ways: 1. To confirm pCPA's inhibitory effect on serotonin synthesis, HPLC-ED was employed to measure pCPA-induced changes in embryonic serotonin content. 2. To elucidate the effects of pCPA treatment on neurite outgrowth of ENC1, embryos were immunostained with a serotonin antibody to examine ENC1 neurites. 3. Since pCPA's inhibitory effect on serotonin synthesis may be manifested as changes in the intensity of serotonin immunostaining of ENC1 somata, ENC1s were also scored for presence or absence of serotonin immunostaining following pCPA treatment.

Another testable prediction of the autoreceptor hypothesis is that experimentally enhanced activation of serotonin autoreceptors should have opposite effects on neurite outgrowth to those induced by pCPA. To test this prediction, 5-HTP was used to increase serotonin synthesis in ENC1s. With enhanced serotonin production, it follows that the pool of releasable serotonin should be increased, thereby increasing activation of serotonin autoreceptors. Increased production of serotonin was confirmed using HPLC and the effects of 5-HTP treatment on ENC1 outgrowth were determined after ENC1s were immunostained, as described previously.[3]

i) Effect of pCPA on whole embryo serotonin content

As described in the Methods, all pCPA experiments involved treating embryos with 0.02% pCPA in APW for 1 hr at stage E15. This treatment was followed by an 48 hr recovery period in APW which permitted the embryos to develop to stage E25. To directly

measure pCPA-induced changes in serotonin content, HPLC-ED was employed. In addition to measurement of serotonin, dopamine (DA) content was also determined to assess the specificity of pCPA action. Although DA was not resolved in early staged *Helisoma* embryos using a tyrosine hydroxylase antibody (Goldberg, 1995), HPLC-ED did reveal low but detectable levels of dopamine. Embryonic serotonin content displayed a dramatic increase in control embryos over the post-treatment period from stage E15 to E25 (Figure 20). pCPA-treatment effectively prevented this developmental increase in serotonin levels, which remained comparable to the stage E15 content of serotonin in control embryos. Both a two-factor ANOVA F-test and Student's t-test confirmed significantly lower serotonin levels in pCPA-treated embryos at stages E20 and E25 with respect to controls ($p < 0.05$; Figure 20A). In contrast, the DA content of control embryos remained unchanged over the post-treatment period from stage E15 to E25 (Figure 20B). Although there appears to be a trend toward reduced DA content resulting from pCPA 1 hr and 24 hr after treatment, this difference was not resolved statistically ($p > 0.05$; ANOVA F-test). Moreover, at 48 hr after treatment, when the greatest changes were observed in embryonic serotonin content, the DA content of control and pCPA-treated embryos was nearly identical ($p > 0.05$; ANOVA F-test). From these direct measurements of embryonic serotonin content, it is apparent that pCPA treatment was effective in establishing and maintaining significantly lower serotonin levels in embryos in spite of a dramatic developmental increase in serotonin levels in control embryos. Furthermore, embryonic DA content was not significantly affected by pCPA treatment, which supports the contention that pCPA treatment specifically inhibited the capacity for serotonin synthesis.

ii) Effect of pCPA on serotonin content of mature CNS of *Helisoma*

To show that the inhibitory effect of pCPA treatment is not limited to *Helisoma* embryos, and as a further test of the specificity of pCPA's action, circumoesophageal ganglia were isolated from adult *Helisoma* and placed for up to 3 days in culture medium

containing 0.02% pCPA. Control ganglia were incubated in culture medium alone. Ganglionic rings were processed for HPLC determination of serotonin and dopamine content at 1, 18, 24, 48 and 72 hr of incubation (6 to 10 ganglia at each time point; Figure 21). By 18 hr of incubation, the serotonin content of control ganglia increased significantly with respect to the initial 1 hr level and remained at an elevated level for the remainder of the incubation period. Ganglia treated with pCPA, however, had serotonin levels that were significantly lower at 24, 48 and 72 hr ($p < 0.05$; Student's t-test) with respect to control ganglia. Thus, it appeared that pCPA treatment prevented the normal increase in ganglionic serotonin content that occurs *in vitro*.

In contrast to the increase in serotonin content of control ganglia, dopamine content actually decreased significantly over the entire 72 hr incubation period. Furthermore, this reduction in dopamine content was unaffected by pCPA treatment. These results suggest that pCPA has a specific inhibitory effect on serotonin production in both *Helisoma* embryos and mature *Helisoma* central nervous system.

iii) Effect of pCPA on serotonin immunoreactivity

An obvious effect of pCPA treatment was a marked, transient reduction of serotonin immunostaining in ENC1s. This effect was so pronounced that in many cases, ENC1 cell bodies were barely visible at best, while the neurites were indistinguishable from the background fluorescence of surrounding tissues (Figure 22). Furthermore, some of these preparations resembled those controls that did not receive secondary antibody during the immunofluorescence procedure. The loss of serotonin immunoreactivity was apparent in as little as 1 hr post-treatment (stage E15). Whereas highly immunofluorescent ENC1s were observed in 93% of the control embryos at stage E15 ($n = 15$ embryos; Figure 23), none of the pCPA-treated embryos ($n = 29$) displayed serotonin-immunostained ENC1s. A complete absence of serotonin immunoreactivity was also observed 24 hr post-treatment in stage E20 embryos. In contrast, by 48 hr post-treatment

(stage E25), serotonin immunostaining had recovered sufficiently (62 % with stained ENC1s; n = 220) to permit quantification of EPN branching. However, the percentage of pCPA-treated embryos with serotonin immunostained ENC1s was still significantly less than that of control embryos at stage E25 ($p < 0.0001$; Chi-squared; n = 61). Thus, pCPA's effect on serotonin immunostaining was long-lasting and partially reversible by 48 hr. These results also complement the HPLC-ED measurements which yielded a significant, albeit persistent, reduction in embryonic serotonin content.

iv) Effect of pCPA on ENC1 neurites

After demonstrating the inhibitory effect of pCPA on whole embryo serotonin content, it was tested whether pCPA treatment alters neurite outgrowth by examining serotonin-immunostained ENC1s. Embryos treated with pCPA at stage E15 and subsequently processed for serotonin immunohistochemistry at stage E25 displayed a unique morphological phenotype not previously observed in the course of examining well over 1000 immunostained embryos. The ENC1 somata and their anteroventrally-directed, unbranched primary neurites were indistinguishable from those of control embryos (Figure 24). However, in the region of the ciliated target cells where the two ENC1 primary neurite homologues conjoin and extend backbranches (Goldberg and Diefenbach, 1992), neurite branching was markedly increased.

In order to quantify the effect of pCPA treatment on neurite branching, the total number of branch points on both the left and right ENC1 were counted (Figure 25). By stage E25, the total number of branch points of pCPA-treated embryos was 45% greater (32.0 ± 2.2; n = 26 embryos) than that of control embryos (22.2 ± 1.1; n = 54; $p < 0.0001$; Student's t-test). The effect of pCPA treatment was even greater in embryos that were treated between stage E10 and E15 and assayed 48 hr later at stage E20. In this case, the total number of branch points in pCPA-treated embryos was increased by approximately 100% over the controls (control: 12.4 ± 1.3; n = 31 versus pCPA: $25.3 \pm$

2.8; n = 8; $p < 0.0001$; Student's t-test). Thus, pCPA treatment increased neurite branching of ENC1 in conjunction with its inhibitory effect on serotonin synthesis.

v) Effects of 5-HTP

Given that the effects of pCPA on ENC1 neurite development are likely a result of the decrease in the amount of serotonin available to bind to autoreceptors, one would predict that a treatment which increases the level of serotonin would result in effects opposite to those of pCPA treatment. We tested this hypothesis by immersing stage E15 embryos for 48 hr in 1.0 mM 5-HTP, a serotonin precursor which serves to increase the synthesis of endogenous serotonin. This elevation was confirmed by HPLC measurements of whole embryo serotonin content. After 1, 24 and 48 hr of incubation in 5-HTP, whole embryo serotonin content was significantly greater in 5-HTP-treated embryos as compared to control ($p < 0.05$, Student's t-test; Figure 26). Dopamine levels were not consistently detectable under the separation conditions used to resolve 5-HT and 5-HTP.

To assess the effects of 5-HTP treatment on ENC1 neurite outgrowth, embryos incubated for 48 hr in either 5-HTP or the control vehicle were isolated and fixed for serotonin immunostaining as in the pCPA treatment protocol. In three experiments, embryos treated with 5-HTP displayed consistently lower numbers of total branch points (Figure 27). There was a significant 5-HTP-induced reduction in total branch point number from 20.3 ± 1.2 (n = 27 embryos) to 14.6 ± 1.1 (n = 30 embryos; $p < 0.002$; Student's t-test). Unlike pCPA treatment, 5-HTP treatment did not reduce serotonin immunostaining intensity. However, background serotonin immunostaining appeared higher in 5-HTP-treated embryos as a result of either cross-reactivity of the serotonin antibody with 5-HTP or the elevated levels of extracellular serotonin. As with pCPA, 5-HTP treatment did not result in changes in the morphology of ENC1 somata. Nor did 5-HTP induce aberrant branching of the neurite segment between the soma and target cell region. Rather, branching outgrowth was consistently confined to the target cell region of the pedal ciliary

band (Figure 24C). Thus, the effects of 5-HTP treatment were consistent with the hypothesis that serotonin released from ENC1 during development binds to ENC1 autoreceptors to regulate the formation of neurite branches.

vi) Effects of dopamine on ENC1 neurites

Since the HPLC experiments revealed detectable dopamine levels in *Helisoma* embryos, it is possible that the effects of pCPA and 5-HTP treatments on ENC1 neurite branching were mediated by dopamine, rather than serotonin. In addition, while pCPA treatment did not significantly alter embryonic dopamine levels, a tendency towards reduced levels was observed 24 hr after treatment in stage E20 embryos (Figure 20B). Therefore, to test whether dopamine could directly affect the development of ENC1 neurites, stage E15 embryos were incubated with 1.0 mM dopamine with 0.04% ascorbic acid for 48 hr and then processed for serotonin immunostaining (Figure 28). There were no differences in ENC1 appearance or the number of ENC1 neurite branches in dopamine-treated embryos when compared with normal controls, or controls which received the ascorbate vehicle. These data support the conclusion that the effects of pCPA and 5-HTP on ENC1 neurite development resulted directly from changes in embryonic serotonin content, rather than through an additional neurotransmitter pathway.

Figure 20: Effect of pCPA treatment on embryonic serotonin and dopamine content. HPLC-ED measurements of embryonic serotonin (A) and dopamine (B) content as a function of time after pCPA treatment (shaded bars: control; open bars: pCPA-treated). Embryos treated for 1 hr with 0.02% pCPA were isolated at 1, 24 and 48 hr after the end of the treatment period and processed for HPLC. Whereas pCPA retarded the normal developmental increase in embryonic serotonin content (*: $p < 0.05$; ANOVA) dopamine levels remained constant over development and were not significantly altered by pCPA treatment (ANOVA). Sample number (E15/E20/E25): 5-HT control: 4/11/11; 5-HT pCPA-treated: 7/11/7; DA control: 3/10/5; DA pCPA-treated: 2/8/2.

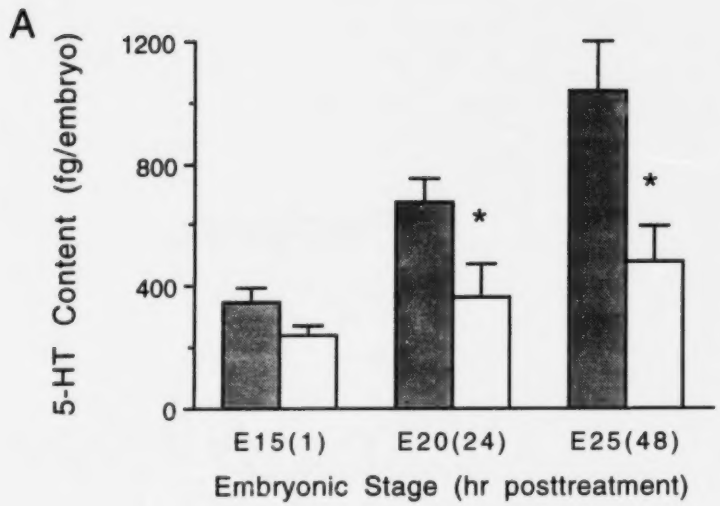
A
5-HT Content (fg/embryo)
1200
800
400
0
*
*
E15(1)
E20(24)
E25(48)
Embryonic Stage (hr posttreatment)

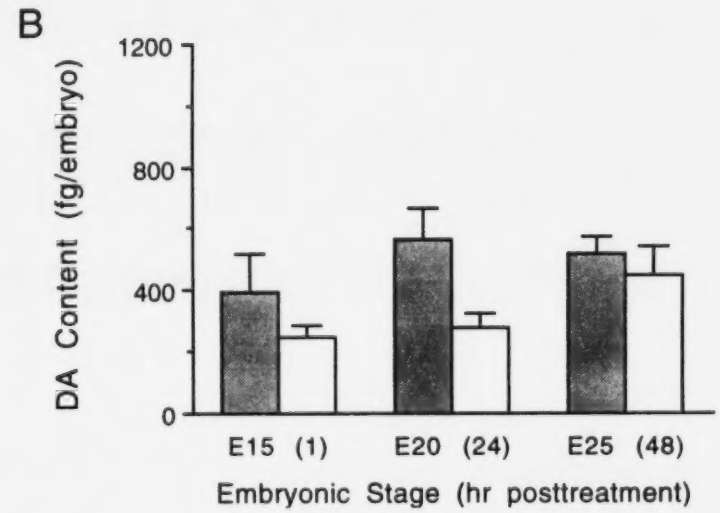
B
DA Content (fg/embryo)
1200
800
400
0
E15 (1)
E20 (24)
E25 (48)
Embryonic Stage (hr posttreatment)

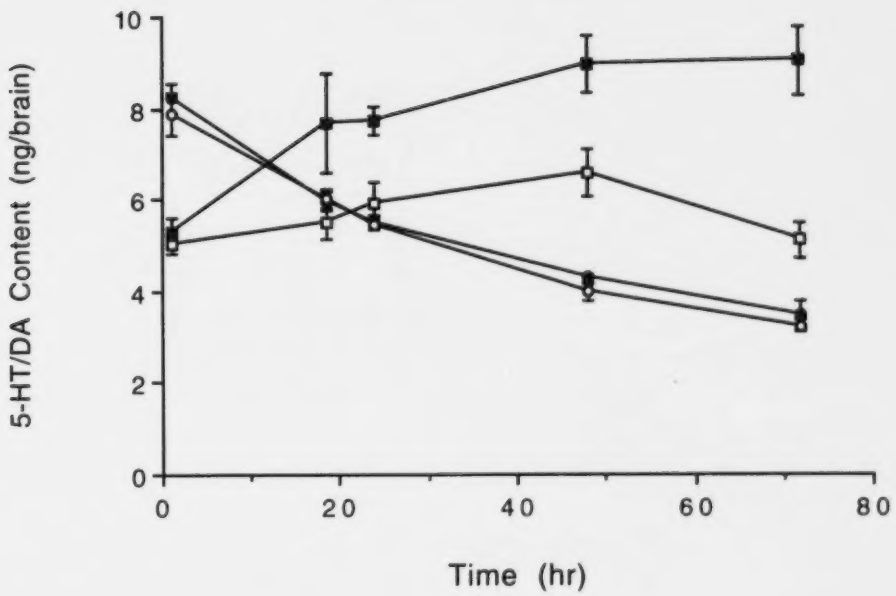

Figure 21: pCPA specifically reduced serotonin content of isolated ganglia from adult *Helisoma*. Ganglia were incubated in culture medium with or without pCPA for up to 72 hr and simultaneously assayed for serotonin and dopamine content using HPLC. Whereas pCPA treatment resulted in significantly reduced ganglionic serotonin content compared to control ganglia at 24, 48, and 72 hr (*: $p < 0.05$; Student's t-test), the negative trend in dopamine content was unaffected by pCPA. Shaded squares: 5-HT control; open squares: 5-HT pCPA-treated; shaded circles: DA control; open circles: DA pCPA-treated. Measurements from between 6 and 10 ganglia per treatment.

Figure 22: Reduction of serotonin immunoreactivity in ENC1 after pCPA treatment. pCPA treatment reduced serotonin immunoreactivity of ENC1s to a level indistinguishable from nonspecific background immunostaining. **A.** Fluorescence micrograph of control stage E25 embryo (anterior profile) 48 hr after pCPA vehicle treatment with serotonin immunostained ENC1s and primary neurites clearly visible. **B.** Stage E20 embryo 24 hr after pCPA treatment with minimal ENC1 cell body staining and no neurite staining. Scale bar = 50 μm for A and B.

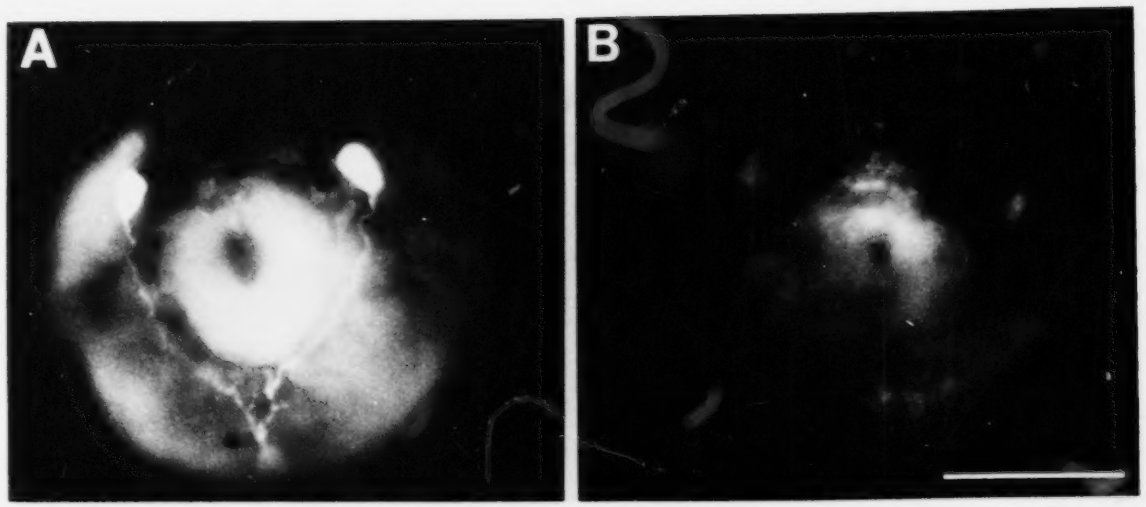
A
B

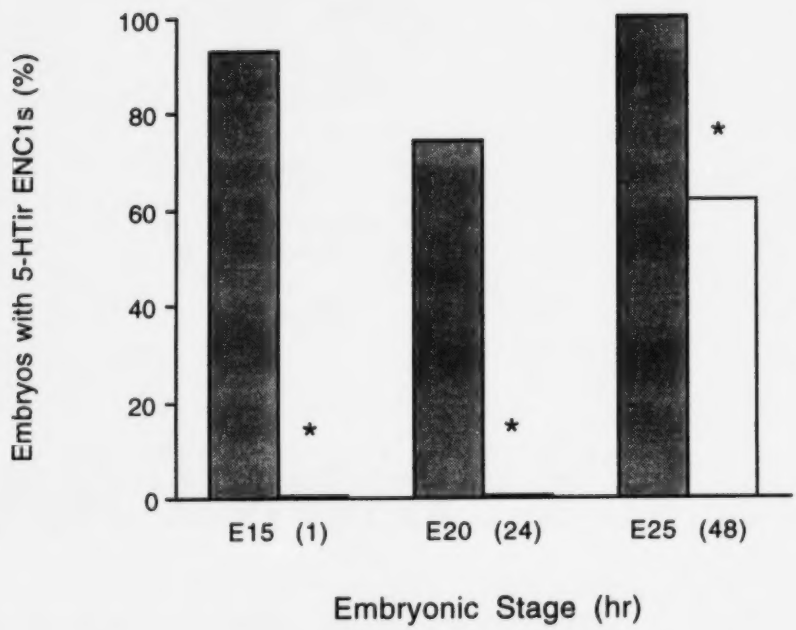

Figure 23: Recovery of serotonin immunostaining after pCPA treatment. Serotonin immunostaining recovered 48 hr after pCPA treatment in 62% of embryos (shaded bars: control; open bars: pCPA-treated; *: $p < 0.0001$; Chi-squared). Number of embryos (control/pCPA): E15: 15/29; E20: 31/47; E25: 61/220.

Figure 24: Effect of pCPA and 5-HTP on ENC1 morphology. Fluorescence micrographs with accompanying photographic tracings of serotonin-immunostained stage E25 embryos (anterior profile) treated with either vehicle (A), pCPA (B) or 5-HTP (C). Since the tracings represent a two-dimensional image, not all the branches are visible. **A.** Control embryo with serotonin-immunostained ENC1s (arrowheads) and primary neurites that extended around the stomodaeum (s) to the pedal band of ciliated cells (p), where neurite branching occurred. **B.** pCPA treatment resulted in a dramatic increase in neurite branching that was confined to the pedal target region. The apparently larger size of the pCPA-and 5-HTP treated embryos, and greater separation between ENC1 somata was caused by excessive compression under a glass coverslip during microscopy. **C.** 5-HTP treated embryo (anterior profile) displaying higher background immunostaining and sparser distribution of neurite branches. The high level of background staining resulted from cross-reactivity of the serotonin polyclonal antibody with residual 5-HTP or extracellular serotonin. Scale bar = 50 µm. Total number of branch points: control: 24; pCPA-treated: 31; 5-HTP treated: 14.

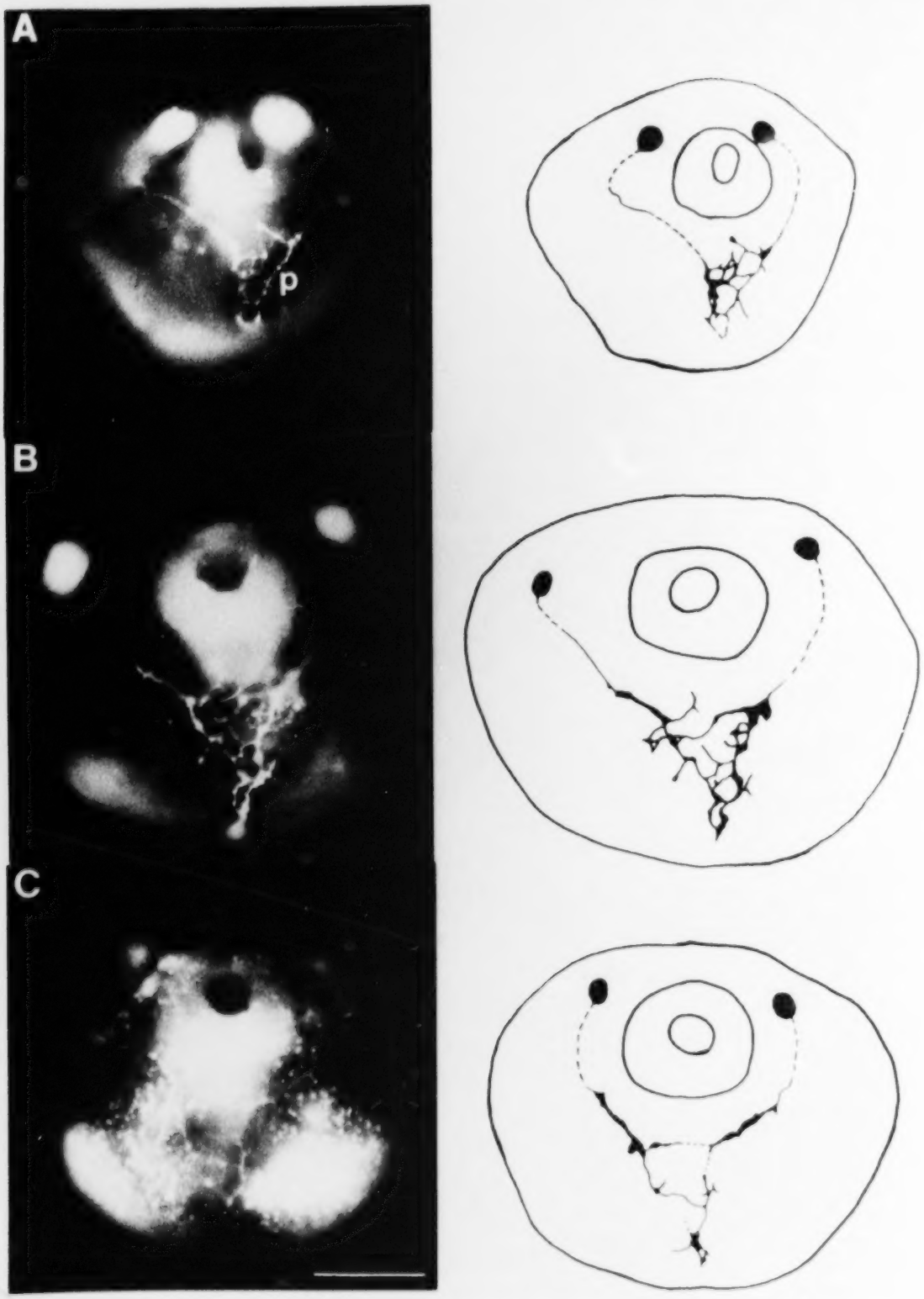
A
p
B
C

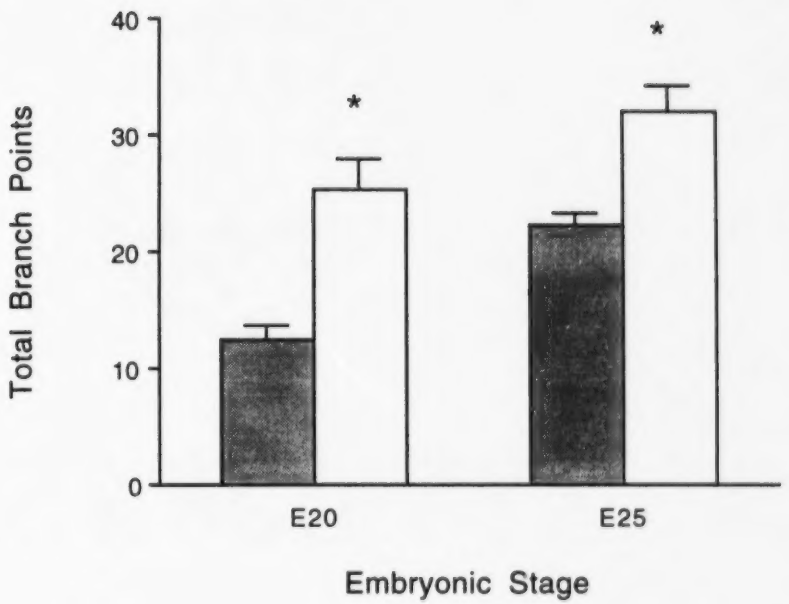

Figure 25: Effect of pCPA treatment on number of ENC1 branch points. The number of branch points was significantly higher in embryos treated with pCPA versus control embryos at both stages E20 and E25 (*: $p < 0.0001$: Student's t-test; shaded bars: control; open bars: pCPA-treated). Number of embryos (control/pCPA): stage E20: 31/8; stage E25: 54/26.

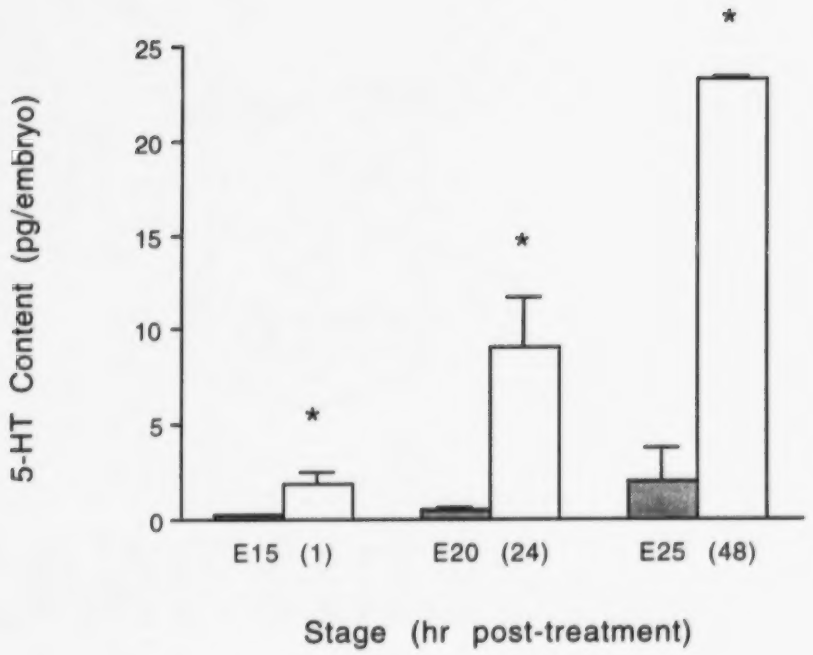

Figure 26: Effect of 5-HTP treatment on serotonin content of *Helisoma* embryos. HPLC-ED determination of changes in whole-embryo serotonin content resulting from continuous exposure to 1.0 mM 5-HTP for 1, 24 and 48 hr durations. Serotonin content was consistently and significantly elevated in 5-HTP-treated embryos (open bars) relative to control embryos (shaded bars) at all developmental stages examined (*: $p < 0.05$; Student's t-test). Sample number (control/5-HTP): E15: 6/8; E20: 5/5 ; E25: 2/3 .

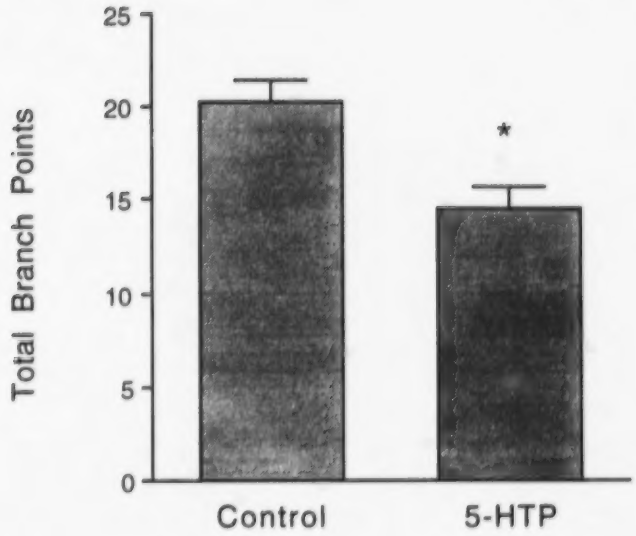

Figure 27: Effect of 5-HTP treatment on ENC1 morphology. Treatment of stage E15 embryos in 1.0 mM 5-HTP for 48 h resulted in a 28% decrease (*: $p < 0.002$; Student's t-test) in total branch point number of stage E25 embryos. Sample size (control/5-HTP): 27/30.

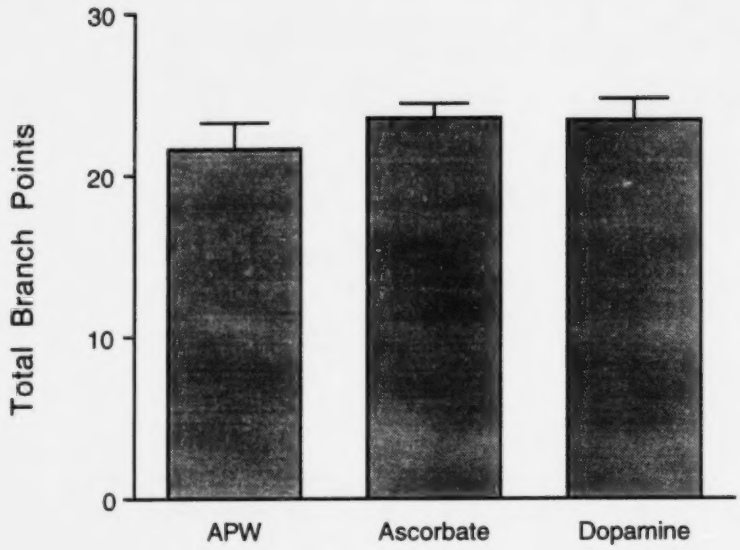

Figure 28: Dopamine treatment did not alter ENC1 morphology. Mean counts of branch point number of ENC1 in stage E25 embryos exposed for 48 hr to artificial pond water (APW), 0.04% ascorbate in APW (Ascorbate), and 1.0 μM dopamine (Dopamine). Branch point number was not significantly different for any of the treatments ($p > 0.05$; Mann-Whitney U-test). Number of embryos: APW: 7, Ascorbate: 20, Dopamine: 11.

III) Role of serotonin in the development of rotational behavior in *Helisoma* embryos.

In some molluscs, serotonin has been implicated as a neurotransmitter in the nervous control of ciliary activity (Aiello, 1962; Audesirk *et al.*, 1979; Catapane, 1983; Koshtoyants *et al.*, 1981; Syed and Winlow, 1989). The first section of the Results in this thesis provides morphological evidence that ENC1 neurites innervate the pedal ciliary band. The activity of cilia generates rotation of the embryo while it develops in the egg capsule. It is therefore possible that ENC1 utilizes serotonin as a neurotransmitter to control cilia-driven rotational behavior during development. This hypothesis was tested by characterizing the rotational behavior of *Helisoma* embryos as a function of development using time-lapse video microscopy. Given the slow time course of the behavior, time-lapse video microscopy was used to resolve the subtle components of rotation and facilitate a quantitative analysis. Following the characterization of the behavior, the effects of exogenous serotonin and a serotonin antagonist on rotational behavior were assessed in a pharmacological study[4,5].

i) Rotational behavior: characteristics of rotation

During embryonic stages E15 to E30, embryos of *H. trivolvis* displayed cilia-driven rotational behavior within the egg capsule. This complex behavior was characterized by four distinct parameters, namely the direction of rotation, rotational surges, periods of inactivity, and rotation rate.

The direction of rotation was determined by the combined activity of two groups of ciliated cells. Activity in the dorsolateral prototrochal cilia (Figure 29) produced a leftward rotation about the dorsoventral axis of the embryo (Table 1), referred to as a yaw movement. Activity of the pedal cilia (Figure 29) produced an upward rotation about the mediolateral axis, referred to as a pitch movement. Coincident activity of both groups of

ciliated cells resulted in an intermediate direction of rotation, namely a rotation in the vector defined by the pitch and yaw movements (Table 1). Rotation could thus occur either as an independent yaw movement, an independent pitch movement or a combined yaw-pitch movement. In addition, during periods when the ciliary activity of both groups of ciliated cells was very low and asynchronous, embryos displayed no rotation.

Rotation rate and rotational surges were also distinctive and variable parameters of rotational behavior. Surges were discrete, transient accelerations through angles of rotation ranging from 20° to 120° (n = 53 embryos, 7 egg masses). Figure 30 illustrates the non-surge and surge components of rotation in a continuous series of video frames captured at 4 second intervals. Surges always occurred in the direction of a pitch movement. Measurement of rotation rate in sequential five-second periods also show the surge and non-surge components of rotation (Figure 31).

ii) Developmental changes in rotation

Rotational behavior underwent marked developmental changes during embryogenesis as a result of specific changes in each of the parameters (Table 1). For example, the direction of rotational movements changed as a function of embryonic stage. At stage E15, when rotational behavior was first expressed, only yaw movements were visible. Combined pitch-yaw movements occurred at stage E20, while independent yaw movements and combined pitch-yaw movements were observed at stage E25. Pitch movements, yaw movements, and combined pitch-yaw movements were all observed at stage E30. Furthermore, periods of inactivity were observed, a behavioral feature restricted to stage E30 embryos. At stage E35, rotational behavior was interrupted by brief periods of crawling behavior along the inner egg capsule wall. Therefore, rotational behavior was not systematically examined beyond stage E30.

In addition to changes in the expression of different rotational movements, the rate of rotation (Figure 32) and frequency of rotational surges (Figure 33) both varied as a

function of developmental stage. The rate of rotation increased significantly from stage E15 (n=53 embryos, 6 egg masses) to stage E25 (n=109 (8); $p<0.001$) after which it declined (n=78 (6); $p<0.0001$; Figure 32). Similarly, the frequency of rotational surges increased from stage E15 (n=31 (3)) to stage E25 (n=74 (5); $p<0.0001$), and then decreased significantly by stage E30 (n=133 (6); $p<0.0001$; Figure 33). Note that most embryos (25 out of 31) did not display any rotational surges at stage E15 (Figure 33, Table 1).

Beyond stage E15, the rate of rotation was a composite measure of rotation both between and during rotational surges. The increase in surge frequency observed at stage E25 must account for at least part of the increase in overall rotation rate at this stage. Measurements of the surge and non-surge components of rotation of stage E25 embryos supported this conclusion. The mean rate of non-surge rotation was 0.41 ± 0.03 rpm and the mean rate of surge rotation was 1.30 ± 0.06 rpm, while the overall rotation rate was 0.82 ± 0.05 rpm (n=28 embryos).

iii) Effects of serotonin on rotation

Given that the onset of rotational surges coincided with the onset of serotonin-immunoreactivity in ENC1 (Figure 2) and the increased innervation of the pedal ciliary band by ENC1 (Figure 13), the effects of exogenous serotonin on rotational behavior were examined. Stage E25 embryos were used in most experiments since both rotation rate and surge frequency reached peak levels at this stage (Figures 32 and 33). Embryos immersed in serotonin increased their rate of rotation in a dose-dependent fashion (Figure 34A). This change in rotation rate resulted specifically from a tonic increase in the pitch component of rotation. Threshold responses were observed at doses of 1.0 μM serotonin; 100 μM serotonin induced a maximal four-fold increase in rotation rate. Prolonged exposure to serotonin (100 μM) for 30 minutes resulted in a gradual increase in rotation rate over that time period (Figure 34B). Rotation rate doubled in the first 10 minutes, and the initial increase in rate was often detectable in under 60 s. The effects of serotonin were completely

reversible over a 60 minute washout period (Figure 34C). The increase in rotation rate was specific for serotonin, since immersion of embryos in either dopamine, octopamine or the serotonin breakdown product, γ-glutamyl serotonin (all 100 μM) (Sloley and Goldberg, 1991) caused no change in rotation rate (Figure 35).

Immersion of stage E25 embryos in exogenous serotonin also resulted in a significant reduction in the frequency of rotational surges (Figure 36A). This reduction was more pronounced with prolonged exposure to serotonin until surges were no longer observed after 30 minutes (Figure 36B). The timecourse of surge frequency reduction was similar to the timecourse of increased rotation rate. Furthermore, after washout of serotonin, the surge frequency returned to basal levels along a similar timecourse as that observed for rotation rate (Figure 36C). In contrast, the sensitivities of the surge frequency response and rate of rotation response were not the same. The threshold concentration for a significant reduction in surge frequency was 10 μM, an order of magnitude less sensitive than the rate of rotation response.

The effects of serotonin on rotation rate (Figure 37A) and rotational surges (Figure 37B) were also examined at different stages of embryonic development. While rotation rate was increased by serotonin at all stages (i. e. E15, E20, E25, E30), the sensitivity of the response was found to be stage-dependent. For stages E20 and E25, the response threshold was 1.0 μM serotonin. Embryos of stages E15 and E30, however, required 10.0 μM serotonin to elicit a response. The sensitivity of the surge response was similarly stage-dependent. Threshold responses occurred at 10 μM serotonin for stage E25 embryos, and at 100 μM serotonin for stage E20 and E30 embryos. These results indicate that both parameters of rotation displayed maximum sensitivity to exogenous serotonin at stage E25.

iv) Effects of a serotonin antagonist on rotation

In order to test whether endogenous serotonin is involved in the regulation of rotational behavior, an effective serotonin antagonist was required. A pharmacological

analysis of the serotonin receptor involved in embryonic rotation revealed mianserin to be an effective antagonist at the receptor (Goldberg *et al.*, 1994). Mianserin (100 μM) was found to reliably prevent the four-fold increase in rotation rate induced by exogenous serotonin (100 μM) on stage E25 embryos (Figure 38A). In the absence of exogenous serotonin, mianserin (100 μM) decreased the rotation rate to a value below the basal level ($p<0.0001$; Figure 38A). A higher concentration of mianserin alone (1000 μM) caused no further decrease in rotation rate ($n = 31$ embryos). Strikingly, analysis of rotational surges revealed that mianserin alone (100 μM) virtually eliminated surge behavior (Figure 38B). Taken together, these data suggest that rotational surges, and their secondary effect on rotational rate, are mediated by endogenous serotonin acting upon specific serotonin receptors, which would likely be located at synapses of ENC1 with pedal ciliated epithelial cells.

Embryonic Stage	Pattern of Cilia	Direction of Rotation	Cessations	Rotational Surges
E15			No	No*
E20			No	Yes
E25		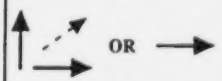	No	Yes
E30		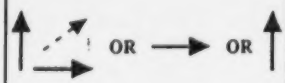	Yes	Yes

Table 1: Summary of qualitative developmental changes in rotational behavior and ciliogenesis of *Helisoma* embryos. Each schematic represents an anterior profile of the embryos as in Figure 28A, with a central black stomodaeum flanked by dorsolateral prototrochal bands of cilia and a single ventromedial pedal band of cilia. Horizontal arrows = the direction of yaw rotation; vertical arrows = pitch rotation; dotted arrows = vectorial sum of combined pitch and yaw rotational components. [1]At stage E15, 25 of 31 embryos exhibited no rotational surges.

Figure 29: Scanning electron micrographs of stage E25 embryos in anterior (A) and left lateral (B) perspective. The arrowhead in panel A points out the right dorsolateral prototrochal band of ciliated epithelial cells and the asterisk indicates the ventromedial pedal band of cilia. Scale bar = 50 μm.

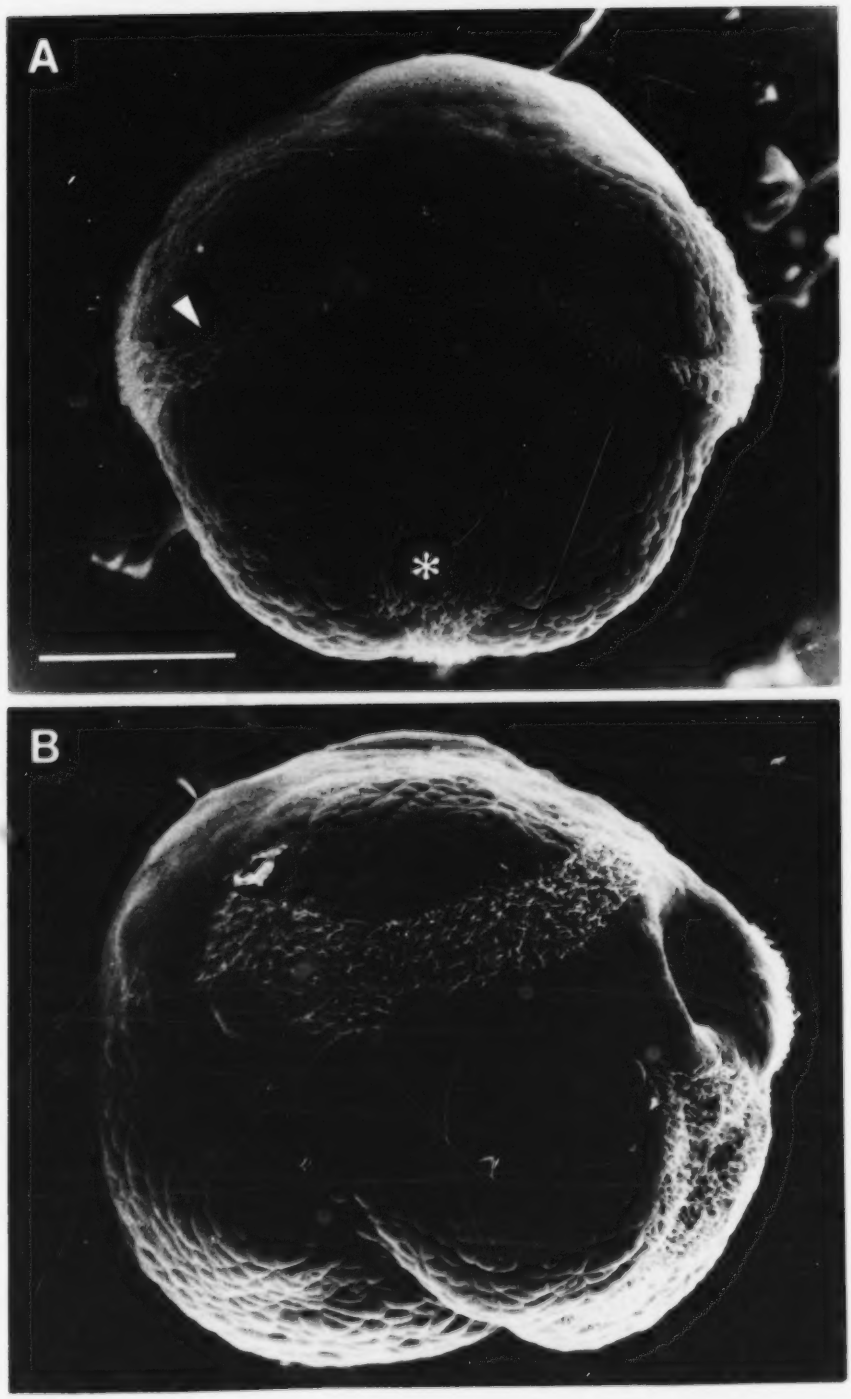
A
B

Figure 30: Surge and non-surge components of rotation. A sequential series of time-lapse video micrographs of a stage E25 embryo taken at four second intervals. Non-surge rotation is seen in the top five frames, while a surge occurs in the bottom five frames. Arrowheads in the first, fifth, sixth and tenth frames of the image series reference the angular change in position of the foot primordium. The diagonal band in the lower left corner of each frame is the egg capsule wall. Scale bar = 100 μm.

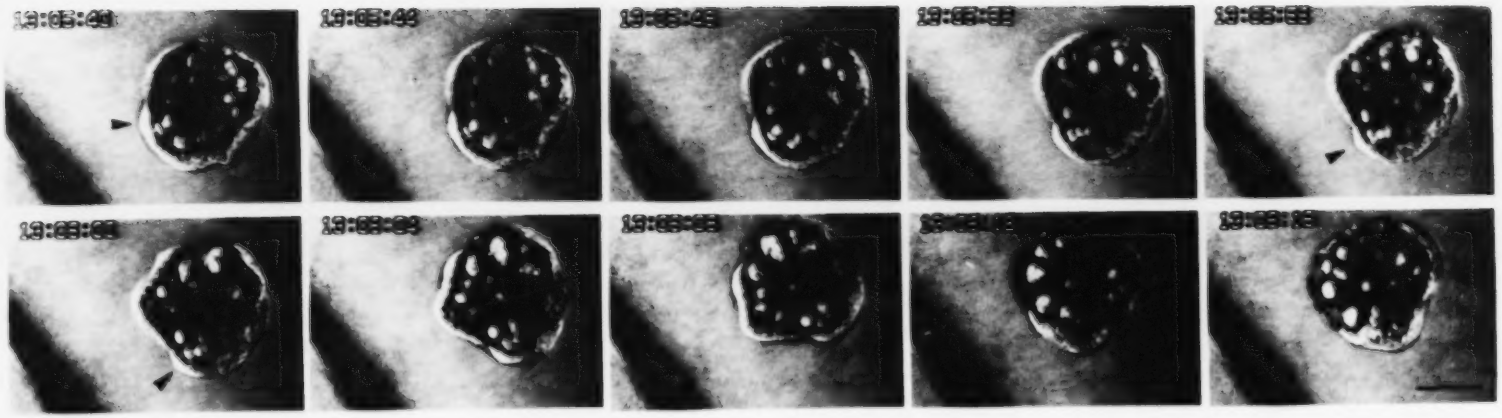

Figure 31: Surges are quantifiable changes in rotation rate. Changes in rotation rate of six representative stage E25 embryos as measured over five second intervals. Non-surge rotation is interrupted by discrete, transient surges that typically reach a maximum rotation rate three to five-fold greater than the rate of non-surge rotation. The top left graph is data taken from the embryo illustrated in Figure 29.

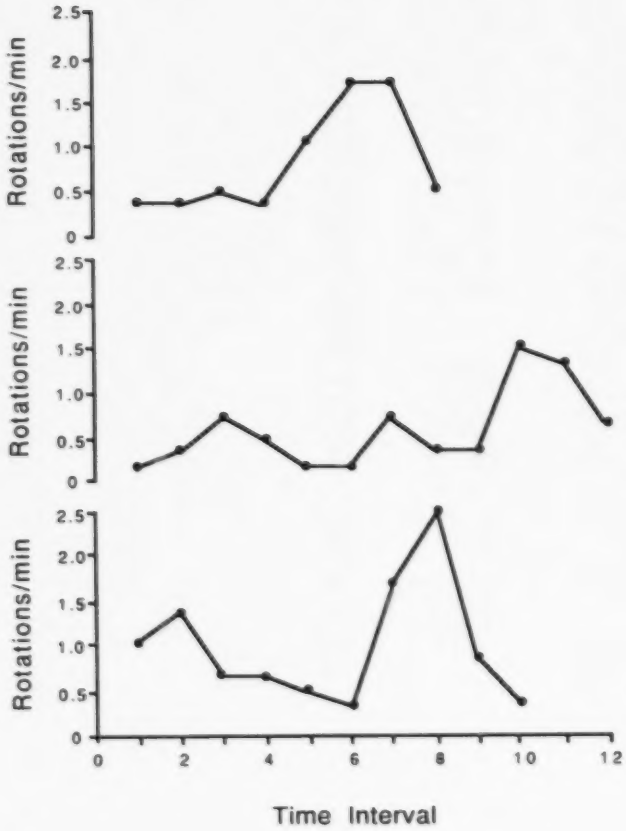
Rotations/min
2.5
2.0
1.5
1.0
0.5
0
0
2
4
6
8
10
12
Time Interval

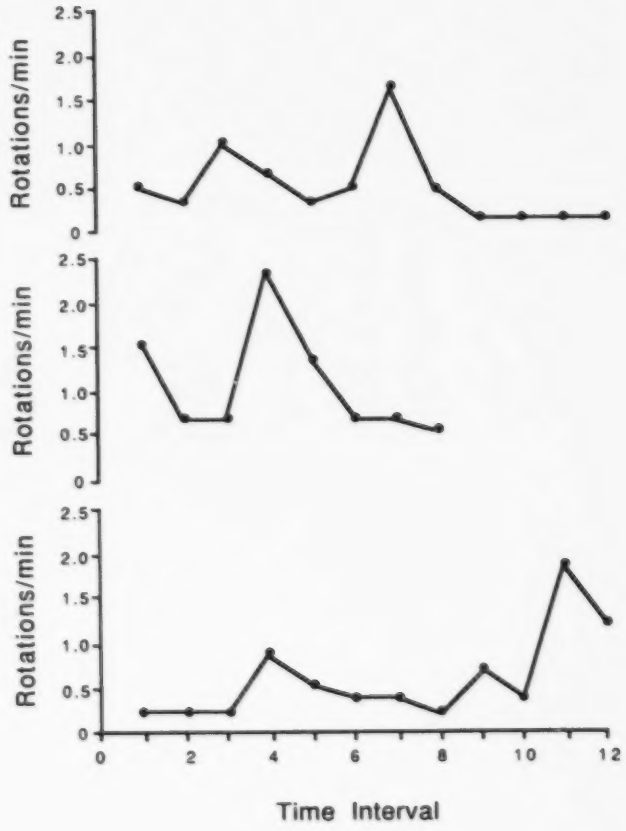
Rotations/min
2.5
2.0
1.5
1.0
0.5
0
0
2
4
6
8
10
12
Time Interval

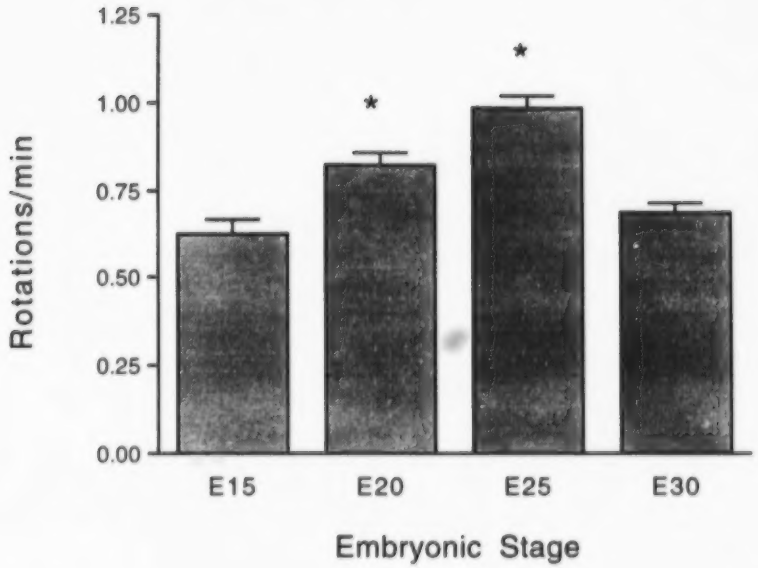

Figure 32: Developmental changes in rotation rate. The number of embryos/egg masses examined at each stage is as follows: E15: 53/6; E20: 89/7; E25: 109/8; E30: 78/6. Asterisk denotes statistically significant difference compared to stage E15 ($p < 0.0001$, ANOVA).

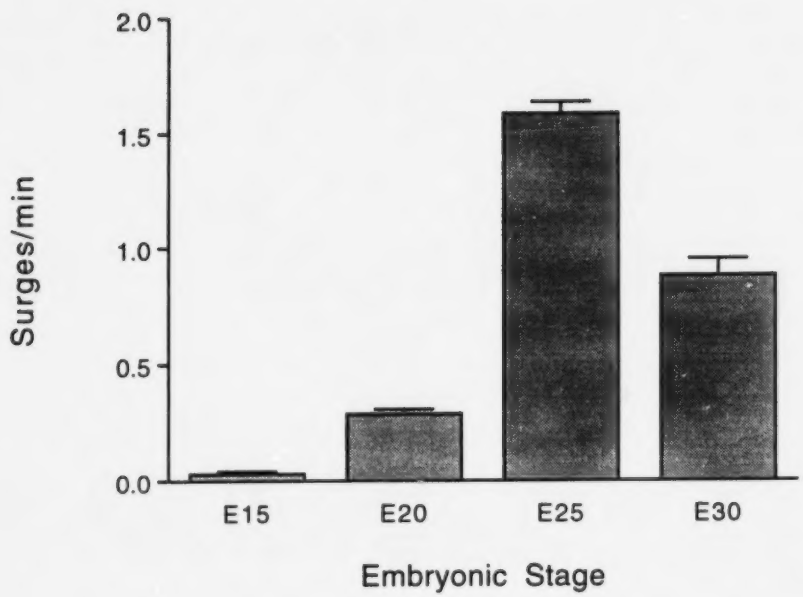

Figure 33: Developmental changes in rotational surge frequency. The number of embryos/egg masses examined at each stage is as follows: E15: 31/3; E20: 190/9; E25: 74/5; E30: 133/6. Statistically-significant differences in surge frequency occurred between all stages examined ($p < 0.0001$, ANOVA).

Figure 34: Effect of serotonin on rotation rate in stage E25 embryos. **A.** Serotonin (5-HT) increased rotation rate in a dose-dependent manner. Each bar represents data from a minimum of 10 embryos. The matched control data (0 μM serotonin) is illustrated in Figure 32. **B.** Prolonged exposure of embryos to 100 μM serotonin induced a gradual increase in rotation rate (n = 23). **C.** The effect of serotonin was completely reversible within 60 minutes of returning embryos to APW (n = 13).

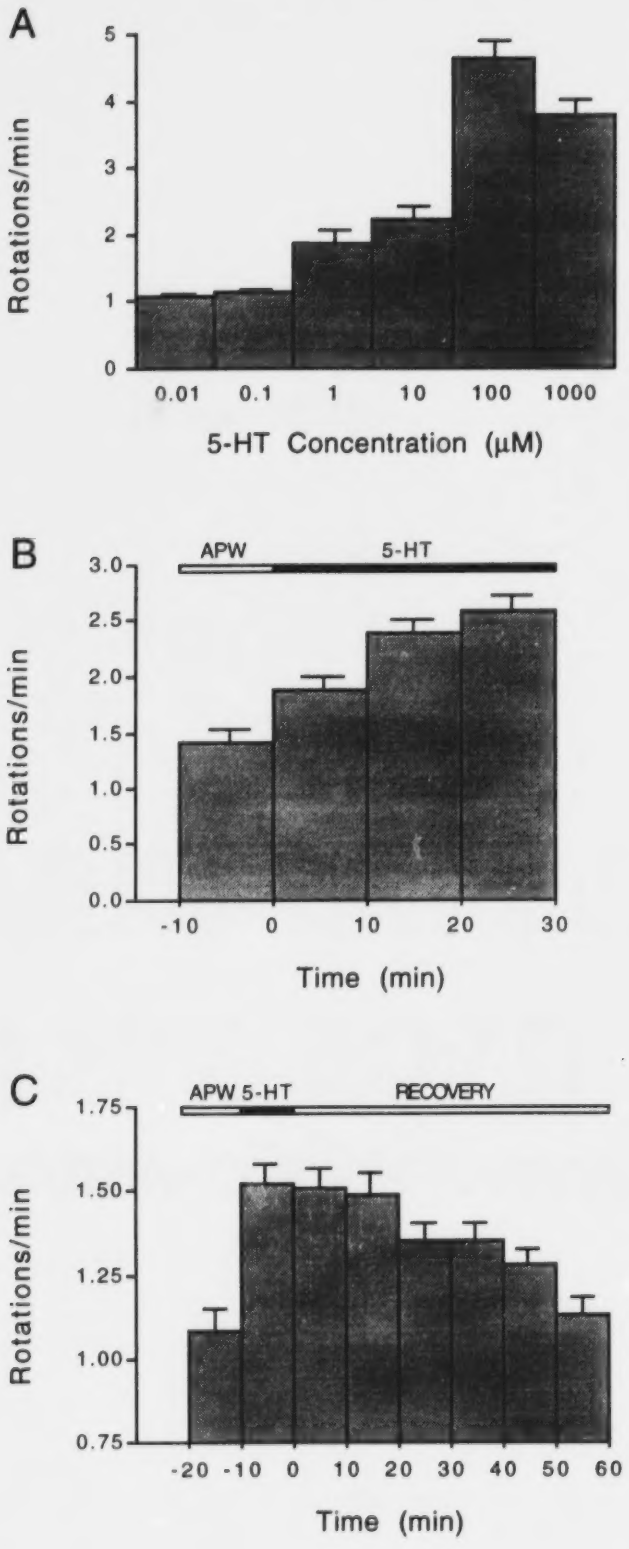
A
Rotations/min
0
1
2
3
4
5
0.01
0.1
1
10
100
1000
5-HT Concentration (μM)
B
APW
5-HT
Rotations/min
0.0
0.5
1.0
1.5
2.0
2.5
3.0
-10
0
10
20
30
Time (min)
C
APW 5-HT
RECOVERY
Rotations/min
0.75
1.00
1.25
1.50
1.75
-20
-10
0
10
20
30
40
50
60
Time (min)

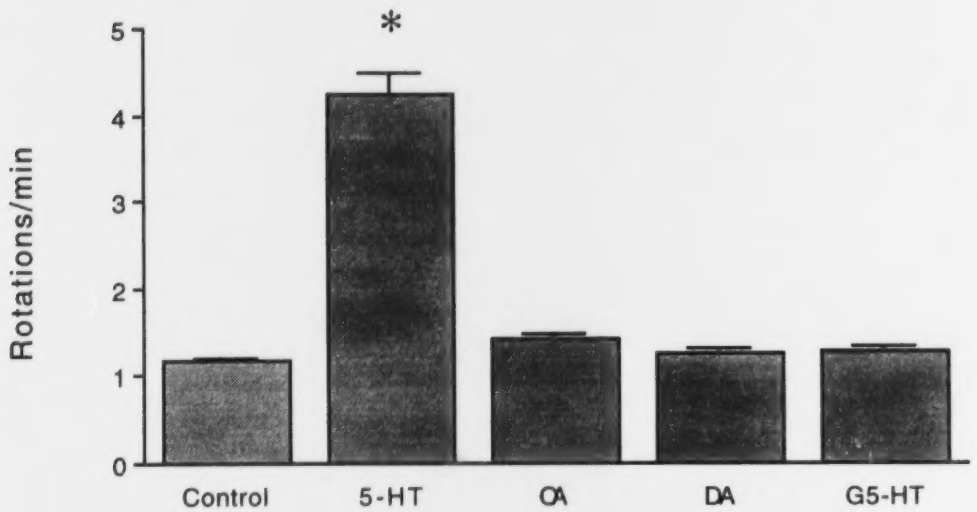

Figure 35: Test for the specificity of the behavioral response of stage E25 embryos to serotonin. Whereas serotonin (100 μM) produced a four-fold increase in rotation rate, other biogenic amines including octopamine (OA), dopamine (DA), and the breakdown product of serotonin in *Helisoma*, γ-glutamyl serotonin (G5-HT; all at 100 μM), were ineffective in producing an increase in rotation rate. The number of embryos/egg masses for each treatment is as follows: control: 26/2; 5-HT: 20/2; OA: 28/2; DA: 24/2; G5-HT: 25/2. Asterisk denotes statistically significant difference compared to control value ($p < 0.0001$; ANOVA).

Figure 36: Effect of serotonin on frequency of rotational surges in stage E25 embryos. **A.** Serotonin decreased surge frequency in a dose dependent manner. **B.** Prolonged exposure of embryos to 100μM serotonin induced a maintained decrease in surge frequency (n =21). **C.** The effect of serotonin on surge frequency was completely reversible within 60 minutes of returning embryos to APW (n = 13).

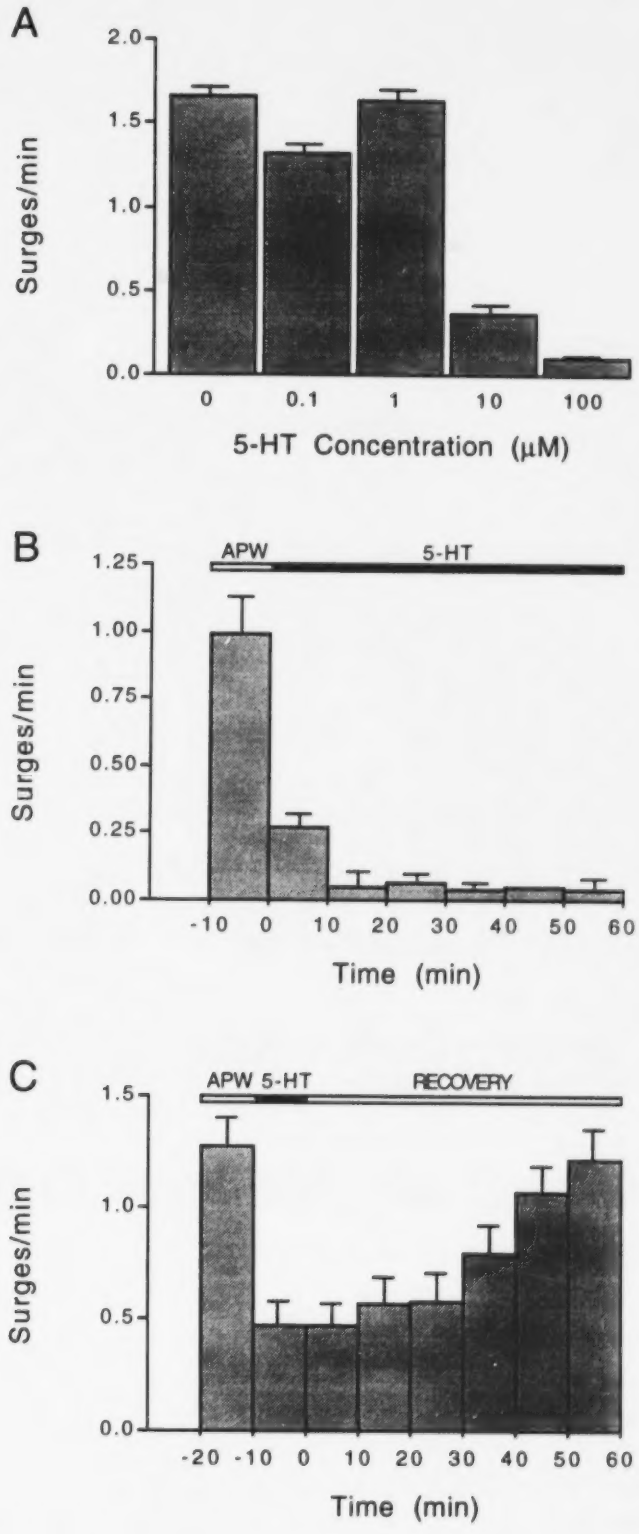
A
Surges/min
2.0
1.5
1.0
0.5
0.0
0
0.1
1
10
100
5-HT Concentration (μM)
B
APW
5-HT
Surges/min
1.25
1.00
0.75
0.50
0.25
0.00
-10
0
10
20
30
40
50
60
Time (min)
C
APW 5-HT
RECOVERY
Surges/min
1.5
1.0
0.5
0.0
-20
-10
0
10
20
30
40
50
60
Time (min)

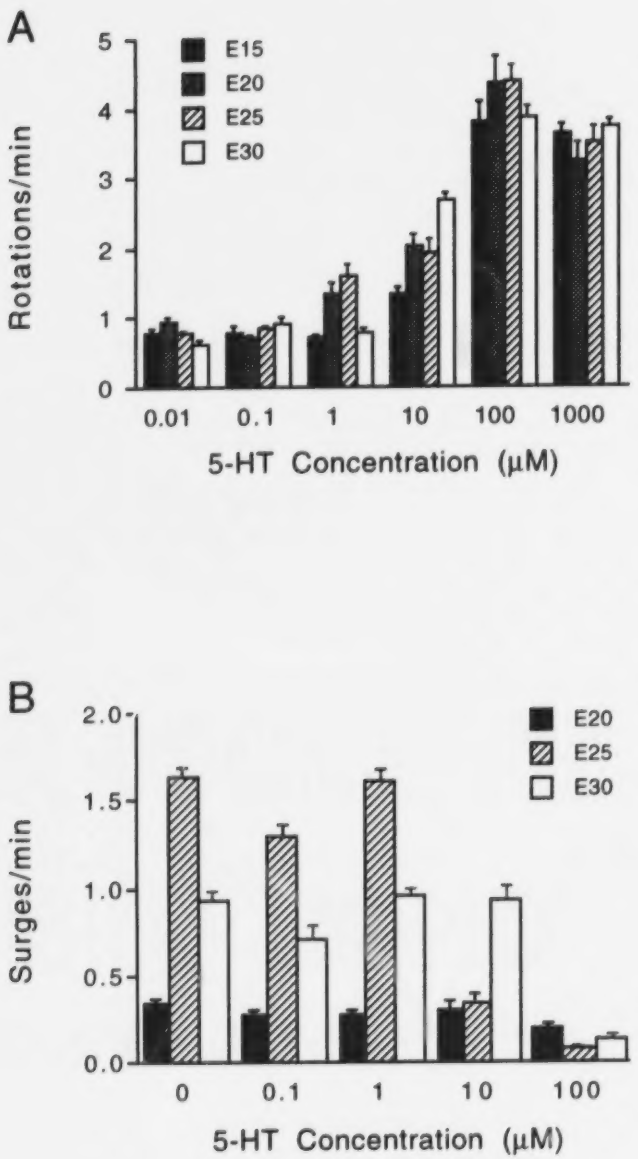

Figure 37: Dose-dependency of serotonin effects on rotation at different embryonic stages. **A.** Rotation rate. The matched control data (0 μM) serotonin) is illustrated in Figure 32. **B.** Frequency of rotational surges.

Figure 38: Effects of mianserin on rotation rate and surge frequency. **A.** When applied with serotonin, mianserin (100 μM) completely prevented the increase in rotation rate normally induced by serotonin (100 μM). When applied alone, mianserin (100 μM) lowered the rate of rotation below basal levels. The number of embryos (egg masses) examined under each treatment was as follows: Control: 25(2); 5-HT: 30(2); 5-HT+Mianserin: 28(2); Mianserin: 30(2). Asterisk denotes statistically significant difference in rotation rate compared to control value ($p < 0.0001$; ANOVA). **B.** Mianserin (100 μM) nearly abolished the occurrence of rotational surges. Control: 26(2); Mianserin: 30(2) (*: $p < 0.0001$; Student's t-test).

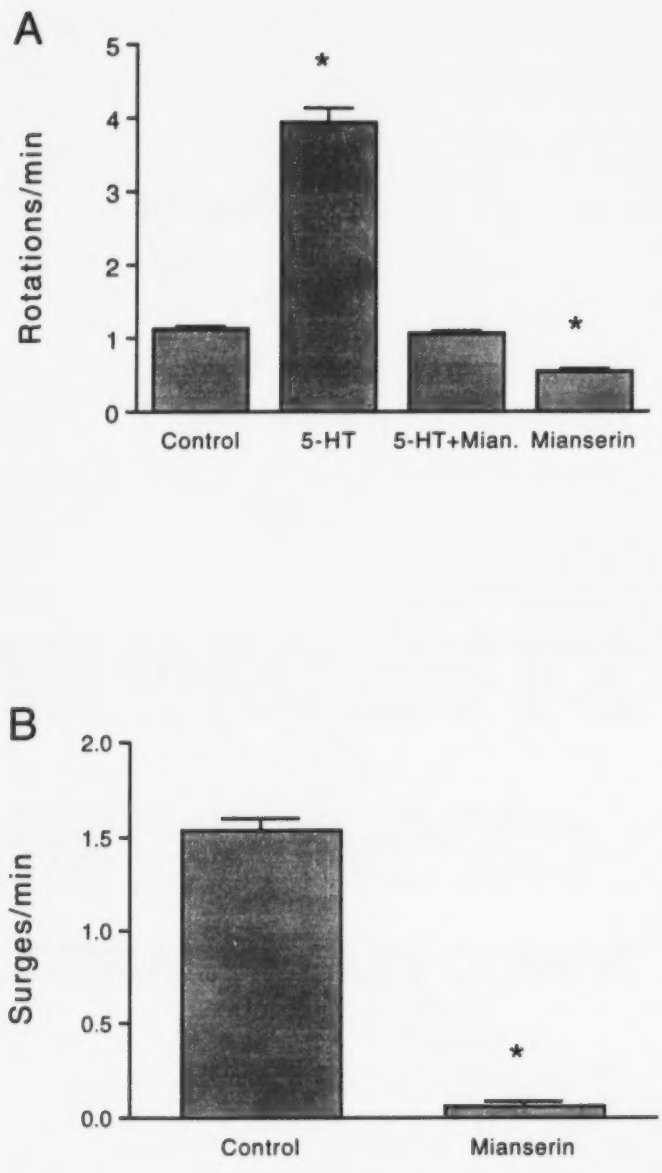
A
Rotations/min
5
4
3
2
1
0
*
*
Control
5-HT
5-HT+Mian.
Mianserin
B
Surges/min
2.0
1.5
1.0
0.5
0.0
*
Control
Mianserin

IV) Identification of ENC1 homologues in embryos of *Lymnaea stagnalis*

Some identified neurons are known to be phenotypically homologous among gastropod species (Granzow and Rowell, 1981; Senseman and Gelperin, 1973). *Lymnaea* has been extensively studied in terms of its development (Morrill, 1982), molecular genetics (Sugamori *et al.*, 1993), and neural basis for behaviors such as respiration (Syed *et al.*, 1993), locomotion (Syed and Winlow, 1989), and feeding (McCrohan and Benjamin, 1980). Given that *Helisoma* and *Lymnaea* are both in the order Limnophila, one may hypothesize that *Lymnaea* embryos possess a cell homologous to ENC1 of *Helisoma*. From a comparative standpoint, finding an ENC1-like cell in *Lymnaea* would strengthen the identity of ENC1 in *Helisoma* in that it would not be restricted to a single species. From a developmental standpoint, it would be interesting to see if ENC1-like cells can be found in the embryos of different gastropod species; that is to say, whether the concept of homology among neurons can be applied to the embryo.

In an immunohistochemical study of *Lymnaea* embryos, a serotonin-immunoreactive cell resembling ENC1 was not observed (Marois and Croll, 1992). In this chapter, an attempt was made to confirm this finding. In addition, a tyrosine hydroxylase antibody was used to determine if there exists an ENC1-like cell in *Lymnaea* which instead expresses dopamine instead of serotonin. Two findings suggest that the ENC1 of *Lymnaea* may express dopamine. First, D. A. Sakharov (personal communication) found that a cell resembling ENC1 in *Lymnaea* displayed fluorescence suggestive of the presence of a catecholamine using the glyoxylic acid technique. Second, Boer *et al.* (1984) found that the giant cerebral neuron of *Lymnaea* possessed both anti-serotonin and anti-dopamine immunoreactivity. This latter finding suggests that some serotonergic neurons may be able to express serotonin or dopamine. To determine if an ENC1-like cell in *Lymnaea* can be

located *in vivo*, the 5,7-DHT fluorescent labeling technique used to identify the *Helisoma* ENC1 *in vivo* was also employed[6,7].

i) Serotonin immunostaining

Given the previous characterization of serotonin expression in *Helisoma* (Goldberg and Kater, 1989) and *Lymnaea* (Marois and Croll, 1992) embryos, the immunohistochemical examination was restricted to embryonic stages which displayed interspecific differences in the distribution of serotonin immunostaining. At stage E45, *Helisoma* embryos possess three pairs of identified serotonergic neurons (Figure 39). Most prominent is the bilateral pair of ENC1 neurons located just anterior and dorsal to the cerebral ganglia (Figure 39A). These neurons first express serotonin at stage E13 (Results section I-i) and each extend a primary neurite anteromedially around the buccal mass primordium and conjoin at the pedal band of ciliated epithelial cells. At stage E45, a second pair of serotonergic neurons were present within the cerebral ganglia and extended a primary neurite which contacted the primary neurite of ENC1. These neurons were provisionally identified as ENC2. Unlike the naming scheme for pedal ciliated cells (Results section I-vii) in which the numerical designation refers to the hypothesized left or right cell homologue, the "2" in ENC2 specifies that ENC2 is the second serotonergic neuron observed in association with the developing cerebral ganglia. There are also two serotonergic neurons present in the pedal ganglia at this stage, ENP1 and ENP2 (Figure 39B). Both extend primary neurites ventrally toward the sole of the foot primordium, where they contact the primary neurite of ENC1. The full complement of serotonergic neurons is schematically represented in Figure 39C.

In *Lymnaea*, serotonin immunoreactive neurons are first visible at approximately stage E40 (Marois and Croll, 1992). Two neuron pairs have previously been identified at this stage (Marois and Croll, 1992), one pair residing in the cerebral ganglia and referred to as the "C4 neurons" and the other pair residing in the pedal ganglia, the "EPe1 neurons".

Lymnaea embryos were processed for serotonin immunostaining, and these findings were confirmed (Figure 40). By stage E40 in *Lymnaea*, a pair of serotonin-immunoreactive cerebral and pedal ganglion neurons are already present. In *Helisoma* embryos, the first pair of pedal ganglion neurons, ENP1, appeared initially at stage E35, a second pair at stage E40 to E45, which will be referred to as ENP2, along with a pair of neurons in the cerebral ganglia posterior to ENC1s , which will be referred to as ENC2 (Diefenbach and Goldberg, in preparation). This sequence of serotonin expression in *Helisoma* is similar to that reported for *Lymnaea* embryos (Marois and Croll, 1992), with the exception that at no time during development of *Lymnaea* embryos is a serotonin immunoreactive ENC1-like neuron observed.

ii) Tyrosine hydroxylase immunostaining

Tyrosine hydroxylase (TH) immunostaining is known to be absent in *Helisoma* embryos until about stage E65, when immunostained cells are first observed in the pedal ganglia and in sensory-like neurons of the developing foot (Goldberg, 1995). Given the disparity in serotonin immunostaining observed in *Helisoma* and *Lymnaea* embryos, I examined whether differences in TH immunostaining also existed. Indeed, TH immunostaining was resolved in early-staged *Lymnaea* embryos using CLSM (Figure 41). In 4 out of 5 stage E25 and 8 out of 11 stage E30 embryos, a single, bilateral pair of TH-positive neurons was observed in a location similar to that of ENC1 of *Helisoma* embryos: dorsolateral to the stomodaeum and one cell layer beneath ectodermal cells of the apical ectodermal plate. Morphologically, this TH-positive cell could be distinguished by an apical dendrite extending to the surface of the apical ectodermal plate, in addition to a ventrally directed neurite (Figure 41). TH immunostaining was confined to cytoplasm in the cell soma, the apical neurite, and about 20 μm along the ventrally-directed neurite proximal to the soma; immunostaining was not observed in distal processes. Thus, TH immunostaining

revealed a single pair of cells with a similar morphology and location as ENC1 of *Helisoma*.

iii) Identification of an ENC1-like cell *in vivo*

5,7-DHT has been shown to selectively stain ENC1 *in vivo* in *Helisoma* embryos (Results section I-v). This cell-labeling technique, followed by DIC microscopy, permits the consistent identification of ENC1 in the living embryo, to the extent that ENC1 is eventually identifiable through DIC optics without a need for prior 5,7-DHT labeling. I used this technique to determine if *Lymnaea* embryos also possess a cell like ENC1 which can accumulate 5,7-DHT. Stage E30 embryos of *Lymnaea* and *Helisoma* were incubated in 5,7-DHT solution overnight and the staining profiles compared. As reported previously, 5,7-DHT positive ENC1s were consistently observed in *Helisoma* embryos. Figure 42 is a DIC micrograph of a stage E30 embryo in right lateral profile. The arrowhead points to the soma of ENC1, the 5,7-DHT staining of which can be observed by switching directly to epifluorescence microscopy (Figure 42B). 5,7-DHT staining was confined to the soma, apical dendrite and the proximal segment of the ventral EPN. 5,7-DHT staining was consistently absent from the distal neurites of ENC1 in the foot primordium. Stage E30 *Helisoma* embryos possessed 5,7-DHT fluorescence, as determined in the previous section of the Results (section I-v) 88% of the time (n =67). The only other 5,7-DHT staining present was in the flame cells of the protonephridium and a subset of yolk cells, most of which were autofluorescent at the excitation wavelength of light used for 5,7-DHT imaging.

Lymnaea embryos treated with 5,7-DHT also possessed a single pair of 5,7-DHT-positive cells in a similar location as ENC1 in *Helisoma* embryos (Figure 43). These cells were located anterolateral to the stomodaeum, but more dorsomedial than ENC1 of *Helisoma*. A 5,7-DHT-positive cell from a stage E30 embryo is shown under fluorescence microscopy (Figure 43B) and at higher magnification under DIC optics (Figure 44). This

cell contained a neurite which extended ventrally toward the stomodaeum, and an apical dendrite which terminated at the lateral margin of the apical ectodermal plate (not visible in Figure 44; refer to Figure 45). In *Lymnaea*, unlike in *Helisoma*, this apical plate is ciliated. The ENC1-like cell in *Lymnaea* was positioned directly beneath the single ectodermal cell layer of the apical plate, in contact with the basal membranes of apical cells (Figure 44). Using 100X DIC optics, distinguishing morphological features were resolved and compared to those of ENC1 (Figure 45), which were described previously (Results section I-v). On the basis of its morphological similarity with ENC1, the ENC1-like cell of *Lymnaea* will be identified as $ENC1_{Lym}$. The nucleus in both ENC1 and $ENC1_{Lym}$ occupied much of the somal volume and possessed a single, centrally-situated nucleolus. Both cells contained numerous granules of different sizes in the cytoplasm. In ENC1, these granules were situated in the apical cytoplasm, whereas in $ENC1_{Lym}$, the granules were distributed throughout the cytoplasm. The granules in $ENC1_{Lym}$ were generally more numerous than in ENC1. Both neurons extended an apical dendrite to the ectodermal surface, terminating at the anterolateral margin of the apical ectodermal plate (in *Helisoma*; Figure 45C) and the apical ciliary band (in *Lymnaea*; Figure 45D) with an array of immotile cilia. The cilia of $ENC1_{Lym}$ appeared longer and were arrayed almost parallel to each other rather than in a radial arrangement as with the cilia of ENC1. Finally, both neurons projected a ventral neurite along the lateral margin of the stomodaeum. Although the primary neurite of $ENC1_{Lym}$ was difficult to follow to the pedal ciliary band, branching neurites were observed under high magnification DIC optics beneath the basal membrane of the pedal ciliated epithelial cells (Figure 46). Thus, both ENC1 and $ENC1_{Lym}$ share many morphological features which serve as identifying characteristics of ENC1.

Collectively, the immunohistochemical, 5,7-DHT, and DIC observations suggest that ENC1 and $ENC1_{Lym}$ are homologous neurons. However, they appear to differ in their neurotransmitter phenotypes, with ENC1 being serotonergic and $ENC1_{Lym}$ being catecholaminergic, based on its TH immunoreactivity. A prediction arising from the

hypothesis that ENC1 and $ENC1_{Lym}$ are homologous neurons is that $ENC1_{Lym}$ regulates cilia-driven rotational behavior through the release of a catecholamine neurotransmitter. Therefore, a pharmacological study was carried out to test the effects of serotonin, dopamine, octopamine, and other putative receptor antagonists on rotational behavior in *Lymnaea* embryos.

iv) Dynamics of rotational behavior of *Lymnaea* embryos

Rotational behavior of *Lymnaea* embryos, as previously characterized in *Helisoma* embryos (Results section II), consists of two components: rotation dorsally around the mediolateral axis, termed pitch rotation, and rotation around the dorsoventral axis, termed yaw rotation. It is known from the study of *Helisoma* that the pedal band of ciliated epithelial cells is responsible for generating pitch rotation, whereas the prototrochal ciliary band generates yaw rotation. Although a systematic examination of the relationship between ciliary activity and the directional components of rotation was not performed with *Lymnaea* embryos, they displayed qualitatively similar rotational components as *Helisoma*. The only observable difference was that *Lymnaea* embryos execute yaw rotation toward their left side, whereas *Helisoma* yaws toward the right. This difference is likely related to the left-handed (sinistral) and right-handed (dextral) body symmetry of *Helisoma* and *Lymnaea*, respectively. As described previously for *Helisoma* at stage E25, the yaw and pitch components of *Lymnaea* rotation can occur independently or in combination to produce transitions in the orientation of the embryo during a rotation cycle. Also similar to *Helisoma* embryos, *Lymnaea* embryos displayed distinct accelerations in rotation rate, or surges, which were best observed and quantified using time lapse video microscopy. Surges occurred predominantly in the pitch direction. Thus, *Lymnaea* embryos express rotational behavior which is qualitatively similar to that of *Helisoma* embryos.

v) Effects of serotonin and dopamine on rotation

All experiments were performed on stage E25 embryos of *Lymnaea*.

Figure 47A shows the response of *Lymnaea* embryos to serotonin, dopamine, and octopamine, all at 1.0 mM. Both 1.0 mM serotonin and 1.0 mM dopamine produced an approximate four-fold increase in rotation rate. The excitatory action of dopamine is in contrast to previous tests on *Helisoma* embryos which showed that dopamine had no effect on rotation rate (see Figure 35). Octopamine (1.0 mM), which is structurally similar to dopamine, had no effect on rotation rate in *Lymnaea*. To see if the increased rotation rate in *Lymnaea* is accompanied by a reduction in surge frequency as seen for *Helisoma* (Results section III-ii), surges were counted for the same embryos exposed to serotonin, dopamine and octopamine (Figure 47B). There were corresponding reductions in surges associated with the increases in rotation rate induced by serotonin and dopamine. Octopamine had no effect on surges.

The positive rotation response to dopamine was dose-dependent (Figure 48A) with a threshold response occurring at 100 µM dopamine. 100 mM dopamine produced a comparable enhancement of rotation as 10 mM dopamine (data not shown). This extremely low sensitivity to dopamine suggested the possibility that the drugs were encountering diffusion barriers to the receptor sites. Although the outer egg mass membrane was cut to expose the egg capsules to the external medium, the intercapsular jelly may impede the passage of drugs. To test this possibility, egg capsules were isolated from the egg masses and stripped of the intercapsular jelly. Isolation resulted in increased effectiveness of dopamine on stimulating rotation, especially at higher concentrations (Figure 48B). However, there was only a slight increase in the potency of dopamine's actions. Thus, the diffusion barrier associated with the intercapsulary fluid had a greater effect on response amplitude than on response sensitivity.

In order to better compare the effectiveness of serotonin and dopamine on rotation rate, a dose-response curve for serotonin was also obtained (Figure 49A). Serotonin

produced threshold increases in rotation rate at 10 µM, ten-fold less than that required to produce a threshold response with dopamine. A maximum rate was not obtained as 100 mM serotonin was not tested. The apparent greater sensitivity of embryos to serotonin than dopamine may be an artifact of differential effects of different barriers on serotonin and dopamine. Thus, *Lymnaea* embryos in isolated egg capsules were also tested for their responsiveness to various concentrations of serotonin (Figure 49B). Isolated embryos showed a threshold response at 1.0 µM serotonin , and a maximum response at 1.0 mM serotonin. Isolation appeared to shift the EC_{50} value to 10 µM, which is at least 10 fold less than that for intact embryos. In comparing the rotation responses of isolated *Lymnaea* embryos to dopamine and serotonin, the results suggest that, independent of the reduced accessibility of the drugs in semi-intact egg masses, *Lymnaea* embryos appear more sensitive to serotonin than to dopamine.

vi) Effects of dopamine receptor antagonists on rotation.

Three dopamine receptor antagonists were tested to determine: 1. Whether dopamine acts specifically on a dopamine receptor and 2. Whether endogenous dopamine, perhaps released from $ENC1_{Lym}$, stimulates rotation in *Lymnaea* embryos. Haloperidol is an antagonist with affinity for both the D_1 and D_2 subtypes of dopamine receptor. In combination with 1.0 mM dopamine, 0.1 mM haloperidol appeared to enhance rotation rate with respect to 1.0 mM dopamine alone (Figure 50A). In addition, 0.1 mM haloperidol by itself almost doubled basal rotation rate. Haloperidol was dissolved in 0.1 % dimethylsulfoxide (DMSO) which, by itself, had no effect on rotation rate. Domperidone, a dopamine D_2 receptor antagonist, at 1.0 mM had no antagonistic effect on rotation rate in combination with 0.1 mM dopamine (Figure 50B). Similarly, domperidone alone (1.0 mM) had no effect on rotation rate, nor did its 1% DMSO vehicle control. SKF83566, a specific antagonist for the dopamine D_1 receptor subtype, was also tested. In combination with 1.0 mM dopamine (the EC_{50} concentration for semi-intact egg masses; Figure 48A),

0.1 mM SKF83566 was completely effective in blocking the dopamine response. The rotation rate resulting from 1.0 mM dopamine and 0.1 mM SKF83566 was not significantly different from its matched control ($p > 0.50$, Student's t-test). SKF83566 alone at 0.1 mM did not have an obvious effect on basal rotation rate, however the rate was lowered slightly with respect to its matched control (*: $p < 0.05$, Student's t-test). SKF83566 at 1.0 mM also had no consistent effect on basal rotation (data not shown). Thus, a specific dopamine receptor antagonist could block the effect of dopamine on rotation rate of *Lymnaea* embryos, and another antagonist acted as an agonist to augment basal rotation rate in addition to the effect of dopamine. Although these results support a possible role for dopamine in regulating rotational behavior, given the inability of SKF83566 to lower rotation rate when applied on its own, more experiments are required to unequivocally demonstrate that dopamine is an endogenous cilioexcitatory neurotransmitter in *Lymnaea* embryos.

Figure 39: ENC1 in *Helisoma* is serotonin-immunoreactive. Conventional epifluorescence micrographs of a stage E45 embryo in left lateral profile illustrating half of the bilateral complement of serotonin-immunoreactive neurons present at this stage. **A.** At a lateral focal plane, two serotonin-immunoreactive neurons can be seen in association with the developing cerebral ganglia. The largest neuron is ENC1. Ventral to it is ENC2 (arrowhead), which extends a primary neurite that contacts the primary neurite of ENC1. **B.** At a more medial focal plane, the two pedal ganglion neurons, ENP1 (arrowhead) and ENP2, are visible. These neurons extend neurites which contact the primary neurite of ENC1 at the base of the foot primordium. **C.** Schematic showing the outline of the embryo and its left bilateral complement of serotonin-immunoreactive neurons. Scale bar = 20 μm.

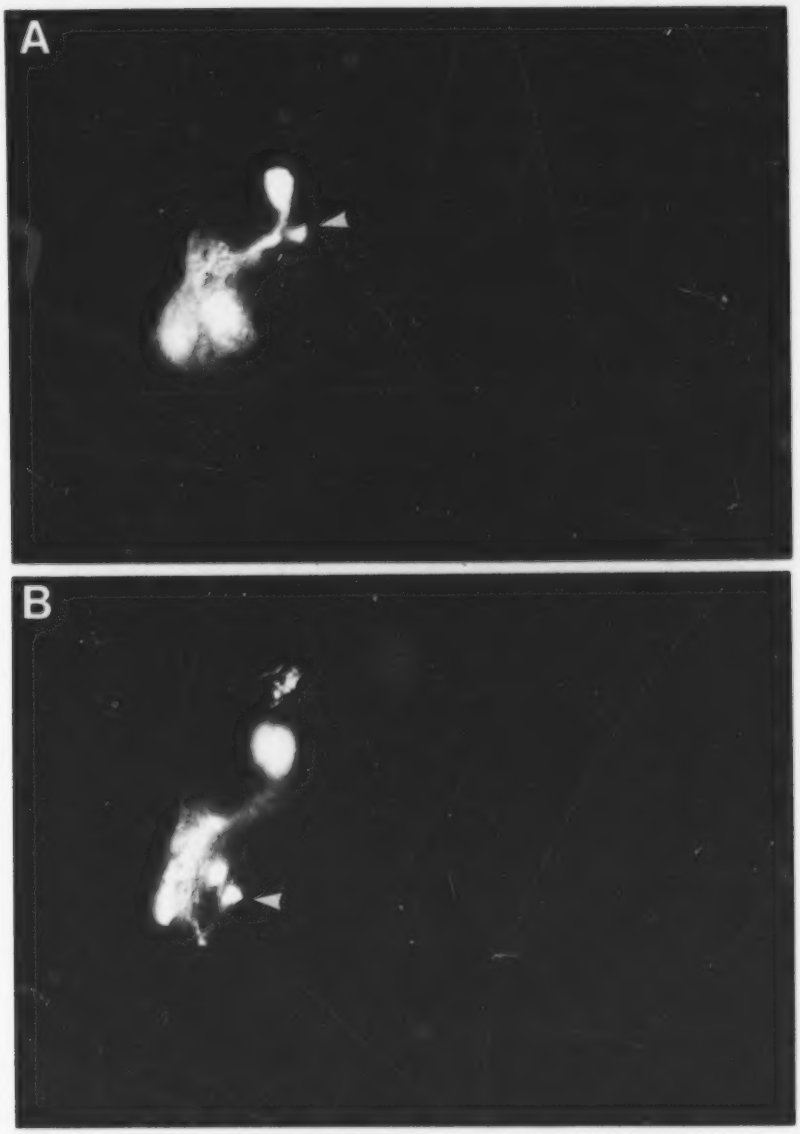
A
B
C

Figure 40: *Lymnaea* embryos lack a serotonin-immunoreactive ENC1. Conventional epifluorescence micrograph of a stage E40 *Lymnaea* embryo in left lateral profile (A) with accompanying schematic (B). The cerebral (C4; arrowhead) and pedal (EPe1) neurons are both present at this stage, but no ENC1-like neuron was observed. Note the immunostained neurite extending ventrally from the EPe1 cell toward the foot (arrow). Scale bar = 20 μm.

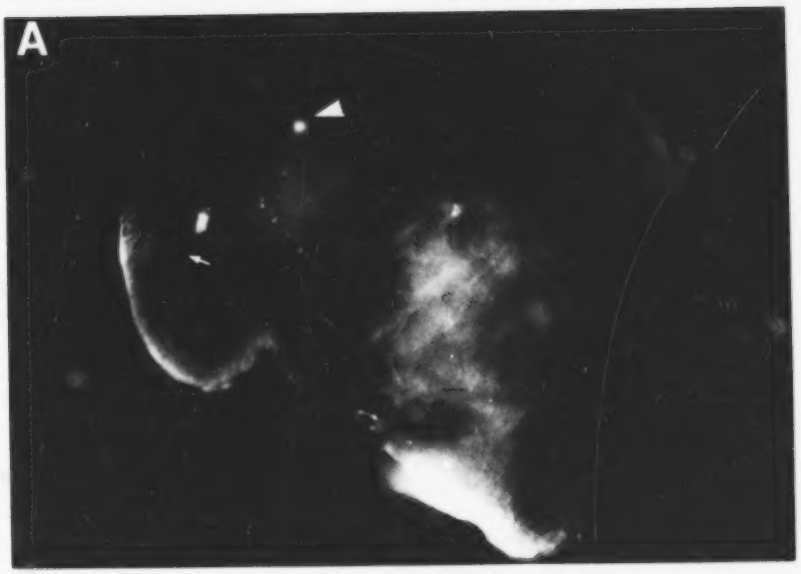
A

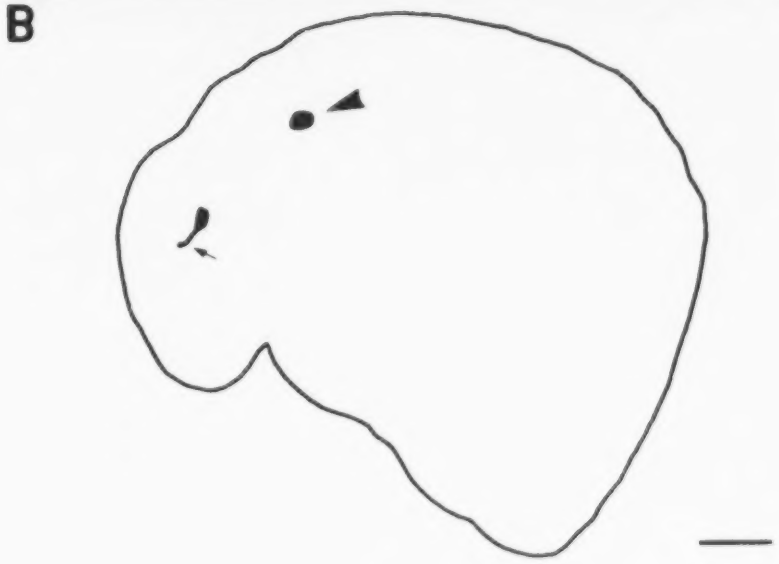
B

Figure 41: An ENC1-like cell in *Lymnaea* embryos shows TH immunoreactivity. Confocal section through a TH-positive cell of a stage E30 *Lymnaea* embryo in left lateral profile. TH immunostaining was resolved in the cell soma and proximal neurite (arrowhead), but was absent from distal neurites. Scale bar = 10 μm.

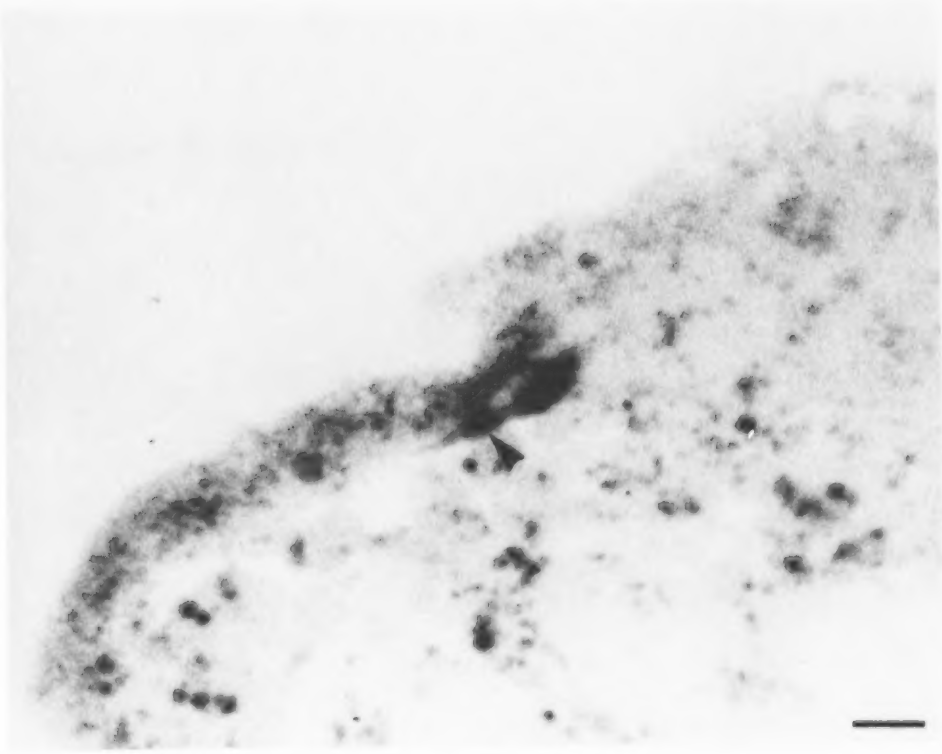

Figure 42: Identification of ENC1 in *Helisoma in vivo* using 5,7-DHT. **A.** DIC micrograph of a stage E30 embryo in left lateral profile showing the large yolk cells (asterisk), the developing foot primordium (f) and the stomodaeum (s). **B.** Complimentary fluorescence micrograph of the same embryo in panel A. ENC1 (arrowhead in panel A and B) was observed with the low intensity but specific 5,7-DHT staining confined to the soma. Although not visible here, staining was also present in the proximal segment of primary neurite, in addition to the apical dendrite. Note that a subpopulation of yolk cells (asterisk) also accumulated 5,7-DHT, while the remainder displayed intense autofluorescence at the excitation wavelength for 5,7-DHT. **C.** Schematic outline of the stage E30 embryo in panels A and B showing the position of ENC1 (arrowhead) in the embryo dorsomedial to the stomodaeum (hatched line). Scale bar = 20 μm.

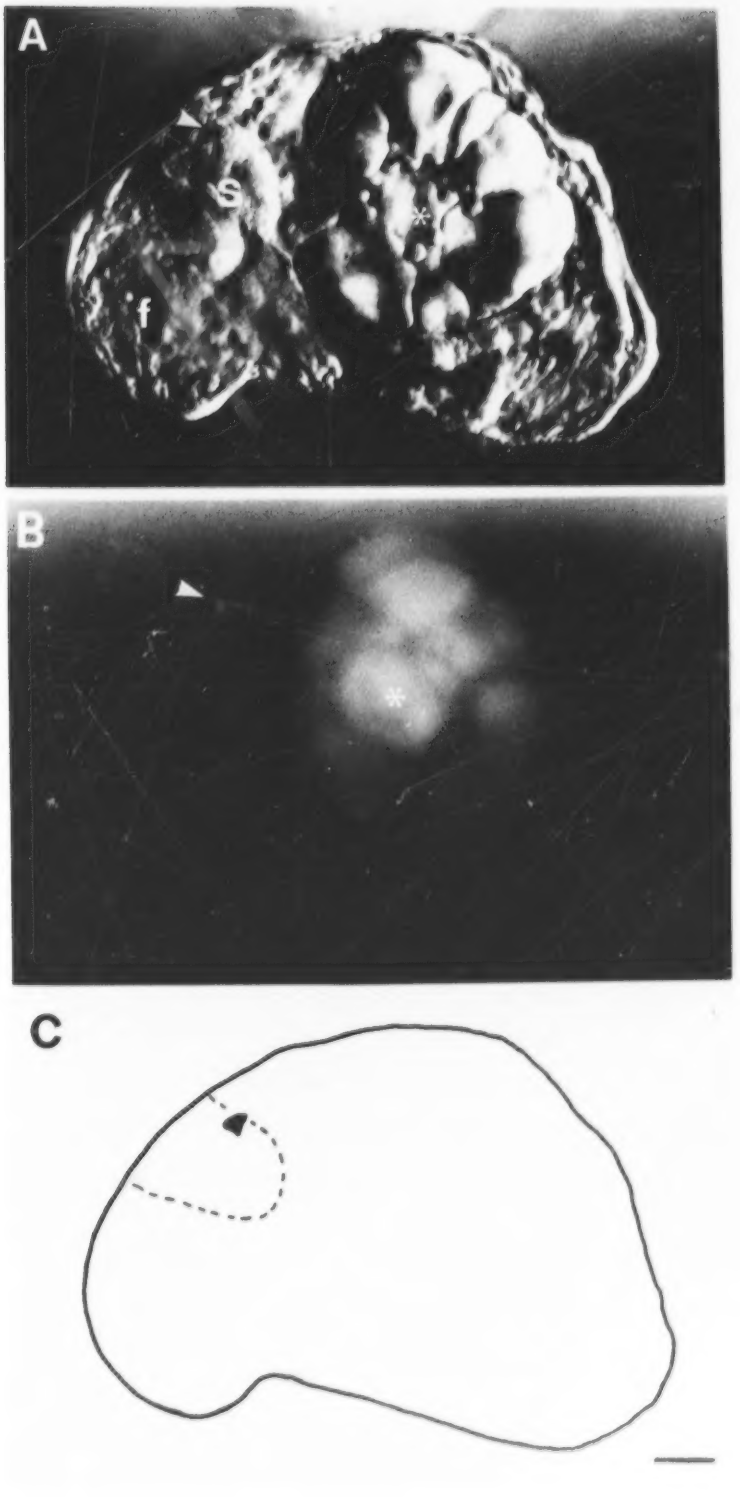
A
S
f
B
C

Figure 43: Identification of an ENC1-like cell in *Lymnaea* ($ENC1_{Lym}$). **A.** DIC micrograph of a left lateral profile of a stage E30 *Lymnaea* embryo. Note the morphological similarity between this embryo and the stage E30 *Helisoma* embryo in Figure 41A. Fluorescence micrograph of the same embryo as in panel A. An ENC1-like cell was observed dorsolateral to the stomodaeum (arrowhead) by virtue of faint 5,7-DHT fluorescence. Its soma is indicated in the DIC micrograph in panel A. A large proportion of the yolk cells at this embryonic stage also showed 5,7-DHT uptake. **C.** Schematic outline of the same embryo, with the dark oblong profile being the left ENC1-like cell (arrowhead). The cell occupied a more dorsomedial position relative to the stomodaeum than in *Helisoma* (compare with *Helisoma* in Figure 41C). Scale bar = 20 μm.

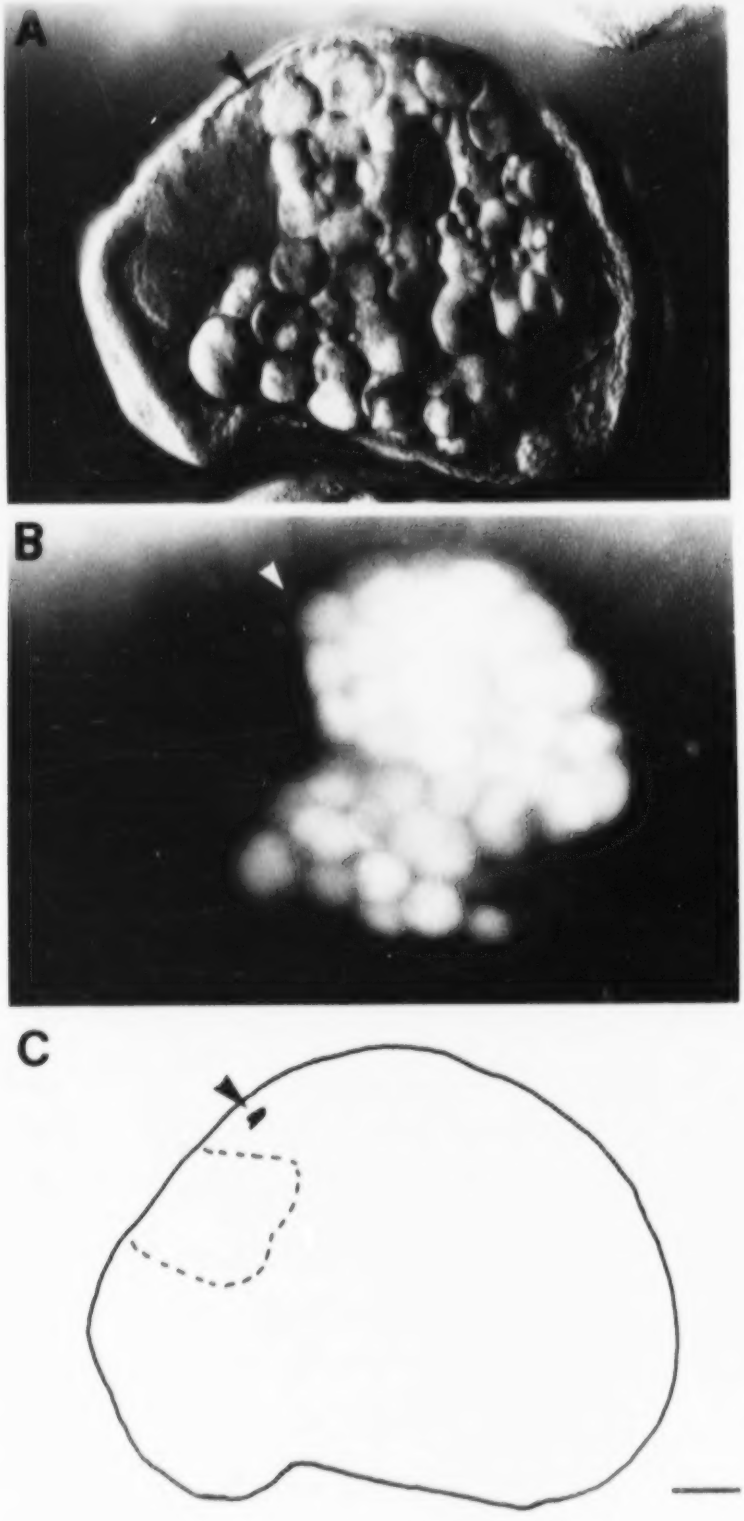
A
B
C

Figure 44: Morphology of $ENC1_{Lym}$ under DIC optics. **A.** High magnification DIC micrograph of $ENC1_{Lym}$ (arrowhead) from the stage E30 embryo in Figure 42. Characteristic morphological features of this cell included a neurite projecting anteroventrally along the lateral margin of the stomodaeum (arrowhead), a large, posteriorly-displaced nucleus with central nucleolus, and numerous granules displaced anteriorly in the cytoplasm. **B.** Schematic outline of the $ENC1_{Lym}$ soma (arrowhead) and neurite. The circular outlines are yolk cells and the array of lines on the dorsal surface represent cilia of the apical ciliary band. Scale bar = 10 μm.

A

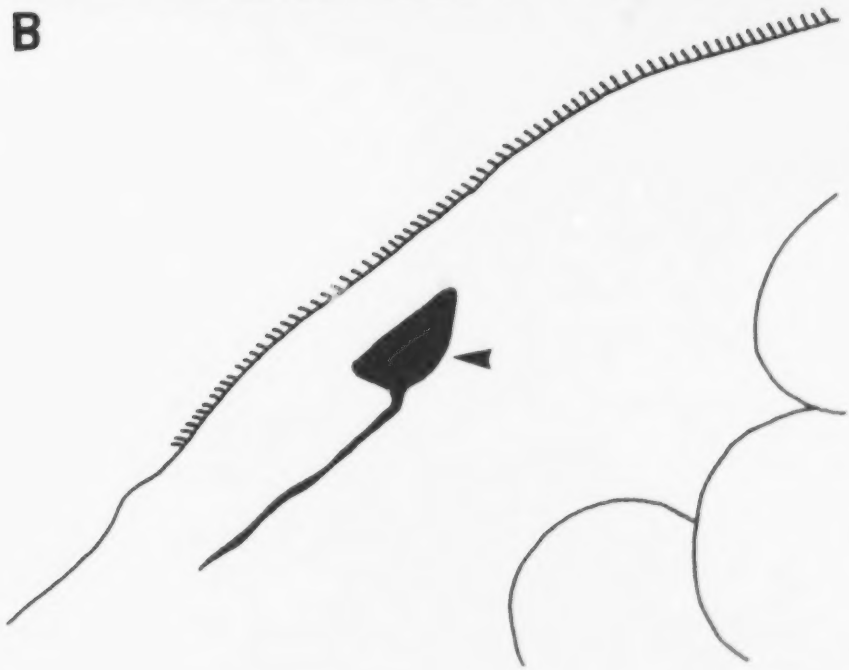
B

Figure 45: Similarity between $ENC1_{Lym}$ and ENC1 from *Helisoma*. High magnification DIC images of an $ENC1_{Lym}$ from *Lymnaea* (A; left dorsolateral profile) and an ENC1 from *Helisoma* (B; left ventrolateral profile), each from stage E25 to E30 embryos. Both neurons possess numerous granules of various sizes, a large nucleus (n) with central nucleolus, and a ventrally-directed primary neurite (arrowheads). Scale bar = 10 μm (A and B). In both *Lymnaea* (C) and *Helisoma* (D), an apical dendrite could be followed from the ENC1 somata to the ectodermal surface where a structure bearing an array of immotile cilia was seen (arrow in B, C and D). In *Lymnaea*, the bilaterally-paired ciliated structures were located on the lateral margins of the apical band of cilia (c), whereas in *Helisoma*, the apical plate is not ciliated (D). Scale bar = 5 μm (C and D).

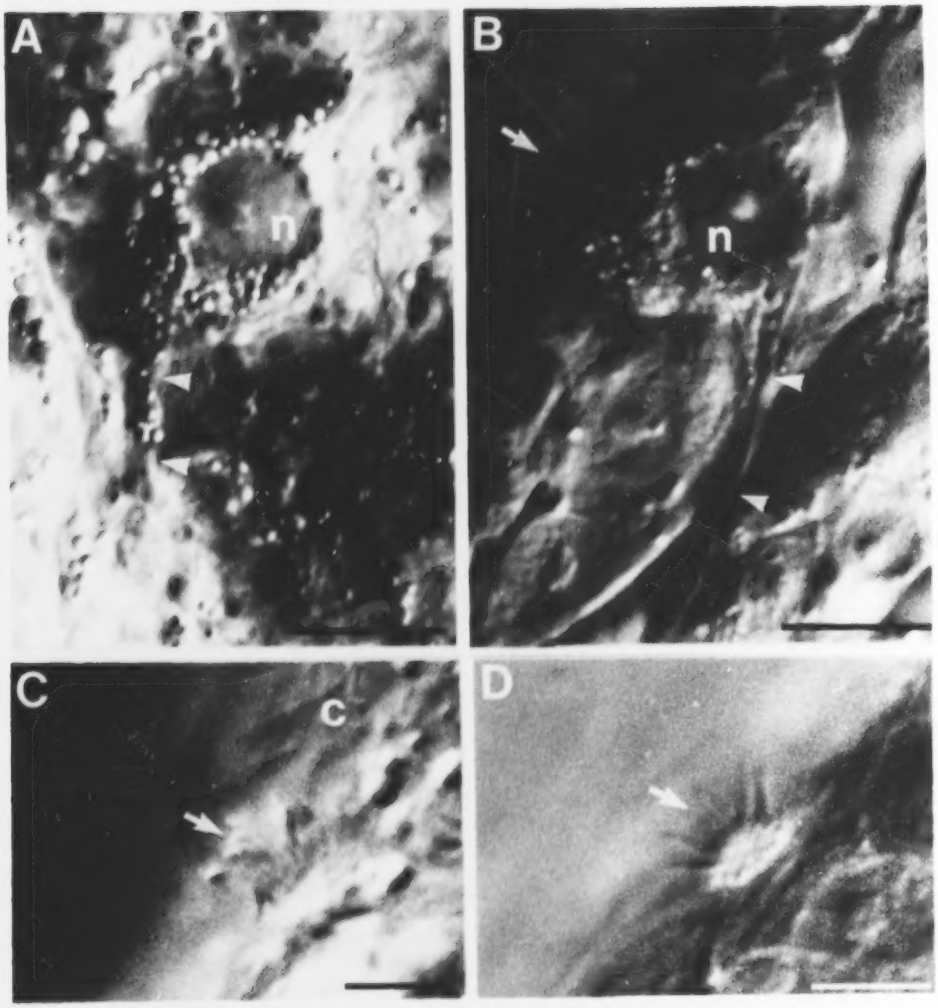
A
n
B
n
C
c
D

Figure 46: Putative neurites were observed associated with the pedal ciliary band of *Lymnaea*. High magnification DIC micrograph of the centre of the pedal ciliary band of a stage E25 *Lymnaea*. This image was obtained by focusing at the basal side of the ciliated cells. Numerous branching processes resembling neurites (small arrowheads outline one prominent branched process) were observed Scale bar = 10 μm.

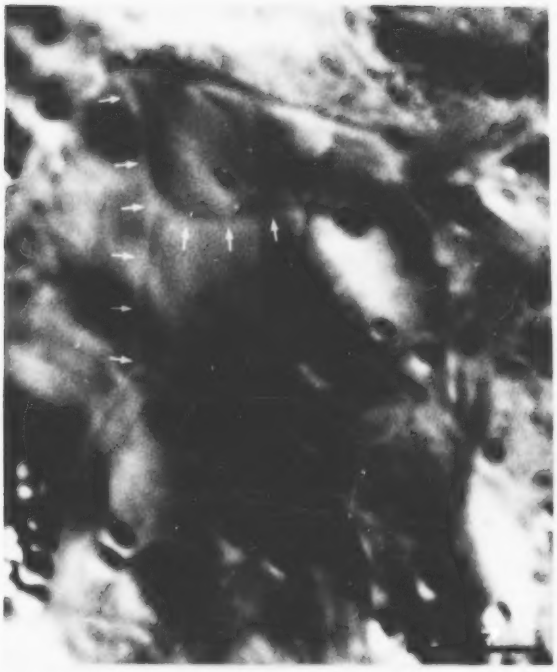

Figure 47: Effects of serotonin, dopamine and octopamine on rotation rate and surge frequency of *Lymnaea* embryos. **A.** 1.0 mM dopamine increased rotation rate by about four-fold, similar to the effect of 1.0 mM serotonin. Octopamine at 1.0 mM had no effect on rotation rate. Control (artificial pond water; APW): 87 embryos/6 egg masses; Serotonin (5-HT): 39/2; Dopamine (DA): 29/2; Octopamine (OCT): 24/2. **B.** Rotation rate increases induced by serotonin and dopamine (panel A) were associated with dramatic reductions in surge frequency. *: $p < 0.0001$; Student's t-test for panels A and B. Surge frequency was unaffected by octopamine.

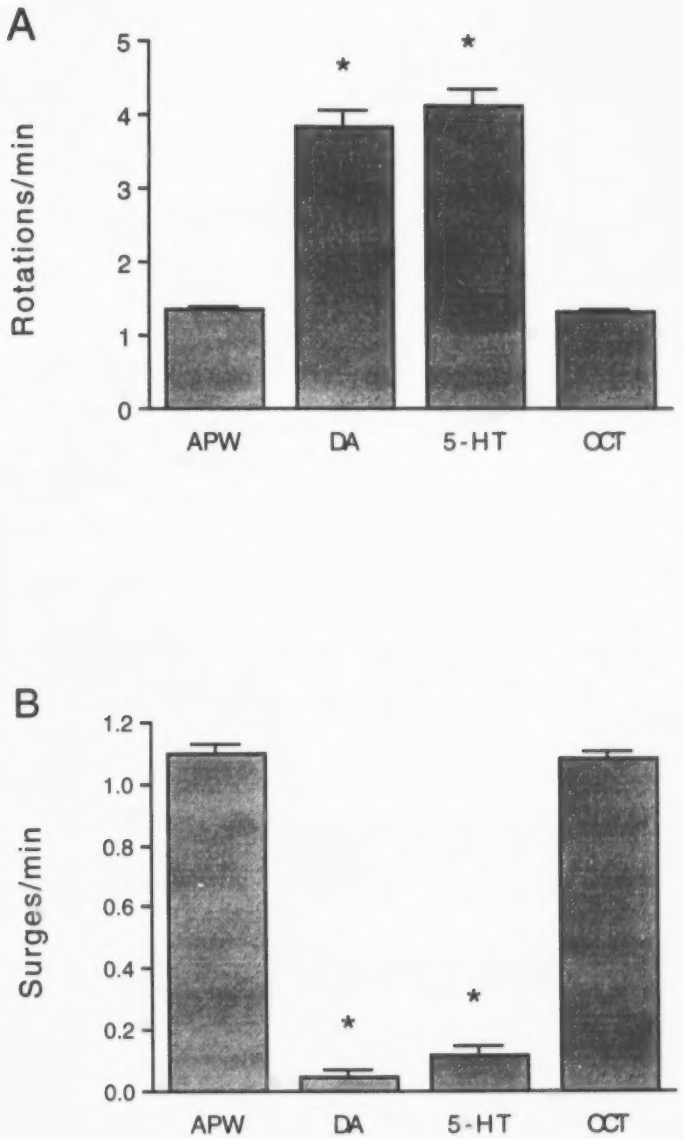
A
Rotations/min
5
4
3
2
1
0
*
*
APW
DA
5-HT
OCT
B
Surges/min
1.2
1.0
0.8
0.6
0.4
0.2
0.0
*
*
APW
DA
5-HT
OCT

Figure 48: Dose-dependent effects of dopamine on rotation rate in *Lymnaea* embryos. **A.** Semi-intact egg masses. Number of embryos/egg masses tested (concentrations in mM): Control (APW): 40/3; 0.001: 28/2; 0.01: 24/2; 0.1: 25:2; 1.0: 29/2; 10: 22/2. **B.** Isolated egg capsules. Isolation resulted in increased rotation, especially at the higher concentrations of dopamine. Number of embryos/egg masses: Control (APW): 62/6; 0.001: 22/2; 0.01: 12/1; 0.1: 12/1; 1.0: 13/1; 10; 10/1.

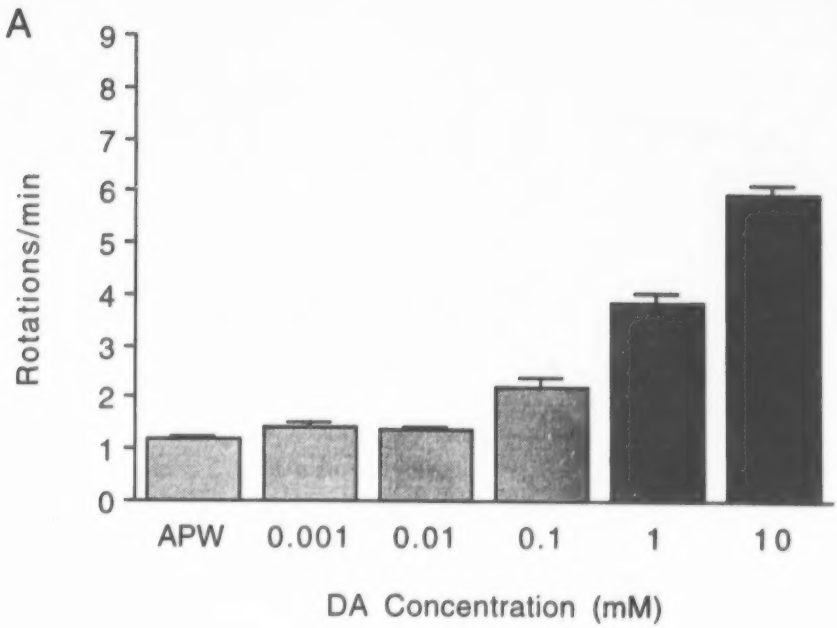
A
Rotations/min
0
1
2
3
4
5
6
7
8
9
APW
0.001
0.01
0.1
1
10
DA Concentration (mM)

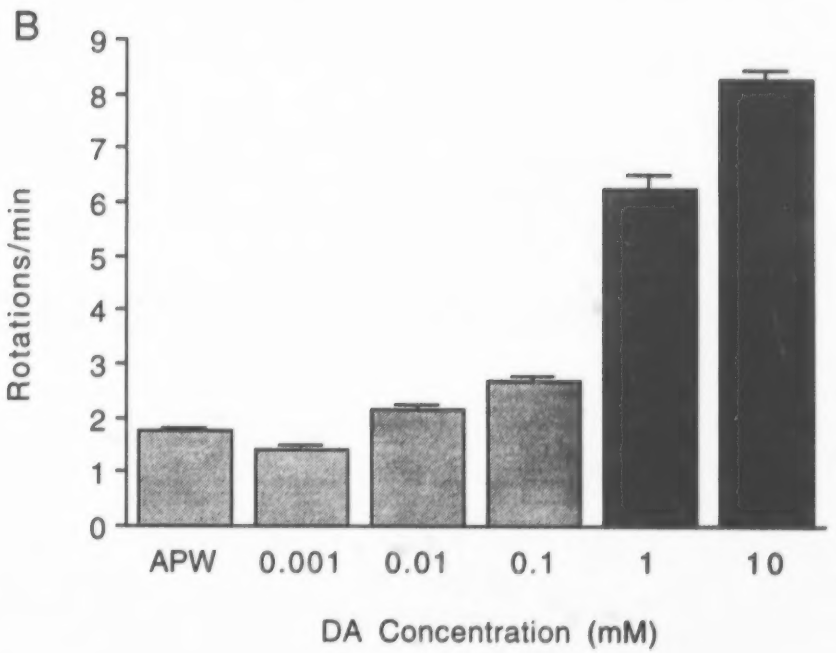
B
Rotations/min
0
1
2
3
4
5
6
7
8
9
APW
0.001
0.01
0.1
1
10
DA Concentration (mM)

Figure 49: Dose-dependent effects of serotonin on rotation rate in *Lymnaea* embryos. **A.** Semi-intact egg masses. Number of embryos/egg masses (concentrations in mM): Control (APW): 119/9; 0.001: 10/1; 0.01: 11/1; 0.1: 37/3; 1.0: 16/1; 10: 9/1. **B.** Isolated egg capsules. Both the amplitude and potency of serotonin's effects were enhanced as a result of isolation. Number of embryos/egg masses (concentrations in mM): Control (APW): 54/5; 0.001: 10/1; 0.01: 11/1; 0.1: 11/1; 1.0: 10/1; 10: 11/1.

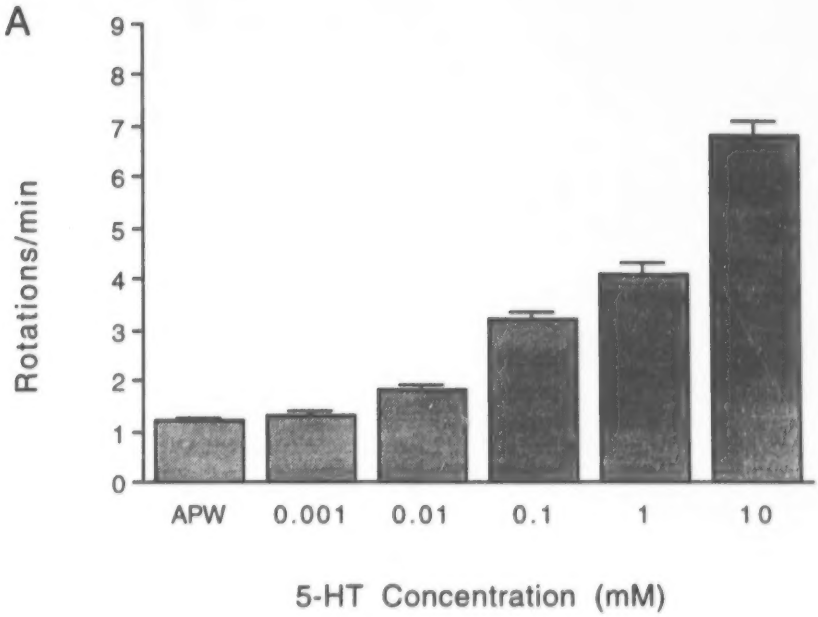
A
Rotations/min
0
1
2
3
4
5
6
7
8
9
APW
0.001
0.01
0.1
1
10
5-HT Concentration (mM)

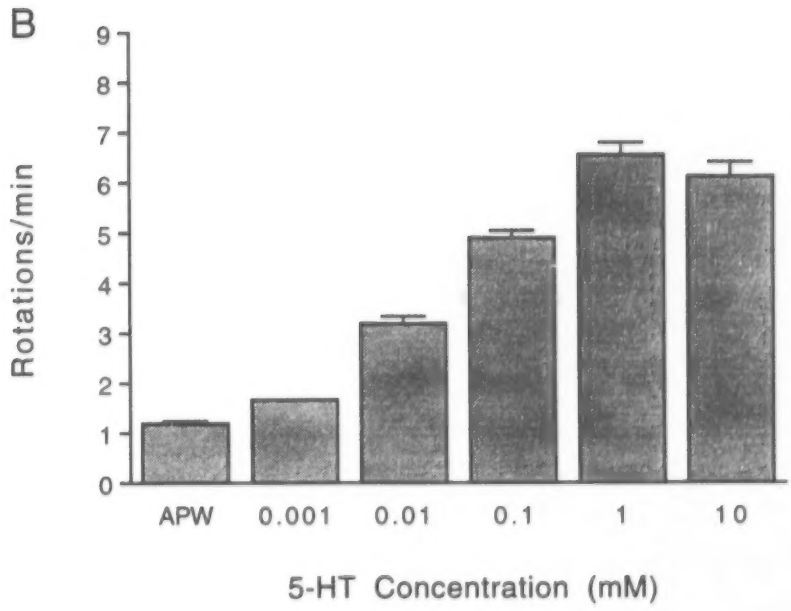
B
Rotations/min
0
1
2
3
4
5
6
7
8
9
APW
0.001
0.01
0.1
1
10
5-HT Concentration (mM)

Figure 50: Effects of dopamine receptor antagonists on rotation rate of *Lymnaea* embryos. **A.** 0.1 mM haloperidol combined with 1.0 mM dopamine resulted in a significant enhancement of rotation rate with respect to 1.0 mM dopamine alone. In addition, haloperidol by itself at 0.1 mM almost doubled rotation rate with respect to its matched APW control ($p < 0.0001$; Student's t-test). Number of embryos/egg masses: pooled control (APW): 65/5; dopamine (DA): 29/2; DA/HP (1.0 mM dopamine and 0.1 mM haloperidol): 24/2; HP (haloperidol, 0.1 mM): 13/1. **B.** 1.0 mM domperidone had no significant effect on rotation induced by 0.1 mM dopamine. Domperidone alone (1.0 mM) had no effect on rotation rate. Number of embryos/egg masses: Control (APW): 90/6; dopamine (DA, 0.1 mM): 25/2; 0.1 mM dopamine and 1.0 mM domperidone (DA/DP): 21/2; domperidone (DP, 1.0 mM): 25/2. **C.** SKF83566 was an effective antagonist of the response of *Lymnaea* embryos to dopamine. In combination with 1.0 mM dopamine, 0.1 mM SKF83566 completely blocked the dopamine response ($p < 0.0001$, Student's t-test). SKF83566 alone at 0.1 mM did not appear to reduce rotation rate, although the reduction was marginally significant ($p < 0.05$, Student's t-test). Number of embryos/egg masses: Control (APW): 79/5; dopamine (DA, 1.0 mM): 29/2; 1.0 mM dopamine and 0.1 mM SKF83566 (DA/SKF): 25/2; SKF83566 alone at 0.1 mM (SKF): 27/2.

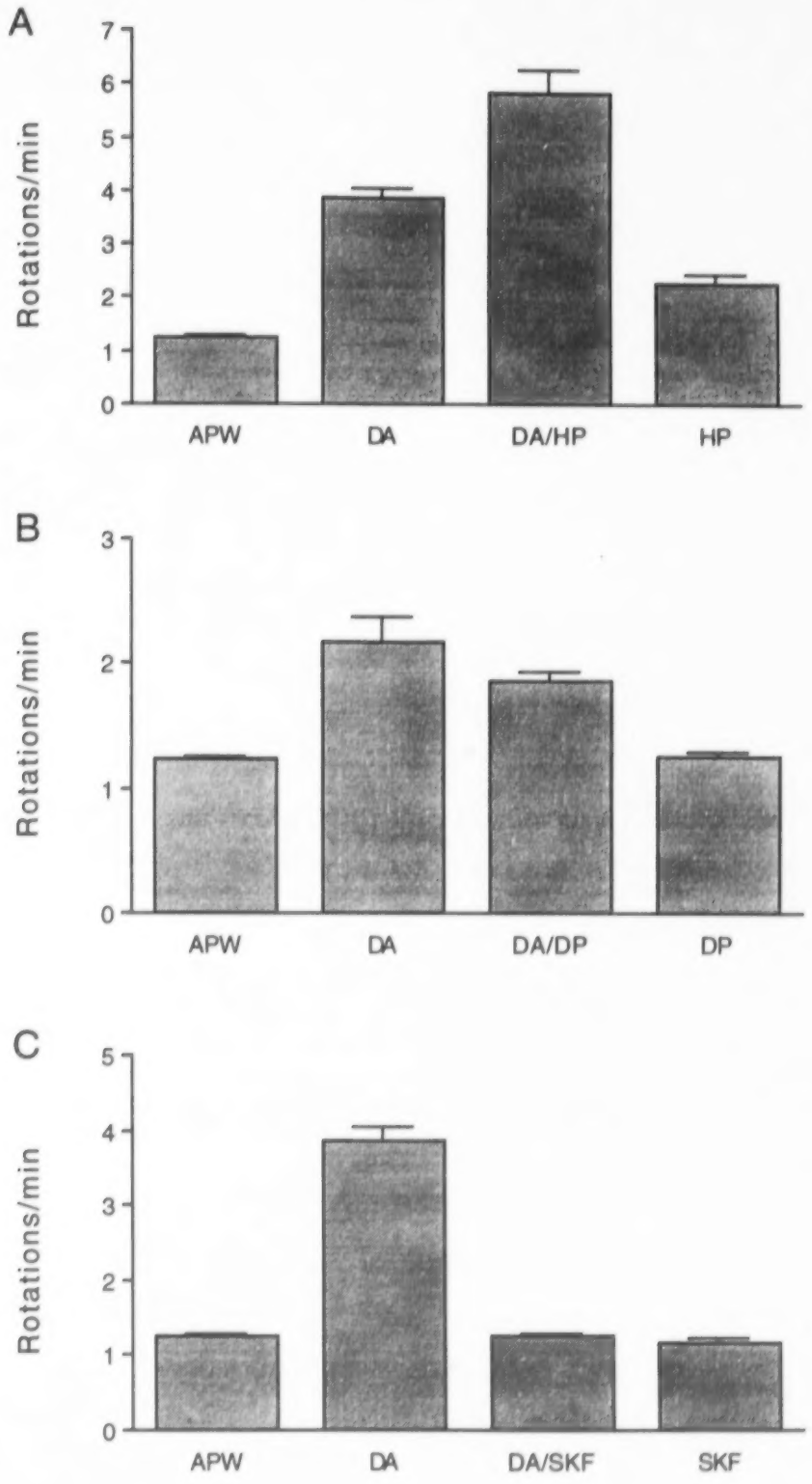
A
Rotations/min
7
6
5
4
3
2
1
0
APW
DA
DA/HP
HP
B
Rotations/min
3
2
1
0
APW
DA
DA/DP
DP
C
Rotations/min
5
4
3
2
1
0
APW
DA
DA/SKF
SKF

Discussion

The results outlined in this thesis provide the first descriptive account of the differentiation and development of an identified molluscan neuron with a defined neurotransmitter phenotype, ENC1. In addition, the possible dual role of serotonin in regulating neuronal development and an embryonic behavior in *Helisoma* was examined. Although previous studies have tested for a role of neurotransmitters in development, this is the first such study conducted at the level of a single identified neuron. In the last section of the results, a possible homologue of ENC1 was found in a related gastropod, *Lymnaea stagnalis*. Based on immunohistochemical and pharmacological findings, the *Lymnaea* homologue may express dopamine rather than serotonin, which is the putative neurotransmitter of ENC1 of *Helisoma*. The results will be discussed in turn and an attempt will be made to assess the significance of these findings in relation to the development and homology of molluscan neurons.

I) Development of ENC1 in *Helisoma*

Three aspects relating to ENC1 development deserve emphasis. First, the identity of ENC1 will be discussed from a morphological and comparative standpoint. Second, ENC1 underwent a stereotyped sequence of differentiation events that will be discussed from a comparative standpoint based on previous work on neurons from other invertebrate and vertebrate systems. Third, the elaboration of backbranches between EPNs in the target cell region was correlated temporally with the development of the pedal band of cilia. This latter result will be discussed in relation to potential cell-cell interactions responsible for the coordination of neurite branching with expansion of the target area.

i) Identity of ENC1 as possible sensorimotor neuron

ENC1 is the first serotonergic neuron to develop in the late gastrula of *Helisoma* and may be the first neuron to develop during embryogenesis. Although originally thought to be a cerebral ganglion neuron (Goldberg and Kater, 1989), three observations point to the contrary. First, ENC1 differentiated from large-celled ectoderm of the apical ectodermal plate, whereas cerebral ganglion neurons differentiate from the bilateral cephalic plates (Raven, 1975; McAllister *et al.*, 1983). Second, although ENC1 sent a projection into the cerebral ganglia, ENC1 was located anterior to, rather than internal to the cerebral ganglia in later-staged embryos and it maintained contact with the epithelial surface up to hatching and in juvenile snails. Third, ENC1 lost its serotonin immunoreactivity between stages E65 and E70. Marois and Croll (1992) reported that the neuron which develops into neuron C1 in *Lymnaea* appears at stage E75. At no time during its expression of serotonin was this neuron observed to be in contact with the epithelial surface via an apical dendrite, nor did it lose its serotonin immunoreactivity later in development. Thus, the development of neuron C1 clearly differs from that of ENC1. Collectively, these findings support the identity of ENC1 as being a heretofore unidentified peripheral neuron with input to the cerebral ganglia.

The morphology of ENC1 suggests that ENC1 may function as both a primary sensory neuron and a motor neuron. In regard to a putative sensory function, a unique feature of ENC1 is its apical dendrite tipped with a structure that bears a striking resemblance to the "dendritic knob" of olfactory neurons in vertebrates (Morrison and Costanz, 1990; Muller and Marc, 1984; Zielinski and Hara, 1988). A previous scanning electron microscopic examination of *Helisoma* embryos revealed these as the only two structures of their kind on the surface of the embryo (McKenney and Goldberg, 1989). Yi and Emery (1991) found similar structures at the tips of receptor cells of the olfactory organ of adult *Helisoma* and likened them to the "sensory knobs" of the optic tentacles of the land snail *Limax maximus* (Kataoka, 1976) and the slug *Arion ater* (Wright, 1974). However,

the sensory knobs of *Helisoma* possessed far fewer cilia than the ciliated structure of ENC1. To facilitate reference to this structure, it will provisionally be referred to as the "spinorbium" from the Latin words *spin* for "spine" and *orbis* for "circle".

It is possible that the spinorbium subserves a chemosensory or mechanosensory function in the embryo. The apical dendrite and spinorbium persisted in ENC1 up to stage E100 (hatching) and in newly hatched juvenile snails (stage P1), as resolved using 5,7-DHT fluorescence (figure not shown). Thus, if ENC1 is retained in the adult snail, it may also serve in chemoreception or mechanoreception. In a preliminary transmission electron microscope study of ENC1, the spinorbium was found to possess longer extensions which were identified as immotile cilia and shorter extensions which were microvilli (Koss, Diefenbach and Goldberg; in preparation). Microvilli have also been found on the sensory knobs of primary olfactory receptors in *Helisoma* and other species (Yi and Emery, 1991). The presence of cilia and microvilli suggests that this sensory terminal may transduce more than one kind of environmental signal, chemosensory or mechanosensory. Possible signals could include the amount of oxygen in the perivitelline fluid (Strathmann and Chaffee, 1984), contact with the interior of the capsular wall which may induce "settlement" as occurs with marine gastropod veligers (Chia *et al.*, 1984), and cues from other embryos to coordinate development. In the squid, *Loligo vulgaris*, the timing of hatching of the embryos may be regulated by a "natural tranquilizing factor" found in the perivitelline fluid which prolongs embryonic development and prevents premature hatching (Weischer and Marthy, 1983). Although report of such a factor in gastropods is lacking, such a factor may maintain the synchrony of development among sibling embryos, which can differ in the onset of first cleavage by between 40 and 60 minutes (Morrill, 1982).

As a possible peripheral sensory neuron, ENC1 shares features with other sensory neurons found in gastropods. ENC1 resembles the "type 2" sensory cells which populate the rhinophores and tentacles of the sea hare *Aplysia californica* (Emery and Audesirk, 1978). However, whereas the cilia of ENC1 are about 3 μm in length, the cilia of the type

2 sensory cell are 10 μm long. ENC1 also resembles the primary sensory cells which populate the chemoreceptor of the ommatophore of the land snail, *Helix pomatia* (Wondrak, 1975). In terms of their location (anterodorsal region of head) and possession of cilia-like projections, it is possible that ENC1s are single-cell functional homologues of the apical sensory organ described in marine nudibranch larvae (Bonar, 1978; Chia and Koss, 1984; Marois *et al.*, 1993). The apical organ consists of three cell types, one of which is the multiciliated cell with an axon projecting into the cerebral ganglia (Bonar, 1978). However, in contrast to the simple apical dendrite and spinorbium of ENC1, the multiciliated cell possesses numerous individual tufts of cilia that project from a luminal compartment which occupies much of the somal volume. Furthermore, the apical organ is unpaired whereas ENC1s are a bilateral neuron pair. Finally, the sensory cells of the apical organ in larval *Aplysia* have been reported *not* to be serotonergic (Marois *et al.*, 1993). Thus, the ciliated cells of the apical organ and ENC1s are cell types with distinct morphologies and neurotransmitter phenotypes. Therefore, from a comparative morphological standpoint, ENC1 may be a primary sensory neuron subserving a chemosensory role in *Helisoma* embryos. Further to this hypothesis, central serotonergic neurons from invertebrates as evolutionarily divergent as *Aplysia* (Rosen *et al.*, 1982), the moth, *Manduca sexta* (Sun *et al.*, 1993), the lobster (Beltz *et al.*, 1992) and crayfish (Sandeman *et al.*, 1988), play roles in chemosensation or olfaction. With further study, it is possible ENC1 may provide another example of serotonin's role in chemoreception.

ENC1 may also be a motor neuron which, through innervation of the pedal ciliary band, may regulate cilia-driven rotational behavior of *Helisoma* embryos as they develop in their egg capsules (Diefenbach *et al.*, 1991). The confocal and DIC studies of ENC1 neurites at the pedal ciliary band resolved EPNs to be in contact with and localized exclusively within the confines of the pedal ciliary band. Furthermore, in a preliminary transmission electron microscope examination of *Helisoma* embryos, neurites of ENC1 were observed to penetrate the basal ciliary membranes and form discrete sites of

membrane-to-membrane contact. In addition, numerous vesicles were localized to the termini of neurites in apposition with ciliated cells (Koss, Diefenbach and Goldberg; in preparation). Thus, ENC1 forms putative synapses with the pedal ciliated cells. These morphological findings, in combination with the cilio-excitatory effect of serotonin on rotational behavior (discussed later), strongly suggest that ENC1 is a motor neuron which utilizes serotonin as its neurotransmitter. Although no sensory role for ENC1 or serotonin has been found, the morphological and behavioral results point strongly to the identity of ENC1 as a "sensorimotor neuron". Typically, neurons have either a sensory or motor function, or communicate between neurons as interneurons. ENC1 is therefore unique in that it shares features of both sensory and motor neurons. Whether ENC1 represents a single-neuron sensorimotor circuit awaits a study of the sensory function of ENC1, and whether this function affects rotational behavior through the release of serotonin onto pedal ciliated cells.

ii) ENC1 as potential pioneer neuron

It is also possible that during embryogenesis, ENC1 serves as a pioneer neuron (Bate, 1976; Wilson and Easter, 1991) for other neurons. Other identified serotonergic neurons from the cerebral and pedal ganglia extended neurites along part of the neurite outgrowth pathway established initially by ENC1. Whether these serotonergic neurons are recognizing ENC1 neurites as a preferential substrate or are guided along by other cues, such as extracellular matrix molecules (Letourneau *et al.*, 1994), awaits further study.

The sequence of appearance of the first cerebral and pedal neurons reported in this thesis differs from that of *Lymnaea stagnalis* (Marois and Croll, 1992) and the preliminary study on *Helisoma* embryos (Goldberg and Kater, 1989). In comparing stage E45 of *Lymnaea* and stage E40 to E45 of *Helisoma*, *Lymnaea* lacks a serotonin-immunostained ENC1, yet both species possess a cerebral ganglion neuron called C4 in *Lymnaea* and ENC2 in *Helisoma*, in addition to a pedal ganglion neuron called EPe1 in *Lymnaea* and

ENP1 in *Helisoma*. The cerebral and pedal neurons are connected through the cerebropedal commissure. As will be discussed later, *Lymnaea* possesses an ENC1-like neuron which does not express serotonin. Marois and Croll (1992) reported that the C4 neuron appears first, followed by the EPe1 and EPe2. Goldberg and Kater (1989) found similarly that, after ENC1, the ENC2 appeared followed by the pedal neurons. From my observations of *Helisoma* embryos, I found that the second serotonergic neuron to appear after ENC1 is ENP1, followed by ENC2 and ENP2 appearing at roughly the same time after ENP1. In short, the cerebral neuron (ENC2) precedes the pedal neurons in *Lymnaea*, whereas the cerebral neuron appears after the pedal neurons in *Helisoma*. Although it is difficult to speculate as to the reason for this difference in time course of serotonin expression in these seemingly homologous neurons, the early expression of serotonin in ENC1 may be a determining factor. For example, expression of serotonin in ENC1 may delay the expression of serotonin in ENC2. This hypothesis could be tested by ablating ENC1 prior to the expression of serotonin in ENC2 and monitor the time course of serotonin expression in ENC2 for delays.

II) Chronology of Differentiation Events

From the results, a tentative sequence of cellular events associated with ENC1 differentiation can be proposed and is illustrated in Figure 51. From stage E13 to E15, ENC1 first displayed serotonin immunoreactivity, followed by neurite outgrowth initiation, pedal ciliary band contact, EPN fasciculation, extension of the apical dendrite and development of the spinorbium. Backbranching of EPNs was then initiated between stage E15 and E20, during which time 5,7-DHT uptake capacity was first visualized. Lateral branching of the EPNs occurred at around stage E30 toE35. Later in development, serotonin immunoreactivity disappeared between stage E65 and E70 (not shown in Figure 51).

i) Expression of serotonin immunoreactivity

It is possible that serotonin was expressed in ENC1 prior to the initiation of neurite outgrowth. In many invertebrate neurons, neurite outgrowth initiation precedes neurotransmitter expression. This is the case for the octopaminergic dorsal unpaired median neurons (DUM) of grasshopper embryos (Goodman and Spitzer, 1979), hermaphrodite specific serotonergic neurons of the nematode, *Caenorhabditis elegans* (Desai *et al.*, 1988), the posteromedial serotonergic neurons of the leech, *Haementeria ghilianii* (Stuart *et al.*, 1987), the FMRFamide-containing L1 and CF neurons of the hawkmoth, *Manduca sexta* (Wall and Taghert, 1991), and the serotonergic cell S1 of the grasshopper (Taghert and Goodman, 1984). However, in cultured embryonic *Drosophila* neurons, expression of choline acetyltransferase and acetylcholine esterase precedes neurite outgrowth initiation (Salvaterra *et al.*, 1987). For vertebrate neurons, neurite outgrowth can precede (Sieber-Blum *et al.*, 1983) or follow (Whitnall *et al.*, 1985) neurotransmitter expression, although there are few studies that have employed the temporal resolution necessary to establish a definite sequence. At least among invertebrates, the differentiation sequence of neurotransmitter expression and neurite outgrowth initiation appears to be specific to the identified neuron in question. In confocal images in which growth cones of EPNs were approaching the target, serotonin-immunoreactive granules were observed in the neurites and in growth cones. Serotonin immunoreactivity was evident even in a growth cone which had progressed one cell body length from ENC1 (figure not shown). Although the outgrowth rate of the EPNs is not known, growth cone advance rates *in vivo* range from 35 to 120 µm/h (Harris *et al.*, 1987; Pike *et al.*, 1993; Wang *et al.*, 1993). Given that the EPNs traverse less than 30 µm to reach their target, it may take the growth cones between 1 h and 15 min to cover this distance, although pauses in outgrowth (for example, see Myers *et al.*, 1986) may lengthen this time. Given that fast axonal transport rates, on the order of 10 400 to 16 700 µm/h (Sheetz *et al.*, 1989) are sufficient to keep up with neurite outgrowth rates *in vivo*, one may assume that there was sufficient serotonin at the time of

neurite outgrowth initiation for it to appear in the growth cone. If this was the case, then serotonin expression commences prior to neurite outgrowth initiation. An alternative scenario would be for neurite outgrowth to begin prior to serotonin expression. This could result from the growth cone pausing long enough in the pathway for serotonin synthesis and transport to catch up with growth cone advance. Observing a serotonin-immunostained ENC1 without a neurite would answer the question of whether serotonin expression precedes neurite outgrowth, however, I have not been able to make such an observation. The relative contribution of intrinsic and extrinsic factors in regulating this sequence await complimentary *in vitro* study, which is afforded by the cell culture techniques already developed for *Helisoma* embryos (Goldberg *et al.*, 1988).

ii) Serotonin immunoreactivity in the EPN growth cone

EPNs displayed greater intensities of serotonin immunostaining in the growth cones than in the neurites. Circular profiles within the neurites and growth cones resembling vesicles were also observed. Wall and Taghert (1991) reported that the expression of FMRFamide-like immunoreactivity in the L1 and CF neurons of *Manduca sexta* appeared in the growth cone prior to the soma and neurite. Growth cones are capable of sustaining protein synthesis, even after being isolated from the parent neuron (Davis *et al.*, 1992) and may thus be able to sustain neurotransmitter synthesis independent of the cell body as long as a sufficient complement of mRNA is present for translation. Growth cones contain polyribosomes and rough endoplasmic reticulum (Davis *et al.*, 1992). Growth cones show characteristics of mature synapses prior to synaptogenesis (Ivgy-May and Gershon, 1994) including neurotransmitter uptake, expression of serotonin-binding protein, and the synaptic vesicle-associated protein synaptophysin (p38). Furthermore, growth cones of embryonic *Xenopus* spinal neurons have been found to spontaneously release acetylcholine (Young and Poo, 1983). These properties of growth cones suggest expression of neurotransmitter in the growth cone prior to synaptogenesis may serve to regulate a specific

feature of neurite outgrowth or target development. As will be discussed later, one candidate process is neurite branching.

iii) Uptake of serotonin by ENC1

Serotonin expression first appeared at stage E13 to E14 in large perinuclear granules concentrated in the apical cell pole. Since ENC1s apical dendrite maintains contact with the egg capsule medium and displays serotonin-like uptake capacity, it is possible that ENC1 is obtaining tryptophan, the amino acid precursor of serotonin, from the perivitelline fluid of the egg capsule. The perivitelline fluid of pulmonates contains amino acids such as tyrosine and tryptophan (Ramasubramaniam, 1979). The serotonergic C1 neuron of the land snail, *Helix pomatia* is reported to possess both serotonin and tryptophan uptake capacity (Pentreath and Cottrell, 1973), with tryptophan uptake being confined to the soma. Tryptophan is converted to 5-hydroxytryptophan, the immediate precursor of serotonin, by tryptophan 5-hydroxylase. Preliminary immunohistochemical findings using a commercially available antibody against tryptophan hydroxylase revealed specific tryptophan hydroxylase immunostaining in the soma of ENC1 (Diefenbach, unpublished observations). Furthermore, ENC1 displayed 5,7-DHT uptake in the soma and apical dendrite, but not in the neurites, although the neurites may be too thin for the 5,7-DHT fluorescence to be resolved. Given the low intensity of 5,7-DHT fluorescence, in addition to the fact that serotonin immunoreactivity is seen in the apical dendrite at stage E13, it is likely that 5-hydroxytryptophan uptake by ENC1 occurs earlier than stage E18. Interestingly, Yi and Emery (1991) found pinocytotic profiles in the dendritic knobs of olfactory receptor neurons in adult *Helisoma*. The spinorbium of ENC1 may thus be a primary site of uptake for tryptophan from the perivitelline fluid.

Although not included in the results section, my experiments also showed that 5,7-DHT-induced fluorescence of ENC1 could be consistently and completely blocked (102/105 stage E30 to E50 embryos lost 5,7-DHT staining) with 1.0 mM mianserin, a

serotonin receptor antagonist. Interestingly, yolk cells which normally displayed 5,7-DHT uptake were unaffected by mianserin. Imipramine, which inhibits serotonin and norepinephrine reuptake (Gandolfi *et al.*, 1984), had no apparent effect on 5,7-DHT uptake (23/26 stage E30 embryos retained 5,7-DHT staining when treated with 0.01 mM imipramine--higher concentrations damaged or killed embryos). From these findings, it is probable that ENC1 utilizes an uptake mechanism which is selective for serotonin-like compounds to accumulate tryptophan from the perivitelline fluid through the apical dendrite for the synthesis of serotonin. Furthermore, the pharmacological results suggest that this uptake mechanism is different than the imipramine-sensitive uptake system that has been well characterized in vertebrate systems (Warrington, 1992) as well as select gastropod species (Cottrell, 1971a; Cottrell, 1971b).

iv) Initial neurite outgrowth and contact with putative guidance cells

Developmental changes in the neurite outgrowth pattern were characterized from stage E15 to E30. EPNs bypassed the prototrochal band of ciliated epithelial cells to grow toward their target, the pedal band of ciliated epithelial cells. The outgrowth of EPNs consisted of three main phases: target-directed unbranched outgrowth, target-localized extension of backbranches, and fasciculation along a subpopulation of median-unpaired-ciliated cells.

EPN growth cones approaching the target were tapered in profile, whereas growth cones extending over the target were club-shaped. The tapered growth cones resemble those of the P neuron axons which extend at later embryonic stages in the leech, *Haementeria ghilianii* (Kuwada and Kramer, 1983) and those of the medial giant interneurons in the grasshopper (Shankland and Goodman, 1982).

EPNs intersected identified cells, the G-cells, at specific intervals along the outgrowth pathway. The consistent location of these cells in an arrangement conducive to converge the outgrowth pathway of the two EPNs provides reason to assume that these

cells may act as cellular guidance points for EPN growth cones, akin to the guidepost cells of grasshopper (Bentley and Caudy, 1983) and *Drosophila* (Blair *et al.*, 1985; Schubiger and Palka, 1985). As in grasshopper (Bentley *et al.*, 1991; Taghert *et al.*, 1982), EPNs were found to make membrane-to-membrane contact with the guidance cells with what may be gap junctions, as found in a transmission electron microscopic study of ENC1 (Koss, Diefenbach and Goldberg, in preparation). In grasshopper and *Drosophila*, guidepost cells differentiate into neurons. The G1 cells of *Helisoma* were in a position similar to that of the serotonergic ENC2 cell. Further study, however, is required to follow the fate of the G1 and other putative guidance cells. Whether these cells serve a guidance function awaits a laser, chemical or electrical ablation study. Thus, molluscs may also utilize a guidepost cell-mediated strategy of neurite pathway establishment during development.

The G-cells were fortuitously identified initially by virtue of their serotonin-immunoreactivity in pCPA-treated stage E15 embryos. Why would a reduction in embryonic serotonin content result in the expression of serotonin in the G-cells? One possible model could involve a mechanism whereby contact by serotonergic processes delays the differentiation of the G-cells into serotonergic neurons. If the G-cells, as suggested above, differentiate into serotonergic neurons, contact between EPNs and the G-cells may delay the differentiation of the G-cells into neurons. This delay may be mediated by exchange of serotonin or other intracellular contents via gap junctions (Bentley *et al.*, 1991). With pCPA treatment, the G-cells would be contacted by EPNs which express very little serotonin. If serotonin is the factor which promotes differentiation (Lauder and Krebs, 1978) of the G-cells into neurons, its virtual absence in the EPNs would result in the premature differentiation and expression of serotonin in the G-cells. However, neurites have not yet been observed extending from any serotonin-immunoreactive G-cell at stage E15, although they may be extended later in development. Although a preliminary study showed that EPNs form gap junctions with the G1 cells (Koss, Diefenbach and Goldberg, in preparation), further analyses are required to determine if the G-cells actually

differentiate into serotonergic neurons and if serotonin is a factor which regulates their differentiation.

v) Target-localized branching outgrowth

Neurite branching of EPNs was termed backbranching, as the branching is confined to a single target as the growth cone navigates over the target (O'Leary and Terashima, 1988). **The** developmental progression of neurite outgrowth from stage E13 to E30 in relation to the pedal ciliary band is summarized schematically in Figure 52. The individual identified pedal ciliated cells are shown as in Figure 11. At stage E13, the two EPN growth cones proceed past the pedal ciliary band which consists of only one ciliated cell, cell PeA (shaded). The two neurites fasciculate at this stage in the target region. Between stages E15 and E20, the remaining pedal ciliated cells differentiate, and the pedal ciliary band enlarges in size. During this time, the ENC1 neurites separate, presumably by defasciculation, and extend neurite branches over the pedal ciliary band, except for the medial PeD cell, over which the EPNs continue to fasciculate. Branching continues at stage E25 to E30 over the pedal ciliary band. Also during this time, lateral neurite branches extend to the lateral PeLA1 and PeLA2 ciliated cells. As described in the results, the only obvious change in the pedal ciliary band from stage E13 to E15 is the differentiation and enlargement of the PeB, PeC cell pairs and the medial PeD cell. Apart from a slight shift in the orientation of the cells within the band, the band remains unchanged until stage E30, when another medial cell, cell PeE, appears posterior to cell PeD.

In a study by Williams *et al.* (1993) backbranching was induced from neurites of *Helisoma* neurons *in vitro* using electric field stimulation. Neurites which had previously ceased their neurite outgrowth did not extend back-branches regardless of the type of stimulation used. Since backbranching occurred in EPNs while the growth cones were pausing to proceed over the next medial ciliated cell, it is possible the EPNs were also in an "active" outgrowth state during that time.

Branching occurred between EPN homologues and so it is possible that the branch of one EPN is somehow attracted to the opposite EPN. Although ablation of one of the ENC1s prior to neurite branch initiation would confirm this possibility, mutant embryos were observed in which one of the ENC1 homologues failed to develop as verified with Nomarski optics (n = 3), or both ENC1s were on one side of the embryo (n = 2). In both cases, EPN growth cones reached the pedal ciliary band and extended numerous branches across the band (results not shown). Thus, EPN branches do not appear to rely on an attractive cue from the opposite neurite to extend over and occupy the entire target.

It is possible that the pedal ciliated cells attract EPN neurites through release of a tropic cue (Bastmeyer *et al.*, 1993; Kennedy *et al.*, 1994). Confirmation of this hypothesis awaits an ablation study of the pedal cells to determine if EPN growth cones are still directed toward the pedal region. Alternatively, ENC1 could be co-cultured close to one or several pedal ciliated cells to determine if ciliated cells are able to attract ENC1 growth cones over a distance, an example of chemotropism (Tessier-Lavigne and Placzek, 1991).

Although the overall pattern of neurite branching is stereotyped, I did not systematically examine the pattern for the degree of stereotypy of individual branches. Nevertheless, there is reason to suggest that much of the neurite branch pattern of ENC1 is stereotyped. For example, the later-developing lateral LB branches were consistently identifiable. These branches are unique in that, unlike the back branches of the EPNs, they formed *prior* to the differentiation of their targets, the lateral ciliated epithelial cells. Since these branches formed prior to target differentiation, their extension, and the extension of other branches, may be regulated through intrinsic mechanisms. Further to the idea that the neurite branch pattern of ENC1 is to some extent stereotyped, when negatives of photomicrographs of different *Helisoma* embryos of identical stage and in similar profiles were superimposed, both the EPNs and some primary neurite branches appeared in perfect register. It is possible the secondary neurites grow along contact margins of the individual pedal ciliated cells, although this hypothesis has not been systematically addressed.

vi) Fasciculation of EPNs on medial ciliated cells

EPNs appeared to fasciculate as they proceeded together across the medial pedal ciliated cells. Since the transition between branched outgrowth and fasciculation occurred at the margin between the paired ciliated cells and the medial ciliated cells, the latter may express a substrate-associated factor which promotes fasciculation of EPN neurites. Possible factors include neural cell adhesion molecules, one of which has been found in another gastropod, *Aplysia*, to mediate serotonin-induced synaptic plasticity by promoting neurite defasciculation and branching (Bailey *et al.*, 1992), or a semaphorin-like molecule, known to mediate axonal fasciculation in insects (Goodman, 1994). That there may be a subset of medial ciliated cells which differ in their expression of cell surface molecules may be revealed in an immunohistochemical examination of the developmental expression of adhesion molecules in *Helisoma* embryos.

vii) Possible factors influencing EPN outgrowth

There are many potential mechanisms which may mediate the transitions in outgrowth displayed by EPNs during pathway navigation. Extracellular matrix (ECM) molecules are important regulators of neuronal development (Letourneau *et al.*, 1994). ECM molecules like laminin, which is a substrate-bound, neurite-outgrowth-promoting factor from *Helisoma* brain-conditioned medium (Miller and Hadley, 1991) and fibronectin, which promotes neurite branching (Mattson and Kater, 1988), are present in the *Helisoma* central nervous system. It needs to be determined whether these compounds are present during *Helisoma* embryogenesis and whether functional deletion experiments using ECM antibodies or injection of antisense mRNA can alter the ENC1 outgrowth pattern. The fasciculation displayed by EPNs on the medial ciliated cells may be mediated by membrane associated adhesion molecules such as Semaphorin I (previously Fasciclin IV; Goodman, 1994) or *Aplysia* CAMs (Zhu *et al.*, 1994). Factors which may regulate

neurite branching of ENC1s will be discussed in greater detail in section III-iii of the discussion.

viii) Asymmetries in the development of ENC1 homologues

Based on the observations of serotonin expression and the progression of neurite outgrowth, the right ENC1 homologue appeared to be at a consistently more advanced developmental stage than the left, and may in fact differentiate prior to the left ENC1. This asymmetry in development may be related to the asymmetrical body plan of *Helisoma*. Indeed, there is a correlation in the asymmetric development of an identified serotonergic neuron cluster in the pedal ganglia with the body asymmetry of *Helisoma* and *Lymnaea* (Diefenbach and Goldberg, 1990). *Helisoma* is sinistral or left-handed (Clarke, 1981; Pip, 1987): the aperture of the shell is on the left of the whorl with the apex dorsal, and reproductive organs are on the left side of the body. *Lymnaea* is right-handed or dextral (Clarke *et al.*, 1978). In *Helisoma*, the serotonergic pedal cluster VII showed an increase in the number of neurons postembryonically in only the left pedal ganglion (Diefenbach and Goldberg, 1990), whereas the apparently homologous PeIb cluster of *Lymnaea* enlarged in the right pedal ganglion (Croll and Chiasson, 1989). Audesirk *et al.* (1985) reported that the serotonin content of neuron C1 in adult *Lymnaea* was greater in the left than in the right neuron. It is interesting that in the right-handed *Lymnaea*, the left neuron C1 had more serotonin, whereas in the left-handed *Helisoma*, the right ENC1 had apparently higher serotonin immunoreactivity. Thus, there appears to be a correlation between body asymmetry and neurotransmitter expression in gastropod development. Why one ENC1 may possess more serotonin than the other is open to speculation. The asymmetry of serotonin expression may serve in mutual electrical stimulation, whereby one neuron could serve as a leader and the other a follower. Goldschmeding *et al.*(1981) found that for neurons C1 of *Lymnaea*, there was a 1:1 driver-follower relationship in firing of action potentials. Interestingly, the left homologue led the firing in 5 out of 9 preparations. This

result makes sense in light of the left neuron possessing between 2.5 and 7% more serotonin than the right (Audesirk *et al.*, 1985). Thus, asymmetry in serotonin content may promote uniform rhythmic output among paired homologous neurons. Evidence that homologous ENC1s may communicate with each other via synapses comes from a recent transmission electron microscopic study of ENC1 (Koss, Diefenbach and Goldberg, in preparation) in which specialized contacts resembling synapses were observed between EPNs of the bilateral ENC1s.

ix) Transient expression of serotonin in ENC1

ENC1 lost its serotonin immunoreactivity between stages E65 and E70, although it retained its 5,7-DHT uptake capacity even in hatchling juvenile snails. Thus, serotonin appeared transiently during embryogenesis. The significance of this transient expression may be related to its developmental and behavioral roles to be discussed later. Serotonin may be co-expressed with other neurotransmitters or neuropeptides, as has been reported for other identified molluscan neurons (Boer *et al.*, 1984; Osborne, *et al.*, 1982) and in vertebrate neurons (Johnson, 1994; Watt, 1992). Thus, when ENC1 no longer expresses serotonin, the second neurotransmitter may prevail. In a transmission electron microscope study of ENC1, both dense core and electron lucent granule types were resolved (Koss, Diefenbach and Goldberg, in preparation). However, these different types of granules may be serotonergic vesicles in the process of turnover, as has been found in synapses of *Aplysia* (Shkolnik and Schwartz, 1980). Alternatively, ENC1 may undergo a phenotype switch to an unknown neurotransmitter, as occurs in neurons of *Lymnaea stagnalis* (Gesser and Larsson, 1985).

The loss of serotonin immunoreactivity in an embryonic molluscan neuron is not unprecedented. In *Aplysia*, an unidentified unpaired median cell, which projects to the velum, is reported to loose its serotonin immunoreactivity coincident with the shedding of the velum during metamorphosis (Marois and Carew, 1990). This neuron was assumed to

undergo cell death, which is unprecedented in molluscs (Jacob, 1984; Goldberg and Cavers, 1993). Similarly, the paired serotonergic V cells, which innervate the velum of red abalone, *Haliotis rufescens*, were assumed to die at metamorphosis (Barlow and Truman, 1992). *H. rufescens* also contained a pair of flask-shaped or F cells, which may be homologous to ENC1 as they possessed an anteriorly-projecting thick process resembling the apical dendrite of ENC1. Prior to metamorphosis, the V cells were located posterior to, and the F cells anterior to serotonergic fibres of the cerebral commissure. The V cells were reported to disappear between day 8 and 16. One may argue that it was the F cells which lost their serotonin immunoreactivity. If the V cells disappeared, the F cells would have to shift from an anterior to posterior position with respect to the cerebral commissure. However, thus far in the literature on gastropod development has there been no such report of a migration of an identified neuron once it becomes differentiated. Like the F cells, ENC1s were consistently located anterior to the cerebral commissure until stage E65, when they lost their immunoreactivity. It is therefore possible that ENC1 and the F cells are homologous not only by virtue of their location but also by their transient expression of serotonin. Labeling of these neurons with 5,7-DHT may confirm this alternative hypothesis. From the present study on ENC1, it is clear that caution is advised in assuming that a loss of neurotransmitter immunoreactivity corresponds to cell death.

Development of ENC1 in *Helisoma* thus provides a model system with which to examine the initial development of a molluscan neuron of a defined neurotransmitter phenotype. The neurite outgrowth pathway is relatively simple and the target cells of ENC1 have been individually identified. This sets the stage for detailed *in vivo*, and potentially *in vitro* (Goldberg *et al.*, 1988), study at the single cell level of factors that regulate development of an identified embryonic neuron of a mollusc. Such a system has eluded neurobiologists, although a previous attempt to culture neurons from larval *Aplysia*, which could be raised in the laboratory, was unsuccessful (Kriegstein *et al.*, 1974) in spite of the

success in culturing adult neurons from *Aplysia* (Dagan and Levitan, 1981). One good reason for looking at neurons of gastropods is that they have retained the capacity to regenerate in the adult. By understanding how a neuron achieves a mature phenotype during development, we may gain insight into why molluscan neurons have retained a capacity to regenerate.

III) Role of serotonin in the development of ENC1 neurites

In this study, I examined whether the development of an identified serotonergic neuron in *Helisoma* embryos depends in part upon serotonin. In both cell culture and *in situ* experiments on regenerating neurons, exogenous serotonin has been found to inhibit the neurite outgrowth of several select identified neurons. A subset of these neurons are actually serotonergic themselves, including pedal ganglion neuron P5 (Haydon *et al.*, 1987) and cerebral ganglion neuron C1 (Murrain *et al.*, 1990). In addition, a subpopulation of serotonin-immunoreactive neurons that direct locomotion in *Pleurobranchea californica* were found to be sensitive to serotonin (Sudlow and Gillette, 1991). Likewise in experiments on developing embryonic neurons, exogenous serotonin was shown to influence neurite outgrowth. However, whereas serotonin typically inhibits neurite outgrowth of adult *Helisoma* neurons (Haydon *et al.*, 1984; Haydon *et al.*, 1987), both inhibitory and stimulatory outgrowth responses were displayed by select embryonic neurons (Goldberg *et al.*, 1991). Embryonic neurons are therefore capable of displaying greater response plasticity to serotonin than adult neurons. Taken together, these observations prompted the hypothesis that the *in situ* development of embryonic serotonergic neurons may be regulated in part by their own serotonin being released and binding to serotonin autoreceptors to regulate neurite outgrowth in an autocrine manner. This autoreceptor hypothesis was tested by treating *Helisoma* embryos with pCPA and 5-HTP, treatments which lowered and raised the endogenous levels of embryonic serotonin, respectively, as verified using HPLC-ED. These compounds produced opposite effects on

the neurite outgrowth of ENC1. Specifically, there was a marked increase in neurite branching after exposure to pCPA and a decrease in branching following 5-HTP treatment. These results implicate a serotonin autoreceptor on ENC1 that regulates the formation of neurite branches during embryonic development.

i) pCPA and ENC1 serotonin content

pCPA was used in this study because of its ability to reduce the levels of embryonic serotonin by inhibiting the rate-limiting enzyme in serotonin synthesis, tryptophan hydroxylase (Gál and Whitacre, 1982; Jéquier *et al.*, 1967). The reduction in serotonin synthesis was confirmed through HPLC-ED measurement of embryonic serotonin content and immunofluorescent labeling of serotonergic cells. pCPA specifically prevented a developmental increase in embryonic serotonin content without significantly altering embryonic dopamine levels. Although the apparent reduction in dopamine content at stage E20 was not statistically significant, it is possible that pCPA may have had a slight effect on dopamine levels by 24 hr. pCPA is considered a selective inhibitor of tryptophan hydroxylase (Gál and Whitacre, 1982). The effectiveness and specificity of pCPA was also shown when ganglia isolated from mature snails were treated *in vitro*. Whereas serotonin levels were significantly lowered following pCPA treatment, dopamine levels were unchanged. Finally, pCPA's effectiveness was confirmed by the transient abolition of serotonin immunoreactivity of ENC1s. Cottrell and Osborne (1970) similarly found that pCPA reduced paraformaldehyde-induced serotonin fluorescence in the metacerebral cells of *Limax maximus*. Although one cannot directly correlate differences in serotonin-immunostaining intensity with actual levels of serotonin in ENC1s (see Ono and McCaman, 1984), pCPA treatment did reversibly abolish serotonin immunoreactivity concomitant with a persistent reduction in embryonic serotonin levels.

An important assumption of the autoregulation hypothesis is that most or all of the serotonin in the embryo at the time of treatment is derived from ENC1s. Otherwise,

serotonin released from alternative sources may directly or indirectly affect ENC1 development. While ENC1s are the only source of intense serotonin immunofluorescence from stages E15 to E25, consistent staining also occurs in two other cell types: the shell gland cells and ectodermal cells bordering the posterior pedal furrow. Serotonin in the shell gland, as indicated by immunofluorescence, first appeared at about stage E25, so its expression is too late to influence the early stages of ENC1 neurite branch formation. On the other hand, since ENC1s project distally to the posterior pedal furrow, the immunofluorescent pedal ectodermal cells may be a site of serotonin uptake, rather than a source of serotonin synthesis. Furthermore, this fluorescence appears close to stage E25, so that even if these cells do in fact produce serotonin, it occurs at too late a stage to affect neurite branch development of ENC1 prior to that stage. Since neurite branching continues to increase from stage E25 to E30, it is unlikely that serotonin from these other sources inhibits neurite branching during this time.

Studies that have quantified the amount of serotonin contained within identified serotonergic molluscan neurons further support the conclusion that most of the serotonin measured in the present study is derived from ENC1s. Giant cerebral ganglion cells isolated from *Aplysia californica* and *Tritonia diomedia* were found to contain 4 to 6 pmol of serotonin (Weinreich *et al.*, 1973; Ono and McCaman, 1984). These cells measure between 200 to 400 µm in diameter, giving them between about 1000 to 10000 times the volume of ENC1 in *Helisoma*. The amount of serotonin present in whole *Helisoma* embryos ranges from around 2 fmol at stage E15 to 6 fmol at stage E25. Thus, *Helisoma* embryos, which have a single pair of serotonin immunofluorescent neurons, contain approximately 1000 to 2000 times less serotonin than serotonergic cells that have about 1000 to 10000 times greater volume. Furthermore, Audesirk *et al.* (1985) found the neuron C1 of *Lymnaea* to contain between 1.12 (wildtype) and 1.54 (lab-reared) pmol of serotonin per neuron of 100 µm diameter (Croll and Chiasson, 1989). In this case, for a serotonergic neuron that is 100 times larger than ENC1, the serotonin content is 200 to 600

times greater. Although neurotransmitter content and soma size are not necessarily directly related (for example, see Ono and McCaman, 1984), ENC1's volume is appropriate for the amount of serotonin measured. Therefore, the serotonin measured in *Helisoma* embryos is probably localized at high concentration in ENC1s relative to other embryonic cell types. After pCPA treatment the whole embryo serotonin content measured by HPLC was roughly halved, while the serotonin immunofluorescence in ENC1 was transiently eliminated. Thus, the remaining portion of the measured serotonin may largely represent the extracellular pool of released serotonin. While it is not possible to directly measure this pool before and after treatment, it is likely that the size of this pool diminishes as its source of serotonin, ENC1, produces less neurotransmitter. Therefore, the end result of these changes would be that less extracellular serotonin is available to bind to ENC1 autoreceptors.

ii) 5-HTP and neurite branching

Continuous 5-HTP treatment resulted in a reduced number of ENC1 neurite branches by stage E25. One possibility is that 5-HTP produced this effect by binding to serotonin autoreceptors, and thus acted directly as a serotonin receptor agonist. No attempt was made to distinguish between this direct effect versus an indirect effect of 5-HTP through enhanced serotonin synthesis. The latter possibility is supported by the 5-HTP-induced increase in whole-embryo serotonin content, as measured using HPLC. In addition, since ENC1s selectively take up 5,7-DHT initially at stage E18, and perhaps earlier, they may also internalize 5-HTP through the same uptake system. Furthermore, the cerebral giant cells of *Helix pomatia* were found to take up 5-HTP and tryptophan (Pentreath and Cottrell, 1973). These results suggest that ENC1s have a functional uptake system for 5-HTP at the time of 5-HTP treatment and are able to convert this precursor into 5-HT. Thus, the effect of 5-HTP could be explained by the following conceptual model. The uptake of 5-HTP by ENC1 increases serotonin synthesis, thus increasing the pool of

releasable serotonin. As a result, more serotonin is released and made available to serotonin autoreceptors. Enhanced activation of the autoreceptors has an inhibitory effect on neurite branching. Whether 5-HTP acts directly on a serotonin autoreceptor or indirectly through enhancing serotonin synthesis, either possibility would require activation of serotonin autoreceptors on ENC1 to cause a reduction in neurite branching.

iii) Serotonin regulation of neurite branching

The results from the serotonin perturbation experiments suggest that endogenous serotonin acts to limit the amount of neurite branching during the development of ENC1. Serotonin regulation of neurite branching was also reported in a cell culture study of non-serotonergic cortical neurons from prenatal rat (Sikich *et al.*, 1990). The effect was to increase the number of secondary neurites; primary neurite number was unaffected. This was also the case for ENC1. There are a number of possible mechanisms through which serotonin could regulate neurite branching. Neurite branching has been shown to be decreased by reduced polysialylation of the cell adhesion molecules L1 and N-CAM (Landmesser *et al.*, 1990; Tang and Landmesser, 1993), microtubule stabilization using taxol (Letourneau *et al.*, 1986), exposure to higher concentrations of substrate-bound laminin (Buettner and Pittman, 1991) and tenascin (Wehrle and Chiquet, 1990), insect hormones such as juvenile hormone (Levine *et al.*,, 1986) and ecdysterone (Weeks *et al.*, 1992) and by treatment with a fibronectin antiserum (Mattson and Kater, 1988). In contrast, neurite branching has been positively regulated by lowered substrate adhesion in culture (Wessels and Nuttall, 1978), blockade of inhibitory glycinergic transmission (Sanes and Chokshi, 1992), exposure to the calcium binding protein S-100b (Liu and Lauder, 1992), increased cholesterol incorporation into membranes (Handelmann *et al.*, 1992), exposure to low ethanol concentration (Zou *et al.*, 1993), an *Antennapedia* homeobox protein (Bloch-Gallego *et al.*, 1993), partial denervation (Brown *et al.*, 1981; Diamond *et al.*, 1976; Murphy and Kater, 1980), postsynaptic receptor blockade (Holland and Brown,

1980; Lipton *et al.*, 1988), appropriate cellular substrates such as astrocytes (Lieth *et al.*, 1990), stress (Bulloch, 1985), and increased aging and body size (Purves *et al.*, 1988). These examples of the many potential mechanisms of neurite branch regulation raises a question in relation to our findings with ENC1: By what mechanism could autoreceptor activation alter neurite branching?

In search of an answer to this question, one should first consider that neurite outgrowth in *Helisoma* can be regulated by a number of neuroactive substances, including neurotransmitters such as serotonin (Haydon et al., 1984; Haydon *et al.*, 1986), dopamine (McCobb *et al.*, 1988a), acetylcholine (McCobb *et al.*, 1988b), and glutamate (Bulloch, 1989). In a study by Budnik *et al.* (1989), a *Drosophila melanogaster* mutant was examined that lacked the enzyme dopa decarboxylase (alternatively referred to as aromatic L-amino acid decarboxylase) which is required for serotonin and dopamine synthesis. In this mutant, serotonergic nerve fibres arrived at their targets, but displayed double the extent of neurite branching. This result parallels our finding that reduced serotonin content in the embryo resulted in increased branching of ENC1 neurites. Neuropeptides, such as somatostatin (Bulloch, 1987), molluscan insulin-related neuropeptide (Kits *et al.*, 1990) and gonadotropin-releasing hormone (Goldberg *et al.*, 1993) and trophic factors such as nerve growth factor (NGF; Ridgway *et al.*, 1991) may also be potential regulators of neurite branching. In vertebrates, NGF may be the target-derived cue responsible for increased branching outgrowth seen in the development of sympathetic and parasympathetic ganglion cells (for review, see Purves *et al.*, 1988). Whether these factors operate independent of or together with classical neurotransmitters awaits future study.

The effects of neurotransmitters on neurite outgrowth are in some instances mediated through depolarization (Cohan, and Kater, 1986; Cohan, 1989) and subsequent increases in intracellular calcium (Kater *et al.*, 1988; Mattson *et al.*, 1988; Kater and Mills, 1991). Recently, the elevation of intracellular calcium by serotonin was also reported for embryonic *Helisoma* neurons in culture (Goldberg *et al.*, 1992). If ENC1s possess

serotonin receptors, as appears to be the case for adult serotonergic neurons in *Helisoma* (Haydon *et al.*, 1987; Murrain *et al.*, 1990), these receptors may mediate autoregulation of intracellular calcium levels, perhaps by directly or indirectly gating a calcium channel (Penington and Kelly, 1990; Price and Goldberg, 1993a). Altered intracellular calcium could in turn promote or prevent neurite branching through regulation of calcium-dependent activities of actin filaments (Lankford and Letourneau, 1989) or microtubules (Gordon-Weeks, 1991). Interestingly, microtubule stabilization by taxol was found to inhibit neurite branching of chick embryo sympathetic and sensory neurons *in vitro* (Letourneau *et al.*, 1986). In addition, microtubule depolymerization *in vitro* is promoted by high calcium (Weisenberg, 1972). Treatment of buccal neuron B19 from *Helisoma* with the inorganic calcium channel blocker lathanum resulted in increased neurite branching (Mattson *et al.*, 1988). However, high intracellular calcium has been found to promote neurite branching in chick embryo dorsal root ganglion cells (Marsh and Letourneau, 1984). Thus, until the roles of calcium and other intracellular mediators in regulating neurite branching are better understood, the mechanisms underlying serotonin's actions will remain unresolved. Nevertheless, given that cultured neurons of stage E25 *Helisoma* embryos possess high-voltage activated calcium currents (Goldberg and Price, 1991) and display serotonin-induced changes in intracellular calcium concentration (Goldberg et al., 1992), membrane depolarization and changes in calcium concentration likely serve as intermediate steps in the sequence of intracellular events leading to altered neurite branching.

Further to the idea that electrical activity may alter branching comes from work on adult *Aplysia*. Exposure to the depolarizing agent KCl resulted in an increase in the number of axonal spines on adult (Bailey and Chen, 1983) and embryonic neurons (Schacher, 1981). This increased branching is caused by down-regulation of an *Aplysia* cell adhesion molecule (apCAM) via cAMP-dependent endocytosis of clathrin-coated vesicles (Hu *et al.*, 1993) upon exposure to serotonin (Bailey *et al.*, 1992; Mayford *et al.*, 1992). CAMs normally promote fasciculation of neurites. With less apCAM, the sensory neurites

defasciculate, which permits branching along the axons of the postsynaptic motor neuron L7 (Zhu *et al.*, 1994). Furthermore, treatment with an antibody against apCAM caused a doubling of neurite branch points in cultured adult *Aplysia* sensory neurons (Mayford *et al.*, 1992). In *Aplysia*, therefore, serotonin may serve to promote neurite branching through its effects on apCAM. Given that serotonin in this report has a negative regulatory effect on neurite branching, it would be interesting to determine whether apCAM is present in *Helisoma*.

iv) Possible role of the target in neurite branch development

There are numerous studies implicating the target tissue in the regulation of neurite branching. For instance, in the medicinal leech, the serotonergic Retzius cells of segments 5 and 6 innervate the gonads and possess fewer neurite branches than their counterparts in other segments which innervate muscle and epidermal target tissues (Loer *et al.*, 1987). In the moth, *Manduca sexta*, motor neuron MN1 displays reduced branching during diapause when the larval target muscle tissue is lost and the adult target muscles are still undeveloped (Truman and Reiss, 1976). In the locust, removal of limb bud target tissue resulted in supernumerary branches forming from the Feti and Dumeti neurons (Whitington *et al.*, 1982). Neurites themselves may also initiate branching of synaptic partners. For example, sensory axons of grasshopper cerci were found to promote dendrite formation of the Medial Giant Interneuron (MGI; Shankland *et al.*, 1982). Retinal ganglion cell neurites of *Xenopus* extend backbranches after arrival of neurites at the optic tectum (Harris *et al.*, 1987). Corticopontine axons in the rat embryo initiate collateralization with a significant delay after reaching the pons (O'Leary and Terashima, 1988). These studies and others underlie the importance of neuron-target interactions in the regulation of neurite branching.

In *Helisoma*, the characteristic branching pattern of ENC1 arises through the latent formation of back branches from the previously extended primary neurites. Given that the branching occurs almost exclusively in the vicinity of the pedal ciliated epithelial cells, these

cells may play an active role in generating the branching pattern. One conceptual model is that the target has two specific actions to regulate ENC1 outgrowth. First, since lowering of embryonic serotonin content through pCPA treatment enhanced branching only in the target region, and not along the proximal neurite segments, the target may release or express a localized cue that is permissive for neurite branching. Candidate cues include extracellular matrix molecules such as laminin and fibronectin, which are known to be important for neurite outgrowth in *Helisoma* (Mattson and Kater, 1988; Miller and Hadley, 1991); or cell adhesion molecules (Hu *et al.*, 1993). Neurite branching has been found to require reduced substrate adhesivity (Buettner and Pittman, 1991; Wessels and Nuttall, 1978). In addition, the decision made by a growth cone to navigate over a particular substrate can be influenced by the relative adhesivity of the substrates to choose from (Gundersen, 1987; Hammarback and Letourneau, 1986; Gomez and Letourneau, 1994; Kuhn *et al.*, 1995). The pedal ciliary band may thus provide a less adhesive substrate. Evidence supporting this idea is the observation using confocal microscopy that the EPNs selectively navigate along the lateral margins of the paired pedal ciliated cells and remain confined to the boundaries of the medial pedal ciliated cells, which may provide a more adhesive substrate.

Although neurite branching may be supported by the suitable substrate of the pedal ciliary band, the presence of a suitable substrate *per se* may not be sufficient for neurite branching to occur. It is possible that the pedal ciliated cells also take up serotonin-like compounds, and thus limit the amount of serotonin available to bind serotonin autoreceptors. By incubating embryos in 5,7-DHT and then dissociating them in culture, ciliated epithelial cells were consistently observed to display 5,7-DHT fluorescence. Ciliated cells *in vivo* were not observed to show 5,7-DHT fluorescence. A possible reason for this is that they are very thin in saggital plane, about 2 to 5 μm as determined using confocal microscopy (see Figure 16 B). Since 5,7-DHT staining has characteristically low intensity emission in the violet part of the visible spectrum, the thin shape of the ciliated

cells may not emit enough fluorescence to be detected with the naked eye. However, on two occasions, individual 5,7-DHT ciliated cells were observed in the pedal ciliary band in embryos which had been excessively compressed under a coverslip to the point where the ciliated cells were partially dissociated. This dissociation resulted in rounding up of the ciliated cells, providing a greater volume through which the 5,7-DHT fluorescence could be seen. It would be interesting to examine 5,7-DHT-stained embryos with a light intensification imaging system to determine if the ciliated cells normally take up 5,7-DHT *in vivo*. Given that ciliated target cells may take up serotonin, a hypothetical model can be presented whereby neurite branching is promoted by the presence of the target (Figure 53). In the first phase of outgrowth, target-directed non-branching outgrowth, EPN growth cones release serotonin, either spontaneously (Hume *et al.*, 1983; Young and Poo, 1983) or as a result of electrical activity (Sun and Poo, 1987). This tonically- or phasically-released serotonin binds serotonin autoreceptors on the growth cones and neurites. Serotonin autoreceptor binding may then initiate a second messenger cascade through a GTP-binding protein which may affect intracellular calcium levels in a way which dramatically reduces the probability of branching. In the second phase of outgrowth, target-localized branching outgrowth, uptake of serotonin by ciliated target cells would reduce the amount of serotonin available to activate the serotonin autoreceptors, which would relieve the inhibition of neurite branching. Further experiments are required to determine whether the target can interact with the autoregulatory mechanism in this fashion.

One way to approach testing this hypothesis *in vivo* would be to find a specific blocker of 5,7-DHT uptake of the pedal ciliated cells. It was already found that mianserin inhibits uptake of 5,7-DHT into ENC1. If one is found which does not affect 5,7-DHT uptake of ENC1 *in vivo* nor autoreceptor binding, embryos could be exposed to it and changes in neurite branching examined using serotonin immunohistochemistry. Alternatively, ENC1 could be isolated in culture and cocultured with ciliated cells to determine if their proximity to ENC1 neurites could promote neurite branching.

v) Significance of serotonin immunoreactivity in the growth cones of ENC1

ENC1 growth cones possessed a high level of serotonin immunoreactivity relative to the neurite shafts of the EPNs. One may argue that the relative abundance of serotonin in EPN growth cones may be a prerequisite for target contact and synaptogenesis, as has been found to be the case for serotonergic projections in rat brain (Ivgy-May and Gershon, 1994). However, the EPN growth cones continue over the target to the end of the outgrowth pathway, and are responsible for extension of the pathway with development of the pedal band of cilia. EPN backbranches, on the other hand, form from neurite shafts and extend over the pedal ciliary band to presumably form synapses. The EPN growth cones, therefore, are not able to form synapses since they proceed along the pedal band long after neurite backbranching has been initiated. Since the EPN growth cones do not immediately form synapses upon target contact, the high level of serotonin may serve to regulate neurite outgrowth. Given the previous model of serotonin regulation of neurite branching, serotonin in the EPN growth cones may be required to limit the amount of neurite branching as they establish the primary neurite pathway.

Why would inhibiting the branching outgrowth of the first growth cones to extend over the target be important? There are basically two strategies by which a pattern of branching could result in complete coverage of the target with neurites (Figure 54): 1. As the growth cones approach or contact the target, branching through bifurcation of growth cones would result in numerous growth cones traversing the target to fill the innervation field. Examples of this strategy include extension of dendrites from the medial giant interneuron of the grasshopper (Shankland and Goodman, 1982), branching of retinal neuron axons in the optic tectum of *Xenopus* (Harris *et al.*, 1987), and innervation of skin of leech by mechanosensory neurons (Kuwada and Kramer, 1983). 2. The growth cone(s) first to arrive at the target traverse the full extent of the target. Primary neurites of these

"pioneering growth cones" then undergo back branching to fill the innervation field. Examples of this strategy include development of the motor endplate in developing rat muscle (Bennett and Pettigrew, 1975), innervation of the body wall of the leech by pressure-sensitive P cells (Kuwada and Kramer, 1983), innervation of the penile sheath by the rostral penile evertor (RPE) neurons of the leech (Macagno *et al.*, 1990), and innervation of the extensor tibiae muscle of locust limb by SETi motor neurons (Myers *et al.*, 1990). There are additional strategies, such as the parallel array of axons extended from the soma of the Comb-cell of the leech to innervate the body wall (Jellies and Kristan, 1991). Although evidence from the literature is lacking, one may hypothesize that once neurite branches are extended, their growth cones may be more committed to forming synapses than the growth cones of the primary neurites, which may have more of a pathfinding function. If primary growth cones are more committed to pathfinding than branch growth cones, the second outgrowth strategy is more suited to targets with changing dimensions, such as the developing pedal ciliary band. If the EPNs of ENC1 chose the first strategy, all of the growth cones would form synapses before the development of the target would be complete, resulting in incomplete innervation. With the second strategy, the EPNs are able to accommodate to the changing size of the pedal ciliary band, while at the same time stimulating the part of the band which is stable. In this way, the pedal ciliary band can function in generating rotational behavior while it is still in the process of development.

IV) Role of serotonin in the development of rotational behavior of *Helisoma* embryos.

The first observable behavior expressed by *Helisoma trivolvis* is cilia-driven rotation, which occurs primarily between embryonic stages E15 and E30. Since the expression of this behavior coincides with the early differentiation of ENC1, the hypothesis that serotonin is an important regulator of rotational behavior during

embryogenesis was tested. Characteristics of this behavior were described as functions of embryonic stage and exposure to serotonin. Developmentally, the rate of rotation and frequency of rotational surges both increased from stages E15 to E25, and decreased thereafter. These parameters of rotation were also affected by the presence of exogenous serotonin. Rotation rate was augmented by serotonin, while surge frequency was reduced. In contrast, both rotation rate and surge frequency were reduced by the serotonin antagonist, mianserin. As discussed below, these data are consistent with the idea that, early in embryogenesis, rotational behavior is regulated in part by the activity of ENC1.

i) Development of embryonic rotational behavior

Developmental changes were observed in all parameters of rotation. For example, the direction of rotation changed from a yaw rotation at stage E15 to a combined yaw-pitch rotation at stage E20. This behavioral change correlates well with the development of ciliated bands of cells on the external surface of the embryo (Figure 1; Table 1). At stage E15, only the dorsolateral prototrochal band of cilia was present, with the pedal band just beginning to form. This band generated a yaw movement, as confirmed by observations of particle movements within the egg capsule. Appearance of the pedal band of cilia by stage E20 coincided with the expression of a pitch component of rotation. Pitch and yaw motions could be expressed independently at later stages (E25 and E30).

Helisoma embryos at stage E30 displayed lower rates of rotation than at stage E25. This reduced rotation rate may arise from the occurrance of complete cessations in rotation possibly resulting from ciliary arrests. However, in the course of observing ciliary activity *in vivo* using time-lapse video microscopy, cilia continued beating out of synchrony with one another during nonsurge activity (results not shown). During a surge in ciliary beating (transient increase in ciliary beat frequency), the cilia appeared coordinated. These changes in ciliary activity were, however, not quantified. Nevertheless, complete ciliary arrests were not observed in *Helisoma* embryos. Ciliary arrests have been examined in larvae of

the gastropods *Mangelia nebula* (Mackie *et al.*, 1976) and *Calliostoma ligatum* (Arkett *et al.*, 1987) and in adult bivalves such as *Mytilus edulis* (Murakami and Takahashi, 1975). These studies have indicated that ciliary arrests result from depolarization of ciliated cells. Yet, preliminary *in vitro* electrophysiological studies of cultured ciliated cells from *Helisoma* embryos have shown that the increase in ciliary beat frequency resulting from serotonin exposure is not accompanied by a change in membrane potential (Goldberg and Collins, unpublished observations.

Another parameter of rotation that changed as a function of embryonic stage was rotation rate. Rotation rate showed an increase from stage E15 to E25. Several possible factors may contribute to this developmental change. First, the number of ciliated cells, ciliary bands, as well as the number of cilia per cell increased from stage E15 to stage E20 (Figures 1 and 10, Table 1), providing a greater number of propulsive units. Second, a decrease in the viscosity of the perivitelline fluid over time (Pechenik *et al.*, 1984) may influence rotation rate. One way to test the effect of viscosity would be to transplant a stage E20 embryo into a capsule emptied of its stage E25 embryo. If viscosity is less in a stage E25 capsule, then the transplanted stage E20 embryo should rotate more rapidly. While changes in ciliation and fluid viscosity may contribute to the developmental increase in rotation rate, the occurrence of rotational surges appears to be the most important factor. For example, at stage E30, rotation rate was less than at stage E25, when one would expect that rotation rate would be higher if the rate changes resulted only from changes in viscosity. Since surge frequency also was significantly reduced at stage E30 in comparison to stage E25, the relationship between rotation rate and surge frequency still holds.

Rotational surges, counted as brief periods of accelerated pitch rotation, were either rare or absent at stage E15, most frequent at stage E25 and intermediate in frequency at stage E30. Since both the rate of non-surge rotation of stage E25 embryos and the overall rate of rotation of stage E15 embryos (which surge very infrequently) were comparable and significantly less than the overall rotation rate of stage E25 embryos, there appears to be a

correlation between increased rotation rate and a capacity for surges. Thus, the increased frequency of rotational surges from stages E15 to E25 appears to be primarily responsible for the increased rate of rotation during this period.

Previous studies on cilia-dependent locomotion in molluscs have concentrated mainly on species whose development includes a planktonic larval period (see Chia *et al.*, 1984 for review). An outcome of this research was the identification of ciliary arrests as a mechanism by which the larval nervous system exerts control over locomotory behavior (Carter, 1926; Mackie *et al.*, 1976; Arkett *et al.*, 1987; Arkett, 1988). In contrast, locomotory surges, such as those observed to occur with *Helisoma*, have not been previously described. Preliminary observations of trocophores of the marine prosobranch gastropod, *Lacuna vincta* (T. J. Diefenbach and A. Martel, unpublished observations) and the freshwater pulmonate *Lymnaea stagnalis* revealed surge events similar to those seen in *Helisoma* . The surge component of rotational behavior may therefore be common to many gastropod trochophores, but requires time-lapse video microscopy to be detected. Given that neurotransmitters such as serotonin have been shown to have cilioexcitatory actions in several molluscan species (Koshtoyants *et al.*, 1961; Audesirk *et al.*, 1979; Catapane, 1983; Murakami, 1987), the present findings on surges also suggest that the embryonic nervous system is likely to impart some degree of excitatory control over ciliary activity in gastropods. Indeed, both *Lacuna* (T. J. Diefenbach and A. Martel, unpublished observations) and *Lymnaea* (Results section VI) showed enhanced rotation upon treatment with serotonin. Furthermore, *Lacuna* and *Lymnaea* embryos were found to possess a pair of 5,7-DHT labeled cells in an anterodorsal position which resembled ENC1 in *Helisoma*. Thus, serotonin may be the excitatory neurotransmitter regulating cilia-driven larval locomotion in a variety of molluscs. However, as section IV of the Results illustrates, cilia-driven locomotion may also be regulated by other neurotransmitters such as dopamine, as may be the case for *Lymnaea*.

ii) Significance of rotation and surges for *Helisoma* embryogenesis

Given that surges have not yet been described in the molluscan literature, their significance for gastropod embryos should be discussed. Rotation in general could facilitate diffusion of oxygen and metabolic wastes through the many diffusion barriers of the egg mass. Strathmann and Chaffee (1984), in a mathematical examination of the constraints of egg mass size and type on ventilation, reported that stirring the capsular fluid should increase the diffusion rate. Since surges increase rotation rate, there would be more "stirring" of the perivitelline fluid by embryos that surge. Surges may also conserve metabolic energy during development, in that occasional, rapid accelerations in rotation are energetically more efficient than rapid, continuous rotation. Rotation resulting from surges may also permit the embryo to collect the contents of the perivitelline fluid within a shorter period of time than would result from passive diffusion of the nutrients toward the embryo. Thus, surge expression in *Helisoma* has potential relevance for embryogenesis in that it may shorten the development time by permitting a balance between energy budgeting and nutrient uptake conducive to a maximal growth rate, or for sustaining a relatively large embryo characteristic of freshwater gastropods (Calow, 1978). In shortening development time, embryos may hatch sooner with less of a nutritional allotment from the adult, which in turn could increase fecundity.

Given the possible role that ENC1 plays in regulating surging of *Helisoma* embryos, coupled with the possibility that ENC1 may have a sensory function, it is possible that surges may occur in response to changes in the egg capsule environment. ENC1 may sense levels of nutritive material in the perivitelline fluid including amino acids such as tyrosine and tryptophan (Ramasubramaniam, 1979), or waste products. Interestingly, the inhibitory neurotransmitter GABA was found to induce settlement leading to metamorphosis in a ciliated marine gastropod (Morse *et al.*, 1979). Therefore, it is possible that ENC1 may regulate rotational behavior based on levels of a serotonin-like

compound in the capsular fluid. ENC1 may also sense the partial pressure of gases such as oxygen and carbon dioxide in the capsular fluid and regulate the activity of the ciliated cells accordingly. For example, in low oxygen conditions, embryos may show initially higher rotation rates to compensate for increased oxygen debt. In a preliminary study, embryos in their egg masses were subjected to carbon dioxide in the medium bathing egg capsules (Young and Goldberg, unpublished observations). This treatment resulted in a noticeable but slight increase in rotation rate, and awaits more systematic study.

iii) Serotonin and embryonic rotational behavior

Immersion of egg masses in serotonin-containing APW induced a rapid increase in rotation rate. Contrary to the developmental increase in rotation rate described previously, this change was not the result of an increase in the frequency of rotational surges. In fact, surge frequency was reduced with higher concentrations of serotonin. The primary effect of serotonin appeared to be an increase in the slow constant rotation that occurs between surges. This probably occurs through direct excitation of the ciliary cells, as has been postulated in other systems (Gosselin, 1961; Koshtoyants *et al.*, 1961; Paparo*et al.*, 1975; Catapane, 1983; Soliman, 1983). A pharmacological study of the serotonin response on cultured ciliated cells isolated from *Helisoma* embryos also suggested that the excitatory effects of serotonin are direct, and not mediated through non-serotonergic neurons (Goldberg *et al.*, 1994). Furthermore, the effects of serotonin appeared to be specific, since biogenic amines such as dopamine or octopamine had no effect on rotation rate in *Helisoma* embryos.

Examination of the dose-dependency of serotonin's effects revealed that rotation rate was affected at a threshold dose of 1.0 μM serotonin. While this dose is within the range for cilioexcitation observed in other molluscan species (Gosselin, 1961; Audesirk et al., 1979; Catapane, 1983), the actual threshold dose may be lower than the measured dose because of restricted access to the site of action. In light of the question of accessibility of

serotonin to receptors on the ciliated epithelial cells, a recent pharmacological study found that cultured ciliated cells from stage E25 *Helisoma* embryos showed a more sensitive dose-response relationship than whole embryos rotating in their egg capsules; the EC_{50} for serotonin-induced cilio-excitation *in vitro* was around 1.0 μM, whereas it was around 10 μM for stimulation of embryo rotation (Goldberg *et al.*, 1994). The capsular environment thus appears to reduce the potency of serotonin. The first potential barriers to serotonin are the egg capsule membranes, which were left intact. However, as indicated in previous experiments on *Helisoma* (Goldberg and Kater, 1989) and *Lymnaea* (Beadle, 1969), molecules in the size range of serotonin readily pass through the membranes and gain access to the embryo. The second type of barrier, and potentially a greater problem for access, is the embryonic tissue itself. If serotonin receptors are located only on the basal surface of the ciliated epithelial cells, then serotonin must access the interior of the embryo to reach the serotonin receptors. Evidence of restricted access comes from a study of several nudibranch and prosobranch species, in which ciliated velar cells displayed increased sensitivity to serotonin after being isolated from the veligers (Koshtoyants et al., 1961). Uptake through the developing gut and epithelial cells may provide general routes for entry of serotonin (McKenney and Goldberg, 1989). Inside the embryo, serotonin may be converted to γ-glutamyl-serotonin, its natural metabolite in gastropods, through the action of a γ-glutamyl transferase (Sloley, 1994; Sloley and Goldberg, 1991). Since γ-glutamyl serotonin was found to have no effect on cilia-driven rotation, its production from serotonin would effectively reduce the intra-embryonic serotonin concentration. Uptake by the yolk cells or extrusion through the larval kidney or protonephridium (which also concentrated 5,7-DHT) could also reduce intra-embryonic serotonin concentrations. Finally, uptake by ENC1 itself may reduce serotonin levels in the immediate vicinity of the synapses.

If serotonin receptors are distributed throughout the plasma membrane of the ciliated epithelial cells, the applied dose would more closely reflect the concentration of

serotonin at the receptor. The timecourse of serotonin action in the present study supports this latter possibility. Rotation rate was often affected in as little as 15 seconds after immersion in a serotonin-containing solution, indicating that access to the serotonin receptors was unrestricted. In a test of serotonin's action on embryos isolated and immobilized on glass slides, ciliary activity increased in less than 5 s after application of serotonin (results not shown). In contrast, the timecourse of recovery after a 10 min serotonin exposure was much slower. This slow recovery may reflect the activity of residual serotonin on internally-located receptors, a long-duration response mediated through a second messenger pathway, or a slow dissociation rate of serotonin from its receptor. Since embryos were incubated in serotonin solution for 10 min, the slow recovery may also reflect the latency for diffusion of residual serotonin from the egg capsule fluid. Given that the capsular membrane may have a negative electrical potential owing to its semipermeability (Taylor, 1973), and given that serotonin is a positively charged ion in solution, serotonin may remain preferentially distributed inside the egg capsule. This possibility could be tested by looking at the time course of rotation rate recovery of embryos treated with serotonin in egg capsules which have been punctured. Thus, the response latency of embryos and ciliated cells to serotonin suggests that serotonin gains rapid access to serotonin receptors on the surface of the ciliated epithelial cells. Ligand-binding studies with radiolabeled-serotonin or fluorescein-labeled serotonin would be helpful in confirming the distribution of serotonin receptors on the ciliated cells, in addition to showing whether ENC1 actually possesses serotonin receptors.

Helisoma embryos displayed stage-dependent sensitivity to serotonin, whereby stage E20 and E25 embryos were more sensitive than stage E15 and E30 embryos. Koshtoyants et al. (1961) also reported that the sensitivity to serotonin in various nudibranch species was stage-dependent, being highest during the veliger stages. However, the change in threshold concentration was far greater for the nudibranchs than for *Helisoma*, becoming as low as 10^{-15} M during veliger stages of nudibranch

development. Why there should be such a disparity in sensitivity between a marine and freshwater gastropod is difficult to explain, especially since serotonin receptors with binding affinities in the femptomolar range are unprecedented. The moderate change in sensitivity in *Helisoma* does parallel a stage-dependency in the occurrence of basal rotation rates and surge frequency. It also correlates with the development of both the pedal ciliary band and the neurite branches of EPNs which contact the band (see results sections III-vi and III-vii, respectively). Thus, the development of ENC1 and the ciliated target cells may underlie the change in sensitivity of *Helisoma* embryos to serotonin.

iv) Serotonin and rotational surges

Immersion of embryos in serotonin produced opposite responses in terms of rotation rate and frequency of rotational surges - the rate of rotation increased while the frequency of surges decreased. The decrease in surge frequency can be explained by one of two possible mechanisms. First, a decrease may result from a serotonin-induced inhibition of the surge generating system. For this hypothesis to be tenable, ENC1s would require inhibitory autoreceptors (Haydon *et al.*, 1987; Murrain *et al.*, 1990) which are activated by exogenous serotonin. Serotonin could inhibit ENC1s through the apical dendrite or, upon gaining access to the embryo, it could act at the terminals of ENC1 neurites, while stimulating the ciliated cells via a different serotonin receptor. Preliminary ligand-binding studies using radiolabeled serotonin resolved two distinct binding profiles suggestive of two receptor subtypes in the CNS of adult *Helisoma* (Goldberg, Christopher and Anctil, unpublished observations). Thus, the differential effect of serotonin on more than one type of serotonin receptor on either ENC1 or the ciliated cells cannot be ruled out and requires further study. A second possibility is that the direct excitatory effect of serotonin on the ciliated epithelial cells is sufficiently large to prevent the expression of surges generated by the release of endogenous serotonin by ENC1. Further experiments are required to distinguish between these two possibilities. One approach would be to examine the surging

of ciliary activity of intact embryos. Preliminary results show that embryos exposed to serotonin display high frequency, continuous ciliary beating with no obvious surge-like changes in frequency (Diefenbach, unpublished results). Thus, surges may be masked by an elevated baseline of non-surge rotation.

There is evidence to suggest that exogenous serotonin can affect ciliary activity in the embryos of different gastropod species (Koshtoyants *et al.*, 1961). This prompted the hypothesis that endogenous serotonin plays an important role in regulating ciliary activity. Only by altering the activity of the endogenous serotonin system can such a hypothesis be tested. In this regard, several serotonin receptor antagonists were screened for their effects on rotation (Goldberg *et al.*, 1994). Mianserin, a serotonin receptor antagonist generally considered more specific for 5-HT_2 receptors (Saudou and Hen, 1994) known to be effective in insects (Baines and Downer, 1991) and molluscan oocytes (Kadam and Koide, 1989), effectively blocked the serotonin-induced increase in rotation rate. More importantly, in the absence of exogenous serotonin, mianserin reduced the overall rotation rate to a level comparable to that of non-surge rotation in control embryos and virtually eliminated rotational surges. These pharmacological results indicate that mianserin blocked the activation of serotonin receptors by endogenous serotonin, thus preventing the serotonin-mediated surges from occurring. Furthermore, since high concentrations of mianserin did not totally abolish rotation, endogenous serotonin appears to be primarily involved in the generation of surges, rather than the maintenance of non-surge rotation. Thus, there is a serotonin-insensitive component to rotation rate. Goldberg *et al.* (1994) recently found that ciliated cells from stage E25 *Helisoma* embryos isolated in culture showed no changes in ciliary beat frequency as a result of exposure to 100 μM mianserin, whereas the response to equimolar serotonin was attenuated by about 50 % by minaserin. Therefore, mianserin appears to inhibit the action of serotonin rather than ciliary activity *per se*.

An extension of the hypothesis that rotational surges are generated by endogenous serotonin is that the paired ENC1s act as cilioexcitatory motor neurons which generate rotational surges. While direct evidence is lacking, several sets of observations are consistent with this hypothesis. First, rotational surges are expressed initially between stages E15 and E20, the same period during which ENC1 first expressed serotonin-immunoreactivity. Second, as discussed previously, ENC1 appears to innervate the pedal ciliary band. Third, preliminary electrophysiological experiments suggest that ENC1 is electrically excitable and exhibits spontaneous bursting activity (data not shown). Fourth, immersion of embryos in exogenous serotonin induces a dose-dependent, reversible increase in the rate of rotation. Fifth, exposure of embryos to ultraviolet (UV) light consistently resulted in increased ciliary activity and rotation (results not shown). In contrast, UV light exposure of isolated ciliated cells resulted in complete cessation of ciliary beating (K. Christopher, personal communication). UV light exposure may therefore stimulate ENC1 to release serotonin, thereby stimulating ciliated cells. Sixth, and most importantly, an effective serotonin antagonist prevents the expression of rotational surges. These results strongly implicate ENC1 as a motor neuron which utilizes serotonin as a cilioexcitatory neurotransmitter. However, a more direct test of ENC1s role in regulating ciliary activity would be to determine whether the ablation of ENC1s results in the abolition of ciliary surges, or, conversely, whether direct electrical stimulation of ENC1 increases ciliary beat frequency.

V) Potential homologue of ENC1 in *Lymnaea* and other molluscs.

A comparative examination of *Lymnaea stagnalis* and *Helisoma trivolvis* was undertaken to determine if *Lymnaea* embryos possess a cell homologous to ENC1. Given that ENC1 is the first neuron of its kind to be identified in a molluscan embryo, this study served to answer the question whether ENC1 is unique to *Helisoma* or if a cell like it is present in another related gastropod species. *Lymnaea* was chosen for the comparative

study since both it and *Helisoma* are in the order of Limnophila, much is known of its development (Morrill, 1982), and many neurons from adult *Lymnaea* and *Helisoma* have been found to be homologous, including the giant metacerebral serotonergic neurons (Granzow and Rowell, 1981). An ENC1-like cell was found in *Lymnaea*, but did not express serotonin. Rather, the immunohistochemical and rotation behavior experiments suggest that the ENC1-like cell of *Lymnaea* utilizes dopamine as a neurotransmitter to regulate rotation of the embryo. As mentioned in the results, these cells will be provisionally referred to as $ENC1_{Lym}$. Neurons homologous to ENC1 may therefore be common in pulmonate gastropods, but differ in their neurotransmitter phenotypes.

i) Morphological and neurotransmitter phenotype of $ENC1_{Lym}$

In the comparative immunohistochemical study of serotonin expression of *Lymnaea* and *Helisoma* embryos, a serotonergic ENC1 was not found in *Lymnaea*, confirming the finding of Marois and Croll (1992) for *Lymnaea* embryos. It should be mentioned that a comparative study by Voronezhskaya and Elekes (1993) revealed in *Helisoma* and *Planorbis corneus* a serotonin-immunoreactive neuron which possessed an apparent apical dendrite and which lost its serotonin immunoreactivity later in development. They also reported that this neuron was absent from *Lymnaea*. This cell was called TS1 and appears to be homologous to ENC1, at least in terms of its gross morphology and neurite outgrowth pattern. As this study was initiated based on the first demonstration of ENC1 by Goldberg and Kater (1989), it supports the idea that ENC1-like cells are found in select gastropod species.

Dopamine is a common neurotransmitter in molluscs that is involved in the regulation of several processes, including locomotion (Audesirk, 1978), feeding (McLean *et al.*, 1989; Nagle and Greenberg, 1982), respiration (Syed *et al.*, 1990), and growth (Stoof *et al.*, 1984). Furthermore, it has also been found to inhibit neurite outgrowth of select neurons from *Helisoma* (McCobb *et al.*, 1988b). It was therefore considered a

possible candidate neurotransmitter for $ENC1_{Lym}$. Immunostaining with a tyrosine hydroxylase antibody revealed a pair of cells similar to ENC1, as distinguished by their location, possession of a ventromedially-directed primary neurite and apical dendrite. Although TH immunostaining was absent from distal neurites, either because of localized expression or low intensity fluorescence, neurites were observed in the pedal region via DIC microscopy and resembled the neurites of ENC1 in their distribution. That these cells were TH immunopositive does not rule out the presence of epinephrine or norepinephrine, which could be produced from dopamine. However, norepinephrine was not detected in *Helisoma* using high performance liquid chromatography (Sloley and Goldberg, 1991). Furthermore, in a study by Trimble *et al.* (1984), ^{3}H-dopamine, but not ^{3}H-norepinephrine, was found to be synthesized from ^{3}H-tyrosine in the CNS of *Helisoma*. This is not to say that norepinephrine is entirely absent from molluscs. An HPLC study of larvae of the pacific oyster, *Crassostrea gigas*, resolved a large amount of dopamine, less norepinephrine, and no epinephrine (Coon and Bonar, 1986). In an earlier study, Coon *et al.* (1985) found that norepinephrine and L-DOPA induced settlement and metamorphosis of oyster larvae. This was the first demonstration of a possible function for norepinephrine in molluscs. Thus, norepinephrine is not a common neurotransmitter in molluscs. These findings strongly suggest that $ENC1_{Lym}$ expresses dopamine rather than norepinephrine. If $ENC1_{Lym}$ does express dopamine, this would likely be the earliest dopaminergic neuron to appear in *Lymnaea* embryos, since no other TH-immunostained cells resembling neurons were observed. $ENC1_{Lym}$ is also the first putative dopaminergic neuron to be identified in a gastropod embryo.

An interesting feature of $ENC1_{Lym}$ is its capacity to take up the fluorescent serotonin analogue, 5,7-DHT. By switching to DIC optics, many morphological features of $ENC1_{Lym}$ were found to be in common with ENC1 of *Helisoma*. If $ENC1_{Lym}$ is a dopaminergic neuron, perhaps the uptake system in $ENC1_{Lym}$ can bind both dopamine and serotonin. Indeed, there are reports of single transporters taking up both dopamine and

serotonin (Faraj *et al.*, 1994), in addition to their precursors, tyrosine and tryptophan (Yorek *et al.*, 1987). It is therefore possible that $ENC1_{Lym}$ and ENC1 of *Helisoma* possess a similar transporter for serotonin and dopamine. Evidence that ENC1 can take up dopamine is, however, lacking. A comparative pharmacological analysis using uptake blockers, or a radiographic binding study could be employed to compare the specificity of uptake between these two cells.

Kerkut *et al.* (1967) found that some neurons in the garden snail *Helix aspersa* showed uptake for both DOPA (3,4-dihydroxyphenylalanine), the immediate precursor of dopamine, and serotonin. An immunohistochemical study by Boer *et al* (1984) found in *Lymnaea* that some serotonergic neurons, including the adult cerebral ganglion neuron C1, possessed anti-dopamine immunoreactivity. That "classical" neurotransmitters may be co-localized in single neurons has also been reported for the L cell of the commissural ganglion of lobster, which expresses serotonin and dopamine (Cournil *et al.*, 1984). Both the amacrine cells in larval salamander (Watt, 1992) and the neurons of rat ventral medulla oblongata (Millhorn *et al.*, 1988) coexpress serotonin and GABA. Furthermore, Johnson (1994) found that serotonergic raphe neurons from rat released both serotonin and glutamate, the effects of which were separated by latencies on the order of tens of milliseconds. These findings support the possibility that select neurons in *Lymnaea* and *Helisoma* can express and take up either neurotransmitter, but that the expression of one neurotransmitter over the other depends on as yet unknown factor(s). Indeed, from the 5,7-DHT results presented here, ENC1 from both *Lymnaea* and *Helisoma* showed serotonin-like uptake capacity, while only ENC1 from *Helisoma* expressed serotonin immunoreactivity.

Whether ENC1 expresses serotonin or dopamine in a given snail species may depend upon the coexpression of neuropeptides. For example, immunohistochemical examination suggests that the serotonergic neuron C1 of *Helix aspersa* expresses cholecystokinin (Osborne *et al.*, 1982) and the neuron C1 of *Lymnaea* expresses vasotocin

(Boer *et al.*, 1984). Similarly, some vertebrate neurons express both dopamine and cholecystokinin (Hoekfelt *et al.*, 1984), whereas substance P, thyrotropin releasing hormone and enkephalin have been found to be colocalized with serotonin in vertebrate serotonergic neurons (Glazer *et al.*, 1981; Johansson *et al.*, 1981). In *Lymnaea*, the light green neuroendocrine cells of the cerebral ganglia appear to express an enkephalin-like peptide in the Spring, a gastrin/cholecystokinin-like peptide in the Fall, and both peptides in the Winter (Gesser and Larsson, 1985). It was additionally found that the caudodorsal cells of the cerebral ganglia showed a gradual switch from enkephalin to gastrin/cholecystokinin-like peptide expression with advancing age. Seasonal or age-related factors may therefore also affect the choice of serotonin versus dopamine in ENC1. In the oyster, significantly more dopamine was found in earlier than later-staged larvae (Coon and Bonar, 1986). There may be neurons in the larval nervous system of oyster which transiently express dopamine, just as ENC1 in *Helisoma* transiently expresses serotonin.

Although one could speculate on numerous potential factors which could determine the neurotransmitter phenotype of ENC1 in *Lymnaea* and *Helisoma*, one factor deserves serious consideration as being key: inbreeding. The strain of *Helisoma* used in the experiments is an inbred albino strain (Kater, 1974). The snails have virtually no pigment and have translucent shells and integuments. Wildtype *Helisoma* have a dark brown, opaque shell and uniform dark brown to black skin pigmentation. *Helisoma* raised in isolation will undergo self-fertilization (Kater, 1974). This results in virtually all of the loci becoming homozygous, causing albinism. Occasional, partial reversions to the wildtype can be distinguished by patches of dark pigment on the shell. The embryos of *Helisoma* are similarly devoid of pigment. Although the *Lymnaea* used in this thesis were laboratory reared and may therefore experience some inbreeding due to confinement, the embryos of *Lymnaea* were pigmented; they began showing patches of black pigment by stage E30 (Diefenbach, personal observation) and are not inbred (Bulloch, personal communication). Audesirk *et al.* (1985) measured the serotonin content of cerebral ganglion neuron C1 and

the giant dopaminergic neuron of the right pedal ganglion (RPeD1) in wildtype and self-fertilized *Lymnaea stagnalis*. They found that the serotonin content of neuron C1 was increased by inbreeding. That is, neurons C1 of the inbred snails possessed consistently higher levels of serotonin, while the wildtype neurons C1 had some neurons with comparable levels of serotonin, but most had much lower levels of expression. In contrast, the dopamine content of RPeD1 was unaffected by inbreeding. The authors concluded that inbreeding could fixate an allele which enhances serotonin production. Thus, ENC1 of inbred *Helisoma* may over-express serotonin to the extent that it is detectable via serotonin immunofluorescence.

Although the Audesirk study provides a reason why ENC1 expresses serotonin, it does not explain why $ENC1_{Lym}$ may express dopamine. This brings us to the fact that *Lymnaea* embryos are pigmented. Dark pigmentation results from melanin, which is synthesized from L-DOPA, the immediate precursor of dopamine (Voet and Voet, 1990). Melanin production may therefore predispose the embryo to synthesize dopamine on account of an abundance of L-DOPA . All that is required to synthesize dopamine from L-DOPA is aromatic amino acid decarboxylase, which $ENC1_{Lym}$ would possess regardless of whether it synthesizes dopamine or serotonin, since this enzyme also catalyzes the conversion of 5-hydroxytryptophan to serotonin. Without pigment production, as in *Helisoma*, dopamine synthesis would not be promoted.

The effect of albinism on dopamine synthesis may also be exerted at the level of tyrosine hydroxylase expression. Park (1990) found that in albino rats, the retina had lower tyrosine hydroxylase expression than in retina from non-albino rats. L-DOPA has been found to inhibit tryptophan hydroxylase, and 5-hydroxytryptophan inhibits tyrosine hydroxylase (Hashiguti *et al.*, 1993). This reciprocal inhibition of the synthetic machinery of serotonin and dopamine could account for reports of their expression being inversely related in molluscs (Stefano *et al.*, 1976). It also could account for the increase in serotonin

and decrease in dopamine content of *Helisoma* ganglia which may have resulted from isolation in culture (Results section II-ii).

Thus, the combined positive effect of inbreeding on serotonin production and a negative effect of albinism on dopamine production may be the reason why ENC1 expresses serotonin and $ENC1_{Lym}$ does not. From this hypothesis, one would predict that embryos of wildtype *Helisoma*, which are highly pigmented, should possess ENC1s which express dopamine instead of serotonin, or have significantly reduced serotonin production. This hypothesis has yet to be tested. If it proves correct, it would be interesting to examine whether dopamine expressed in ENC1 of wildtype *Helisoma* could also play an autoregulatory role.

From the comparative study of *Helisoma* and *Lymnaea*, it is apparent that population inbreeding may influence the choice of neurotransmitter by a neuron. It also underscores the need for criteria in addition to neurotransmitter phenotype when assigning an identity to a neuron. And finally, this comparative system could provide an invertebrate model of a human disorder which claims many lives: anorexia nervosa. Individuals with this condition, which is characterized by self-imposed undernourishment and starvation, have recently been found to have depressed tyrosine hydroxylase activity and enhanced tryptophan hydroxylase activity (Hirata *et al.*, 1990). Therefore, understanding the interactions between these two neurotransmitter systems in an identified molluscan neuron may yield insight into the etiology of this disorder.

ii) Characteristics of rotational behavior in *Lymnaea*

Lymnaea embryos displayed rotational behavior characteristics comparable to those of *Helisoma* including two vectors of rotation; the occurrence of surges, and continuous rotation at stage E25. The major difference between *Lymnaea* and *Helisoma* embryos was that *Lymnaea* embryos yawed clockwise when viewed dorsally, whereas *Helisoma* embryos yawed counterclockwise. These opposite directions of rotation correlate with the

type of body symmetry of these two species, with *Lymnaea* being dextral (right-handed) and *Helisoma* being sinestral (left-handed). Given the similarity in the embryonic rotational behavior of the two species, it is likely that they share common cellular machinery regulating the behavior. This possibility is strongly supported by the identification of an ENC1-like cell in *Lymnaea*.

iii) Dopamine, serotonin and embryonic rotational behavior

Given that the ENC1-like cell of *Lymnaea* embryos express dopamine or some other catecholamine rather than serotonin, the rotational behavior of *Lymnaea* embryos may be subject to regulation by the endogenous neurotransmitter of $ENC1_{Lym}$. The goals of the pharmacological experiments were thus to determine whether *Lymnaea* embryos display changes in rotational behavior resulting specifically from exposure to exogenous dopamine, whether the effects of dopamine are specific receptor-mediated responses, and whether an endogenous dopamine-like compound normally regulates the rotational behavior.

Lymnaea embryos responded to both dopamine and serotonin with an increase in rotation rate, whereas octopamine had no effect. The lack of an effect of octopamine implies that the effects of dopamine and serotonin are specific. Furthermore, embryos showed dose-dependent increases in rotation rate in response to both compounds. However, the sensitivity of the embryos to serotonin and dopamine appeared to be very low, with EC_{50} values approaching the mM range. A serotonin receptor was recently cloned from *Lymnaea* which had moderate affinity for serotonin, with a dissociation constant of 0.9 nM (Sugamori *et al.*, 1993). It is possible that, either the receptors involved have very low affinity, or that egg mass structures impede the diffusion of the compounds to the site of action, thereby lowering their effective concentration at the sites of action. To distinguish between these possibilities, embryos were exposed to dopamine and serotonin under two conditions: in semi-intact egg masses which have incisions made in the external egg mass membrane, and in isolated egg capsules. For both dopamine and serotonin,

isolation of egg capsules resulted in an increase in the maximal responses of the embryos to most of the concentrations tested. The increase in effectiveness was more evident with serotonin. With the outer egg mass membrane being essentially absent in semi-intact egg masses, other barriers to diffusion could include the intercapsular jelly, the inner and outer capsular membranes and the perivitelline fluid of the egg capsule itself. In a study of the permeability properties of the capsular membranes of *Lymnaea* embryos (Beadle, 1969), molecules in the size range of serotonin were found to pass through the membranes. If the capsular membranes are not a barrier to diffusion, the difference in responses of embryos in semi-intact egg masses versus isolated egg capsules may result from the presence of intercapsular jelly. Furthermore, if the neurotransmitter receptors are located primarily on the intraembryonic basal membrane of ciliated cells, then the tissues through which serotonin and dopamine gain entry into the embryo present additional diffusion barriers. It is not known for either *Helisoma* or *Lymnaea* where receptors are concentrated on the ciliary membranes.

The role of diffusion barriers would be best addressed by testing the responses of isolated ciliated cells in culture to serotonin and dopamine. Indeed, in a pharmacological study of *Helisoma* embryos, isolated ciliated cells in culture were found to be between 10 and 100 times more sensitive to serotonin than whole embryos (Goldberg *et al.*, 1994). Therefore, although the observed responses to dopamine and serotonin do not reflect the actual affinity of the receptor or receptors involved, the fact that serotonin produced consistently greater increases in rotation rate than dopamine, whether the curves from semi-intact egg masses or isolated egg capsules are compared, argues for a greater sensitivity of the embryos to serotonin than dopamine.

Since *Lymnaea* embryos responded to both dopamine and serotonin, it is possible that the ciliated cells of the embryos can express both serotonin and dopamine receptors. If ENC1-like cells can express dopamine or serotonin, it follows that the target cells should be capable of responding to either neurotransmitter. In addition, since in adult *Lymnaea*

serotonin is the primary cilioexcitatory neurotransmitter of pedal cilia (Syed and Winlow, 1989), it is not surprising that pedal cilia of *Lymnaea* embryos are responsive to serotonin. *Helisoma* embryos were found to be insensitive to dopamine, which is consistent with the fact that dopamine has not been found in cilioexcitatory motor neurons of *Helisoma*. Just as *Lymnaea* embryos appear more sensitive to serotonin than dopamine, *Helisoma* embryos may also be less sensitive to dopamine so that a response cannot be resolved in whole embryo assays. From the results with *Lymnaea* embryos, it may be the case that isolated ciliated cells from *Helisoma* are also weakly sensitive to dopamine.

If dopamine does serve as a neurotransmitter to regulate the rotation rate of *Lymnaea* embryos, its effect should be inhibited by a dopamine receptor antagonist. Of the three antagonists tested, domperidone had no effect, haloperidol acted as an agonist, and SKF83566 antagonized the dopamine-induced increases in rotation rate. Since SKF83566 did not reduce basal rotation rate with anywhere near the magnitude of that seen with mianserin in *Helisoma* embryos, this result could argue against dopamine being the endogenous neurotransmitter released by $ENC1_{Lym}$ onto the pedal ciliated cells. At least two factors may explain why SKF83566 did not work. Since the experiments were performed on embryos in semi-intact egg masses, SKF83566 may not be reaching the receptor sites at sufficient concentration to block the effect of dopamine released by $ENC1_{Lym}$. If accessibility is a problem, a higher concentration of SKF83566, or SKF83566 added to isolated egg capsules may have an effect. However, 1.0 mM SKF83566 had no consistent effect on rotation rate, and 0.1 mM SKF83566 had no effect on the rotation rate of isolated egg capsules (data not shown). SKF83566 may in fact not be able to penetrate embryos and act at $ENC1_{Lym}$ ciliary synapses, but may act only on extraembryonic dopamine receptors. Another possibility is that the three bands of cilia may be differentially responsive to dopamine. *Lymnaea* embryos differ from *Helisoma* embryos in that they possess an apical band of cilia, which lies along the same medial plane as the pedal band and may generate the pitch component of rotation which contributes the main

thrust to rotation. It is possible that, if the apical band is insensitive to dopamine, SKF83566 could block the effect of dopamine on the pedal ciliary band, and the insensitive apical band could still maintain basal rotation rate. SKF83566 by itself would therefore be ineffective because of the larger component of rotation contributed by the apical ciliary band. This hypothesis would best be addressed be testing whether isolated ciliated cells in culture respond differentially to dopamine, and whether cells which do respond show sensitivity to the antagonistic effect of SKF83566.

The findings that a cell resembling ENC1 in *Helisoma* exists in *Lymnaea*, that this putative ENC1 homologue shows tyrosine hydroxylase immunoreactivity, and that *Lymnaea* embryos respond specifically to dopamine suggest that an ENC1-like cell may utilize dopamine in *Lymnaea* to regulate rotational behavior, much as ENC1 utilizes serotonin in *Helisoma*. Further experiments to confirm the dopaminergic identity of $ENC1_{Lym}$ would include immunostaining embryos with a dopamine antibody and cell culture experiments to further characterize the specificity of the dopamine response.

In summary, the results from this set of studies provide for the first time evidence that serotonin can serve a dual role as a neurotransmitter which regulates the development of an embryonic behavior, in addition to a factor which determines the extent of neurite outgrowth of a neuron from which it is released. A role for the target in mediating the effects of serotonin on neurite branching was also suggested, providing a novel mechanism through which the target can communicate with a nascent neurite to initiate branching. The development of an identified molluscan neuron was characterized for the first time, with evidence that this neuron may act as a motor neuron to regulates an early embryonic behavior. Finally, a comparative study of *Helisoma* and *Lymnaea* uncovered two potentially homologous neurons with different neurotransmitter phenotypes.

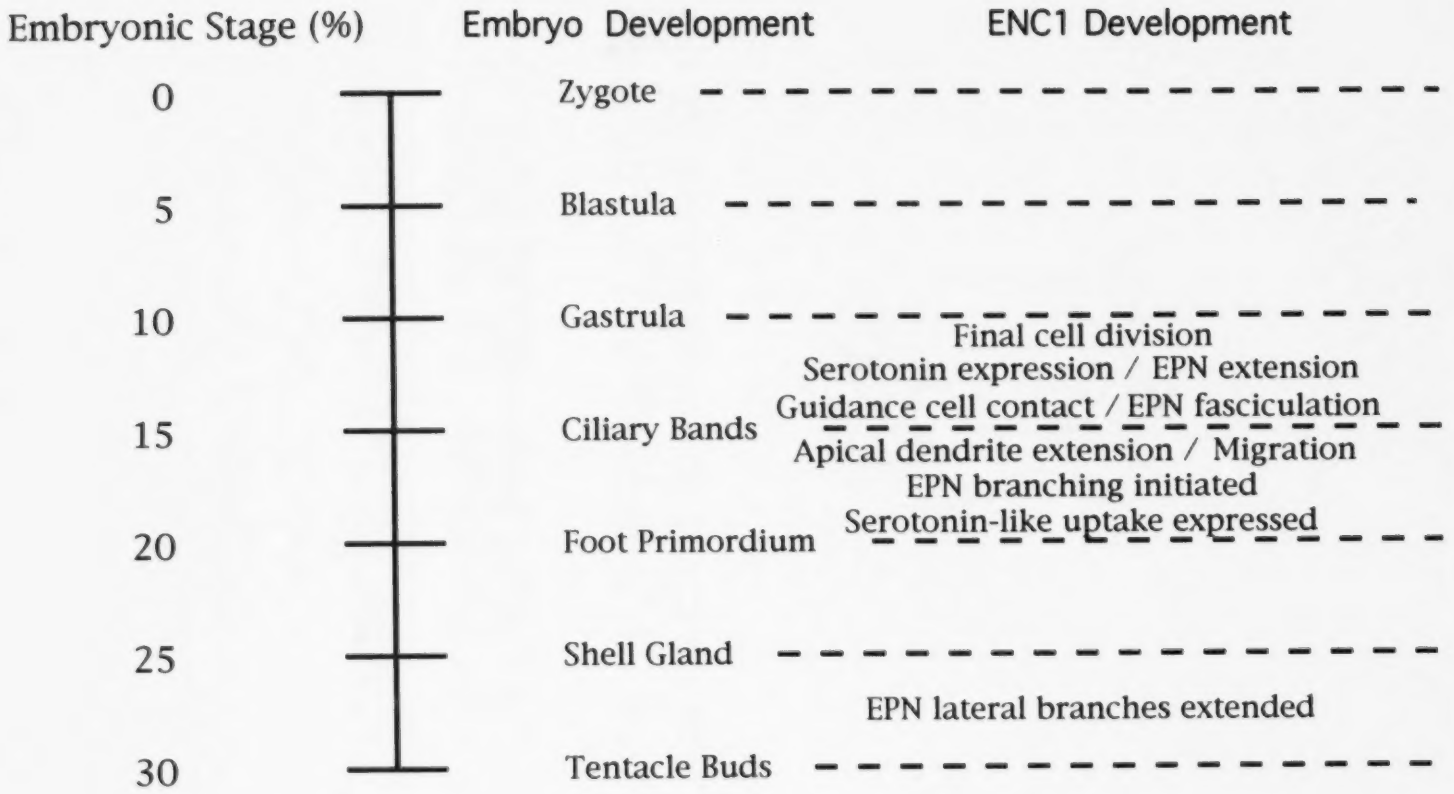

Figure 51: Tentative chronology of events associated with the differentiation and early development of ENC1. These events are shown in a time line of percent embryogenesis, with major distinguishing characteristics of the embryo provided for reference. Events sharing a single line occur close enough together in time to be considered coincident.

Figure 52: Schematic illustrating the developmental progression of neurite outgrowth of the EPNs over the pedal ciliary band. Each identified ciliated cell is shown as they appear labelled in Figure 11. The two dark circles represent the somata of ENC1s. The oval between the ENC1 somata is the stomodaeum. The initial pathway is established by stage E13 to E15, with the right EPN preceding the left one as they proceed toward the midline, where they fasciculate. At this stage, only cell PeA is ciliated (see Figure 11). From stage E15 to E20, neurite back-branching is initiated in conjuction with the differentiation of the other pedal ciliated cells. Between stage E20 and E25, neurite branching proceeds without any obvious morphological changes in the pedal ciliary band. Further back-branching occurs between stages E25 to E30, in addition to elongation of the pedal ciliary band and appearance of the medial cell PeE (not shown because of it ventral position on the foot primordium) and the lateral cells PeLA1 and PeLA2. Note that ENC1s extend lateral neurites over this bilateral pair of ciliated cells.

E13

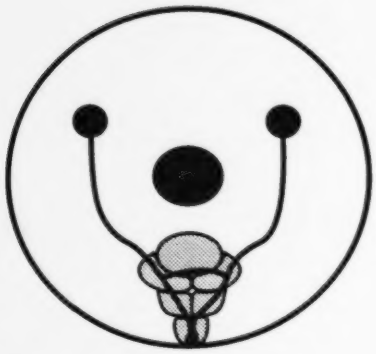

E15-E20

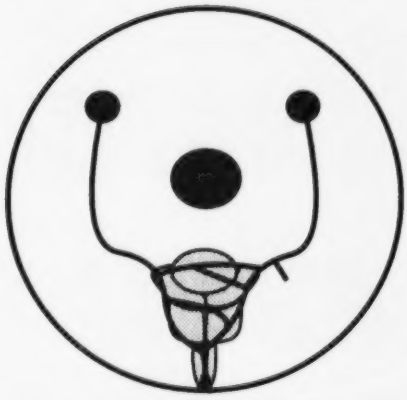

E25

E30

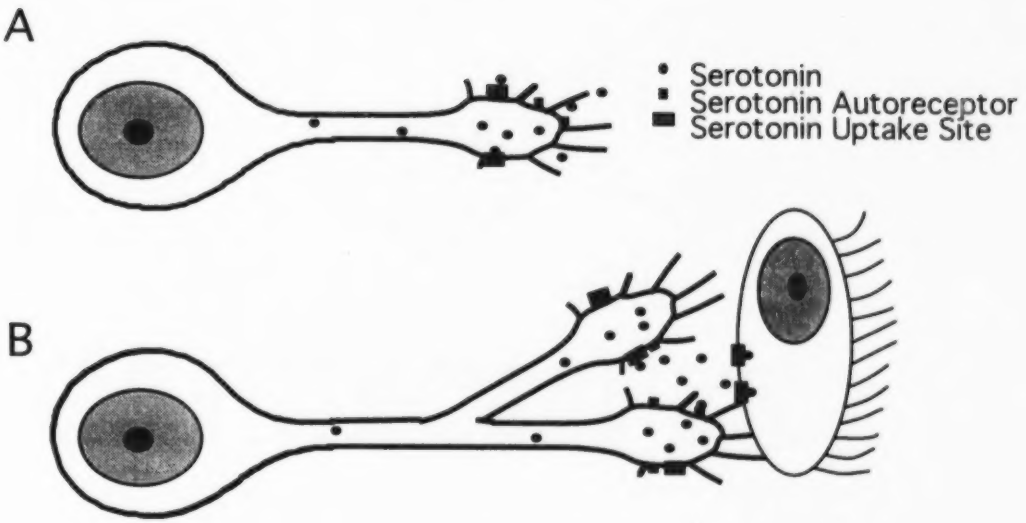

Figure 53: Model of possible mechanism whereby serotonin autoreceptors regulate neurite outgrowth in the target cell region. **A.** While approaching the target, EPNs and EPN growth cones spontaneously release serotonin, which, upon binding to serotonin autoreceptors, prevent neurite branching. **B.** As EPNs grow over the ciliated target cells, the target cells bind and take up serotonin released by EPNs, thereby reducing the amount of serotonin available to bind serotonin autoreceptors, and releasing the neurites from inhibition of branching.

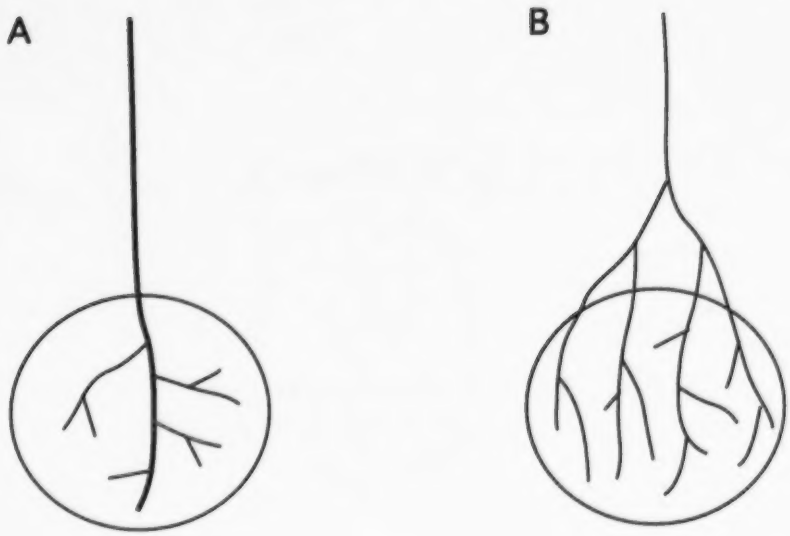

Figure 54: Modeled patterns of neurite branching in the target region. Two schematic representations of how a pattern of neurite branching could be established are shown. **A.** In the first strategy, the growth cone of a primary neurite (thick line) first arrives at the target (circle) and traverses the target. Back-branching then occurs as secondary neurites are elaborated from the primary neurite to complete full coverage of the target region. This is the strategy observed to occur during innervation of the pedal ciliary band by neurites of ENC1. **B.** In the second strategy, the primary neurite undergoes branching by bifurcation either prior to or after contact with the target, resulting in numerous growth cones traversing the target to complete coverage.

Footnotes

1. A version of this section of the Results will be submitted to the Journal of Neuroscience for review.

2. I wish to acknowledge the technical assistance of Ron Koss with immunostaining and confocal microscopy.

3. A version of this section of the Results has been published. Diefenbach, T. J., Sloley, B. D. and Goldberg, J. I. 1995. Developmental Biology 167: 232-293.

4. A version of this section of the Results has been published. Diefenbach, T. J., Koehncke, N. K. and Goldberg, J. I. 1991. Journal of Neurobiology 22(9): 922-934.

5. The technical assistance of Niels Koehncke in testing the antagonistic effect of mianserin and the specificity of serotonin's effect is greatly appreciated.

6. The technical assistance of Dennis Djogovic in carrying out most of the pharmacological experiments on *Lymnaea* embryos is greatly appreciated. The technical assistance of Ron Koss with slide preparation for confocal microscopy is also appreciated.

7. Part of the results of this section of the Results have appeared in abstract form. Diefenbach and Goldberg, 1994. Bull. Can. Soc. Zool. 24: 45

Literature Cited

Aiello, E. 1962. Identification of the cilioexcitatory substance present in the gill of the mussel Mytilus edulis. J. Cell Comp. Physiol. 60: 17-21.

Al-Mohanna, F. A., Cave, J. and Bolsover, S. R. 1992. A narrow window of intracellular calcium concentration is optimal for neurite outgrowth in rat sensory neurones. Dev. Brain Res. 70: 287-290.

Arregui, C. O., Carbonetto, S. and McKerracher, L. 1994. Characterization of neural cell adhesion sites: point contacts are the sites of interaction between integrins and the cytoskeleton in PC12 cells. J. Neurosci. 14(11): 6967-6977.

Arkett, S. A. 1988. Development and senescence of control of ciliary locomotion in a gastropod veliger. J. Neurobiol. 19: 612-623.

Arkett, S. A., Mackie, G. O. and Singla, C. L. 1987. Neuronal control of ciliary locomotion in a gastropod veliger (Calliostoma). Biol. Bull. 173: 513-526.

Audesirk, G. 1978. Properties of central motor neurons exciting locomotory cilia in *Tritonia diomedea*. J. comp. Physiol. 128: 259-267.

Audesirk, G., Audesirk, T., McCaman, R. E. and Ono, J. K. 1985. Evidence for genetic influences on neurotransmitter content of identified neurones of *Lymnaea stagnalis*. Comp. Biochem. Physiol. 81C(1): 57-60.

Audesirk, G., McCaman, E. and Willows, A. O. D. 1979. The role of serotonin in the control of pedal ciliary activity by identified neurons in *Tritonia diomedea*. Comp. Biochem. Physiol. 62C: 87-91.

Azmitia, E. C. and Whitaker-Azmitia, P. M. 1987. Target cell stimulation of dissociated serotonergic neurons in culture. Neurosci. 20(1): 47-63.

Azmitia, E. C., Dolan, K. and Whitaker-Azmitia, P. M. 1990. S-100B but not NGF, EGF, insulin or calmodulin is a CNS serotonergic growth factor. Brain Res. 516(2): 354-356.

Bailey, C. H. and Chen, M. 1983. Morphological basis of long-term habituation and sensitization in *Aplysia*. Science 220: 91-93.

Bailey, C. H. and Chen, M. 1988. Morphological basis of short-term habituation in *Aplysia*. J. Neurosci. 8(7): 2452-2459.

Bailey, C. H. and Chen, M. 1989. Time course of structural changes at identified sensory neuron synapses during long-term sensitization in *Aplysia*. J. Neurosci. 9(5): 1774-1780.

Bailey, C. H., Chen, M., Keller, F. and Kandel, E. R. 1992. Serotonin-mediated endocytosis of apCAM: an early step of learning-related synaptic growth in *Aplysia*. Science 256: 645-648.

Baines, R. A. and Downer, R. G. 1991. Pharmacological characterization of a 5-hydroxytryptamine-sensitive receptor/adenylate cyclase complex in the mandibular closer muscles of the cricket, *Gryllus domestica*. 16(3): 153-163.

Bamburg, J. R., Bray, D. and Chapman, K. 1986. Assembly of microtubules at the tip of growing axons. Nature 321: 788-790.

Barlow, L. A. and Truman, J. W. 1992. Patterns of serotonin and SCP immunoreactivity during metamorphosis of the nervous system of the Red Abalone, *Haliotis rufescens*. J. Neurobiol. 23(7): 829-844.

Bate, M. 1976. Pioneer neurons in an insect embryo. Nature 260: 54-55.

Battelle, B.-A., Edwards, S. C., Kass, L., Maresch, H. M., Pierce, S. K. and Wishart, A. C. 1988. Identification and function of octopamine and tyramine conjugates in the *Limulus* visual system. J. Neurochem. 51: 1240-1251.

Beadle, L. C. 1969. Salt and water regulation in the embryos of freshwater pulmonate molluscs. J. Exp. Biol. 50: 475-479.

Bear, M. F. and Singer, W. 1986. Modulation of visual cortical plasticity by acetylcholine and noradrenalin. Nature 320: 172-176.

Beltz, B. S., Helluy, S. M., Ruchhoeft, M. L. and Gammill, L. S. 1992. Aspects of the embryology and neuronal development of the American lobster. J. Exp. Zool. 261: 288-297.

Ben-Ari, Y., Cherubini, E. and Krnjevic, K. 1988. Changes in voltage dependence of NMDA currents during development. Neurosci. Lett. 94: 88-92.

Benjamin, P. R. and Rose, R. M. 1979. Central generation of bursting in the feeding system of the snail, *Lymnaea stagnalis*. J. Exp. Biol. 80: 93-118.

Bennett, M R. and Pettigrew, A. G. 1975. The formation of synapses in amphibian striated muscle during development. J Physiol. (Lond.) 252: 203-239.

Bentley, D. and Caudy, M. 1983. Pioneer axons lose directed growth after selective killing of guidepost cells. Nature 304: 62-65.

Bentley, D., Guthrie, P. B. and Kater S. B. 1991. Calcium ion distribution in nascent pioneer axons and coupled preaxonogenesis neurons *in situ*. J. Neurosci. 11(5): 1300-1308.

Bentley, D., Keshishian, H., Shankland, M. and Toroian-Raymond, A. 1979. Quantitative staging of embryonic development of the grasshopper, *Schistocerca nitens*. J. Embryol. Exp. Morphol. 54: 47-74.

Berdan, R. C. and Easaw, J. C. 1992. Modulation of sprouting in organ culture after axotomy of an identified molluscan neuron. J. Neurobiol. 23(4): 433-450.

Berdan, R. C., Shivers, R. R. and Bulloch, A. G. M. 1987. Chemical synapses, particle arrays, pseudo-gap junctions and gap junctions of neurons and glia in the buccal ganglion of *Helisoma*. Synapse 1: 304-323.

Berry, M. S. and Pentreath, V. W. 1976. Properites of a symmetric pair of serotonin-containing neurones in the cerebral ganglia of *Planorbis*. J. Exp. Biol. 65: 361-380.

Bishop, G. A., Ho, R. H. and King, J. G. 1985. A transient serotonergic pathway in the cerebellum. Anat. Embryol. 171: 325-338.

Blair, S. S., Murray, M. A. and Palka, J. 1985. Axon guidance in cultured epithelial fragments of *Drosophila* wing. Nature 315: 406-409.

Boer, H. H., Schot, L. P. C., Steinbusch, H. W. M., Montagne, C. and Reichelt, D. 1984. Co-existence of immunoreactivity to anti-dopamine, anti-serotonin and anti-vasotocin in the cerebral giant neuron of the pond snail *Lymnaea stagnalis*. Cell Tissue Res. 238: 411-412.

Bonar, D. B. 1978. Ultrastructure of a cephalic sensory organ in larvae of the gastropod *Phestilla sibogae* (aeolidacea, nudibranchia). Tiss. Cell 10(1): 153-165.

Bradford, M. 1976. Rapid quantitative and sensitive method for the quantitation of microgram quantities of protein utilizing the principle of protein dye-binding. Analyt. Biochem. 72: 248-254.

Bray, D. and Chapman, K. 1985. Analysis of microspike movements on the neuronal growth cone. J. Neurosci. 5(12): 3204-3213.

Bridgman, P. C. 1992. Functional anatomy of the growth cone in relation to its role in locomotion and neurite assembly. *In* The Nerve Growth Cone (P. C. Letourneau, S. B. Kater and E. R. Macagno, Eds.), Raven Press, New York. pp.39-53.

Brown, M. C., Holland, R. L. and Hopkins, W. G. 1981. Motor nerve sprouting. Annu. Rev. Neurosci. 4: 17-42.

Bubel, A. 1983. Epidermal cells, Ch. 24. *In* Mollusca. Vol. 7. (A. O. D. Willows, Ed.), pp. 400-447. Academic Press, Inc., New York.

Bulloch, A. G. M. 1985. Development and plasticity of the molluscan nervous system. *In* The Mollusca Vol. 8. Neurobiology and Behavior. Part 1, Ch. 4. (A. O. D. Willows, Ed.). Academic Press, Inc., New York. pp. 335-410.

Bulloch, A. G. M. 1987. Somatostatin enhances neurite outgrowth and electrical coupling of regenerating neurons in *Helisoma*. Brain Res. 412: 6-17.

Bulloch, A. G. M. 1989. Sprouting by intact *Helisoma* neurons: role for glutamate. J. Neurosci. Res. 23(4): 384-395.

Bulloch, T. H. and Horridge, G. A. 1965. Stucture and Function in the Nervous Systems of Invertebrates. Vol. 2 W. H. Freeman, San Francisco.

Burmeister, D. W. and Goldberg, D. J. 1988. Micropruning: The machanism of turning of *Aplysia* growth cones at substrate borders *in vitro*. J. Neurosci. 8(9): 3151-3159.

Burrell, D. E. and Stefano, G. B. 1981. Analysis of monoamine accumulations in the neuronal tissues of *Mytilus edulis* (bivalvia) I. Ganglionic variations. Comp. Biochem. Physiol. 70C: 71-76.

Buettner, H. M. and Pittman, R. N. 1991. Quantitative effects of laminin concentration on neurite outgrowth *in vitro*. Dev. Biol. 145; 266-276.

Buznikov, G. A. 1984. The action of neurotransmitters and related substances on early embryogenesis. Pharmc. Ther. 25: 23-59.

Buznikov, G. A. and Shmukler, Y. B. 1981. The possible role of "prenervous" neurotransmitters in cellular interactions of early embryogenesis: a hypothesis. Neuorchem. Res. 6 (1): 55-69.

Buznikov, G. A., Chudakova, I. V. and Zvezdina, N. D. 1964. The role of neurohumors in early embryogenesis. I. Serotonin content of developing embryos of sea urchin and loach. J. Embryol. Exp. Morph. 12: 563-573.

Buznikov, G. A., Kost, A. N., Kucherova, N. F., Mndzhoyan, A. L., Suvorov, N. N. and Berdysheva, L. V. 1970. The role of neurohumours in early embryogenesis.

III. Pharmacological analysis of the role of neurohumours in cleavage divisions. J. Embryol. Exp. Morph. 23: 549-569.

Buznikov, G. A., Mileusnic, R., Yurovskaya, M. A. and Rakic, L. 1984. Effect of calcium ionophore A23187 on the sensitivity of early sea urchin embryos to cytotoxic neuropharmacological drugs. Comp. Biochem. Physiol. 79C: 425-427.

Calow, P. 1978. The evolution of life-cycle strategies in fresh-water gastropods. Malacologia. 17(2): 351-364.

Carter, G. S. 1926. On the nervous control of the velar cilia of the nudibranch veliger. J. Exp. Biol. 4: 1-25.

Castellucci, V. and Kandel, E. R. 1976. Presynaptic facilitation as a mechanism for behavioral sensitization in *Aplysia*. Science 194: 1176-1178.

Catapane, E. J. 1983. comparative study of the control of lateral ciliary activity in marine bivalves. Comp. Biochem. Physiol. 75C: 403-405.

Chia, F. S., Buckland, J. and Young, C. M. 1984. Locomotion of marine invertebrate larvae: a review. Can. J. Zool. 62: 1205-1222.

Chia, F. S. and Koss, R. 1984. Fine structure of the cephalic sensory organ in the larva of the nudibranch *Rostanga pulchra* (Mollusca, Opisthobranchia, Nudibranchia). Zoomorphology 104: 131-139.

Chien, C.-B., Rosenthal, D. E., Harris, W. A. and Holt, C. E. 1993. Navigational errors made by growth cones without filopodia in the embryonic xenopus brain. Neuron 11: 237-251.

Chubakov, A. R., Gromova, E. A., Konovalov, G. V., Sarkisova, E. F. and Chumasov, E. I. 1986. The effects of serotonin on the morphofunctional development of rat cerebral neocortex in tissue culture. Brain Res. 369: 285-297.

Clarke, A. H. 1981. The freshwater molluscs of Canada. National Museum of Natural Sciences, National Museums of Canada, Ottawa.

Clarke, B., Arther, W., Horsley, D. T. and Parkin, D. T. 1978. Genetic variation and natural selection in polmonate molluscs. *In* Pulmonates, vol. 2A (V. Fretter and J. Peake, Ed.), pp. 220-267. Academic Press, London.

Clarke, P. G. H. 1985. Neuronal death in the development of the vertebrate nervous system. TINS 8: 345-349.

Cohan, C. S. 1990. Frequency-dependent and cell-specific effects of electrical activity on growth cone movements of cultured *Helisoma* neurons. J. Neurobiol. 21(3): 400-413.

Cohan, C. S. and Kater, S. B. 1986. Suppression of neurite elongation and growth cone dynamics by electrical activity. Science 232: 1638-1640.

Cohan, C. S., Connor, J. A. and Kater, S. B. 1987. Electrically and chemically mediated increases in intracellular calcium in neuronal growth cones. J. Neurosci. 7(11): 3588-3599.

Conn, P. J., Strong, J. A., Azhderian, E. M., Nairn, A. C., Greengard, P. and Kaczmarek, L. K. 1989. Protein kinase inhibitors selectively block phorbol ester- or forskolin-induced changes in excitability of *Aplysia* neurons. J. Neurosci. 9: 473-479.

Coon, S. L. and Bonar, D. B. 1986. Norepinephrine and dopamine content of larvae and spat of the pacific oyster, *Crassostrea gigas*. Biol. Bull. 171: 632-639.

Coon, S. L., Bonar, D. B. and Weiner, R. M. 1985. Induction of settlement and metamorphosis of the Pacific oyster, *Crassostrea gigas* (*Thunberg*), by L-DOPA and catecholamines. J. Exp. Mar. Biol. Ecol. 94: 211-221.

Cooper, J. A. 1991. The role of actin polymerization in cell motility. Annu. Rev. Physiol. 53: 585-605.

Cottrell, G. A. 1971a. Action of imipramine of 5-hydroxytryptaminergic transmission and on 5-hydroxytryptamine uptake in the snail (*Helix pomatia*) brain. Brit. J. Pharmacol. 43(2): 437P.

Cottrell, G. A. 1971b. Action of imipramine on a serotonergic synapse. Comp. Gen. Pharmacol. 2(6): 125-128.

Cottrell, G. A. and Osborne, N. N. 1969. Localization and mode of action of cardioexcitatory agents in molluscan hearts. Experientia Suppl. 15: 230-231.

Cottrell, G. A. and Osborne, N. N. 1970. Subcellular localization of serotonin in an identified serotonin-containing neurone. Nature 225: 470-472.

Cottrell, G. A. and Powell, B. 1971. Formation of serotonin by isolated serotonin-containing and by isoaled non-amine-containing neurons. J. Neurochem. 18: 1695-1697.

Cournil, I., Geffard, M., Moulins, M. and Le Moal, M. 1984. Coexistence of dopamine and serotonin in an identified neuron of the lobster nervous system. Brain Res. 310: 397-400.

Croll, R. P. and Chiasson, B. J. 1989. Postembryonic development of serotoninlike immunoreactivity in the central nervous system of the snail, *Lymnaea stagnalis*. J. Comp. Neurol. 280: 122-142.

Croll, R. P. and Lo, R. Y. S. 1986. Distribution of serotonin-like immnoreactivity in the central nervous system of the periwinkle, *Littorina littorea* (gastropoda, prosobranchia, mesogastropoda). Biol. Bull. 171: 426-440.

Cumin, R. 1972. Normentafel zur Organogenese von *Lymnaea stagnalis* (Gastropoda, Pulmonata) mit besonderer Beruecksichtigung der Mitteldarmdruese. Rev. Suisse Zool. 79: 709-774.

Dagan, D., and Levitan, I. B. 1981. Isolated identified *Aplysia* neurons in cell culture. J. Neurosci. 1(7): 736-740.

D'Amato, R. J., Blue, M. E., Largent, B. L. *et al.* 1987. Ontogeny of the serotoninergic projection to rat neocortex: Transient expression of a dense innervation to primary sensory areas. Proc. Natl. Acad. Sci. USA 84: 4322-4326.

Davenport, R. W. and McCaig, C. D. 1993. Hippocampal growth cone responses to focally applied electric fields. J. Neurobiol. 24(1): 89-100.

Davenport, R. W., Dou, P., Rehder, V. and Kater, S. B. 1993. A sensory role for neuronal growth cone filopodia. Nature 361: 721-724.

Davis, L., Dou, P., DeWit, M. and Kater, S. B. 1992. Protein synthesis within neuronal growth cones. J. Neurosci. 12(12): 4867-4877.

Deeb S. S. 1972. Inhibition of cleavage and hatching of sea urchin embryos by serotonin. J. Exp. Zool. 181: 79-86.

DeMello, F. G. 1978. The ontogeny of dopamine-dependent increase of adenosine 3'-5'-cyclic monophosphate in the chick retina. J. Neurochem. 31: 1049-1053.

Desai, C., Garriga, G., McIntire, S. L. and Horvitz, H. R. 1988. A genetic pathway for the development of the *Caenorhabditis elegans* HSN motor neurons. Nature 336: 638-646.

Diamond, J., Cooper, E., Turner, C. and Macintyre, L. 1976. Trophic regulation of nerve sprouting. Science 193: 371-377.

Diefenbach, T. J. and Goldberg, J. I. 1990. Postembryonic expression of the serotonin phenotype in *Helisoma trivolvis*: comparison between laboratory-reared and wild-type strains. Can. J. Zool. 68: 1382-1389.

Diefenbach, T. J. and Goldberg, J. I. 1994. Distinct neurotransmitter phenotypes in homologous embryonic neurons from *Helisoma trivolvis* and *Lymnaea stagnalis*. Bull. Can. Soc. Zool. 25: 45.

Diefenbach, T. J., Koehncke, N. K. and Goldberg, J. I. 1991. Characterization and development of rotational behavior in *Helisoma* embryos: role of endogenous serotonin. J. Neurobiol. 22: 922-934.

Diefenbach, T. J., Sloley, B. D. and Goldberg, J. I. 1995. Neurite branch development of an identified serotonergic neuron from embryonic *Helisoma*: evidence for autoregulation by serotonin. Dev. Biol. 167: 282-293.

Edmonds, B. W., Klein, M., Dale, N. and Kandel, E. R. 1990. Contribution of two types of calcium channels to synaptic transmission and plasticity. Science Wash. DC 250: 1142-1147.

Edson, K., Weisshaar, B. and Matus, A. 1993. Actin depolymerisation induces process formation on MAP2-transfected non-neuronal cells. Development 117: 689-700.

Ekstroem, P, Nyberg, L. and van Veen, T. 1985. Ontogenetic development of serotoninergic neurons in the brain of a teleost, the three-spined stickleback. An immunohistochemical analysis. Brain Res. 349 (1-2): 209-224.

Elekes, K. 1991. Serotonin-immunoreactive varicosities in the cell body region and neural sheath of the snail, *Helix pomatia*, ganglia: an electron microscopic immunocytochemical study. Neurosci. 42(2): 583-591.

Emanuelsson, H. 1992. Autoradiographic localization in polychaete embryos of tritiated mesulergine, a selective antagonist of serotonin receptors that inhibits early polychaete development. Int. J. Dev. Biol. 36: 293-302.

Emanuelsson, H. 1974. Localization of serotonin in cleavage embryos of *Ophryotrocha labronica* LaGreca and Bacci. Roux Arch. Dev. Biol. 175: 253-271.

Emanuelsson, H. 1992. Autoradiographic localization in polychaete embryos of tritiated mesulergine, a selective antagonist of serotonin receptors that inhibits early polychaete development. Int. J. Dev. Bioll. 36(2): 293-302.

Emanuelsson, H., Carlberg, M. and Lowkvist, L. 1988. Presence of serotonin in early chick embryos. Cell Diff. 24: 191-199.

Emerit, M. B. 1992. Trophic effects of neurotransmitters during brain maturation. Biol. Neonate 62: 192-201.

Emery, D. G. and Audesirk, T. E. 1978. Sensory cells in *Aplysia*. J. Neurobiol. 9(2): 173-179.

Faraj, B. A., Olkowski, Z. L. and Jackson, R. T. 1994. Active [^{3}H] -dopamine uptake by human lymphocytes: correlates with serotonin transporter activity. Pharmacology 48(5): 320-327.

Forda, S. and Kelly, J. S. 1985. The possible modulation of the development of rat dorsal root ganglion cells by the presence of 5-HT-containing neurones of the brainstem in dissociated cell culture. Brain Res. 354(1): 55-65.

Forscher, P. 1989. Calcium and polyphosphoinositide control of cytoskeletal dynamics. TINS 12(11): 468-474.

Forscher, P. and Smith, S. J. 1988. Actions of cytochalasins on the organization of actin filaments and microtubules in neuronal growth cone. J. Cell Biol. 107: 1505-1516.

Franquinet, R. and Martelly, I. 1981. Effects of serotonin and catecholamines on RNA synthesis in planarians: in vitro and in vivo studies. Cell Differentiation 10: 201-209.

Fretter, V. 1975. Introduction. *In* Pulmonates, Functional Anatomy and Physiology, Vol. 1. (V. Fretter and J. Peake, Ed.),p. xxvii. Academic Press, London.

D., Bauce, Bauce, L. G., Lukowiak, K. and Bulloch, A. G. M. 1986. Transient depletion of serotonin in the nervous system of *Helisoma*. J. Neurobiol. 17(5): 431-447.

Gál, E. M. and Whitacre, D. H. 1982. Mechanism of irreversible inactivation of pheylalanine-4- and tryptophan-5-hydroxylase by [4-36Cl, 2-14C] *p*-chorophenylalanine: A revision. Neurochem. Res. 7(1): 13-26.

Gandolfi, O., Barbaccia, M. L. and Costa, E. 1984. Comparison of iprindole, imipramine and mianserin action on brain serotonergic and beta adrenergic receptors. J. Pharm. Exp. Ther. 229(3): 782-786.

Garyantes, T. K. and Regehr, W. G. 1992. Electrical activity increases growth cone calcium but fails to inhibit neurite outgrowth from rat sympathetic neurons. J. Neurosci. 12(1): 96-103.

Gerschenfeld, H. M., Hamon, M. and Paupardin-Tritsch, D. 1978. Release of endogenous serotonin from two identified serotonin-containing neurones and the physiological role of serotonin re-uptake. J. Physiol. 274: 265-278.

Gesser, B. P. and Larsson, L.-I. 1985. Changes from enkephalin-like to gastrin/cholecystokinin-like immunoreactivity in snail neurons. J. Neurosci. 5(6): 1412-1417.

Gillette, R. 1991. On the significance of neuronal gigantism in gastropods. Biol. Bull. 180: 234-240.

Gillette, R. and Davis, W. J. 1977. the role of the metacerebral giant neuron in the feeding behavior of *Pleurobranchaea*. J. Comp. Physiol. 116: 129-159.

Glanzman, D. L., Kandel, E. R. and Schacher, S. 1990. Target-dependent structural changes accompanying long-term synaptic faciliatation in *Aplysia* neurons. Science 249: 799-802.

Glazer, E. J., Steinbusch, H., Verhofstad., A. and Basbaum, A. I. 1981. Serotonin neurons in nucleus raphe dorsalis and paragigantocellularis of the cat contain enkephalin. J. Physiol. (Paris) 77: 241-245.

Glover, J. C. and Kramer, A. P. 1982. Serotonin selectively ablates identified neurons in the leech embryo. Science 216: 317-319.

Goldberg, J. I. 1995. Neuronal development in embryos of the mollusc, *Helisoma trivolvis*. Multiple roles of serotonin. *In* Advances in Neural Science, Vol. II (S. Malhotra, Ed.), GAI Press, Greenwich, Conneticut (in press).

Goldberg, J. I. and Cavers, K. J. 1993. Growth of neuronal populations during postembryonic development in *Helisoma trivolvis*. Soc. Neurosci. Abst. 19: 533.8.

Goldberg, J. I. and Diefenbach, T. J. 1992. Early development of an identified serotonergic neuron in embryos of the gastropod, *Helisoma trivolvis*. Soc. Neurosci. Abstr. 20: 261.7.

Goldberg, J. I. and Kater, S. B. 1989. Expression and function of the neurotransmitter serotonin during development of the *Helisoma* nervous system. Dev. Biol. 131: 483-495.

Goldberg, J. I. and Price, C. J. 1991. Voltage-gated ionic currents in neurons isolated from *Helisoma trivolvis* embryos. *In* Molluscan Neurobiology (K. S. Kits, H. H. Boer, and J. Joose, Ed.), pp. 161-167. Proc. 3rd Symp. Mollusc. Neurobiol. North Holland, Amsterdam.

Goldberg, J. I., Koehncke, N. K., Christopher, K. J., Neumann, C. and Diefenbach, T. J. 1994. Pharmacological characterization of a serotonin receptor involved in an early embryonic behavior of *Helisoma trivolvis*. J. Neurobiol. 25(12): 1545-1557.

Goldberg, J. I., McCobb, D. P., Guthrie, P. B., Lawton, R. A., Lee, R. E. and Kater, S. B. 1988. Characterization of cultured embryonic neurons from the snail *Helisoma*.. *In* Cell Culture Approaches to Invertebrate Neurosciences (D. Beadle, G. Lees, and S. B. Kater, Ed.), Academic Press, London. pp. 85-108.

Goldberg, J. I., Mills, L. R. and Kater, S. B. 1991. Novel effects of serotonin on neurite outgrowth in neurons cultured from embryos of *Helisoma trivolvis*. J. Neurobiol. 22(2): 182-194.

Goldberg, J. I., Mills, L. R., and Kater, S. B. 1992. Effects of serotonin on intracellular calcium in embryonic and adult *Helisoma* neurons. Int. J. Dev. Neurosci. 10(4): 255-264.

Goldschmeding, J. T., Van Duivenboden, Y. A. and Lodder, J. C. 1981. Axonal branching pattern and coupling mechanisms of the cerebral gaint neurones in the snail, *Lymnaea stagnalis*. J. Neurobiol. 12(5): 405-424.

Goldstein, R., Kistler, Jr., H. B., Steinbusch, H. W. M. and Schwartz, J. H. 1984. Distribution of serotonin-immunoreactivity in juvenile *Aplysia*. Neurosci. 11(2): 515-547.

Gomez, T. M. and Letourneau, P. C. 1994. Filopodia initiate choices made by sensory neuron growth conees at Laminin/Fibronectin borders *in vitro*. J. Neurosci. 14(10): 5959-5972.

Goodman, C. S. 1994. The likeness of being: phylogenetically conserved molecular mechanisms of growth cone guidance. Cell 78: 353-356.

Goodman C. S. and Spitzer N. C. 1979. Embryonic development of identified neurones: differentiation from neuroblast

Gordon-Weeks, P. R. 1991. Growth cones: the mechanism of neurite advance. BioEssays 13(5): 235-239.

Gosselin, R. E. 1961. The cilioexcitatory activity of serotonin. J. Cell. Comp. Physiol. 58: 17-25.

Granzow, B. and Kater, S. B. 1977. Identified higher-order neurons controlling the feeding motor program of *Helisoma*. Neurosci. 2: 1049-1063.

Granzow, B. and Rowell, C. H. F. 1981. Further observations on the serotonergci cerebral neurones of *Helisoma* (mollusca, gastropoda): the case for homology with the metacerebral giant cells. J. exp. Biol. 90: 283-305.

Gromova, H. A., Chubakov, A. R., Chumasov E. I., Konovalov, H. V. 1983. Serotonin as a stimulator of hippocampal cell differentiation in tissue culture. Int. J. Dev. Neurosci. 1: 339-349.

Gundersen R. W. 1987. Response of sensory neurites and growth cones to patterned substrata of laminin and fibroectin *in vitro*. Dev. Biol. 121: 423-431.

Gustafson, T. and Toneby, M. 1970. On the role of serotonin and acetylcholine in sea urchin morphogenesis. Exp. Cell Res. 62: 102-117.

Hammarback, J. A. and Letourneau, P. C. Neurite extension across regions of low cell-substratum adhesivity: implications for the guidepost hypothesis of axonal pathfinding. Dev. Biol. 117: 655-662.

Handelmann, G. E., Boyles, J. K.., Weisgraber, K. H., Mahley, R. W. and Pitas, R. E. 1992. Effects of apolipoprotein, E, β-very low density lipoproteins, and cholesterol on the extension of neurites by rabbit dorsal root ganglion neurons *in vitro*. J. Lipid Res. 33: 1677-1688.

Hanson, P. I. and Schulman, H. 1992. Neuronal Ca^{2+}/calmodulin-dependent protein kinases. Annu. Rev. Biochem. 61: 559-601.

Harris, W. A., Holt, C. E. and Bonhoffer, F. 1987. Retinal axons with and without their somata growing to and arborizing in the tectum of frog embryos: a time-lapse video study of single fibres *in vivo*. Development 101: 123-133.

Harrison, R. G. 1907. Observations on the living developing nerve fiber. Anat. Rec. 1: 116-118.

Harrison, R. G. 1910. The outgrowth of the nerve fiber as a mode of protoplasmic movement. J. Exp. Zool. 9: 787-846.

Hashiguti, H., Nakahara, D., Maruyama, W., Naoi, M. and Ikeda, T. 1993. Simultaneous determination of *in vivo* hydroxylation of tyrosine and tryptophan in rat striatum by microdialysis-HPLC: relationship between dopamine and serotonin biosynthesis. J. Neural Trans. 93(3): 213-223.

Haydon, P. G. and Man-Son-Hing, H. 1988. Low- and high-voltage-activated calcium currents: their relationship to the site of neurotransmitter release in an identified neuron of *Helisoma*. Neuron 1: 919-927.

Haydon, P. G., Cohan, C. S., McCobb, D. P., Miller, H. R. and Kater, S. B. 1985. Neuron-specific growth cone properites as seen in identified neurons of *Helisoma*. J. Neurosci. Res. 13: 135-147.

Haydon, P. G., McCobb, D. P. and Kater, S. B. 1984. Serotonin selectively inhibits growth cone motility and synaptogenesis of specific identified neurons. Science 226: 561-564.

Haydon, P. G., McCobb, D. P. and Kater, S. B. 1987. The regulation of neurite outgrowth, growth cone motility, and electrical synaptogenesis by serotonin. J. Neurobiol. 18(2): 197-215.

Heidemann, S. R., Lamoureux, P. and Buxbaum, R. E. 1990. Growth cone behavior and production of traction force. J. Cell Biol. 111: 149-157.

Hickmott, P. W. and Carew, T. J. 1991. An autoradiographic analysis of neurogenesis in juvenile *Aplysia californica*. J. Neurobiol. 22(4): 313-326.

Hirai, S., Kishimoto, T., Kadam, A. L., Kanatani, H., and Koide, S. S. 1988. Induction of spawning and oocyte maturation by 5-hydroxytryptamine in the surf clam. J. Exp. Zool. 245: 318-321.

Hirata, Y., Sawada, M., Minami, M., Arai, H., Iizuka, R. and Nagatsu, T. 1990. Tyrosine hydroxylase, tryptophan hydroxylase, biopterin, and neopterin in the brain of *anorexia nervosa*. J. Neural Trans. 80(2): 145-150.

Hiripi, L. 1970. Examination of monoamine synthesis and breakdown in the nervous system and other tissues of *Lymnaea stagnalis* L. Annal. Biol. Tihany 35: 3-11.

Hiripi, L. and Salanki, J. 1971. The role of monoamine oxidase in the inactivation of serotonin in the nervous system and other tissues of *Anodonta cygena* L. Annal. Biol. Tihany 36: 19-24.

Hoekfelt, T. Johansson, O. and Goldstein, M. 1984. Chemical anatomy of the brain. Science 225: 1326-1334.

Hoekfelt, T., Ljungdahl, Å., Steinbusch, H., Verhofstad, A., Nilsson, G., Brodin, E., Pernow, B. and Goldstein, M. 1978. Immunohistochemical evidence of substance P-like immunoreactivity in some 5-hydroxytryptamine-containing neurons in the rat central nervous system. Neurosci. 3: 517-538.

Holland, R. L. and Brown, M. C. 1980. Postsynaptic transmission block can cause terminal sprouting of a motor nerve. Science 207: 649-651.

Horvitz, H. R., Ellis H. M. and Sternberg P. W. 1982. Programmed cell death in nematode development. Neurosci . Comm. 1: 56-65.

Hu, Y., Chen, M., Bailey, C. H. and Kandel, E. R. 1993. 5-HT and cAMP induce the formation of coated pits and vescicles and increase the expression of clathrin light chain in sensory neurons of *Aplysia*. Neuron 10: 921-929.

Hubendick, B. 1972. Systematics and comparative morphology of the basommatophora. Ch. 1. *In* The Mollusca Vol. 2A. Systematics, Evolution and Ecology (V. Fretter and J. Peakes, Eds.) Academic Press, New York. pp.1-47.

Hume, R. I., Role, L. W. and Fischbach. 1983. Acetylcholine release from growth cones detected with patches of acetylcholine receptor-rich membranes. Nature 305: 632-634.

Hynes, R. O. 1992. Integrins: versatility, modulation, and signaling in cell adhesion. Cell 69: 11-25.

Igarashi, M., Strittmatter, S. M., Vartanian, T. and Fishman, M. C. 1993. Mediation by G proteins of signals that cause collapse of growth cones. Science 259: 77-79.

Ivgy-May, N. and Gershon, M. D. 1994. Synaptic properites of serotonergic growth cones in developing rat brain. J. Neurosci. 14(3): 1011-1029.

Ivins, J. K., Raper, J. A. and Pittman, R. N. 1991. Intracellular calcium levels do not change during contact-mediated collapse of chick DRG growth cone structure. J. Neurosci. 11(6): 1597-1608.

Jacob, M. H. 1984. Neurogenesis in *Aplysia californica* resembles nervous system formation in vertebrates. J. Neurosci. 4(5): 1225-1239.

Jahan-Parwar, B, S.-Rozsa, K., Salanki, J., Evans, M. L. and Carpenter, D. O. 1987. In vivo labeling of serotonin-containing neurons by 5,7-dihydroxytryptamine. Brain Res. 426: 173-178.

Jellies, J. and Kristan, W. B., Jr. 1991. The oblique muscle organizer in *Hirudo medicinalis*, an identified embryonic cell projecting multiple parallel growth cones in an orderly array. Dev. Biol. 148: 334-354.

Jéquier, E., Lovenberg, W. and Sjoerdsma, A. 1967. Tryptophan hydroxylase inhibition: The mechanism by which p-chlorophenylalanine depletes rat brain serotonin. Mol. Pharmacol. 3: 274-278.

Johansson, O., Hokfelt., T., Pernow, B., Jeffcoate, S. L., White, N., Steinbusch, H. W. M., Verhofstad, A. A. J., Emson, P. C. and Spindel, E. 1981. Immunohistochemical support for three putative transmitters in one neuron: coexistence of 5-hydroxytryptamine, substance P-, and thyrotropin releasing hormone-like immunoreactivity in medullary neuron projecting to the spinal cord. Neuroscience 6: 1857-1881.

Johnson, M. D. 1994. Synaptic glutamate release by postnatal rat serotonergic neurons in microculture.

Kadam A. L. and Koide S. S. 1989. Serotonin analogs and *Spisula* oocyte maturation. Invert. Reprod. Dev. 15(3): 225-227.

Kalb, R. G. 1994. Regulation of motor neuron dendrite growth by NMDA receptor activation. Development 120(11): 3053-3071.

Kalb, R. G., Lidow, M. S., Halsted, M. J. and Hockfield, S. 1992. N-methyl-D-aspartate receptors are transiently expressed in the developing spinal cord ventral horn. Proc. Natl. Acad. Sci. USA 89(18): 8502-8506.

Kandel, E. R. 1991. Nerve cells and behavior. Ch. 2 *In* Principles of Neural Science, 3rd ed. (E. R. Kandel, J. H. Schwartz, T. M. Jessell, Eds.), Elsevier, New York. pp. 18-34.

Kandel, E. R., Kriegstein, A. and Schacher, S. 1980. Development of the central nervous system of *Aplysia* in terms of the differentiation of its specific identifiable cells. Neurosci. 5: 2033-2063.

Kasamatsu, T. 1991. Adrenergic regulation of visuocortical plasticity: a role of the locus coeruleus system. Prog. Brain Res. 88: 599-616.

Kataoka, S. 1976. Fine structure of the epidermis of the optic tentacle in a slug, *Limax flavus*. Tissue Cell 8: 47-60.

Kater, S. B. 1974. Feeding in *Helisoma trivolvis*: the morpholgical and physiological bases of a fixed action pattern. Am. Zool. 14: 1017-1036.

Kater, S. B. and Kaneko, C. R. S. 1972. An endogenously bursting neuron in the gastropod mollusc, *Helisoma trivolvis*. Characterization of activity *in vivo*. J. comp. Physiol. 70: 1-14.

Kater, S. B. and Mills, L. R. 1991. Regulation of growth cone behavior by calcium. J. Neurosci. 11: 891-899.

Kater, S. B., Mattson, M. P., Cohan, C. and Connor, J. 1988. Calcium regulation of the neuronal growth cone. TINS 11: 315-321.

Kennedy, T. E., Serafini, T., de la Torre, J. R. and Tessier-Lavigne, M. 1994. Netrins are diffusible chemotropic factors for commissural axons in the embryonic spinal cord. Cell 78: 425-435.

Kerkut, G. A., Cottrell, G. A. 1963. 5-hydroxytryptamine and acetylcholine in the snail brain. Comp. Biochem. Physiol. 8: 53-63.

Kerkut, G. A., Sedden, C. B., Walker, R. J. 1967. Uptake of DOPA and 5-hydroxytryptophane by monoamine forming neurones in the brain of *Helix*. Comp. Bioch. Physiol. 23: 159-162.

Kits, K. S., de Vries, N. J. and Ebberink, R. H. M. 1990. Molluscan insulin-related neuropeptide promotes neurite outgrowth in dissociated neuronal cell cultures. Neurosci. Lett. 109: 253-258.

Klemm, H. P., Baumgarten, H. G. and Schlossberger, H. G. 1980. polarographic measurements of spontaneous and mitochondria-promoted autooxidation of 5,6- and 5,7-dihydroxytryptamine. J. Neurochem. 35(6): 1400-1408.

Koshtoyants, K. S., Buznikov, G. A. and Manukhin, B. N. 1961. The possible role of 5-hydroxytryptamine in the motor activity of embryos of some marine gastropods. Comp. Biochem. Physiol. 3: 20-26.

Kostenko, M. A., Musienko, V. S. and Smolikhina, T. I. 1983. Ca^{2+} and pH affect the neurite formation in cultured mollusc isolated neurones. Brain Res. 276: 43-50.

Krantic, S., Dubé, F. and Guerrier, P. 1993a. Evidence for a new serotonin receptor in oocytes of the surf clam *Spisula solidissima*. Gen. Comp. Endocrinol. 90: 125-131.

Krantic, S., Guerrier, P. and Dubé, F. 1993a. Meiosis reinitiation in surf clam oocytes is mediated via a 5-hydroxytryptamine high affinity binding site. J. Biol. Chem. 268(11): 7983-7989.

Kriegstein, A. R. 1997. Development of the nervous system of *Aplysia californica*. Proc. Natl. Acad. Sci. U. S. A. 74: 375-378.

Kruglyanskaya, Z. Ya. and Sakharov, D. A. 1975. Appearance of biogenic amines in the developing nervous system of embryos of the mollusk *Lymnaea stagnalis*. Ontogenez 6(2): 194-197.

Kuhn, T. B., Schmidt, M. F. and Kater, S. B. 1995. Laminin and fibronectin guideposts signal sustained but opposite effects to passing growth cones. Neuron 14(2): 275-285.

Kuwada, J. Y. and Kramer, A. P. 1983. Embryonic development of the leech nervous system: Primary exon outgrowth of identified neurons. J. Neurosci. 10: 2098-2111.

Lamoureux, P., Buxbaum, R. E. and Heidemann, S. R. 1989. Direct evidence that growth cones pull. Nature 340: 159-162.

Landmesser, L., Dahm, L., Tang, J. and Rutishauser. U. 1990. Polysialic acid as a regulator of intramuscular nerve branching during embryonic development. Neuron 4: 655-667.

Lankford, K. L. and Letourneau, P. C. 1989. Evidence that calcium may control neurite outgrowth by regulating the stability of actin filaments. J. Cell Biol. 109: 1229-1243.

Lankford, K. L. and Letourneau, P. C. 1991. Roles of actin filaments and three second-messenger systems in short term regulation of chick dorsal root ganglion neurite outgrowth. Cell Motil. Cytoskel. 20: 7-29.

Lankford, K. L., DeMello, F. G., Klein, W. L. 1987. A transient embryonic dopamine receptor inhibits growth cone motility and neurite outgrowth in a subset of avian retina neurons. Neurosci. Lett. 75: 169-174.

Lankford, K. L., DeMello, F. G. and Klein, W. L. 1988. D1-type dopamine receptors inhibit growth cone motility in cultured retina neurons: evidence that neurotransmitters act as morphogenic growth regulators in the developing central nervous system. Proc. Natl. Acad. Sci. USA 85: 2839-2843.

Lauder, J. M. 1988. Neurotransmitters as morphogens. Prog. Brain Res. 73: 365-387.

Lauder, J. M. 1993. Neurotransmitters as growth regulatory signals: role of receptors and second messengers. TINS 16(6): 233-239.

Lauder, J. M. and Bloom, F. E. 1974. Ontogeny of monoamine neurons in the locus coeruleus, raphe nuclei and substantia nigra of the rat. I. Cell differentiation. J. Comp. Neurol. 155: 469-481.

Lauder, J. M. and Krebs, H. 1976. Effects of p-chlorphenylalanine on time of neuronal origin during embryogenesis in the rat. Brain Res. 107(3): 638-644.

Lauder, J. M. and Krebs, H. 1978. Serotonin as a differentiation signal in early neurogenesis. Dev. Neurosci. 1: 15-30.

Lauder, J. M. and Zimmerman, E. 1988. Sites of serotonin uptake in the epithelia of the developing mouse palate, oral cavity and face: Possible role in morphogenesis. J. Craniofac. Genet. devl Biol. 8: 265-276.

Lauder, J. M., Tamir, H. and Sadler, T. W. 1988. Serotonin and morphogenesis: I. Sites of serotonin uptake and -binding protein immunoreactivity in the midgestation mouse embryo. Development 102: 709-720.

Lauder, J. M., Towle, A. C., Patrick, K., Henderson, P. and Krebs, H. 1985. Decreased serotonin content of embryonic raphe neurons following maternal administration of *p*-chlorophenylalanine: a quantitative immunocytochemical study. Dev. Brain Res. 20: 107-114.

Lauder, J. M., Wallace, J. A, Krebs, H., Petrusz, P. and McCarthy, K. 1982. *In vivo* and *In vitro* development of serotonergic neurons. Brain Res. Bull. 9: 605-625.

Lawrence, I. E., Jr. and Burden, H. W. 1973. Catecholamines and morphogenesis of the chick neural tube and notochord. Am. J. Anat. 137: 199-208.

LeDouarin, N. M. 1980. Migration and differentiation of neural crest cells. Curr. Top. Dev. Biol. 16: 31-85.

Lee, S. L., Wang, W. W., Lanzillo, J. J. and Fanburg, B. L. 1994. Regulation of serotonin-induced DNA synthesis of bovine pulmonary artery smooth muscle tissue. Am. J. Physiol. 266: 53-60.

Lein, P. J. and Higgins, D. 1991. Protein synthesis is required for the iniation of dendritic growth in embryonic rat sympathetic neurons*in vitro*. Devel. Brain Res. 60: 187-196.

Lenicque, P. M. and Feral, J. P. 1976. A mechanism of the action of neurotransmitters on the regeneration of the planarian worm, *Dugesia tigrina*: Role of acetylcholine as a negative feedback. Acta Zoologica 57: 1-5.

Lent, C. M. 1984. Quantitative effects of a neurotoxin upon serotonin levels within tissue compartments of the medicinal leech. J. Neurobiol. 15: 309-325.

Lent, C. M. and Dickinson, M. H. 1984. Retzius cells retain functional membrane properties following 'ablation' by the neurotoxin 5,7-DHT. Brain Res. 300: 167-171.

Le Prince, G., Copin, M.-C., Hardin, H., Belin, M.-F., Bouilloux, J.-P. and Tardy, M. 1990. Neuron-glia interactions: effect of serotonin on the astroglial expression of GFAP and of its encoding message. Dev. Brain Res. 51: 295-298.

Letourneau, P. C., Condic, M. L. and Snow, D. M. 1994. Interactions of developing neurons with the extracellular matrix. J. Neurosci. 14(3): 915-928.

Letourneau, P. C., Shattuck, T. A. and Ressier, A. H. 1986. Branching of sensory and sympathetic neurites *in vitro* is inhibited by treatment with taxol. J. Neurosci. 6(7): 1912-1917.

Levine, R. B., Truman, J. W., Linn, D. and Bate, C. M. 1986. Endocrine regulation of the form and function of axonal arbors during insect metamorphosis. J. Neurosci. 6(1): 293-299.

Lieth, E., McClay, D. R. and Lauder, J. M. 1990. Neuronal-glial interactions: complexity of neurite outgrowth correlates with substrate adhesivity of serotonergic neurons. Glia. 3: 169-179.

Lin, S. S. and Levitan, I. B. 1991. Concanavalin A: a tool to investigate neuronal plasticity. TINS 14(7): 273-278.

Lipton, S. A., Frosch, M. P., Phillips, M. D., Tauck, D. L. and Aizenman, E. 1988. Nicotinic antagonists enhance process outgrowth by rat retinal ganglion cells in culture. Science 239: 1293-1296.

Liu, J. P. and Lauder, J. M. 1992. S-100b and insulin-like growth factor-II differentially regulate growth of developing serotonin and dopamine neurons in vitro. J. Neurosci. Res. 33: 248-256.

Lloyd, P. E., Kupfermann, I., and Weiss, K. R. 1984. Evidence for parallel actions of a molluscan neuropeptide and serotonin in mediating arousal in *Aplysia*.. Proc. Natl. Acad. Sci. USA 81: 2934-2937.

Macagno, E. R., Gao, W.-Q., Baptista, C. A. and Passani, M. B. 1990. Competition or inhibition? Developmental strategies in the establishment of peripheral projections by leech neurons. J. Neurobiol. 21(1): 107-119.

Mackie, G. O., Singla, C. L. and Thiriot-Quievreux, C. 1976. Nervous control of ciliary activity in gastropod larvae. Biol. Bull. 151: 182-199.

Mandelbaum, D. E., Koester, J., Schonberg, M. and Weiss, K. R. 1979. Cyclic AMP mediation of the excitatory effect of serotonin in the heart of Aplysia. Brain Res. 177: 388-394.

Marois, R. 1989. Embryonic Development of *Lymnaea stagnalis*: General, Neuronal and Behavioral Aspects. M. Sc. thesis, Dalhousie University, Halifax, N. S..

Marois, R. and Carew, T. J. 1990. The gastropod nervous system in metamorphosis. J. Neurobiol. 21(7): 1053-1071.

Marois, R. and Croll, R. P. 1992. Development of serotoninlike immunoreactivity in the embryonic nervous system of the snail *Lymnaea stagnalis*. J. Comp. Neurol. 322: 255-265.

Marsh, L. and Letourneau, P. C. 1984. Growth of neurites without filopodial or lamellipolial activity in the presence of cytochalasin B. J. Cell Biol. 99: 2041-2047.

Martelly, I. 1984. Calcium thresholds in the activation of DNA and RNA synthesis in culturedd planarian cells: relationship with hormonal and DB cAMP effects. Cell Diff. 15(1): 25-36.

Mattson, 1988. Neurotransmitters in the regulation of neuronal cytoarchitecture. Brain Res. Rev. 13: 17-212.

Mattson, M. P. and Kater, S. B. 1987. Calcium regulation of neurite elongation and growth cone motility. J. Neurosci. 7: 4034-4043.

Mattson, M. P. and Kater, S. B. 1988. Fibronectin-like immunoreactivity in *Helisoma* buccal ganglia: evidence that an endogenous fibronectin-like molecule promotes neurite outgrowth. J. Neurobiol. 19(3): 239-256.

Mattson, M. P. and Kater, S. B. 1989. Excitatory and inhibitory neurotransmitters in the generation and degeneration of hippocampal neuroarchitecture. Brain Res. 478: 337-348.

Mattson, M. P., Dou, P. and Kater, S. B. 1988a. Outgrowth regulating actions of glutamate in isolated hippocampal pyramidal neurons. J. Neurosci. 8: 2087-2100.

Mattson, M. P., Taylor-Hunter, A. and Kater, S. B. 1988b. Neurite outgrowth in individual neurons of a neuronal population is differentially regulated by calcium and cyclic AMP. J. Neurosci. 8(5): 1704-1711.

Mayford, M., Barzilai, A., Keller, F., Schacher, S. and Kandel, E. R. 1992. Modulation of an NCAM-related adhesion molecule with long-term synaptic plasticity in *Aplysia*. Science 256: 638-644.

McAllister, L. B., Scheller, R. H., Kandel, E. R. and Axel, R. 1983. *In situ* hybridization to study the origin and fate of identified neurons. Science 222: 800-808.

McCaman, M. W., Ono, J. K. and McCaman, R. E. 1984. 5-hydroxytryptamine measurements in molluscan ganglia and neurons using a modified radioenzymatic assay. J. Neurochem. 43(1): 91-99.

McCaman, M. W., Stetzler, J. and Clark, B. 1985. Synthesis of gamma-glutamyldopamine and other peptidoamines in the nervous system of *Aplysia californica*.. J. Neurochem. 45(6): 1828-1835.

McCobb, D. P. and Kater, S. B. 1988. Membrane voltage and neurotransmitter regulation of neuronal growth cone motility. Dev. Biol. 130: 599-609.

McCobb, D. P., Cohan, C. S., Connor, J. A. and Kater, S. B. 1988a. Interactive effects of serotonin and acetylcholine on neurite elongation. Neuron 1: 377-385.

McCobb, D. P., Haydon, P. G. and Kater, S. B. 1988b. Dopamine and serotonin regulation of neurite outgrowth of different identified neurons. J. Neurosci. Res. 19: 19-26.

McCrohan, C. R. and Benjamin, P. R. 1980. Synaptic relationships of the cerebral gaint cells with motoneurones in the feeding system of *Lymnaea stagnalis*. J. exp. Biol. 85: 169-186.

McKenney, K. and Goldberg, J. I. 1989. *Helisoma* embryogenesis: morphological, behavioral and neural development. Soc. Neurosci. Abstr. 15: 1016.

McLean, E. M., Behhatnia, B. and Murphy, A. D. 1989. An identified "dopaminergic" buccal interneuron activates patterned motor activity in *Helisoma*. Soc. Neursci Abst. 297.7.

McMahon, D. 1974. Chemical messengers in development: a hypothesis. Science 185: 1012-1021.

Miller, J. D. and Hadley, R. D. 1991. Laminin-like immunoreactivity in the the snail *Helisoma*: involvement of a ~ 300 kD extracellular matrix protein in promoting outgrowth from identified neurons. J. Neurobiol. 22(5): 431-442.

Millhorn, D. E., Hoekfelt, T., Seroogy, K. and Verhofstad, A. A. J. 1988. Extent of colocalization of serotonin and GABA in neurons of the ventral medulla oblongata in rat. Brain Res. 461: 169-174.

Moffett, S. B. and Ridgway, R. L. 1988. Structural repair and functional recovery following cerebral ganglion removal in the pulmonate snail *Melampus*. Amer. Zool. 28: 1109-1122.

Morrill, J. B. 1982. Development of the pulmonate gastropod, *Lymnaea*. *In* Developmental Biology of Freshwater Invertebrates. (F. W. Harrison and R. R. Cowden, Eds.). Alan R. Liss Inc., New York. pp. 399-483.

Morrison, E. E. and Costanzo, R. M. 1990. Morphology of the human olfactory epithelium. J. Comp. Neurol. 297: 1-13.

Morse, D. E., Hooker, N., Duncan, H. and Jensen, L. 1979. γ-aminobutyric acid, a neurotransmitter, induces planktonic abalone larvae to settle and begin metamorphosis. Science 204: 407-410.

Mueller, W. A. 1984. Retinoids and pattern formation in a hydroid. J. Embryol. Exp. Morph. 81: 253-271.

Muller, J. F. and Marc, R. E. 1984. Three distinct morphological classes of receptors in fish olfactory organs. J. Comp. Neurol. 222: 482-495.

Murakami, A. 1983. Control of ciliary beat frequency in *Mytilus*. J.Submicrosc. Cytol. 15(1): 313-316.

Murakami, A. 1987. Control of ciliary beat frequency in the gill of *Mytilus*--I. Activation of the lateral cilia by cyclic AMP. Comp. Biochem. Physiol. 86C(2): 272-279.

Murakami, A. and Takahashi, K. 1975. Correlation of electrical and mechanical responses in nervous control of cilia. Nature 257: 48-49.

Murphy, A. D. and Kater, S. B. 1980. Sprouting and functional regeneration of an identified neuron in *Helisoma*. Brain Res. 186: 251-272.

Murrain, M., Murphy, A. D., Mills, L. R. and Kater, S. B. 1990. Neuron-specific modulation by serotonin of regenerative outgrowth and intracellular calcium within the CNS of *Helisoma trivolvis*. J. Neurobiol. 21(4): 611-618.

Myers, P. Z., Eisen, J. S., and Westerfield, M. 1986. Development and axonal outgrowth of identified motoneurons in the zebrafish. J. Neurosci. 6(8): 2278-2289.

Myers, C. M., Whitington, P. M. and Ball, E. E. 1990. Embryonic development of the innervation of the locust extensor tiiae muscle by identified neurons: formation and elimination of inappropriate axon branches. Dev. Biol. 137: 194-206.

Negre-Aminou, P. and Pfenninger, K. H. 1993. Arachidonic acid turnover and phospholipase A2 activity in neuronal growth cones. J. Neurochem. 60(3): 1126-1136.

Nemecek, G. M., Coughlin, S. R., Handley, D. A. and Moskowitz, M. A. 1986. Stimulation of aortic smooth muscle cell mitogenesis by serotonin. Proc. Natl. Acad. Sci. USA 83: 674-678.

Newton, B. W., Burkhart, A. B. and Hamill, R. W. 1989. Immunohistochemical distribution of serotonin in spinal autonomic nuclei: II. Early and late postnatal ontogeny in the rat. J. Comp. Neurol. 279: 82-103.

Nichol, C. A., Smith, G. K., and Duch, D. S. 1985. Biosynthesis and metabolism of tetrahydrobiopterin and molybdopterin. Annu. Rev. Biochem. 54: 729-764.

O'Connor, T. P. and Bentley, D. 1993. Accumulation of actin in subsets of pioneer growth cone filopodia in response to neural and epithelial guidance cues *in situ*. J. Cell Biol. 123: 935-948.

O'Leary, D. D. M. and Terashima, T. 1988. Cortical axons branch to multiple subcortical targets by interstitial axon budding: implications for target recognition and "waiting periods." Neuron 1: 901-910.

Ono, J. K. and McCaman, R. E. 1984. Immunocytochemical localization and direct assays of serotonin-containing neurons in *Aplysia*.. Neurosci. 11(3): 549-560.

O'Rourke, N. A. and Fraser, S. E. 1990. Dynamic changes in optic fiber terminal arbors lead to retinotopic map formation: An *in vivo* confocal microscope study. Neuron 5: 159-171.

Osborne, N. N. 1972. The in vivo synthesis of serotonin in an identified serotonin-containing neuron of *Helix pomatia*.. Int. J. Neurosci. 3: 215-228.

Osborne, N. N. and Cottrell, G. A. 1971. Amine and amino acid microanalysis of two identified snail neurons with known characteristics. Experientia 28: 656-658.

Osborne, N. N., Cuello, A. C. and Dockray, G. J. 1982. Substance P and cholecystokinin-like peptides in *Helix* neurons and cholecystokinin and serotonin in a giant neuron. Science 216: 409-411.

Osborne, N. N., Hiripi, L. and Neuhoff, V. 1975. The *in vitro* uptake of biogenic amines by snail (*Helix pomatia*) nervous tissue. Biochem. Pharmacol. 24: 2141-2148.

Palén, K., Thoerneby L. and Emanuelsson, H. 1979. Effects of serotonin and serotonin antagonists on chick embryogenesis. Wilhelm Roux' Archiv. 187: 89-103.

Paparo, A. A. and Murphy, J. A. 1975. The effects of calcium on the rate of beating of lateral cilia in *Mytilus edulis*. II. A response to electrical stimulation of the brachial nerve. Comp. Biochem. Physiol. 50C: 15-19.

Pearce, I. A., Cambray-Deakin, M. A. and Burgoyne, R. D. 1987. Glutamate acting on NMDA receptors stimulates neurite outgrowth from cerebellar granule cells. FEBS Lett. 223: 143-147.

Pechenik, J. A., Chang, S. C. and Lord, A. 1984. Encapsulated development of the marine prosobranch gastropod *Nucella lapillus*. Marine Biol. 78: 223-229.

Penington, N. J. and Kelly, J. S. 1990. Serotonin receptor activation reduces calcium current in an acutely dissociated adult central neuron. Neuron 4: 751-758.

Pentreath, V. W. and Cottrell, G. A. 1973. Uptake of serotonin, 5-hydroxytryptophan and tryptophan by giant serotonin-containing neurones and other neurones in the central nervous system of the snail (*Helix pomatia*). Z. Zellforsch. 143: 21-35.

Pentreath, V. W., Osborne, N. N. and Cottrell, G. A. 1973. Anatomy of giant serotonin-containing neurones in the cerebral ganglia of *Helix pomatia* and *Limax maximus*. Z. Zellforsch. 143: 1-20.

Pentreath, V. W., Radojcic, T., Seal, L. H. and Winstanely, E. K. 1985. The glial cells and glia-neuron relations in the buccal ganglia of *Planorbis corneus* (L.): cytological, qualitative and quantitative changes during growth and aging. Phil. Trans. Royal Soc. Lond. Ser. B 307(1133): 399-455.

Peter, N., Aronoff, B., Wu, F. and Schacher, S. 1994. Decrease in growth cone-neurite fasciculation by sensory or motor cells *in vitro* accompanies downregulation of *Aplysia* cell adhesion molecules by neurotransmitters. J. Neurosci. 14(3): 1413-1421.

Peterson, C., Neal, J. H. and Cotman, C. W. 1989. Development of N-methyl-D-aspartate excitotoxicity in cultured hippocampal neurons. Dev. Brain Res. 48: 187-195.

Pfenninger, K. H. and Friedman, L. B. 1993. Sites of plasmalemmal expansion in growth cones. Dev. Brain Res. 71: 181-192.

Pike, S. H., Marinovich, A., and Smith, S. J. 1993. Target selection and synapse formation within the spinal cord of living zebrafish embryos. Soc. Neurosci. Abstr. 259.7.

Pip, E. 1987. Morphological anomalies in the shall of natural populations of *Helisoma trivolvis* Say (Gastropoda: Planorbidae). Nautilus 101(3): 140-142.

Plesch, B., De Jong-Brink, M. and Boer, H. H. 1971. Histological and histochemical observations on the reproductive tract of the hermaphrodite pond snail *Lymnaea stagnalis*. (L.). Neth. J. Zool. 21: 180-201.

Polak, K. A., Edelman, A. M., Wasley, J. W. F. and Cohan, C. S. 1991. A novel calmodulin antagonist, CGS 9343B, modulates calcium-dependent changes in neurite outgrowth and growth cone movements. J. Neurosci. 11(2): 534-542.

Pollock, J. D., Bernier, L. and Camardo, J. S. 1985. Serotonin and cyclic adenosine 3':5'-monophosphate modulate the potassium current in tail sensory neurons in the pleural ganglion of *Aplysia*. J. Neurosci. 5: 1862-1871.

Popov, S., Brown, A. and Poo, M.-m. 1993. Forward plasma membrane flow in growing nerve processes. Science 259: 244-246.

Price C. J. and Goldberg, J. I. 1993a. Serotonin activation of a cyclic AMP-dependent sodium current in an identified neuron from *Helisoma trivolvis*. J. Neurosci. 13(11): 4979-4987.

Price, C. J. and Goldberg, J. I. 1993b. Pharmacological properties of a serotonin-activated sodium current in an identified neuron from *Helisoma trivolvis*. Soc. Neurosci. Abstr. 19: 527.1.

Purves, D. and Hadley, R. D. 1985. Changes in the dendritic branching of adult mammalian neurones revealed by repeated imaging *in situ*. Nature 315: 404-406.

Purves, D., Snider, W. D. and Voyvodic, J. T. 1988. Trophic regulation of nerve cell morphology and innervation in the autonomic nervous system. Nature 336: 123-128.

Purves, D., Voyvodic, J. T., Magrassi, L. and Yawo, H. 1987. Nerve terminal remodeling visualized in living mice by repeated examination of the same neuron. Science 238: 1122-1126.

Ramasubramaniam, R. 1979. A histochemical study of the sections of reproductive glands and of the egg envelopes of *Achatina fulica* (Pulmonata: Stylommatophora). Int. J. Invert. Reprod. 1: 333-346.

Ramón y Cajal S. 1890. A quelle epoque apparaissent les expansions des cellule nerveuses de la moelle epinere du poulet. Anat. Ang. 5: 609-613.

Raven, C. P. 1966. Gastrulation and formation of germ layers. Ch. IV *In* Morphogenesis: The Analysis of Molluscan Development. Vol. 2. Permagon Press, London. pp. 110-174.

Raven, C. P. 1975. Development. Ch. 8. *In* Pulmonates Vol. 1. Functional Anatomy and Physiology (V. Fretter and J. Peake, Eds.). Academic Press, New York. pp.367-400.

Rehder, V., Jensen, J. R. and Kater, S. B. 1992. The initial stages of neural regeneration are dependent upon intracellular calcium levels. Neurosci. 51(3): 565-574.

Reinsch, S. S., Mitchison, T. J. and Kirscher, M. 1991. Microtubule polymer assembly and transport during axonal elongation. J. Cell Biol. 115(2): 365-379.

Renaud, F., Parisi, E., Capasso, A. and DePrisco, P. 1983. On the role of serotonin and 5-methoxytryptamine in the regulation of cell division in sea urchin eggs. Dev. Biol. 98: 37-46.

Rodríguez, N. and Renaud, F. L. 1980. On the possible role of serotonin in the regulation of regeneration of cilia. J. Cell Biol. 85: 242-247.

Rosen, S. C., Kupfermann, I. Goldstein, R. S. and Weiss, K. R. 1983. Lesion of a serotonergic modulatory neuron in *Aplysia* produces a specific defect in feeding behavior. Brain Res. 260: 151-155.

Rosen, S. C., Weiss, K R., Cohen, J. L. and Kupfermann, I. 1982. Interganglionic cerebral-buccal mechanoafferents of Aplysia: receptive fields and synaptic connections to different classes of neuron involved in feeding behavior. J. Neurophysiol. 48: 271-288.

Rosen, S. C., Weiss, K. R., Goldstein, R. S. and Kupfermann, I. 1989. The role of a modulatory neuron in feeding and satiation in *Aplysia*: effects of lesioning of the serotonergic metacerebral cells. J. Neurosci. 9(5): 1562-1578.

Salvaterra, P. M., Bournaiss-Vardiabasis, N., Nair, T., Hou, G., and Lieu, C. 1987. *In vitro* neuronal differentiation of *Drosophilia* embryo cells. J. Neurosci. 7(1): 10-22.

Sandeman, D. C., Sandeman, R. E. and Aitken. 1988. Atlas of serotonin-containing neurons in the optic lobes and brain of crayfish, *Cherax destructor*. J. Comp. Neural. 269: 465-478.

Sanderson, M. J., Dirksen, E. R. and Satir, P. 1985. The antagonistic effects of 5-hydroxytryptamine and methylxanthine on the gill cilia of *Mytilus edulis*. Cell Motil. 5(4); 293-309.

Saudou, R. and Hen R. 1994. 5-Hydroxytryptamine receptor subtypes in vertebrates and invertebrates. Neurochem. Int. 25(6): 503-532.

Sanes, D. H. and Chokski, P. 1992. Glycinergic transmission influences the development of dendrite shape. Neuroreport 3(4): 323-326.

Schacher, S. M. 1981. The role of support cells in the growth and differentiation of neurones in the abdominal ganglion of *Aplysia*. J. Exp. Biol. 95: 205-214.

Schacher, S. M. and Proshansky, E. 1983. Neurite regeneration by *Aplysia* neurons in dissociated cell culture: modulation by *Aplysia* hemolymph and the presence of the initiatl axonal segment. J. Neurosci. 3(12): 2403-13.

Schacher, S., Kandel, E. R. and Wolley R. 1979a. Development of neurons in the abdominal ganglion of *Aplysia californica*. I. Axosomatic synaptic contacts. Dev. Biol. 71: 163-175.

Schacher, S., Kandel, E. R. and Wolley R. 1979b. Development of neurons in the abdominal ganglion of *Aplysia californica*. II. Nonneural support cells. Dev. Biol. 71: 176-190.

Scheller, R. H., Kaldany, R.-R., Kreiner, R., Mahon, A. C., Nambu, M. S. and Taussig, R. 1984. Neuropeptides: mediators of behavior in *Aplysia*. Science 225: 1300-1308.

Schubert, D., LaCorbiere, M., Whitlock, C. and Stallarp, W. 1978. Alterations in the surface properties of cells responsive to nerve growth factor. Nature 273: 718-723.

Schubiger, M. and Palka, J. 1985. Genetic suppression of putative guidepost cells: Effect on establishment of nerve pathways in *Drosophila* wings. Dev. Biol. 108: 399-410.

Senseman, D. and Gelperin, A. 1973. Comparative aspects of the morphology and physiology of a single identifiable neuron in *Helix aspersa*, *Limax maximus*, and *Ariolimax californica*. Malacol. Rev. 7: 51-52.

Seuwen, K., Magnaldo, I. and Pouyssegur, J. 1988. Serotonin stimulates DNA synthesis in fibroblasts acting through 5-HT_{1B} receptors coupled to a G_1-protein. Nature 335: 254-256.

Shankland, M. 1984. Positional determination of supernumerary blast cell death in the leech embryo. Nature. 307: 541-543.

Shankland, M. and Goodman, C. S. 1982. Development of the dendritic branching pattern of the medial gaint interneuron in the grasshopper embryo. Dev. Biol. 92: 489-506.

Sheetz, M. P., Steuer, E. R. and Schroer, T. A. 1989. The mechanism and regulation of fast exonal transport. TINS 12(11): 474- 478.

Shkolnik, L. J. and Schwartz, J. H. 1980. Genesis and maturation of serotonergic vesicles in identified giant cerebral neuron of *Aplysia*. J. Neurophysiol. 43: 945-967.

Shuey, D. L., Sadler, T. W., Tamir, H. and Lauder J. M. 1993. Serotonin and morphogenesis. Transient expression of serotonin uptake and binding protein during craniofacilal morphogenesis in the mouse. Anat. Embryol. 187: 75-85.

Shuster, M. J., Camardo, J. S., Siegelbaum, S. A., and Kandel, E. R. 1985. Cyclic AMP-dependent protein kinase closes the serotonin-insensitive K^+ channels of *Aplysia* sensory neurones in cell-free membrane patches. Nature 313: 392-395.

Siegelbaum, S. A., Camardo, J. S. and Kandel, E. R. 1982. Serotonin and cyclic AMP close single K channels in *Aplysia* sensory neurones. Nature 299: 413-417.

Sikich, L., Hickok, J. M. and Todd, R. D. 1990. 5-HT_{1A} receptors control neurite branching during development. Dev. Brain Res. 56: 269-274.

Silver, R. A., Lamb, A. G. and Bolsover, S. R. 1989. Elevated cytosolic calcium in the gowth cone inhibits neurite elongation in neuroblastoma cells: correleation of behavioral states with cytosolic calcium concentration. J. Neurosci. 9(11): 4007-4020.

Skelton, M. Alevizos, A. and Koester, J. 1992. Control of the cardiovascular system of *Aplysia* by identified neurons. Experientia 48(9): 809-817.

Sloley, B. D. 1994. γ-glutamyl conjugation of 5-hydroxytryptamine (serotonin) in the earthworm (*Lumbricus terrestris*). Neurochem. Res. 19(2): 217-222.

Sloley, B. D. and Downer, R. G. H. 1990. Catabolism and disposition of exogenous 5-hydroxytryptamine in cockroach, *Periplaneta americana*, tissues. Insect Biochem. 20: 165-171.

Sloley, B. D. and Goldberg, J. I. 1991. Determination of γ-glutamyl conjugates of monoamine by means of high-performance liquid chromatography with electrochemical detection and application to gastropod tissues. J. Chromatog. 567: 49-56.

Sloley, B. D., Juorio, A. V. and Durden, D. A. 1990. High-performance liquid chromatogrpahic analysis of monoamines and some of their γ-glutamyl conjugates produced by the brain and other tissues of *Helix aspersa* (Gastropoda). Cell Mol. Biol. 10: 175-192.

Smith, S. J. 1988. Neuronal cytomechanics: The actin-based motility of growth cones. Science 242: 708-715.

Sobue, K. and Kanda, K. 1989. Alpha-actinins, calspectin (brain spectrin or fodrin), and actin participate in adhesion and movement of growth cones. Neuron 3(3): 311-319.

Soliman, S. 1983. Pharmacological control of ciliary activity in the young sea urchin larva. Effects of monoaminergic agents. Comp. Biochem. Physiol. 76C: 181-191.

Sossin, W. S. and Schwartz, J. H. 1992. Selective activation of Ca (2+) - activated PKCs in *Aplysia* neurons by 5-HT. J. Neurosci. 12(4): 1160-1168.

S.-Rózsa, K. 1984. The pharmacology of molluscan neurons. Prog. Neurobiol. 23: 79-150.

S.-Rózsa, K. and Perényi, L. 1966. Chemical identification of the excitatory substance released in *Helix* heart during stimulation of the extracardial nerve. Comp. Biochem. Physiol. 85C: 419-425.

Strathmann, R. R. and Chaffee, C. 1984. Constraints on egg masses. II. Effect of spacing, size, and number of eggs on ventilation of masses of embryos in jelly, adherent groups, or thin-walled capsules. J. Exp. Mar. Biol. Ecol. 84: 85-93.

Stefano, G. B., Catapane, E. and Aiello, E. 1976. Dopaminergic agents: influence on serotonin in the molluscan nervous system. Science 194: 539-541.

Stephens, R. E. and Prior. G. 1990. Cyclic AMP-dependent dynein light chain phosphorylation in neuronally controlled mussel gill cilia. J. Cell Biol. 111: 295a.

Stephens, R. E. and Prior, G. 1992. Dynein from serotonin-activated cilia and flagella: extraction characteristics and distinct sites for cAMP-dependent protein phosphorylation. J. Cell Sci. 103: 999-1012.

Stommel, E. W. 1984. Calcium activation of mussel gill abfrontal cilia. J. Comp. Physiol. A 155: 457-469.

Stoof, J. C., de Vlieger, T. A. and Lodder, J. C. 1984. Opposing roles for D-1 and D-2 dopamine receptors in regulating the excitability of growth hormone-producing cells in the snail *Lymnaea stagnalis*. Euro. J. Pharmacol. 106: 431-435.

Strittmatter, S. M., Valenzuela, D. and Fishman, M. C. 1994. An amino-terminal domain of the growth-associated protein GAP-43 mediates its effects on filopodial formation and cell spreading. J. Cell Sci. 107: 195-204.

Strittmatter, S. M., Vartanian, T. and Fishman, M. C. 1992. GAP-43 as a neuronal plasticity protein in neuronal form and repair. J. Neurobiol. 23: 507-520.

Stuart, D. K., Blair, S. S. and Weisblat, D. A. 1987. Cell lineage, cell death, and the developmental origin of identified serotonin and dopamine containing neurons in the leech. J. Neurosci. 7: 1107-1122.

Sudlow, L. and Gillette, R. 1991. Serotonin-sensitive neurons in the pedal ganglion of *Pleurobranchaea californica* are serotonin immunoreactive. Soc. Neurosci. Abstr. 17: 1390.

Sugamori, K. S., Sunahara, R. K., Guan, H.-C., Bulloch, A. G. M., Tensen, C. P., Seeman, P., Niznik, H. B. andVan Tol, H. H. M. 1993. Serotonin receptor cDNA cloned from *Lymnaea stagnalis*. Proc. Natl. Acad. Sci. USA 90: 11-15.

Sullivan, W. D. and Sullivan, C. F. 1964. The acetylcholine content and the effects of hexamethonium on this compound at various phases of division of *Tetrahymena pyriformis* Broteria. Cienc. Natur. 33: 17-33.

Sun, Y.-a. and Poo, M.-m. 1987. Evoked release of acetylcholine from the growing embryonic neuron. Proc. Natl. Acad. Sci. USA 84: 2540-2544.

Sun, X. J., Tolbert, L. P., and Hildebrand, J. G. 1993. Ramification pattern and ultrastructural characters of the serotonin-immunoreactive neuron in the antennal lobe of the moth *Manduca sexta*: a laser scanning confocal and electron microscope study. J. Comp. Neurobiol. 338: 5-16.

Syed, N. I. and Winlow, W. 1989. Morphology and electrophysiology of neurons innervating the ciliated locomotor epithelium in *Lymnaea Stagnalis* (L.). Comp. Biochem. Physiol. 93A(3): 633-644.

Syed, N. I., Bulloch, A. G. M. and Lukowiak, K. 1990. In vitro reconstruction of the respiratory central pattern generator of the mollusk *Lymnaea*.. Science 250: 282-285.

Taghert, P. H. and Goodman, C. S. 1984. Cell determination and differentation of identified serotonin-immunoreactive neurons in the grasshopper embryo. J. Neurosci. 4: 989-1000.

Taghert, P. H., Bastiani, M. J., Ho, R. K. and Goodman, C. S. 1982. Guidance of pioneer growth cones: Filopodial contacts and coupling revealed with an antibody to Lucifer Yellow. Dev. Biol. 94: 391-399.

Tang, J. and Landmesser, L. 1993. Reduction of intramuscular nerve branching and synaptogenesis is correlated with decreased motoneuron survival. J. Neurosci. 13(7): 3095-3103.

Taylor, H. H. 1973. The ionic properties of the capsular fluid bathing embryos of *Lymnaea stagnalis*, a freshwater pulmonate mollusc. J. Exp. Biol. 69: 143-172.

Tessier-Lavigne, M. and Placzek, M. 1991. Target attraction: are developing exons guided by chemotropism? TINS 14(7): 303-310.

Todd, R. D. 1992. Neural development is regulated by classical neurotransmitters: dopamine D2 receptor stimulation enhances neurite outgrowth. Biol. Psychiatry 31: 794-807.

Trimble, D. L., Barker, D. L. and Bullard, B. J. 1984. Dopamine in a molluscan nervous system: synthesis and fluorescence histochemistry. J. Neurobiol. 15(1): 27-36.

Truman, J. W. and Reiss, S. E. 1976. Dendritic reorganization of an identified motorneuron during metamorphosis of the tobacco hornworm moth. Science 192: 477-479.

Vaney, D. I. 1986. Morphological identification of serotonin-accumulating neurons in the living retina. Science 233: 444-446.

Ventura, A. L. M., Kein, W. L. and De Mello, F. G. 1984. Differential ontogenesis of D_1- and D_2-dopaminergic receptors in the chick embryo retina. Dev. Brain Res. 12: 217-223.

Vigers, A. J. and Pfenninger, K. H. 1991. N-type and L-type calcium channels are present in nerve growth cones. Numbers increase on synaptogenesis. Dev. Brain Res. 60: 197-203.

Voet, D. and Voet, J. G. 1990. Biochemistry. John Wiley and Sons, New York. 1223 pp.

Voronezhskaya, E. E. and Elekes, K. 1993. Distribution of serotonin-like immunoreactive neurones in the embryonic nervous system of lymnaeid and planorbid snails. Neurobiol. 1(4): 371-383.

Walczak, C. E. and Nelson, D. L. 1994. Regulation of dynein-driven motility in cilia and flagella. Cell Motil. Cytoskel. 27: 101-107.

Wall, J. B. and Taghert, P. H. 1991. The timing of initial neuropeptide expression by an identified insect neuron does not depend on interactions with its normal peripheral target. J. Neurobiol. 22(9): 935-956.

Wallace, J. A. 1985. An immunocytochemical study of the development of central serotonergic neurons in the chick embryo. J. Comp. Neurol. 236: 443-453.

Wallace, J. A. and Lauder, J. M. 1983. Development of the serotonergic system in the rat embryo: an immunocytochemical study. Brain Res. Bull. 10: 459-479.

Walter, J., Allsopp, T. E. and Bonhoeffer, F. 1990. A common denominator of growth cone guidance and collapse? TINS 13(11): 447-452.

Wang, L. -C., Godement, P. and Mason, C. A. 1993. Growth cone form is behavior- and position specific. Soc. Neurosci. Abstr. 259.5.

Warrington, S. J. 1992. Clinical implications of the pharmacology of serotonin reuptake inhibitors. Int. Clin. Psychopharmacol. 7 Suppl 2: 13-19.

Watt, C. B. 1992. A double-label study demonstrating that all serotonin-like immunoreactive amacrine cells in the larval tiger salamander retina express GABA-like immunoreactivity. Brain Res. 583: 336-339.

Wehrle, B. and Chiquet, M. 1990. Tenascin is accumulated along developing peripheral nerves and allows neurite outgrowth *in vitro*.. Development 110: 401-415.

Weinreich, D., McCaman, M. W., McCaman, R. E. and Vaughn, J. E. 1973. Chemical, enzymatic and ultrastructural characterization of 5-hydroxytryptamine-containing neurons from the ganglia of *Aplysia californica* and*Tritonia diomedia*.. J. Neurochem. 20: 969-976.

Weischer, M.-L. and Marthy, H.-J. 1983. Chemical and physiological properties of the natural tranquilliser in the cephalopod eggs. Mar. Behav. Physiol. 9: 131-138.

Weiss, K. R. and Kupfermann, I. 1976. Homology of the giant serotonergic neurons (metacerebral cells) in *Aplysia* and pulmonate molluscs. Brain Res. 117: 33-49.

Weiss, K. R., Cohen, J. and Kupfermann, I. 1975. Potentiation of muscle contraction: a possible modulatory function of an identified serotonergic cell in *Aplysia*. Brain Res. 99: 381-386.

Weiss, K. R., Mandelbaum, D. E., Schonberg, M. and Kupfermann, I. 1979. Modulation of buccal muscle contractility by serotonergic metacerebral cells in *Aplysia*: evidence for a role of cyclic adenosine monophosphate. J. Neurophysiol. 43(3): 791-803.

Welsh, J. H. and Williams, L. D. 1970. Monoamine-containing neurons in planaria. J. Comp. Neurol. 138: 103-116.

Wessells, N. K. and Nuttall, R. P. 1978. Normal branching, induced branching and steering of cultured parasympathetic motor neurons. Exp. Cell Res. 115: 111-122.

Whitaker-Azmitia, P. M. and Azmitia, E. C. 1989. Stimulation of astroglial serotonin receptors produces culture media which regulates growth of serotonergic neurons. Brain Res. 497: 80-85.

Whitaker-Azmitia, P. M., Murphy, R. and Azmitia, E. C. 1990. Stimulation of astroglial 5-HT1A receptors releases the serotonergic growth factor, protein S-100, and alters astroglial morphology. Brain Res. 528(1): 155-158.

Whitington, P. M., Bate, M., Seifert, E., Ridge, K. and Goodman, C. S. 1982. Survival and differentiation of identified embryonic neurons in the absence of their target muscles. Science 215: 973-975.

Whitnall, M. H., Key, S., Ben-Barak, Y., Ozato, K. and Gainer, H. 1985. Neurophysin in the hypthalamo-neurohypophysial system II. Immunocytochemical studies of the ontogeny of oxytocinergic and vasopressinergic neurons. J. Neurosci. 5: 98-109.

Wildering, W. C. and Janse, C. 1992. Serotonergic modulation of junctional conductance in an identified pair of neurons in the mollusc *Lymnaea stagnalis*. Brain Res. 595: 343-352.

Williams, C. V., Davenport, R. W., Dou, P. and Kater, S. B. 1995. Developmental regulation of plasticity along neurite shafts. J. Neurobiol. (in press).

Wilson, S. W. and Easter, S. S., Jr. 1991. A pioneering growth cone in a vertebrate brain. Proc. Natl. Acad. Sci. USA 88: 2293-2296.

Wollemann, M. and S.-Rózsa, K. 1975. Effects of serotonin and catecholamines on the adenylate cyclase of molluscan heart. Comp. Biochem. Physiol. 51C: 63-66.

Wondrak, G. 1975. The ultrastructure of the sensory cells in the chemoreceptor of the ommatophore of *Helix pomatia* L. Cell Tiss. Res. 159: 121-140.

Wong, R. G., Barker, D. L., Kater, S. B. and Bodnar, D. A. 1984. Nerve growth-promoting factor produced in culture media conditioned by specific CNS tissues of the snail *Helisoma*. Brain Res. 292:81-91.

Wong, R. G., Hadley, R. D., Kater, S. B and Hauser, G. C. 1981. Neurite outgrowth in molluscan organ and cell cultures: the role of conditioning factor(s). J. Neurosci. 1(9): 1008-1021.

Wright, B. R. 1974. Sensory structure of the tentacles of the slug *Arion ater* (Pulmonata, Mollusca) 1. Ultrastructure of thedistal epithelium, receptor cells and tentacular ganglion. Cell Tissue Res. 151: 229-244.

Yavarone, M. S., Shuey, D. L., Sadler, T. W. and Lauder, J. M. 1993a. Serotonin uptake in the ectoplacental cone and placenta of the mouse. Placenta 14 (2): 149-161.

Yavarone, M. S., Shuey, D. L., Tamir, H., Sadler, T. W. and Lauder, J. M. 1993b. Serotonin and cardian morphogenesis in the mouse embryo. Teratology 47(6): 573-584.

Young, S. H. and Poo, M.-M. 1983. Spontaneous release of transmitter from growth cones of embryonic neurons. Nature 305: 634-637.

Yorek, M. A., Strom, D. K. and Spector, A. A. 1987. Synthesis and high affinity uptake of serotonin and dopamine by human Y79 retinoblastoma cells. J. Neurochem. 49(4): 1316-1323.

Yu, W., Ahmad, F. J. and Baas, P. W. 1994. Microtubule fragmentation and partitioning in the axon during collateral branch formation. J. Neurosci. 14(10): 5872-5884.

Zhu, H., Wu, F. and Schacher, S. 1994. *Aplysia* cell adhesion molecules and serotonin regulate sensory cell-motor cell interactions during early stages of synapse formation *in vitro*. J. Neurosci. 14(11): 6886-6900.

Zielinski, B. and Hara, T. J. 1988. Morphological and physiological development of olfactory receptor cells in rainbow trout (*Salmo gairdneri*) embryos. J. Comp. Neurol. 271: 300-311.

Zoran, M. J., Haydon, P. G. and Matthews, P. J. 1989. Aminergic and peptidergic modulation of motor function at an identified neuromuscular junction in *Helisoma*. J. exp. Biol. 142: 225-243.

Zou, J.-y., Rabin, R. A. and Pentney, R. J. 1993. Ethanol enhances neurite outgrowth in primary cultures of rat cerebellar macroneurons. Dev. Brain Res. 72: 75-84.

Zs.-Nagy, I. and Sakharov, D. A. 1969. Axo-somatic synapses in procerebrum of Gastropoda. Experientia 25: 258-259.